ANTILARVAL SUBSTITUTED PHENOLS, DISTRIBUTION OF TRICYCLIC PYRONES IN MICE, AND SYNTHESIS OF UNNATURAL AMINO ACIDS

by

THI D.T. NGUYEN

B.Sc., Cantho University, Vietnam, 2001

AN ABSTRACT OF A DISSERTATION

submitted in partial fulfillment of the requirements for the degree

DOCTOR OF PHILOSOPHY

Department of Chemistry
College of Arts and Sciences

KANSAS STATE UNIVERSITY
Manhattan, Kansas

2014

Abstract

Three research projects were carried out and they are described below.

The synthesis of substituted phenolic compounds including halogenated di- and trihydroxybenzenes, aminophenols, and substituted di-*tert*-butylphenols are described. Redox potentials of the synthesized molecules along with various known laccase substrates were measured, and an inverse relationship between the oxidation potential and the efficiency of oxidation by laccase of halogenated hydroxybenzenes and aminophenols is demonstrated. The synthesized substituted phenols were found to be substrates but not inhibitors of laccase. We discovered a new class of di-*tert*-butylphenols compounds that inhibits the growth of mosquito larvae at low concentrations. Compound **17**, 2,4-di-*tert*-butyl-6-(3-methyl-2-butenyl) phenol caused greater than 98% mortality of third-instar larvae of *Anopheles gambiae* in the concentration of 0.18 μM. These compounds do not inhibit laccases. It appears that they affect a new target of the mosquito that is different from those of currently existing pesticides.

Two anti-Alzheimer molecules, CP2 and TP70, discovered in our laboratory were studied for their pharmacokinetics and distribution. The distribution of CP2 and TP70 in mouse brain region and various tissues of mice were examined. HPLC analysis revealed that CP2 treatment in primary neurons accumulates in mitochondria fraction. Similarly, the amount of CP2 in the brain tissue from wild type and APP/PS1 mice treated with 25 mg/kg/daily for 2 months also have the highest concentration in the mitochondria fractions in the hippocampus. The results show that CP2 and TP70 can penetrate the blood brain barrier and accumulate in the tissue in significant amounts. Pharmacokinetics and bioavailability of compound TP70 were determined. Area under the curve and bioavailability value F were calculated, and data show that TP70 has a good PK profile and bioavailability.

For the preparation of a novel tripeptidyl norovirus 3C-like protease ($3CL^{pro}$) inhibitor, the P3 unnatural amino acid, (*S*)-3-hydroxyphenylalanine was synthesized. The P3 is designed to increase the polarity with the addition of the alcohol group. After combining the P3 unnatural amino acid with the P1 and P2 to form the novel tripeptidyl compound, a study comparing the relations between the structure and its activity (SAR) will confirm whether prediction is correct in our pursuit for an antiviral therapeutic drug in the form of a protease inhibitor.

ANTILARVAL SUBSTITUTED PHENOLS; DISTRIBUTION OF TRICYCLIC PYRONES IN MICE; AND SYNTHESIS OF UNNATURAL AMINO ACIDS

by

THI D.T. NGUYEN

B.Sc., Cantho University, Vietnam, 2011

A DISSERTATION

submitted in partial fulfillment of the requirements for the degree

DOCTOR OF PHILOSOPHY

Department of Chemistry
College of Arts and Sciences

KANSAS STATE UNIVERSITY
Manhattan, Kansas

2014

Approved by:

Major Professor
Duy H. Hua

Abstract

Three research projects were carried out and they are described below.

The synthesis of substituted phenolic compounds including halogenated di- and trihydroxybenzenes, aminophenols, and substituted di-*tert*-butylphenols are described. Redox potentials of the synthesized molecules along with various known laccase substrates were measured, and an inverse relationship between the oxidation potential and the efficiency of oxidation by laccase of halogenated hydroxybenzenes and aminophenols is demonstrated. The synthesized substituted phenols were found to be substrates but not inhibitors of laccase. We discovered a new class of di-*tert*-butylphenols compounds that inhibits the growth of mosquito larvae at low concentrations. Compound **17**, 2,4-di-*tert*-butyl-6-(3-methyl-2-butenyl) phenol caused greater than 98% mortality of third-instar larvae of *Anopheles gambiae* in the concentration of 0.18 μM. These compounds do not inhibit laccases. It appears that they affect a new target of the mosquito that is different from those of currently existing pesticides.

Two anti-Alzheimer molecules, CP2 and TP70, discovered in our laboratory were studied for their pharmacokinetics and distribution. The distribution of CP2 and TP70 in mouse brain region and various tissues of mice were examined. HPLC analysis revealed that CP2 treatment in primary neurons accumulates in mitochondria fraction. Similarly, the amount of CP2 in the brain tissue from wild type and APP/PS1 mice treated with 25 mg/kg/daily for 2 months also have the highest concentration in the mitochondria fractions in the hippocampus. The results show that CP2 and TP70 can penetrate the blood brain barrier and accumulate in the tissue in significant amounts. Pharmacokinetics and bioavailability of compound TP70 were determined. Area under the curve and bioavailability value F were calculated, and data show that TP70 has a good PK profile and bioavailability.

For the preparation of a novel tripeptidyl norovirus 3C-like protease ($3CL^{pro}$) inhibitor, the P3 unnatural amino acid, (*S*)-3-hydroxyphenylalanine was synthesized. The P3 is designed to increase the polarity with the addition of the alcohol group. After combining the P3 unnatural amino acid with the P1 and P2 to form the novel tripeptidyl compound, a study comparing the relations between the structure and its activity (SAR) will confirm whether prediction is correct in our pursuit for an antiviral therapeutic drug in the form of a protease inhibitor.

Table of Contents

List of Figures

List of Tables

List of Abbreviations

ABTS	2,2'-azino-bis(3-ethylbenzothiazoline-6-sulphonic acid)
ABCA1	ATP-binding cassette subfamily A member 1
AD	Alzheimer's disease
AMPK	activated protein kinase
ATP	adenosine triphosphate
AβO	amyloid beta oligomers
Aβ	amyloid-beta peptide
ACAT	Acyl-CoA: cholesterol acyltransferase
APOE	apolipoprotein E
APP	amyloid precursor protein
AUC	area under the curve
BTA	1,2,4,5-benzenetetracarboxylic acid
C_{max}	maximum concentration
CV	cyclic voltametry
DMAP	4-(dimethylamino)pyridine
DMF	N, N-dimethylformamide
DMSO	dimethyl sulfoxide
EDTA	N, N, N', N'- ethylenediaminetetraacetic acid
ETC	electron transport chain
Glu	Glutamic acid
HM	heavy mitochondria
HPLC	high performance liquid chromatography
HAS	hydroxylamine-*O*-sulfonic acid
IBX	*o*-iodoxybenzoic acid
IP	intraperitoneal
IV	intravenous
LM	light mitochondria
MCPBA	*m*-chloroperbenzoic acid

mtDNA	mitochondrial DNA
NBS	*N*-bromosuccinimide
NFTs	neurofibrillary tangles
NV	norovirus
ORFs	open reading frames
PK	pharmacokinetics
PS1	presenilin 1
PS2	presenilin 2
TBAF	tetra-*n*-butylammonium fluoride
THF	tetrahydrofuran
T_{max}	time needed to reach the maximum concentration
TP	tricyclic pyrone
WT	wild type

List of Schemes

List of Structures

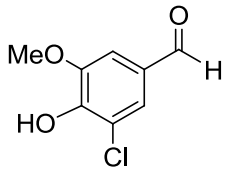

1

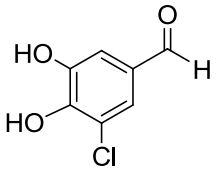

2

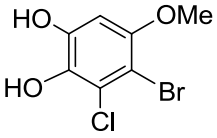

3

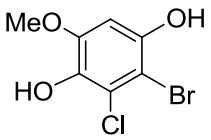

4

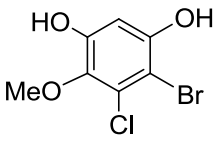

5

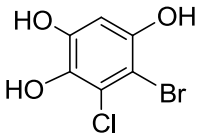

6

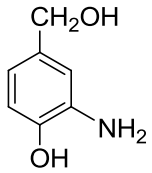

7

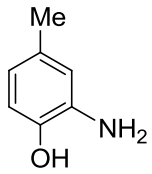

8

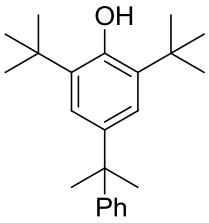

9
MON-0585

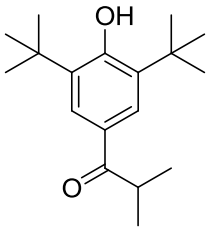

10

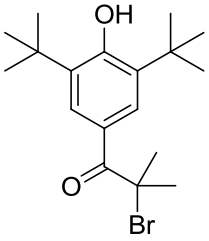

11

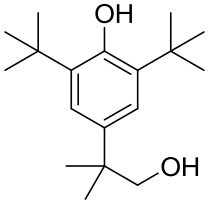

12

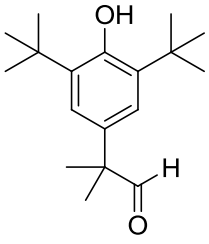

13

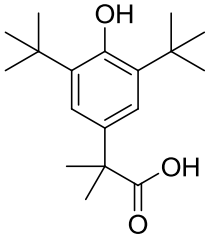

14

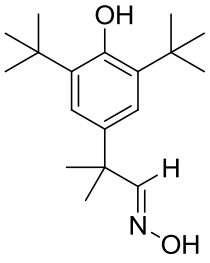

15

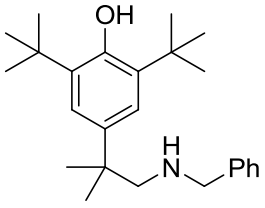

16

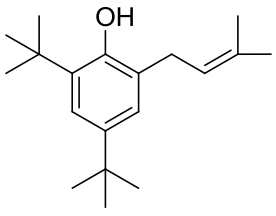

17

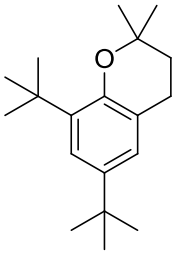

18

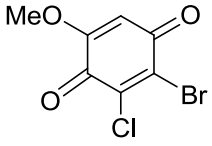

19

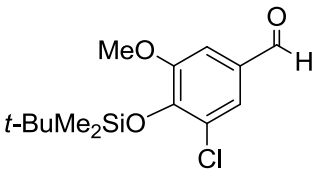

20

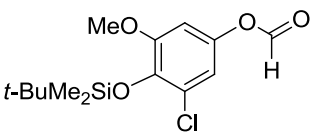

21

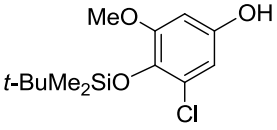

22

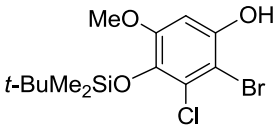

23

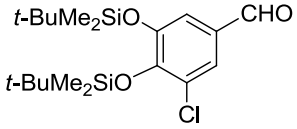

24

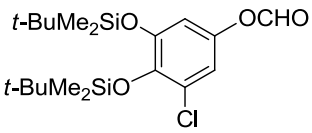

25

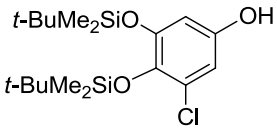

26

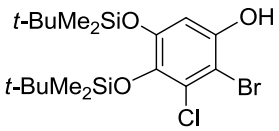

27

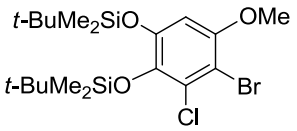

28

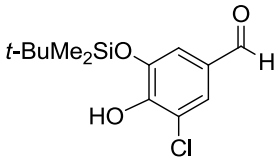

29

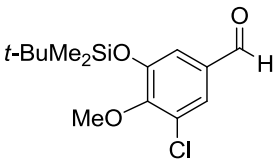

30

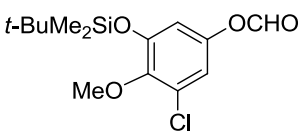

31

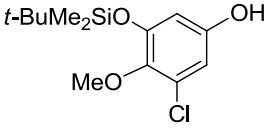

32

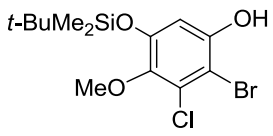

33

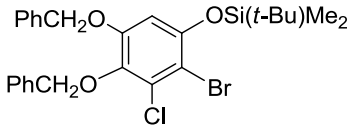

34

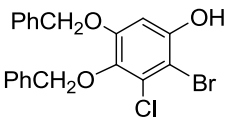

35

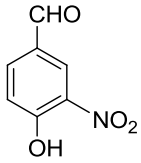

36

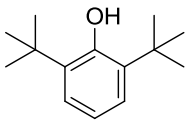

37

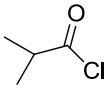

38

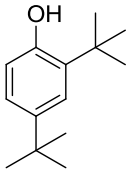

39

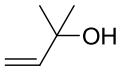

40

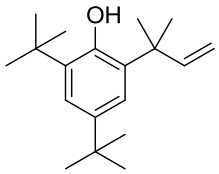

41

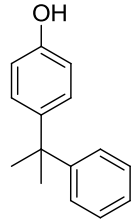

42

43

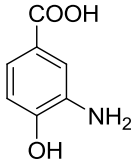

44

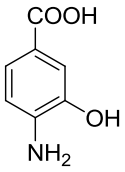

45

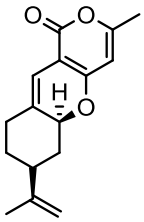

46

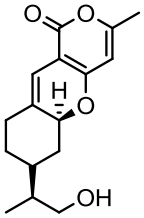

47

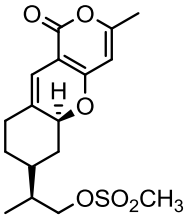

48

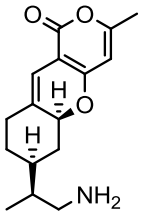

49

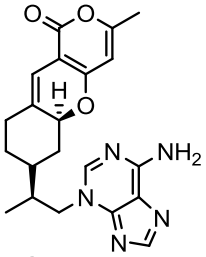

CP2

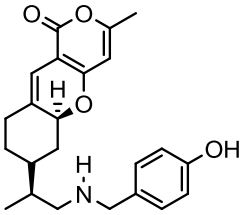

TP70

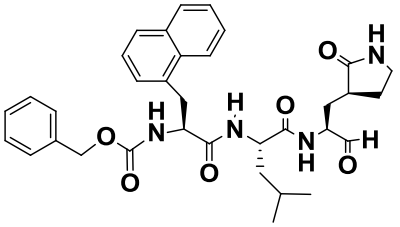

50

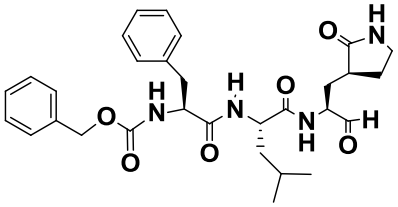

51

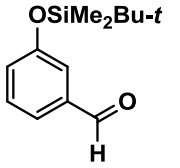

52

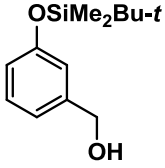

53

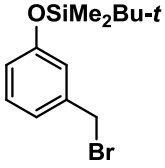

54

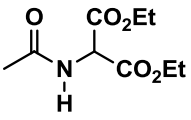

55

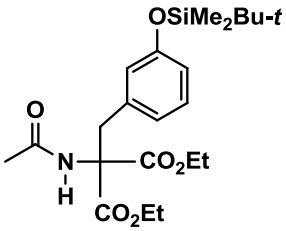

56

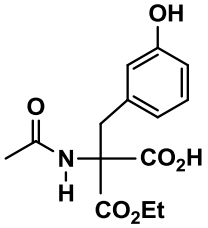

57

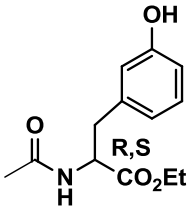

58a, 58b

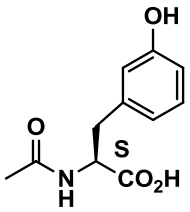

59a

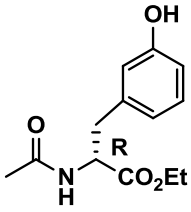

59b

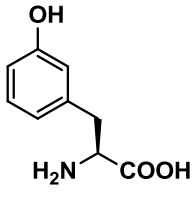

60

Acknowledgements

I would like to express my gratitude to my advisor, Dr. Duy H. Hua for his support and guidance throughout my graduate studies. He has taught me so much about being a scientist. I gained a lot from his professional and academic experience. I am thankful to the members of my advisory committee for their valuable time and valuable discussions. I would like to acknowledge the Department of Chemistry, Kansas State University, for providing me an opportunity to be a Ph.D. student. I am also grateful to all the faculties and staffs for their helpfulness and invaluable technical assistance. I would also like to thank my past and present labmates for their assistance and friendship. Finally, I would like to thank my family members in Vietnam and my husband for their love and continuous encouragements.

Chapter 1. Antilarval substituted phenols

1.1 Introduction

Mosquitoes are important arthropods affecting human health. Mosquitoes transmit some of the deadliest diseases known to man, such as malaria, yellow fever, dengue, Ebola, etc., claiming many millions of lives.[1] In fact, over 100 countries and about half of the world population are at risk of being infected with malaria. This leads to about 300 - 500 million malaria cases and between 1 - 1.5 million people die worldwide every year. Insecticides have played a significant role in public health; however, the use of insecticides for mosquito control is in jeopardy. Currently, pyrethroids are the primary insecticides used for mosquito control, and resistance to this class of compounds develops rapidly in the mosquitoes. These facts clearly prove that malaria is an especially serious problem and it is urgent to develop new insecticides that have novel targets to combat the transmission of malaria.

Laccases, copper-containing oxidases, are important enzymes found in many species of bacteria, fungus, plants and insects, and are utilized in a variety of ways depending on the species.[2] In plants, for example, tissues undergoing lignin synthesis express high levels of the laccase gene, and laccase is also believed to be used by plants to detoxify environmental pollutants affecting the plants.[3,4] Fungal laccase, on the other hand, involves in lignin degradation as seen in white rot fungi.[5,6] Our research focuses on insect laccases, particularly in the malaria transmitted mosquito, *Anopheles gambie*. Laccase is an important enzyme involving in the formation of external insect cuticle.[7-9] The formation of the cuticle, including sclerotization or tanning, is essential to insect survival because it protects insect from the environment and is involved in other key processes such as communication, locomotion, and respiration. Therefore, it is vital to understand the laccase enzyme as it might serve as an important target for controlling insect populations, especially the malaria mosquito, *Anopheles gambiae*.

As a class, laccases are glycoproteins that typically contain multiple copper atoms at the enzyme's active site. Laccases are oxidoreductases that reduce oxygen to water while oxidizing various organic compounds, particularly substituted *o*-, *m*-, and *p*-phenols, polyphenols, aromatic amines and *N*-hydroxamines.[10-13]. However, laccase inhibitors are rare and few useful organic compounds have been found.[14-16] Ideal compounds would bind irreversibly to the enzyme's active site, effectively cross-linking the enzyme. Other compounds, that serve as competitive substrates might also be good inhibitors, but are not ideal because the enzyme eventually regains activity.

The goals of this work were to synthesize classes of halogenated polyphenols, substituted aminophenols, and di-*tert*-butyl substituted phenols, and study their redox potentials, laccase activities, and mosquito larval inhibitory activities. The results may shed light onto future design of environmentally compatible laccase inhibitors and mosquito larvicides. The synthesis of these compounds was done by Dr. Keshar Prasain and me. The redox potentials of these compounds were measured by me using the facilities in Dr. Jun Li's laboratory. The laccase substrate activities were measured by Dr. Maureen Gorman and Zeyu Peng in Dr. Michael Kanost's laboratory, Kansas State University and the anti-mosquito larval activities were studied in Dr. Kun Yan Zhu's laboratory, Kansas State University. Since the biological works were performed in other laboratories, limited discussions are described in this thesis.

1.2 Background

Laccases are typically monomeric extracellular enzymes containing four copper atoms per monomer bound to three redox sites designated as T1, T2 and T3.[5] These coppers can be differentiated by UV/Vis and electronic paramagnetic resonance. The trinuclear cluster (containing one Cu T2 and two Cu's T3) is located approximately 12 Å away from the T1 site, and it is the place where molecular oxygen is reduced to water. Type I copper is the site where substrate oxidation takes place due to its high redox potential of around +790 mV.[17-18] In fungal laccase, T1 copper exhibits a planar trigonal geometry by coordinating with one cysteine and imidazole side chains of two histidines through sulfur and nitrogen atoms respectively. One T2 and two T3 copper atoms are arranged in a trinuclear cluster and coordinated to two and six histidines residues, respectively (**Figure 1.1**).[3] The electrons from the T1 copper site are transferred through the highly conserved His-Cys-His tripeptide to the T2/T3 copper trinuclear cluster, where four-electron reduction of molecular oxygen to water takes place.[12]

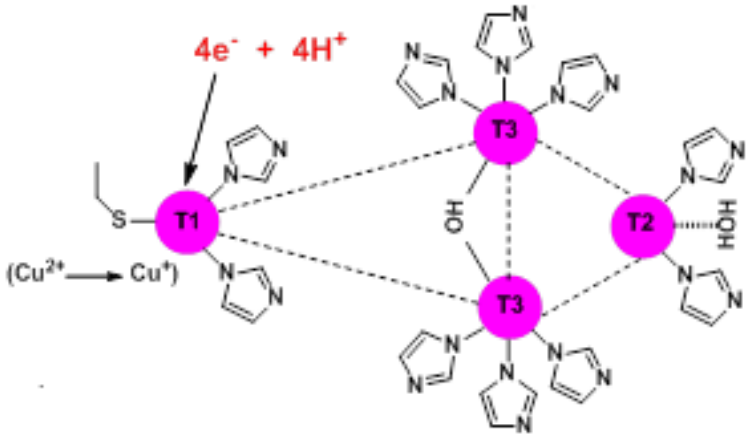

Figure 1.1 Schematic representation of tricopper site in fungal laccase.[3,12]

The typical reaction of laccase is oxidation of a phenolic compound with the concurrent reduction of molecular oxygen to water. After four cycles of single-electron oxidations forming free radicals, the enzyme reduces one molecule of oxygen, generating two molecules of water (**Figure 1.2**). The unstable radical may undergo further laccase-catalyzed oxidation or non-enzymatic reactions such as hydration and polymerization or couple to other phenolic structures.[44]

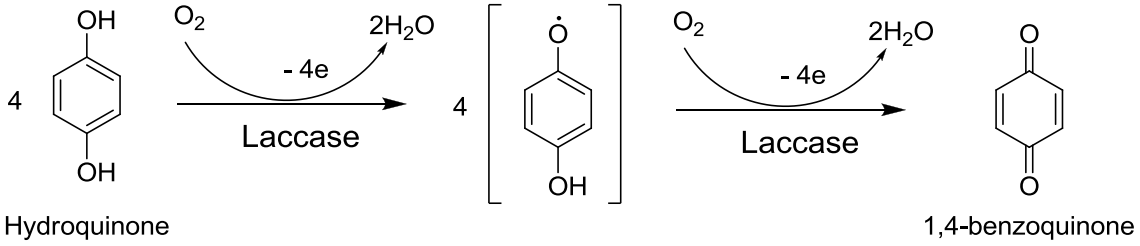

Figure 1.2 Schematic representation of oxidation of phenolic substrates (hydroquinone) to 1,4-benzoquinone and reduction of molecular oxygen to water by laccase.

Laccases can be strongly inhibited by various reagents with IC_{50} values in the high concentrations (mM ranges). Small anions such as azide, halides, cyanide, thiocyanide, fluoride and hydroxide bind to the type 2 and type 3 trinuclear copper sites, resulting in an interruption of the internal electron transfer and inhibition of activity. Smaller sized and low electronegativity halides inhibit laccases more effectively than those latter in the periodic table (fluoride > chloride > bromide). Other inhibitions include metal ions, fatty acids, hydroxylglycine, kojic acid by causing amino acid residue changes, conformational changes or copper chelation.[14, 34, 41-43]

The cuticle of insects, also known as exoskeleton of the insect, is mainly composed of chitin, protein, and catecholamine derivatives.[19] Insect cuticle does not expand readily and continuously; as a result, insects must often shed their old cuticle and make a new cuticle for growth. The newly formed cuticle is usually soft and pale, and soon it becomes hard and tanned by a process known as sclerotization. Sclerotization also aids the hardening of the pupal cuticle and protects the pupae during larval-pupal transformation. Disruption of sclerotization can lead to the death of insects because without sclerotization the organism would be vulnerable to its environmental enemies and die from desiccation. In cuticular sclerotization, two types of phenol

oxidases present in the cuticle, tyrosinases or laccases catalyze oxidation *N*-acetyl catecholamines to highly reactive quinones followed by reacting with nucleophilic side chains of histidines and other amino acids of cuticular proteins to form the inter-protein cross linking and polymer as shown in **Figure 1.3**.[8] This formation play a major role in strengthening and stabilization the cuticle. In 2005 and 2009, Arakane et al.[9,20] using the RNA interference experiments demonstrated the importance of laccase 2 not only for hardening of the cuticle but proper morphology and pigmentation as well. Reducing the level of laccase 2 (TcLac2) in the red flour beetle *Tribolium castaneum* resulted in insects failed to tan normally and physical deformities. These phenomena were also observed at the larval, pupa, and adult stages causing death within days of molting.

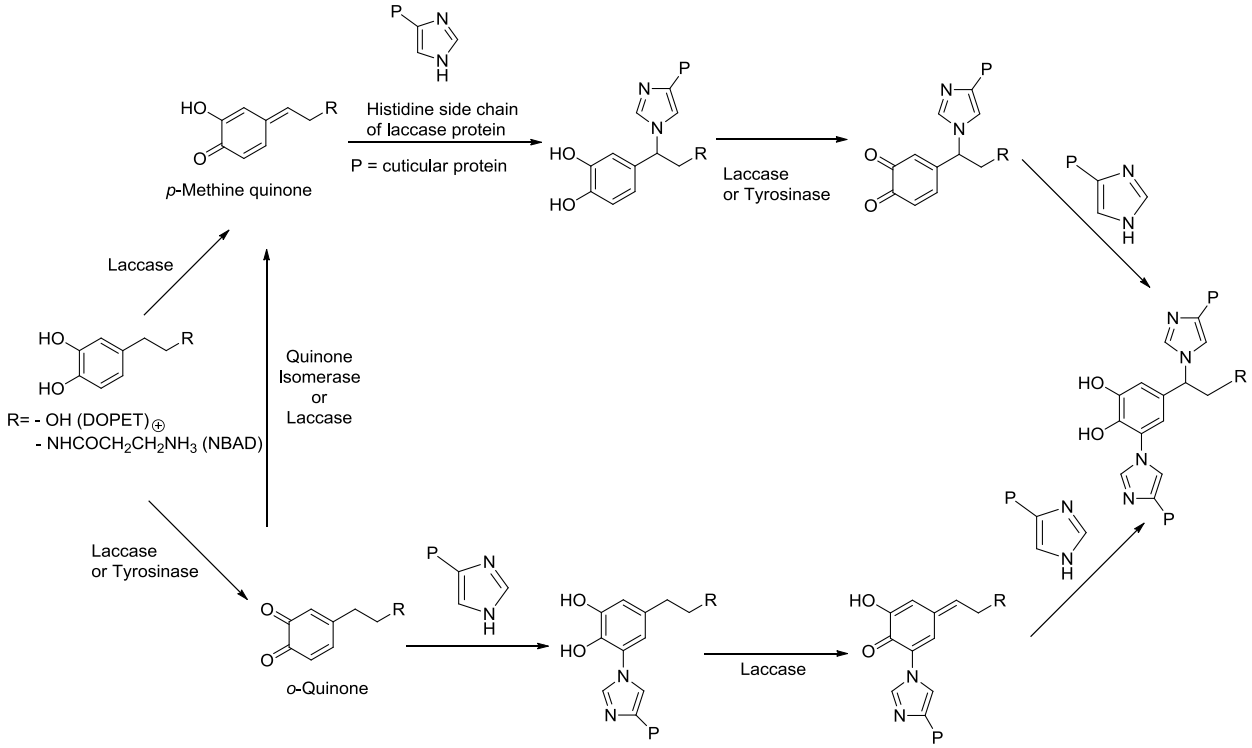

Figure 1.3 Proposed protein cross-linking during cuticle sclerotization in pupa of *Manduca sexta*.[8] The figure is copied from Karmer et al. *Tetrahedron* 2001, 57, 385-392 without permission.

1.3 Results and discussion

1.3.1 Synthesis and redox potential of halogenated phenols and amino phenols.

Laccase is known to be an important enzyme in insect cuticle sclerotization, it might serve as an important target for controlling insect populations, especially the malaria mosquito, *Anopheles gambiae*. With this in mind, our initial plan was to discover, design, and synthesize novel chemicals which can be laccase inhibitors and may lead to the inhibition of mosquito laccase. Halides are known to inhibit laccases at the Type 2/3 trinuclear copper site, hence compounds **1 - 6** were incorporated a leaving group such as chlorine (compound **1** – **2**) or both bromine and chlorine (compound **3** – **6**). To examine the activity of different positional isomers, compounds **3** – **5** have the hydroxyl groups oriented towards ortho, para and meta positions, respectively. Compound **6** (triol) having both ortho and para oriented hydroxyl groups was expected to have the highest laccase activity among the synthesized halogen substituted phenols. In addition, it has been reported that the introduction of methoxy group in phenolic compounds increases their laccase oxidative activity[21]; therefore, the presence of methoxy group in compound **1**, **3 - 5** might enhance their laccase oxidative activity. The amino function of synthesized *o*-aminophenols **7**[22] and **8**[23] were investigated since the resulting iminoquinones might complex with the copper in the laccase binding site (T1 site) and upon laccase oxidation would produce more reactive iminoquinones than the quinone analogs. The nucleophilic moieties like amino or hydroxyl function present in the laccase protein close to the T1 copper site might add irreversibly to the iminoquinone producing a covalently linked adduct and inhibit laccase activity.[24-25] With these ideas in mind, various halogen containing phenols and polyphenols, and aminophenols, were synthesized (**Figure 1.4**).[33] Synthesis of compound **1** has been previously reported by Dr. Hua's laboratory.[26]

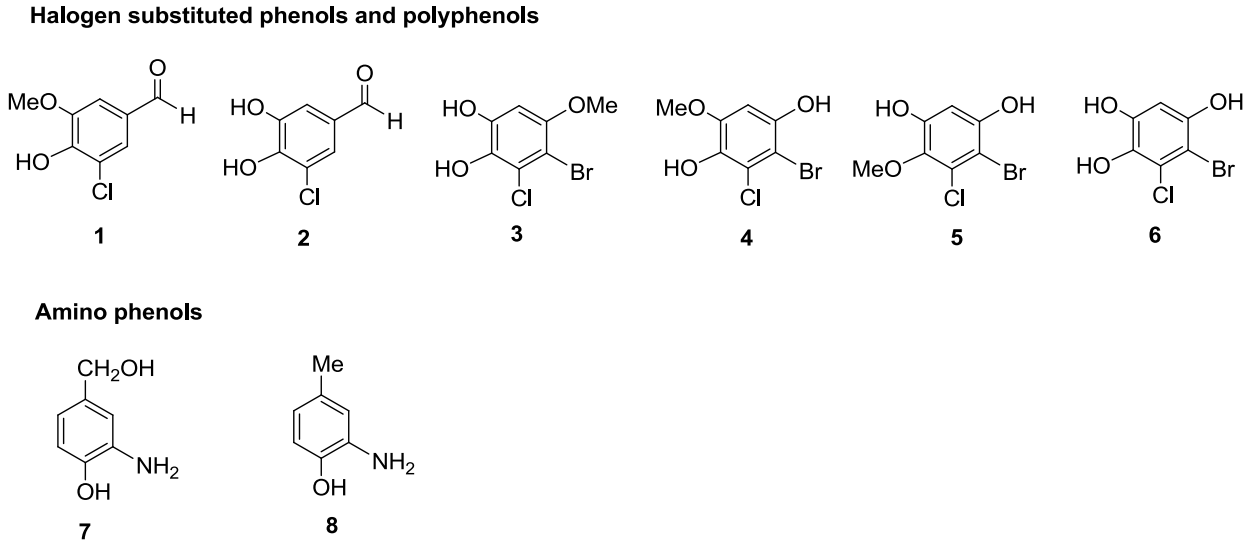

Figure 1.4 Synthesized halogenated polyphenols, and aminophenols.

1.3.1.1 Syntheses of compounds 2 and 3.

The synthetic route of 3-chloro-4,5-dihydroxybenzaldehyde (**2**) and 4-bromo-3-chloro-5-methoxybenzene-1,2-diol (**3**) is outlined in **Scheme 1.1**.

Scheme 1.1 Syntheses of compound **2** and **3.**

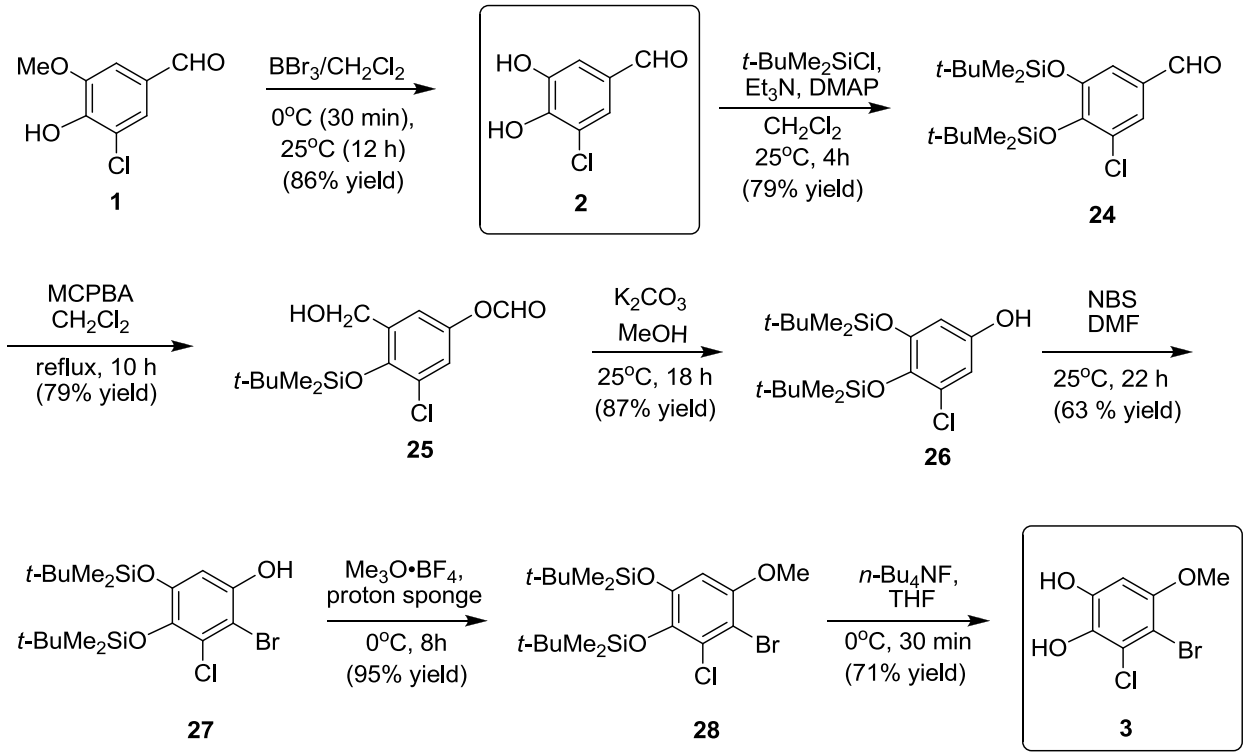

Compound **2** was obtained in 86% yield by demethylation of 3-chlorovanillin (**1)** with boron tribromide (BBr_3) in CH_2Cl_2 at 0°C for 30 minutes and 25°C for 12 hours. The two hydroxyl functions on C-4 and C-5 positions of compound **2** were then protected by the use of *tert*-butyldimethylsilyl chloride, triethylamine, and 4-dimethylaminopyridinene (DMAP) in CH_2Cl_2 at 0°C for 1 hour and 25°C for 3 hours to give 3,4-bis(*tert*-butyldimethylsilyloxy)-5-chlorobenzaldehyde (**24**) in 79% yield. Compound **24** on Baeyer-Villiger oxidation using *m*-chloroperbenzoic acid (MCPBA) (70% pure) in CH_2Cl_2 under reflux for 10 hours afforded 3,4-bis(*tert*-butyldimethylsilyloxy)-5-chlorophenyl formate (**25**) in 79% yield. Basic methanolysis of formate **25** was carried out with K_2CO_3 in methanol at 25°C for 12 hours to give 3,4-bis(*tert*-butyldimethylsilyloxy)-5-chlorophenol (**26**) in 87% yield. The less hindered C-2 position of compound **26** was regioselectively brominated by the use of *N*-bromosuccinimide (NBS) in dimethylformamide (DMF) for 22 hours to give 2-bromo-4,5-bis(*tert*-butyldimethylsilyloxy)-3-chlorophenol (**27**) in 63% yield; based on recovered starting material. Methylation of the phenolic hydroxyl moiety in compound **27** was achieved by the use of trimethyloxonium

tetrafluoroborate ($Me_3O•BF_4$) in the presence of proton sponge in CH_2Cl_2 at 0°C for 8 hours to give 2-bromo-4,5-bis-(*tert*-butyldimethylsilyloxy)-3-chloro-1-methoxybenzene (**28)** in 95% yield. Finally, the desired compound **3** was obtained by the desilylation of compound **28** with tetra-*n*-butylammonium fluoride (TBAF) in THF at 0°C for 30 minutes in 71% yield.

1.3.1.2 Synthesis of compound 4.

2-Bromo-3-chloro-5-methoxy-1,4-dihydroxybenzene (**4**) was synthesized from aldehyde **1**[26] following a sequence of reactions as outlined in **Scheme 1.2**.

Protection of the hydroxyl function of **1** by using *tert*-butyldimethylsilyl chloride in the presence of triethylamine and DMAP in CH_2Cl_2 at 25°C for 12 hours gave 4-(*tert*-butyldimethylsilyloxy)-3-chloro-5-methoxybenzaldehyde (**20**) in 85% yield. Baeyer-Villiger oxidation of compound **20** with the use of MCPBA in CH_2Cl_2 under reflux for 8 hours gave 4-(*tert*-butyldimethylsilyloxy-3-chloro-5-methoxyphenyl formate (**21**) along with the hydrolyzed product 4-(*tert*-butyldimethylsilyloxy)-3-chloro-5-methoxyphenol (**22)** in the yield of 63% and 27%, respectively. The formate function of compound **21** was hydrolyzed to the phenolic function by basic methanolysis using potassium carbonate (K_2CO_3) in methanol at 25°C for 4 hours to give phenol **22** in 90% yield. The less hindered C-2 position in compound **22** was regioselectively brominated by the use of NBS in DMF at room temperature for 12 hours following the literature published by Hua's group in the total synthesis of (+)-chloropuupehenone.[26] However**,** bromination of compound **22** under NBS condition gave 2-bromo-3-chloro-5-methoxy-1,4-benzoquinone (**19**) along with the desilylated product 2-bromo-4-(*tert*-butyldimethylsilyloxy)-3-chloro-5-methoxyphenol (**23**) in 48% and 31% yield, respectively. Compound **19** might have formed by the hydrolytic cleavage of silyl ether **23** by the HBr generated from the action of NBS and trace amount of water in the reaction mixture followed by the oxidation to the quinone. NBS oxidation of dihydroquinone to benzoquinone has been previously reported by Barakat et al.[27] Interestingly, deprotection of compound **23** by the use of TBAF in THF at 0°C for 30 minutes gave quinone **19** in 81% yield. Reduction of compound **19** in presence of 10% palladium/carbon in ethanol under hydrogen (1 atm.) at 25°C

for 15 minutes afforded the desired compound **4** in 100% yield. Infrared spectrum of compound **19** does not show a characteristic hydroxyl stretch but shows a quinone stretch at 1683 cm^{-1}, whereas compound **4** shows hydroxyl absorption at 3303 cm^{-1} implying compounds **19** and **4** are quinone and dihydroquinone, respectively.

Scheme 1.2 Synthesis of compound **4**.

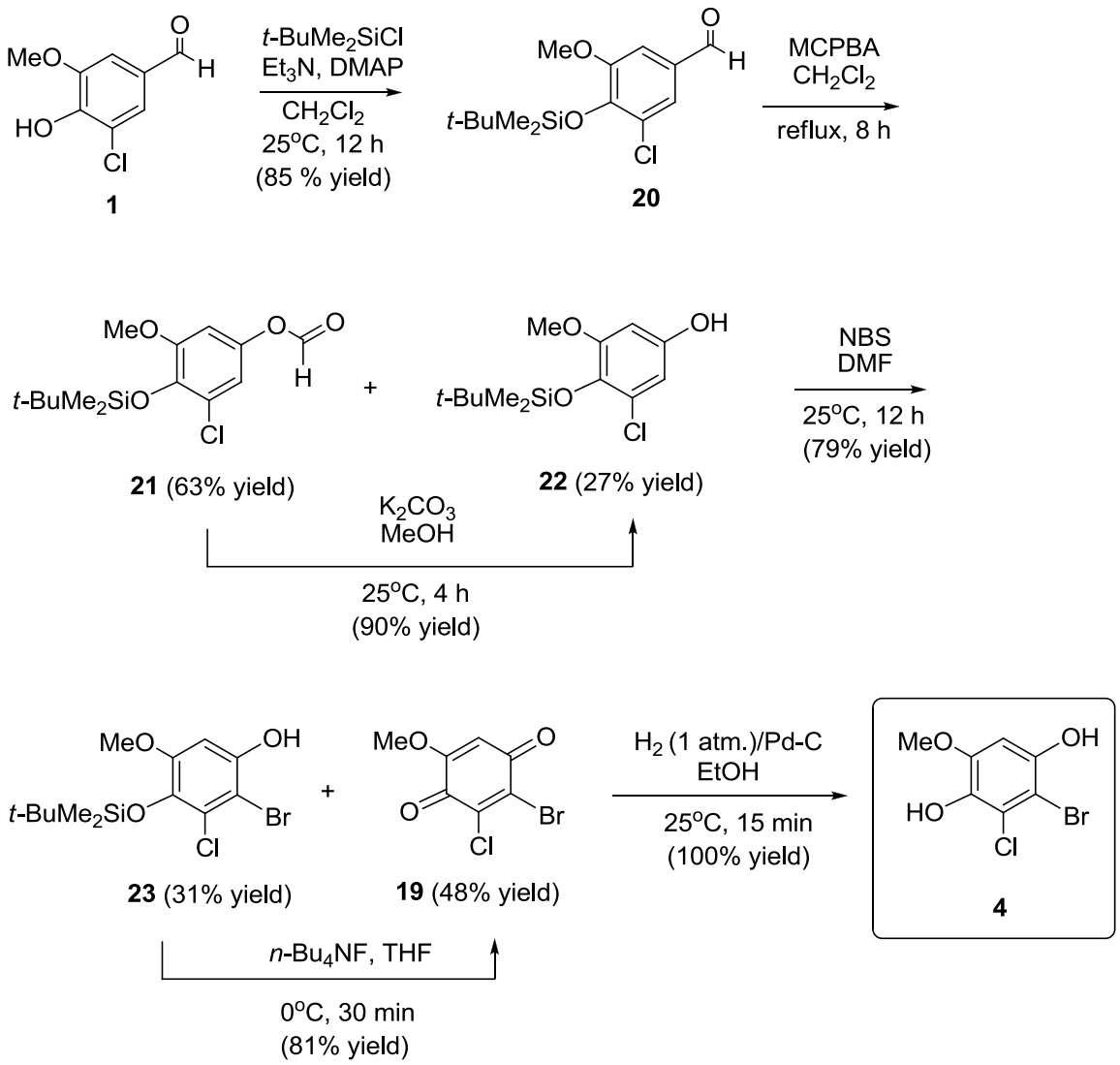

1.3.1.3 Synthesis of compound 5.

The synthesis of 4-bromo-5-chloro-6-methoxybenzene-1,3-diol (**5**) is outlined in **Scheme 1.3**. Selective protection of hydroxyl moiety on C-5 position of compound **2** was achieved by the use of equivalent amount of *tert*-butyldimethylsilyl chloride in the presence of triethylamine and DMAP in CH_2Cl_2 at 25^oC for 8 h to give 3-(*tert*-butyldimethylsilyloxy)-5-chloro-4-hydroxybenzaldehyde (**29**) and compound **24** (with both protected hydroxyl groups) in 70% and 11% yield, respectively. The structure of compound **29** was confirmed by a single-crystal X-ray analysis as shown in **Figure 1.5**. The less hindered C-5 hydroxyl moiety in compound **2** is likely to react faster with *tert*-butyldimethylsilyl chloride than the more hindered C-4 hydroxyl moiety giving compound **29** predominantly. Methylation of the phenolic hydroxyl moiety in compound **29** was achieved by the treatment with trimethyloxonium tetrafluoroborate and proton sponge in CH_2Cl_2 at 0^oC for 8 hours to give 3-(*tert*-butyldimethylsilyloxy)-5-chloro-4-methoxybenzaldehyde (**30**) in 78% yield; based on the recovery of starting material **29**. Compound **30** on Baeyer-Villiger oxidation by the use of MCPBA (70% pure) in CH_2Cl_2 under reflux for 12 hours afforded 3,4-bis(*tert*-butyldimethylsilyloxy)-5-chloro-4-methoxyphenyl formate (**31**) along with the hydrolyzed product 3-(*tert*-butyldimethylsilyloxy)-5-chloro-4-methoxyphenol (**32**) in 42% and 44% yield, respectively. Basic methanolysis of the formate function in compound **31** with K_2CO_3 in methanol at 25^oC for 12 hours afforded phenol **32** in quantitative yield. Regioselective bromination on the less hindered C-2 position of compound **32** was achieved by the use of NBS in DMF for 12 hours giving 2-bromo-5-(*tert*-butyldimethylsilyloxy)-3-chloro-4-methoxyphenol (**33**) in 67% yield. Finally, desilylation of compound **33** by treating with TBAF in THF at 0 ^oC for 30 minutes led to the formation of desired product **5** in 60% yield.

Scheme 1.3 Synthesis of compound **5**.

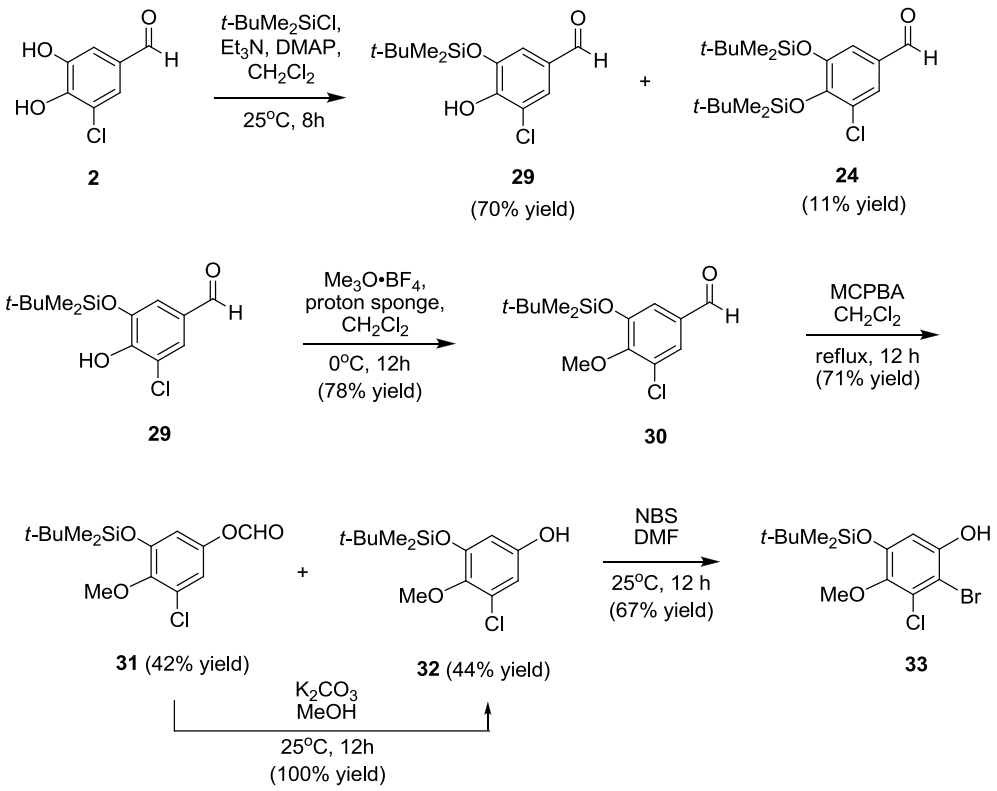

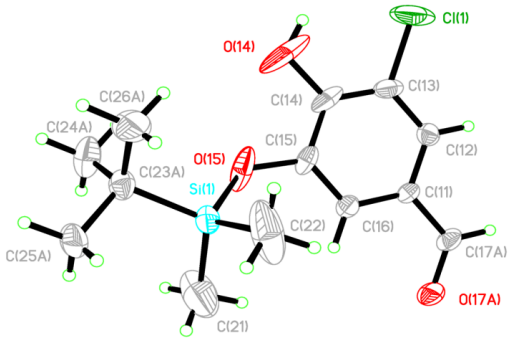

Figure 1.5 Crystal structure of compound **29**.

1.3.1.4 Synthesis of compound 6.

5-Bromo-6-chlorobenzene-1,2,4-triol (**6**) was synthesized from 4-bromo-3-chloro-1,2-dibenzyloxy-5-(*tert*-butyldimethylsiloxy)benzene (**34**), an intermediate previously reported by Hua's lab in the synthesis of (+)-chloropuupehenone,[26] in two steps as outlined in **Scheme 1.4**.

Scheme 1.4 Synthesis of compound **6**.

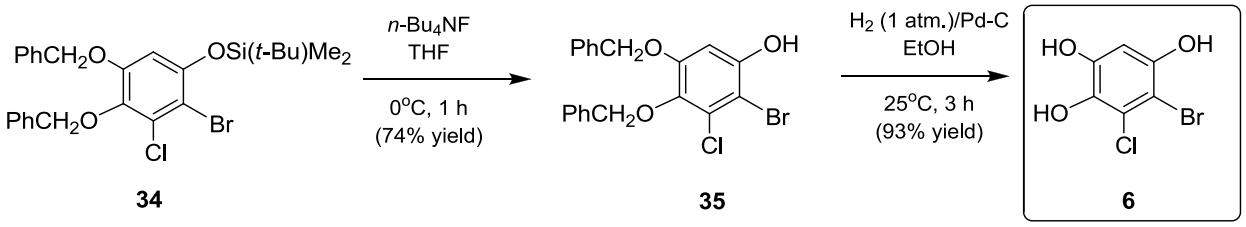

Desilylation of **34** by the use of TBAF in THF at 0°C for 1 hour afforded 2-bromo-3-chloro-4,5-dibenzyloxyphenol (**35**) in 74% yield. Finally, removal of two benzyl groups in compound **35** by catalytic hydrogenation (H_2, 1 atm.) in the presence of 10% palladium/carbon in ethanol at 25°C for 3 hours gave **6** as the desired product in 93 % yield. The infrared spectrum of triol **6** shows strong hydroxyl absorption at 3382 cm^{-1}. Triol **6** upon standing in air produced a black solid which might have resulted from its air oxidation to quinone followed by decomposition. Hence, triol **6** was immediately stored in a dry box under nitrogen atmosphere and used as soon as possible for the laccase activity study.

1.3.1.5 Syntheses of aminophenols 7 and 8.

A reaction for the selective reduction of the nitro function in 4-hydroxy-3-nitrobenzaldehyde (**36**) by the use of iron in the presence of acetic acid led to the formation of a mixture of several compounds, as indicated by TLC analysis, which could not be separated and analyzed. However, catalytic hydrogenation of 4-hydroxy-3-nitrobenzaldehyde by the use of a catalytic amount of palladium/carbon under 30 psi of hydrogen in ethanol for 4 hours gave 2-amino-4-(hydroxymethyl)phenol (**7**)[22] and 2-amino-4-methylphenol (**8**)[23] each with 41% yield as

shown in **Scheme 1.5**. The products were formed by the reduction of both nitro and aldehyde functions of 4-hydroxy-3-nitrobenzaldehyde. Compound **8** is formed by further reduction of benzylic hydroxyl function in compound **7** under hydrogenation condition. No reaction was observed when the catalytic hydrogenation of **36** was carried out in the presence of Raney Nickel under similar reaction conditions.

Scheme 1.5 Syntheses of compound **7**[22] and **8**[23].

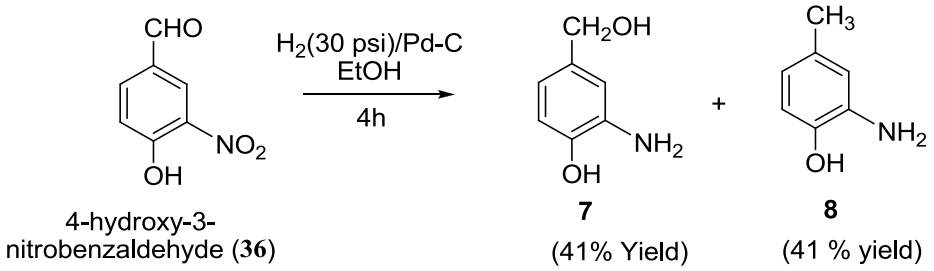

4-hydroxy-3-nitrobenzaldehyde (**36**)

7 (41% Yield)

8 (41 % yield)

Laccase oxidation activity of compounds **1** – **8** along with known laccase substrates such as hydroquinone, catechol, 2-aminophenol, 1,2-diphenyleneamine, and ABTS were tested with fungal laccase *Tramestes versicolor*. This study was carried by Dr. Maureen Gorman and Zeyu Peng in Dr. Michael Kanost's laboratory and results have been published.[33] The known laccase substrates were used as positive control for comparison. In summary, the results showed that these halogenated phenols and amino phenols were not laccase inhibitors; however, the laccase oxidation efficiency of most of the synthesized polyphenols and aminophenones were found to be higher than that of known substrates indicating their role as better laccase substrates.

After knowing that synthesized halogenated phenols and amino phenols (compounds **1** – **8**) were not laccase inhibitors but may serve as laccase substrates, the electrochemical properties of these compounds were investigated to better understand the oxidation ability of these compounds. Therefore, cyclic voltammetry (CV) experiments were carried out to study the redox properties of compounds **1** – **8** and other known laccase substrates (**Figure 1.6**) like hydroquinone, catechol, 2-aminophenol, 1,2-phenylenediamine, and 2,2'-azino-bis-(3-

ethylbenzothiazoline-6-sulfonic acid) (ABTS), 3-amino-4-hydroxybenzoic acid (**44**) and 4-amino-3-hydroxybenzoic acid (**45**) which were used as positive control in the experiment.

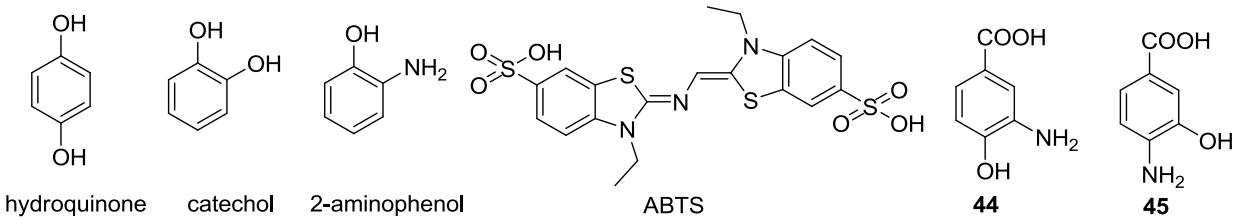

Figure 1.6 Known laccase substrates used in CV experiments.

Most of the synthesized polyphenols and aminophenones having lower or similar values of oxidation peak potential (E_{pa}) as that of known substrates could be easily oxidized by laccase. Different positions of two hydroxy groups in the benzene rings are responsible for different rates of their oxidation. Since the ease of oxidation of dihydroxybenzenes is para (dihydroquinone) > ortho (catechol) > meta (resorcinol), [37-38] dihydroxyquinone (**4)** had lower redox potential as compared to catechols **2** and **3**. Moreover, resorcinol **5** was found to have highest redox potential among the polyphenols. As expected, triol **6** was found to have the lowest oxidation potential (80 mV) thus gives the highest laccase activity. An inverse relationship between laccase oxidation efficiency (K_{cat}/K_m) and redox potential of studied compounds including compounds **1** – **8**, **44**, **45**, ABTS, 2-aminophenol, catechol, hydroquinone, and 1,2-phenylenediamine is highlighted in **Figure 1.7**. These results are in agreement with previous studies which showed that the higher the oxidation potential, the lower laccase oxidation efficiency is.[34-36]

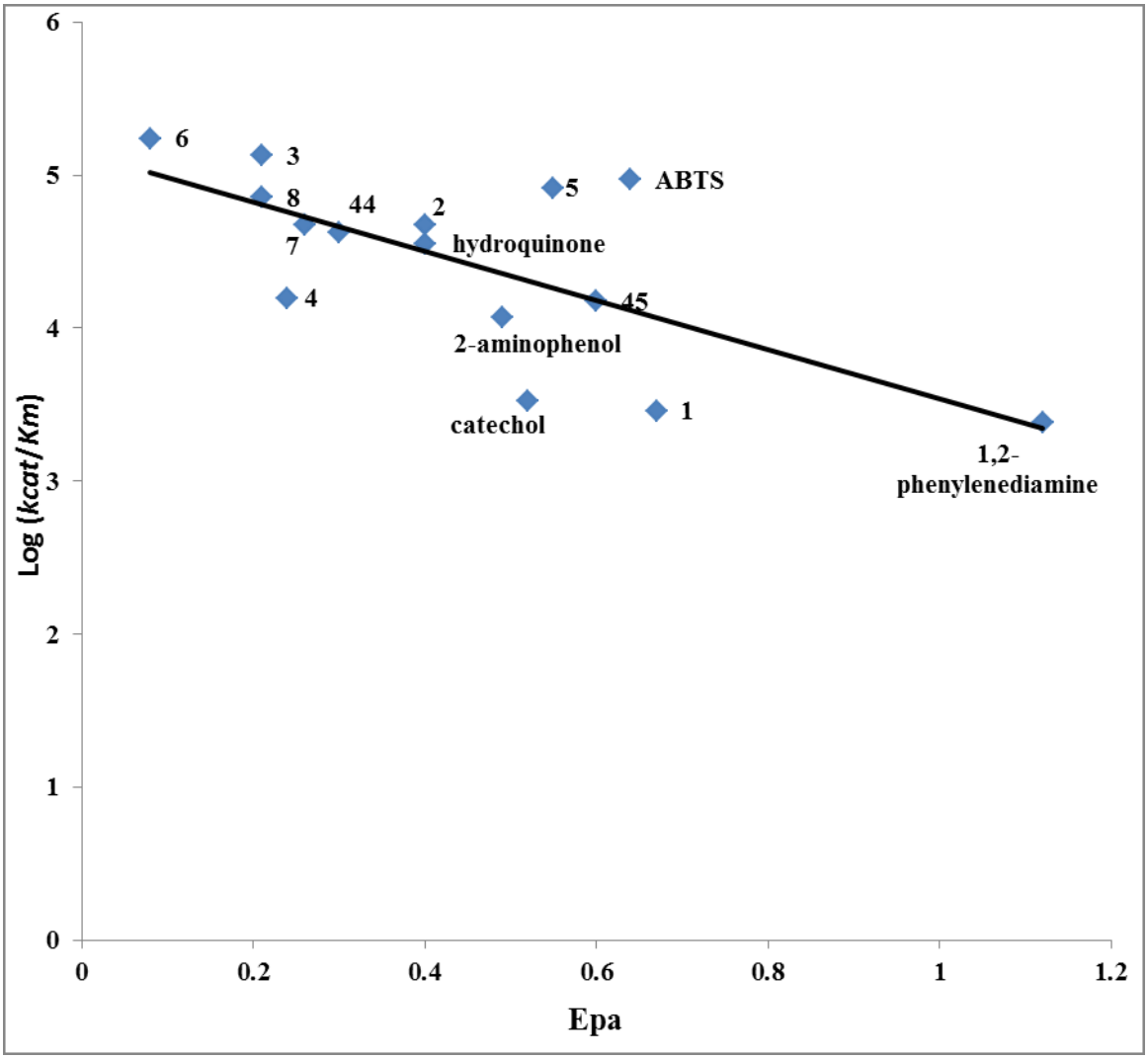

Figure 1.7 Correlation of laccase activities and redox potentials of compounds **1** – **8**, **44**, **45**, ABTS, 2-aminophenol, catechol, hydroquinone, and 1,2-phenylenediamine.

E_{pa} : oxidation peak potential (Volt)

1.3.2 Synthesis and anti-mosquitoes larval activity of substituted di-tert-butyl phenols.

After failing in synthesizing a class of laccase inhibitors (compounds **1** – **8**), our research efforts focus on searching for new anti-larval agents which have a different target in controlling mosquitoes. In insect, juvenile hormone refers to a group of hormone, secreted from a pair of glands behind the brain, that promotes the growth of larva while preventing metamorphosis. The juvenile hormone inhibits development of adult characteristics until the insects reach a proper stage. Juvenile hormones also play a prominent role for the production of eggs in female insects and in regulating reproductive maturation in adult insects. Therefore, synthetic juvenile hormone mimics have been widely used as pesticides for mosquito controls since they can cause premature molting of young immature stages, disrupting larval development. MON-0585 (**9, Figure 1.8**), developed by Monsanto, is a juvenile hormone mimic and implicated as insect growth regulators.[28] MON-0585 is also known to affect cuticle sclerotization in mosquitoes.[29] To investigate how the nature of the phenyl group on the side chain of MON-0585 affects activity, we started by changing it into different functional groups such as alcohol, aldehyde, carboxylic acid and oxime analogs (compound **11** – **15, Figure 1.9**).[33]

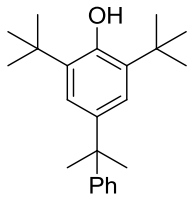

9

MON-0585 [2,6-di-*tert*-butyl-4-(2-phenylpropan-2-yl)phenol]

Figure 1.8 Chemical structure of MON-0585 (**9**).

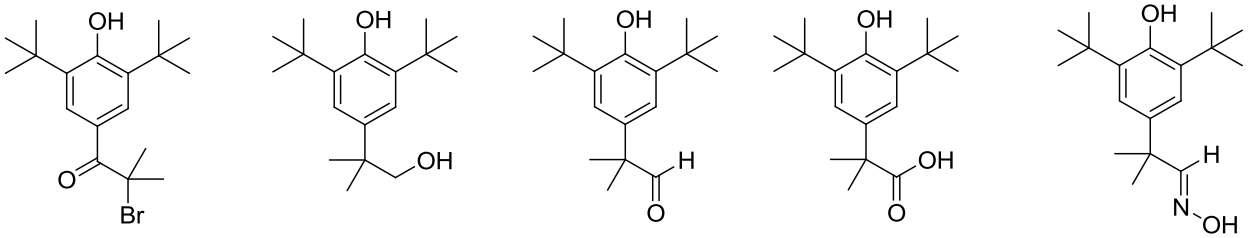

11 **12** **13** **14** **15**

Figure 1.9 Synthesized substituted di-tert-butyl phenols (compounds **11** - **15**).

Several 2,6-di-tert-butyl phenols **11** – **15** were synthesized mimicking the structure of MON-0585 as outlined in **Scheme 1.6**.

Scheme 1.6 Synthesis of compound **11** – **15**.

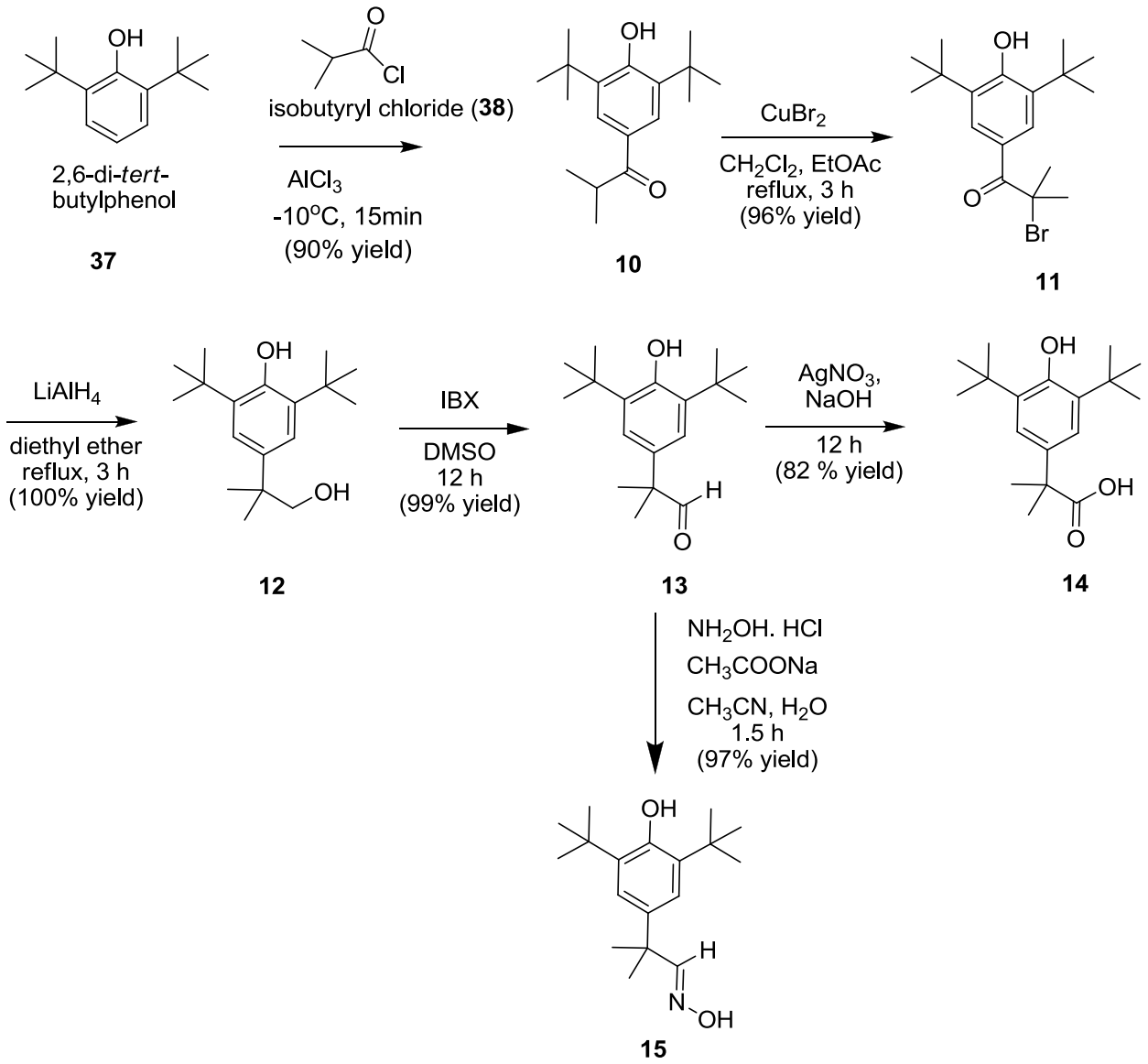

Following the reported procedure,[30] Friedel-Craft acylation of 2,6-di-*tert*-butylphenol (**37**) with isobutyryl chloride (**38**) in the presence of anhydrous aluminum chloride ($AlCl_3$) at -10°C for 15 minutes gave compound 1-(3,5-di-*tert*-butyl-4-hydroxyphenyl)-2-methylpropan-1-

one (**10**) in 90% yield. Bromination of compound **10** with cupric bromide in a solvent mixture of dichloromethane and ethyl acetate for 3 h afforded 2-bromo-1-(3,5-di-*tert*-butyl-4-hydroxyphenyl)-2-methylpropan-1-one (**11**) in 96% yield which on further treatment with excess of lithium aluminum hydride ($LiAlH_4$) in dry diethyl ether under reflux for 3 h gave 2,6-di-*tert*-butyl-4-(1-hydroxy-2-methylpropan-2-yl)phenol (**12**) in 100% yield. Compound **12** is likely formed by the hydride attack on the carbonyl carbon followed by aryl group rearrangement (**Scheme 1.7**).[31] The para-hydroxyl group facilitates the 1,2-shift of aryl group in the epoxide intermediate **11a**.

Scheme 1.7 Proposed mechanism for the formation of **12**.

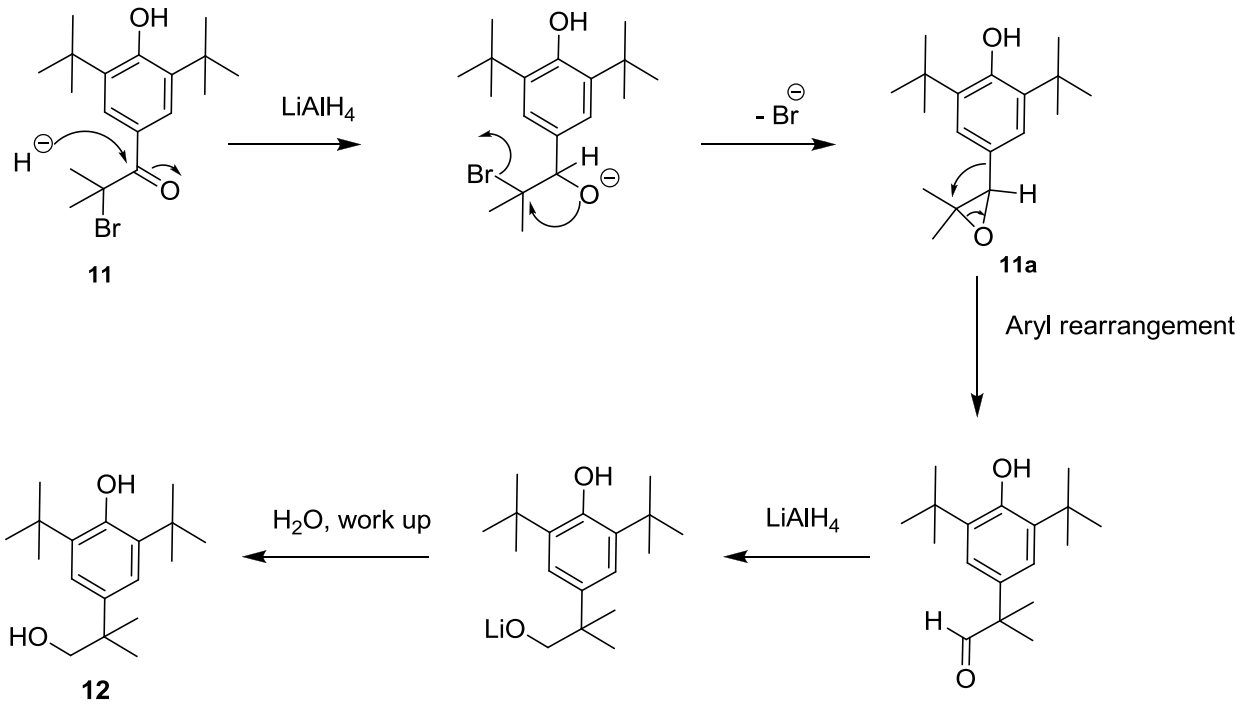

Compound **12** on oxidation with *o*-iodoxybenzoic acid (IBX) in dimethyl sulfoxide (DMSO) for 12 hours furnished 2-(3,5-di-*tert*-butyl-4-hydroxyphenyl)-2-methylpropanal (**13**) in 99% yield. Aldehyde **13** was further oxidized to 2-(3,5-di-*tert*-butyl-4-hydroxyphenyl)-2-methylpropanoic acid (**14**)[32] in 82% yield by treating with silver oxide, prepared in situ by reacting silver nitrate ($AgNO_3$) and sodium hydroxide (NaOH) in the solvent mixture of water and 1,4-dioxane at 25°C for 12 hours. Treatment of aldehyde **13** with hydroxylamine

hydrochloride and sodium acetate in a solvent mixture of acetonitrile and water (2:1) for 1.5 hour gave (*E*)-2-(3,5-di-*tert*-butyl-4-hydroxyphenyl)-2-methylpropanal oxime (**15**) in 97% yield.

The next goal was to synthesize amine from the oxime **15**; however, the oxime **15** could not be reduced to its corresponding amine on a catalytic hydrogenation by the use of 10% palladium/carbon in ethanol under 30 psi of hydrogen for 16 hours (**Scheme 1.8**). Therefore, reductive amination of aldehyde **13** was carried out by the use of benzylamine in toluene under reflux conditions for 12 hours followed by the removal of toluene under rotovapor and addition of methanol and sodium cyanoborohydride ($NaBH_3CN$) to give 4-(1-(benzylamino)-2-methylpropan-2-yl)-2,6-di-*tert*-butylphenol (**16**) in 97% yield. The removal of benzyl group in compound **16** leading to the corresponding amine was not achieved under catalytic hydrogenation conditions by the use of hydrogen (30 psi) in the presence of 10% palladium/carbon in ethanol for 12 hours. Moreover, increasing the temperature to 50^{o}C had no effect on the reaction and resulted in the recovery of the starting material. Changing the catalyst to platinum oxide (PtO_2) also failed in the removal of benzyl group.

Scheme 1.8 Synthesis of compound **16**.

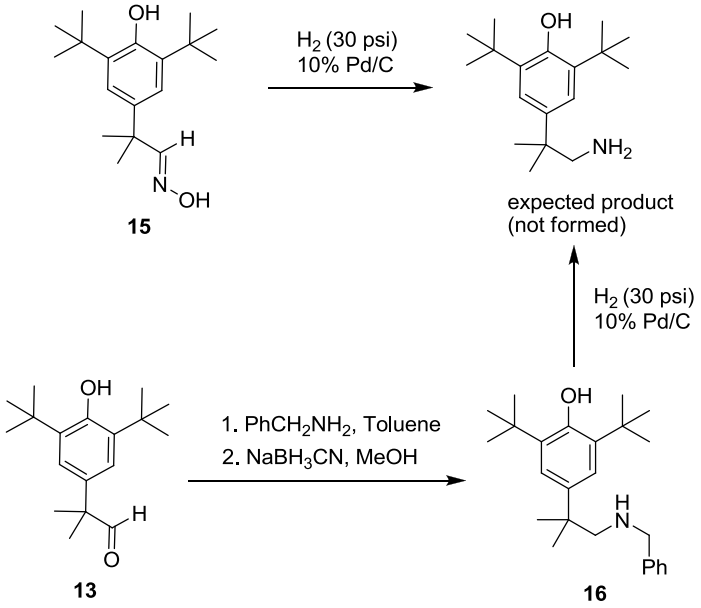

In addition to the 2,6-di-*tert*-butyl phenolic compounds, synthesis of 2,4-di-*tert*-butyl-6-(2-methylbut-3-en-2-yl)phenol (**41)** was envisioned by following Friedel-Crafts alkylation of 2,4-di-*tert*-butyl phenol (**39**) and 2-methyl-3-buten-2-ol (**40**) as highlighted in **Scheme 1.9a**. Compound **41** would have all the major structural features of MON-0585; moreover, would have an additional side chain with a terminal double bond that could be manipulated into different functional groups as desired. However, instead of giving compound **41**, treatment of 2,4-di-*tert*-butylphenol with 2-methyl-3-buten-2-ol in the presence of boron trifluoride.ether (BF_3•$O(Et)_2$) in CH_2Cl_2 at 25^{o}C for 1 hour afforded 2,4-di-*tert*-butyl-6-(3-methyl-2-butenyl)phenol (**17**) and 6,8-di-*tert*-butyl-2,2-dimethyl-3,4-dihydro-2*H*-chromene (**18**) in 46% and 10% yield respectively. Benzopyran **18** appears to be derived from an acid-catalyzed ring closing reaction of compound **17** as highlighted in **Scheme 1.9b.**

Scheme 1.9 a) Syntheses of compound **17** and **18** and b) proposed mechanism for the formation of **18**.

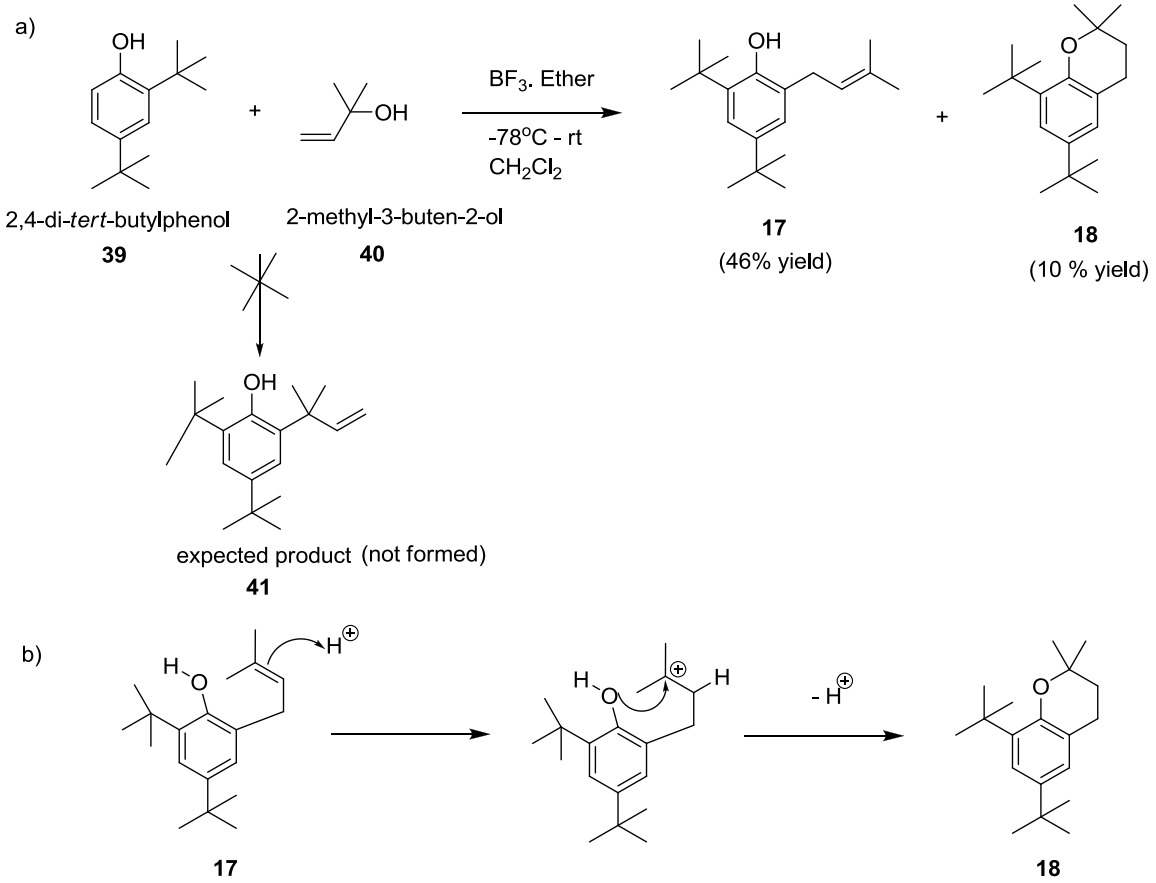

MON-0585 (**9**) was used as a positive control and was prepared by a Friedel-Crafts alkylation reaction of 4-cumylphenol (**42**) and isobutylene (**43**) in the presence of catalytic amount of sulfuric acid in dichloroethane in a sealed tube at 80°C for 6 h as shown in **Scheme 1.10**.[39]

Scheme 1.10 Synthesis of MON-0585.

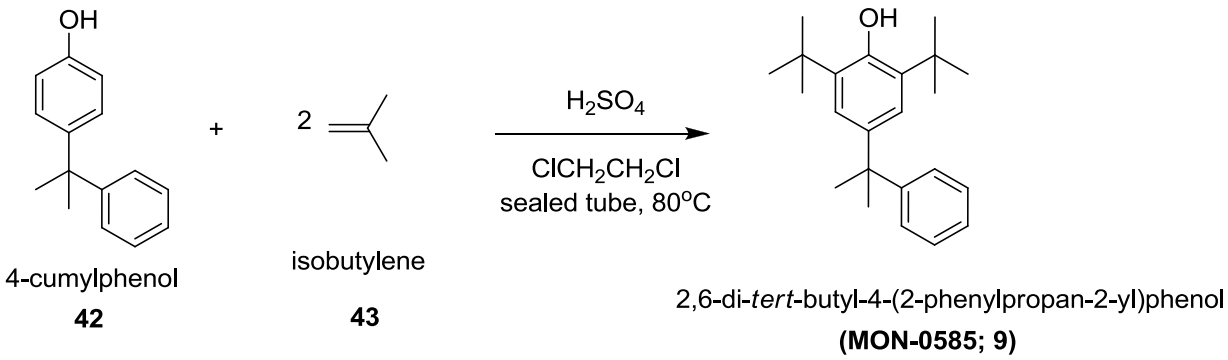

Substituted di-*tert*-butyl phenolic compounds **10 - 16**, benzopyran **17**, and MON-0585 were not oxidized by laccase and their laccase activity could not be detected due to their water insolubility. Cyclic voltammetry (CV) experiments were carried out to study the redox properties of compounds **10 - 17**, MON-0585 (**9**), including other known laccase substrates like hydroquinone, catechol, 2-aminophenol, 1,2-phenylenediamine, and 2,2'-azino-bis-(3-ethylbenzothiazoline-6-sulfonic acid) (ABTS), 3-amino-4-hydroxybenzoic acid (**44**) and 4-amino-3-hydroxybenzoic acid (**45**). These compounds show only one of the redox waves and have broad peak separation (> 540 mV). These compounds caused unreliable CV measurements due to their most water-insoluble property in the phosphate-buffered saline (PBS) solution containing 20% ethanol.

Laccase are used as the building blocks in the insect cuticle sclerotization. Therefore, laccase substrates such as triol **6**, MON-0585 (**9**), dihydroquinone, and various di-*tert*-butyl phenolic compounds including compound **10 - 16**, and di-*tert*-butyl substituted benzopyran **17** were investigated for their anti-larval activities by using the third-instar larvae of *Anopheles*

gambiae in a three-day bioassay. MON-0585 known as an insect growth regulator was used as a positive control and for comparison. This study was performed in Dr. Kun Yan Zhu's laboratory at Kansas State University by him and his assistant and the result has been published.[33] For the anti-larval assay, water soluble compounds like hydroquinone and triol **6** were dissolved in water and used; whereas water-insoluble compounds such as di-*tert*-butyl phenol derivatives **10 - 16** and benzopyran **17** were first dissolved in acetone and used for the assay in aqueous solution. The larval toxicity studies were investigated for two concentrations per compound; 50 and 1000 µg/mL.

Table 1.1 Toxicities of substituted phenols to third-instar larvae of Anopheles gambiae in a three-day bioassay.[33]

Compound	**% Mortality (mean ± SE)**	
	50 µg/L	**1000 µg/L**
Control	0 ± 0b	3.50 ± 3.50 d
Dihydroquinone	1.25 ± 1.25 b	5.38 ± 1.80 d
MON-0585 (**9**)	93.3 ± 4.71 a	100 ± 0 a
Compound **6**	0 ± 0b	11.4 ± 3.85 d
Compound **11**	0 ± 0b	60.0 ± 11.5 c
Compound **12**	0 ± 0b	46.7 ± 3.25 c
Compound **13**	0 ± 0b	65.0 ± 5.00 c
Compound **14**	5.50 ± 3.455 b	12.3 ± 1.35 d
Compound **15**	5.41 ± 3.28 b	93.1 ± 3.99 ab
Compound **16**	3.71 ± 2.14 b	7.70 ± 3.14 d
Compound **17**	98.1 ± 1.93 b	98.3 ± 1.68 ab
Compound **18**	5.77 ± 3.69 b	91.7 ± 6.31 d

Results are mean ± standard errors (SE) of four replicates (n = 4); each with 12 – 15 third-instar larvae. Means followed by the same letter in the same column are not significantly different (P >0.05) according to Fisher's LSD multiple comparison test after arcsine square root transformation of the percentage date (ProStat; PolySoftware International, 2002).[33]

Water soluble laccase substrates such as compound **6,** compound **14** and **16** (used as a sodium salt and trifluoroacetic acid salt respectively) and dihydroquinone did not produce any toxicity at the studied concentrations. In contrast, water-insoluble materials such as di-*tert*-butyl

phenolic compounds (**11 – 13)** showed more that 46% mortality of larvae at 1000 µg/mL concentration. Interestingly, compound **17** was found to have similar toxicity towards the larvae as compared to MON-0585 at both studied concentrations. Compound **17** appears to have higher toxicity than methoprene (**Figure 1.10**), an insect growth regulator mimicking natural juvenile hormone of insects and commonly used insecticides, which caused only 60% mortality at 100 µg/L in 3 days bioassay against the third-instar larvae of *Culex molestus*.[40] Compound **15** and benzopyrane **17** also produced significant toxicity to the mosquito larvae with mortality of 93% and 91% at the concentration of 1000 µg/mL. Only water insoluble compounds were found to be toxic to the larvae suggesting that these compounds may be absorbed through the body of the larvae resulting in its death. The mosquito has four distinct stages in its life cycle: egg, larva, pupa, and adult. The larvae treated with di-*tert*-butyl phenolic compounds died just before pupation and over the course of 3 days indicating that the target does not involve the neurological system, a common target of most insecticides.

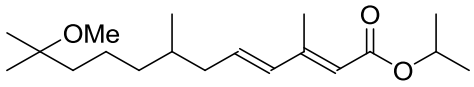

Figure 1.10 Chemical structure of methoprene.

To better understand what causes the death of larvae when treating with our compounds, the microscopic sections of the larvae killed by most active compound **17** were compared with that of untreated larvae (**Figure 1.11**). The larva needs to remove its old cuticle and form a new one to grow up. Interestingly, the larvae treated with compound **17** had thin cuticle and appeared to start molting; however, failed to remove the old cuticle. Moreover, the larvae treated with compound **17** showed very little synthesis of new pupal cuticle as compared to the untreated larvae. This phenomenon not only happens in the head of the larva but also in the thorax and abdomen. This indicates that compound **15**, other toxic di-*tert*-butyl phenolic derivatives and compound **17** might attack the target related to the insect cuticle formation. However, the target and mechanism of action of these water insoluble di-*tert*-butyl phenolic compounds and benzopyran **17** remain to be investigated.

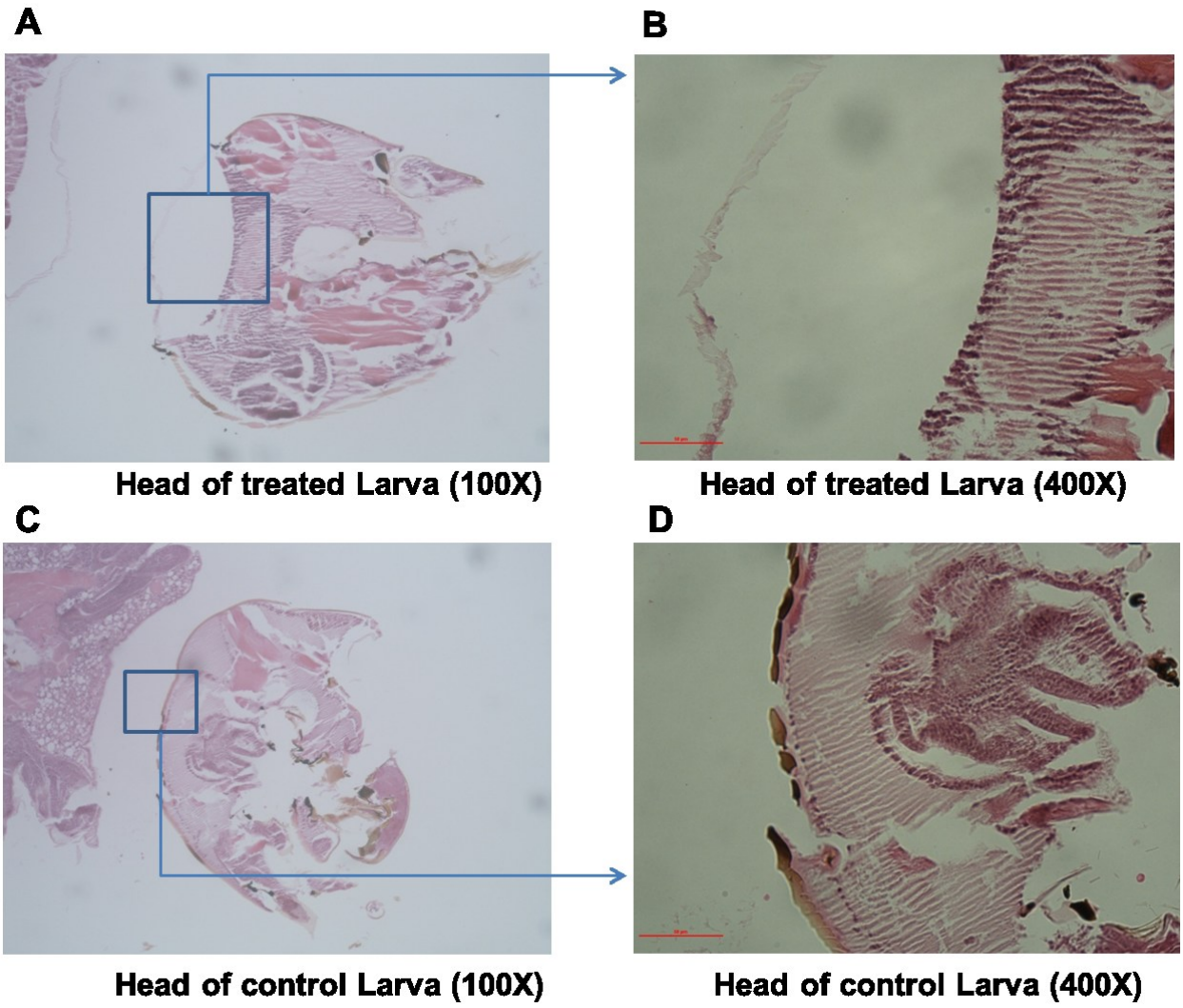

Figure 1.11 Microscopic slides of larvae of Anopheles gambiae treated and untreated with compound **16**.[33] **A**. Head of treated Larva (100X). **B**. Head of treated Larva (400X). **C**. Head of control Larva (100X). **D**. Head of control Larva (400X).

1.4 Conclusion

A new class of phenolic compounds containing halide, hydroxyl, aldehyde, methoxy, amino, and di-*tert*-butyl functions were synthesized and their redox potential, laccase oxidation, and mosquito anti-larval activities were examined. Synthesized phenolic compounds **1 - 8** were found to be laccase substrates but not the inhibitors of laccase. Redox potentials of the synthesized molecules along with various known substrates were measured, and the relationship with the efficiency of oxidation by laccase is analyzed. Compounds **15** and **17** were found to have potent anti-larval activity at low concentrations. Treatment of 50 μg/L (or 0.18 μM) of compound **17** to third-instar larvae of *Anopheles gambiae* caused greater than 98% mortality. It appears that these compounds affect a new target of the mosquito that is different from those of currently existing pesticides.

1.5 Experimental section

General Methods

Nuclear magnetic resonance (NMR) spectra were recorded on a Varian Unity plus 400 MHz or 200 MHz spectrometer for ^{1}H and ^{13}C in deuteriochloroform ($CDCl_3$), unless otherwise indicated. Tetramethylsilane was used as the internal reference and the data reported in ppm. Infrared (IR) spectra were recorded on a Nicolet 380 FT-IR and are reported in wavenumbers (cm^{-1}). Low-resolution mass spectra were taken from an API 2000-triple quadrupole ESI-MS/MS mass spectrometer (from Applied Biosystems). High-resolution Mass spectra were recorded on LCT Premier (Waters corp., Milford MA), a time of flight mass analyzer with an electrospray ion source. Column chromatography was carried out on silica gel (200 – 400 mesh) from the University of Kansas. Tetrahydrofuran (THF) and diethyl ether were distilled over sodium and benzophenone, methylene chloride was distilled over calcium hydride (CaH_2), and toluene was distilled over $LiAlH_4$ prior for usage. The purity of compounds, **1 - 17** and MON 0585 were found to be ~ 98% as indicated by HPLC analysis carried on Varian Prostar 210 with a UV-Vis detector and a reverse phase column from Phonomenex (250 x 21.20 mm, 10 micron).

Experimental section for synthesis

4-(*tert*-Butyldimethylsilyloxy)-3-chloro-5-methoxybenzaldehyde (20)

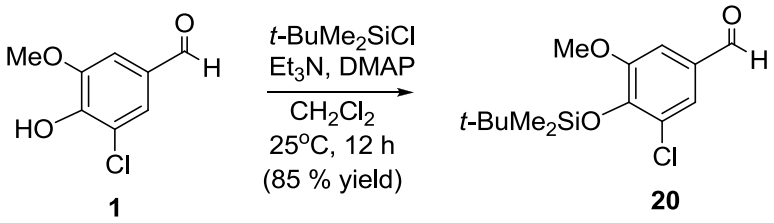

To a solution of 0.40 g (2.15 mmol) of 3-chloro-4-hydroxy-5-methoxybenzaldehyde (**1**)[26] in 5 mL of dichloromethane at 0°C under argon, were added 0.6 mL (4.3 mmol) of triethylamine, 40 mg (0.33 mmol) of 4-dimethylaminopyridine (DMAP), and 0.65 g (4.3 mmol) of *tert*-butyldimethylsilyl chloride and the solution was stirred at 25°C for 12 hours. The reaction was diluted with 100 mL of diethyl ether and washed with 20 mL of saturated aqueous NH_4Cl solution, 20 mL of water, and 20 mL of brine. The organic layer was dried over anhydrous $MgSO_4$, concentrated, and the crude product was column chromatographed on silica gel using a mixture of hexane and diethyl ether (4:1) as eluent to give 0.55 g of **20** in 85% yield. ^{1}H NMR δ 9.76 (s, 1 H), 7.45 (d, J = 2.0 Hz, 1 H), 7.27 (d, J = 2.0 Hz, 1 H), 3.85 (s, 3 H), 1.01 (s, 9 H), 0.21 (s, 6 H); ^{13}C NMR δ 190.0, 151.9, 147.7, 130.0, 126.6, 126.3, 108.4, 55.6, 25.8 (3 C), 19.0, -3.8 (2 C); HRMS calcd for $C_{14}H_{22}ClO_3Si$ ($M+H^+$) 301.1021, found 301.1028.

4-(*tert*-Butyldimethylsilyloxy)-3-chloro-5-methoxyphenyl formate (21) & 4-(*tert*-butyldimethylsilyloxy)-3-chloro-5-methoxyphenol (22)

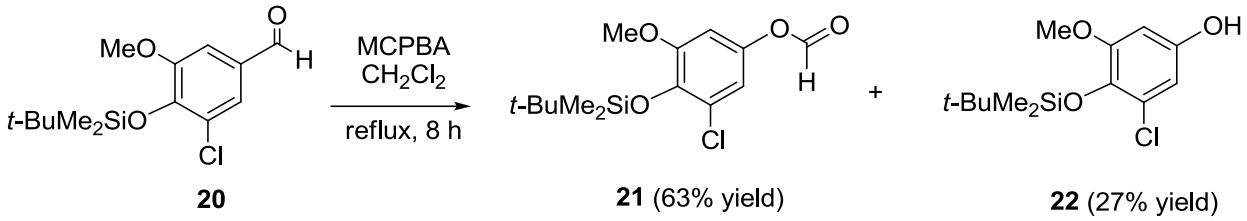

20 **21** (63% yield) **22** (27% yield)

To a solution of 0.60 g (2 mmol) of **20** in 5 mL of dichloromethane at 0°C under argon, was added 0.75 g (3 mmol) of *m*-chloroperbenzoic acid (70% pure) and heated to reflux for 8 hours. The reaction was cooled to room temperature and 5 mL of aqueous sodium thiosulfate and 200 mL of diethyl ether were added to it. The solution was washed with 20 mL of saturated aqueous $NaHCO_3$, 20 mL of water, and 20 mL of brine. The organic layer was dried over anhydrous $MgSO_4$, concentrated, and column chromatographed on silica gel using a mixture of hexane and diethyl ether (5:1) as an eluent to give 0.40 g of **21** and 150 mg of **22** in 63% and 27% yield, respectively. **Formate 21:** ^{1}H NMR δ 8.26 (s, 1H, OCHO), 6.78 (d, J = 2.9 Hz, 1 H), 6.58 (d, J = 2.9 Hz, 1 H), 3.80 (s, 3 H), 1.03 (s, 9 H), 0.20 (s, 6 H); ^{13}C NMR δ 159.3, 151.8, 143.2, 140.4, 125.9, 114.4, 104.1, 55.7, 26.0, 19.0, -3.9; HRMS calcd for $C_{14}H_{22}ClO_4Si$ ($M+H^+$) 317.0976, found 317.0968. **Phenol 22:** ^{1}H NMR δ 6.43 (d, J = 2.9 Hz, 1 H), 6.32 (d, J = 2.9 Hz, 1 H), 3.78 (s, 3 H), 1.02 (s, 9 H), 0.17 (s, 6 H); ^{13}C NMR δ 152.2, 149.8, 135.8, 125.7, 108.2, 99.2, 55.5, 26.1 (3 C), 19.0, -4.0 (2 C); HRMS calcd for $C_{13}H_{22}ClO_3Si$ ($M+H^+$) 289.1027, found 289.1000.

Conversion of formate 21 to phenol 22

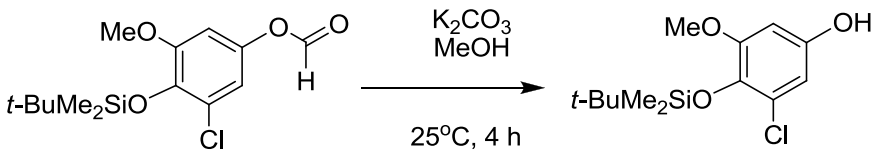

21 **22** (27% yield)

To a solution of 45 mg (0.142 mmol) of **21** in 2 mL of methanol, was added 98 mg (0.71 mmol) of K_2CO_3 and stirred at 25°C for 4 hours. The reaction was diluted with 100 mL of diethyl ether and washed with 10 mL of aqueous NH_4Cl, 10 mL of water, and 10 mL of brine. The organic layer was dried over anhydrous $MgSO_4$, solvent evaporated, and the crude product was column chromatographed on silica gel using a mixture of hexane and diethyl ether (2:1) as eluent to give 37 mg of phenol **22** in 90% yield, which ^{1}H NMR spectral data is identical to that described above.

2-Bromo-4-(*tert*-butyldimethylsilyloxy)-3-chloro-5-methoxyphenol (23) & 2-bromo-3-chloro-5-methoxy-1,4-benzoquinone (19)

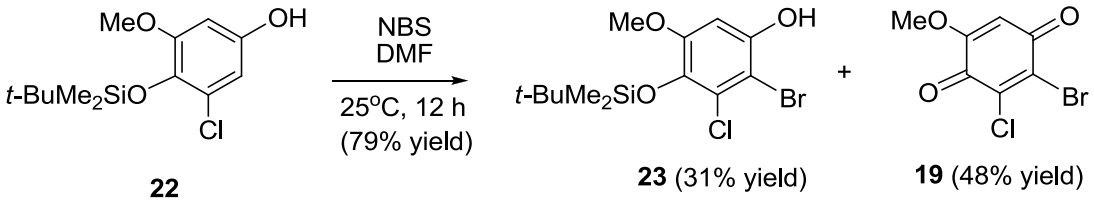

To a solution of 84 mg (0.29 mmol) of **22** in 2 mL of DMF under argon, was added 57 mg (0.32 mmol) of NBS and was stirred at 25°C for 12 h. The reaction solution was diluted with 100 mL of diethyl ether and washed with 10 mL of water followed by 10 mL of brine. The organic layer was dried over anhydrous $MgSO_4$, concentrated, and column chromatographed on silica gel using a gradient mixture of hexane and diethyl ether as an eluent to give 27 mg of **23** and 35 mg of **19** in 31% and 48% yield, respectively. **Bromophenol 23**: ^{1}H NMR δ 6.56 (s, 1 H), 5.33 (s, 1 H, OH), 3.78 (s, 3 H), 1.03 (s, 9 H), 0.18 (s, 6 H); ^{13}CNMR δ 151.5, 147.4, 136.8, 125.8, 101.5, 98.4, 55.6, 26.1, 19.0, -3.9; HRMS calcd for $C_{13}H_{19}BrClO_3Si$ (M-H) 364.9975, found 365.0076; $C_{13}H_{20}BrClO_3SiNa$ ($M+Na^+$) 388.9951, found 388.9934. ***p*-Benzoquinone 19** **(**light yellow solid): Mp. 167 – 170°C; IR (neat) υ 2953, 2913, 2839, 1683, 1638, 1613, 1556, 1454, 1229, 1168 cm^{-1}; ^{1}H NMR δ 6.16 (s, 1 H), 3.89 (s, 3 H); ^{13}C NMR δ 177.5, 172.4, 158.9, 137.4, 107.9, 107.2, 57.3; HRMS calcd for $C_7H_5BrClO_3$ ($M+1^+$) 250.9105, found 251.0593.

Conversion of silyl ether 23 to *p*-benzoquinone 19

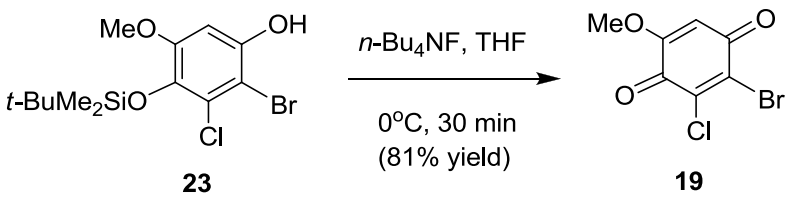

23 **19**

To a solution of 25 mg (0.068 mmol) of silyl ether **23** in 2 mL of THF was added 68 μL (0.068 mmol) of *n*-Bu_4NF (1 M in THF) and stirred under argon from 0°C for 30 minutes. The reaction was diluted with 50 mL of diethyl ether and washed with 10 mL of aqueous NH_4Cl, 10 mL of water, and 10 mL of brine. The organic layer was dried over anhydrous $MgSO_4$, concentrated, and column chromatographed on silica gel using a mixture of hexane and diethyl ether (1:1) as an eluent to give 14 mg of *p*-benzoquinone **19** in 81% yield, which ^1H NMR spectrum is identical to that described above.

2-Bromo-3-chloro-5-methoxy-1,4-dihydroxybenzene (4)

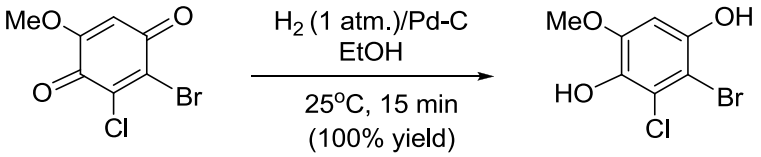

19 **4**

A mixture of 10 mg (0.040 mmol) of **19** and 2 mg of 10% palladium over carbon in 1 mL of ethanol under 1 atm. of hydrogen (a balloon filled with hydrogen connected to the round bottom flask) was stirred at 25°C for 15 minutes, filtered through Celite, and rinsed with 10 mL of ethanol. The filtrate was concentrated to give 10 mg of **4** in quantitative yield: IR (neat) υ 3303, (s), 2935, 2851, 1601, 1497, 1441, 1210, 1071, 1046, 994, 864, 842, 825 cm^{-1}; ^1H NMR δ 6.60 (s, 1 H), 5.50 (bs, 1 H, OH), 5.30 (bs, 1 H, OH), 3.89 (s, 3 H, OMe); ^{13}C NMR δ 148.2, 147.7, 136.7, 121.1, 100.2, 99.4, 56.0; HRMS calcd for $C_7H_6BrClO_3$ (M^+) 251.9189, found 252.0427.

3-Chloro-4,5-dihydroxybenzaldehyde (2)[26]

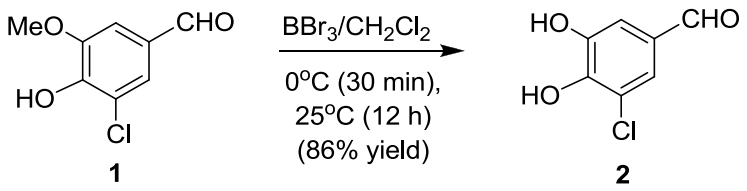

To a solution of 10.14 g (5.43 mmol) of **2**[26] in 40 mL of dry CH_2Cl_2 at 0°C, was added 0.57 mL (6 mmol) of boron tribromide (BBr_3) drop wise and the mixture was stirred under argon at 0°C for 30 minutes and then at 25°C for 12 hours. The reaction was quenched with a slow addition of 50 mL of methanol followed by evaporation under rotavap. The addition and evaporation of methanol were repeated 3 times (50 mL each time) to remove excess BBr_3. The crude product was then treated with 30 mL of 1:1 hexane and diethyl ether solution, filtered and washed with small amount of 1:1 hexane and diethyl ether solution to give 8.80 g (93.9%) of 2[26] as pure green solid. ^{1}H NMR (Acetone-*d6*) δ 9.78 (s, 1H), 7.47 (d, *J* = 2.0 Hz), 7.34 (d, *J* = 2.0 Hz); ^{13}C NMR (Acetone-*d6*) δ 190.6, 148.8, 147.4, 130.8, 125.2, 121.5, 113.8.

3,4-Bis(*tert*-butyldimethylsilyoxy)-5-chlorobenzaldehyde (24)[26]

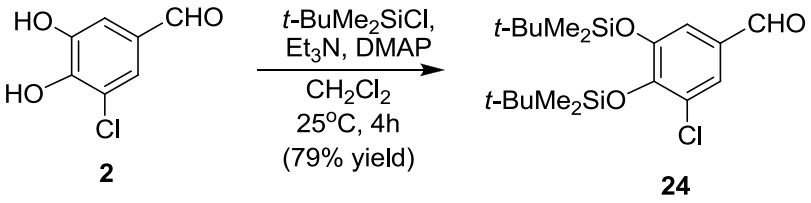

To a solution of 0.80 g (4.64 mmol) of **2**[26] and 0.17 g (1.39 mmol) of 4-dimethylaminopyridine (DMAP) in 10 mL of dry CH_2Cl_2 at 0°C under argon, were added 2.6 mL (18.56 mmol) of triethylamine and 2.8 g (18.56 mmol) of *tert*-butyldimethylsilyl chloride and stirred at 0°C for 1 hour and then at 25°C for 3 hours. The reaction mixture was diluted with 100 mL of diethyl ether, washed with 20 mL of aq. NH_4Cl followed by 20 mL of brine, dried over anhydrous $MgSO_4$, and concentrated. The crude product was column chromatographed on silica gel using a 10:1 mixture of hexane and diethyl ether as an eluent to give 1.46 g of desired

24[26] in 79% yield. ^{1}H NMR δ 9.78 (s, 1 H), 7.50 (d, *J* = 2 Hz, 1 H), 7.29 (d, *J* = 2 Hz, 1 H), 1.05 (s, 9 H), 0.99 (s, 9 H), 0.27 (s, 6 H), 0.24 (s, 6 H); ^{13}C NMR δ 190.1, 149.9, 149.4, 130.3, 128.0, 126.0, 119.0, 26.3 (3 C), 26.2 (3 C), 19.0, -3.2, -3.4; HRMS calcd for $C_{19}H_{34}ClO_3Si_2$ ($M+H^+$) 401.1735, found 401.1747.

3,4-Bis(*tert*-butyldimethylsilyloxy)-5-chlorophenyl formate (25)[26]

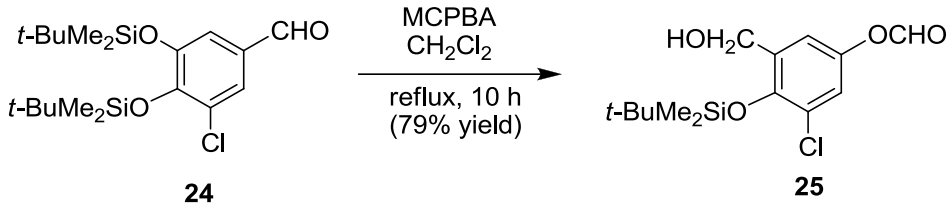

24 **25**

To a solution of 1.01g (5.43 mmol) of **24** in 20 mL of dry CH_2Cl_2 was added 1.6 g (6.45 mmol) of *m*-chloroperoxybenzoic acid (70% pure) and refluxed at 50^{o}C for 10 hours. The reaction mixture was diluted with 500 mL of diethyl ether, washed with 100 mL of aq. $NaHCO_3$, 100 mL of water and 100 mL of brine. The organic layer was dried over anhydrous $MgSO_4$, concentrated, and column chromatographed on silica gel using a mixture of diethyl ether and hexane (10:1) as an eluent to give 1.42 g of **25**[26] in 79% yield . ^{1}H NMR *δ* 8.22 (s, 1 H, OCHO), 6.79 (d, *J* = 3.2 Hz, 1 H), 6.58 (d, *J* = 3.2 Hz, 1 H), 1.03 (s, 9 H, *t*-Bu), 0.96 (s, 9 H, *t*-Bu), 0.22 (s, 6 H, Me), 0.19 (s, 6 H, Me); ^{13}C NMR *δ* 159.0 (CHO), 148.8, 143.0, 142.4, 127.1, 115.5, 113.1, 26.2 (6 C, *t*-Bu), 18.8 (2 C, *t*-Bu), -3.3 (2 C, Me), -3.6 (2 C, Me).

3,4-Bis(*tert*-butyldimethylsilyloxy)-5-chlorophenol (26)[26]

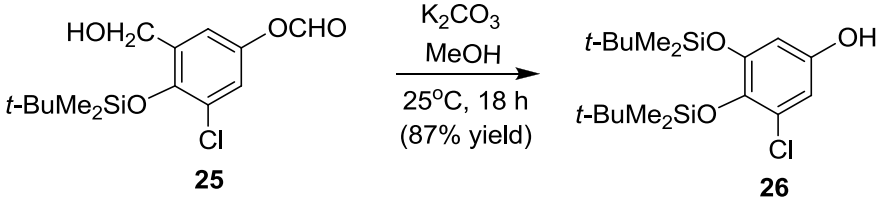

25 **26**

To a solution of 1.24 g (3 mmol) of **25** in 30 mL of methanol, was added 2.21 g (15 mmol) of K_2CO_3 and stirred at room temperature for 12 h. The reaction was diluted with 70 mL

ethyl acetate and washed with 20 mL of aq. NH_4Cl followed by 20 mL of brine. The organic layer was dried over anhydrous $MgSO_4$ and concentrated to give 0.6 g of **26**[26] which was used in the next step without further purification. ^{1}H NMR δ 6.47 (d, J = 2.9 Hz, 1 H), 6.30 (d, J = 2.9 Hz, 1 H), 1.02 (s, 9 H, *t*-Bu), 0.97 (s, 9 H, *t*-Bu), 0.22 (s, 6 H, Me), 0.17 (s, 6 H, Me); ^{13}C NMR δ 149.7, 148.9, 137.7, 126.9, 109.8, 107.8, 26.3 (3 C), 26.2 (3 C), -3.6 (2C, Me), -3.4 (2 C, Me).

2-Bromo-4,5-bis(*tert*-butyldimethylsilyloxy)-3-chlorophenol (27)[26]

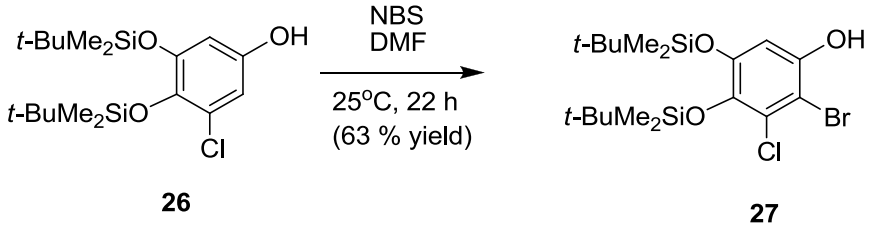

26 **27**

To a solution of 0.42 g (1.08 mmol) of **26** in 8 mL of dry DMF under argon at 25°C, was added 0.19 g (1.08 mmol) of *N*-bromosuccinimide and stirred at 25 °C for 22 hours. The reaction was diluted with 50 mL of ethyl acetate and washed twice with 15 mL of water followed by 15 mL of brine. The organic layer was dried over anhydrous $MgSO_4$, concentrated, and column chromatographed using a gradient mixture of hexane and diethyl ether as an eluent to give 0.18 g of **27**[26] in 63% yield; based on the recovery of 0.18 g of starting material **26**. ^{1}H NMR δ 6.65 (s, Ar, 1 H), 5.27 (s, OH), 1.03 (s, *t*-Bu, 9 H), 0.97 (s, *t*-Bu, 9 H), 0.23 (s, CH_3, 6 H), 0.17 (s, CH_3, 6 H); ^{13}C NMR δ 148.3, 147.4, 138.8, 127.0, 106.9, 102.9, 26.2 (*t*-Bu), 18.8, -3.3 (Me), -3.5 (Me).

2-Bromo-4,5-bis-(*tert*-butyldimethylsilyloxy)-3-chloro-1-methoxybenzene (28)

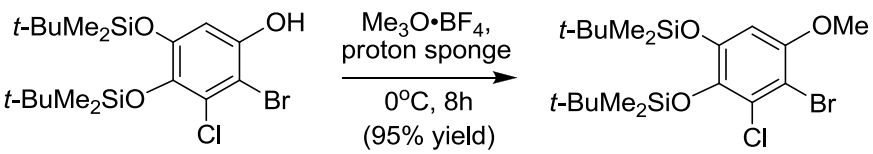

27 **28**

To a solution of 0.10 g (0.21 mmol) of **27** in 2 mL of dichloromethane at 0°C and under argon, were added 55 mg (0.26 mmol) of proton sponge and 38 mg (0.26 mmol) of trimethyloxonium tetrafluoroborate, and the mixture was stirred at 0°C for 8 h. The reaction was diluted with 15 mL of water and extracted twice with 50 mL of diethyl ether. The organic layer was washed with 10 mL of water followed by 10 mL of brine, dried over anhydrous $MgSO_4$, concentrated, and column chromatographed on silica gel using a mixture of hexane and diethyl ether (10:1) as eluent to give 67 mg of **28** in 95% yield; based on the recovery of 31 mg of compound **27**. ^{1}H NMR δ 6.43 (s, 1 H), 3.80 (s, 3 H), 1.03 (s, 9 H), 0.98 (s, 9 H), 0.23 (s, 6 H), 0.17 (s, 6 H); ^{13}C NMR δ 151.0, 147.5, 138.9, 128.9, 104.7, 104.5, 56.9, 26.3 (6 C), 18.9, 18.8, -3.3 (2 C), -3.5 (2 C); HRMS calcd for $C_{19}H_{35}BrClO_3Si_2$ ($M+H^+$) 481.0996, found 481.0951.

4-Bromo-3-chloro-5-methoxybenzene-1,2-diol (3)

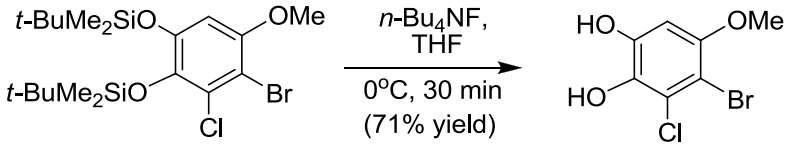

28 **3**

To a solution of 51 mg (0.10 mmol) of **28** in 2 mL of THF at 0°C under argon, was added 0.20 mL (0.20 mmol) of *n*-Bu_4NF, and the solution was stirred for 30 min. The reaction was diluted with 100 mL of diethyl ether, washed with 10 mL of water followed by 10 mL of brine, dried over anhydrous $MgSO_4$, concentrated, and column chromatographed on silica gel using a gradient mixture of dichloromethane and methanol as an eluent to give 19 mg of **3** in 71% yield. IR (neat) υ 3436, 3219 (broad & s), 2917, 2851, 1580, 1462, 1417, 1315, 1188, 1070, 984, 820

cm^{-1}; ^{1}H NMR δ 6.59 (s, 1 H), 5.60 (bs, 1 H, OH), 5.24 (bs, 1 H, OH), 3.83 (s, 3 H); ^{13}C NMR δ 151.4, 144.4, 134.2, 121.8, 101.7, 99.7, 57.1; HRMS calcd. for C7H7BrClO3 $C_7H_7BrClO_3$ ($M+H^+$) 252.9267, found 252.9254.

3-(*tert*-Butyldimethylsilyloxy)-5-chloro-4-hydroxybenzaldehyde (29)

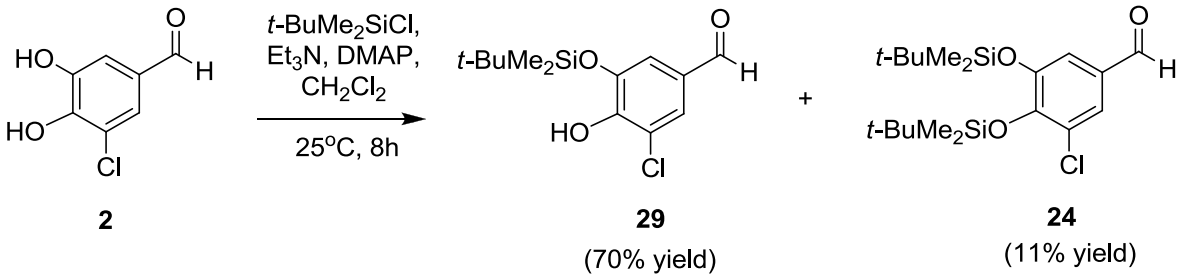

To a solution of 3.2 g (19 mmol) of **2** in 60 mL of CH_2Cl_2 at 0°C under argon, were added 2.9 mL (22 mmol) of triethylamine, 0.45 g (3.7 mmol) of 4-dimethylaminopyridine, and 3.4 g (22 mmol) of *tert*-butyldimethylsilyl chloride and the solution was stirred at 25°C for 8 h. The reaction was diluted with 500 mL of diethyl ether and washed with 50 mL water and 50 mL of brine. The organic layer was dried over anhydrous $MgSO_4$, concentrated, and column chromatographed on silica gel using hexane and dichloromethane (1:1) as an eluent to give 3.7 g of **29** and 0.84 g of **24** in 70% and 11% yield, respectively. Compound **29** was crystallized from diethyl ether to provide single crystals and its structure was unequivocally identified by a single-crystal X-ray analysis (**Figure 1.5**). **Compound 29:** ^{1}H NMR δ 9.76 (s, 1H, CHO), 7.51 (d, J = 2.8 Hz, 1 H), 7.27 (d, J = 2.8 Hz, 1 H), 6.24 (s, 1 H, OH), 1.03 (s, 9 H), 0.32 (s, 6 H); ^{13}C NMR δ 189.9, 149.9, 144.2, 129.4, 126.8, 120.7, 115.9, 25.8, 18.4, -4.2; HRMS calcd for $C_{13}H_{20}ClO_3Si$ ($M+H^+$) 287.0870, found 287.0858. **Compound 24:** ^{1}H NMR δ 9.78 (s, 1 H), 7.50 (d, J = 2 Hz, 1 H), 7.29 (d, J = 2 Hz, 1 H), 1.05 (s, 9 H), 0.99 (s, 9 H), 0.27 (s, 6 H), 0.24 (s, 6 H); ^{13}C NMR δ 190.1, 149.9, 149.4, 130.3, 128.0, 126.0, 119.0, 26.3 (3 C), 26.2 (3 C), 19.0, -3.2, -3.4; HRMS calcd for $C_{19}H_{34}ClO_3Si_2$ ($M+H^+$) 401.1735, found 401.1747.

3-(*tert*-Butyldimethylsilyloxy)-5-chloro-4-methoxybenzaldehyde (30)

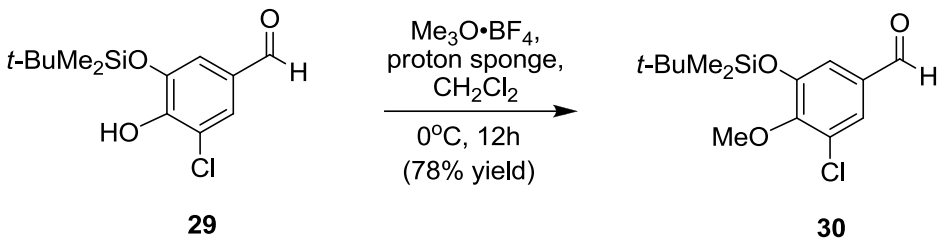

29 **30**

To a solution of 0.45 g (1.57 mmol) of **29** in 10 mL of dichloromethane at 0°C under argon, were added 0.67 g (3.14 mmol) of proton sponge and 0.47 g (3.14 mmol) of trimethyloxonium tetrafluoroborate, and stirred at 0°C for 12 hours. The reaction mixture was diluted with 200 mL of diethyl ether and washed with 30 mL of aqueous NH_4Cl solution, 30 mL of water, and 30 mL of brine. The organic layer was dried over anhydrous $MgSO_4$, concentrated, and column chromatographed on silica gel using a mixture of hexane and diethyl ether (10:1) as an eluent to give 0.20 g of **30** in 78% yield; based on the recovery of 0.21 g of **29** : ^{1}H NMR δ 9.83 (s, 1H, CHO), 7.54 (d, *J* = 1.8 Hz, 1 H), 7.28 (d, *J* = 1.8 Hz, 1 H), 3.91 (s, 3 H), 1.03 (s, 9 H), 0.23 (s, 6 H); ^{13}C NMR δ 190.1, 153.4, 150.9, 132.8, 129.8, 125.5, 119.9, 60.7, 25.8, 18.4, -4.4; HRMS calcd for $C_{14}H_{22}ClO_3Si$ ($M+H^+$) 301.1027, found 301.1421; negative ion detection mode: $C_{14}H_{20}ClO_3Si$ (M-H) 299.0870, found 298.9978.

3-(*tert*-Butyldimethylsilyloxy)-5-chloro-4-methoxyphenyl formate (31) & 3-(*tert*-butyldimethylsilyloxy)-5-chloro-4-methoxyphenol (32)

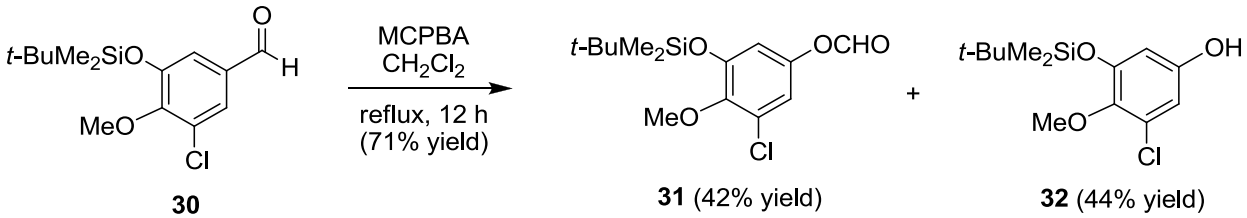

30 **31** (42% yield) **32** (44% yield)

To a solution of 0.13 g (0.432 mmol) of **30** in 2 mL of dichloromethane at 0 ^{o}C and under argon, was added 0.16 g (70% pure; 0.648 mmol) of *m*-chloroperbenzoic acid, and the solution was refluxed for 12 hours. The reaction solution was diluted with 5 mL of aqueous sodium thiosulfate and 200 mL of diethyl ether. The solution was washed with 20 mL water followed by 20 mL of brine. The organic layer was dried over anhydrous $MgSO_4$, concentrated, and column chromatographed on silica gel using a mixture of hexane and diethyl ether (10:1) as an eluent to give 58 mg of **31** and 55 mg of hydrolyzed product **32** in 42% and 44% yield, respectively. **Compound 31**:^{1}H NMR δ 8.23 (s, 1 H, OCHO), 6.83 (d, *J* = 2.6 Hz, 1 H), 6.59 (d, *J* = 2.6 Hz, 1 H), 3.81 (s, 3 H), 1.01 (s, 9 H), 0.21 (s, 6 H); ^{13}C NMR δ 158.9, 150.7, 146.6, 145.4, 129.1, 115.8, 113.6, 60.7, 25.8 (3 C), 18.4, -4.5; HRMS calcd for $C_{14}H_{22}ClO_4Si$ ($M+H^+$) 317.0976, found 317.1355. **Compound 32:** ^{1}H NMR δ 6.48 (d, *J* = 2.6 Hz, 1 H), 6.29 (d, *J* = 2.6 Hz, 1 H), 3.75 (s, 3 H), 1.01 (s, 9 H), 0.20 (s, 6 H); ^{13}C NMR δ 152.0, 150.7, 142.6, 128.1, 110.8, 108.6, 60.7, 25.8 (3 C), 18.4, -4.5; HRMS calcd for $C_{13}H_{22}ClO_3Si$ ($M+H^+$) 289.1027, found 289.1041.

Conversion of formate 31 to phenol 32

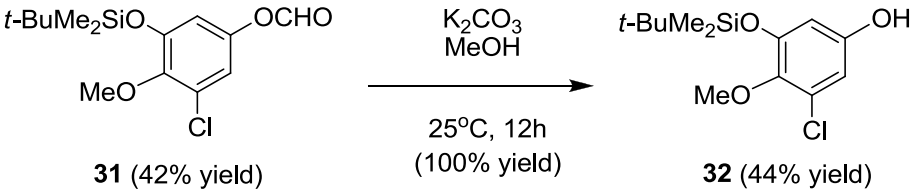

31 (42% yield) **32** (44% yield)

A solution of 55 mg (0.18 mmol) of compound **31** and 0.13 g (0.91 mmol) of K_2CO_3 in 1 mL of methanol was stirred at 25^{o}C for 12 h. The reaction was diluted with 10 mL of water and 30 mL of ethyl acetate and the solution washed with 5 mL of aqueous NH_4Cl solution, 5 mL of water, and 5 mL of brine. The organic layer was dried over anhydrous $MgSO_4$, concentrated, and column chromatographed on silica gel using a mixture of hexane and diethyl ether (10: 1) as an eluent to give 50 mg of compound **32** in quantitative yield, which ^{1}H NMR spectrum is identical to that described above.

2-Bromo-5-(*tert*-butyldimethylsilyloxy)-3-chloro-4-methoxyphenol (33)

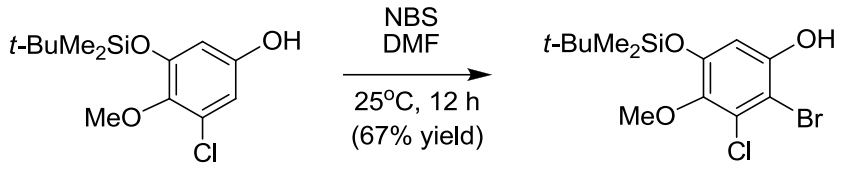

32 **33**

To a solution of 75 mg (0.26 mmol) of **32** in 2 mL of dimethylformamide (DMF) under argon, was added 51 mg (0.28 mmol) of *N*-bromosuccinimide and the solution was stirred at 25°C for 12 h. The reaction mixture was diluted with 100 mL of diethyl ether, washed with 10 mL of water followed by 10 mL of brine, and the organic layer was dried over anhydrous $MgSO_4$. The solvent was evaporated and the crude product was column chromatographed on silica gel using a mixture of hexane and diethyl ether (10:1) as an eluent to give 64 mg of **33** in 67% yield: Mp. 44 – 45°C; ^{1}H NMR δ 6.55 (s, 1 H), 5.42 (s, 1 H, OH), 3.77 (s, 3 H), 1.01 (s, 9 H), 0.20 (s, 6 H); ^{13}C NMR δ 150.2, 149.6, 143.1, 124.2, 107.2, 103.0, 60.8, 25.8 (3 C), 18.5, -4.5; HRMS calcd for $C_{13}H_{21}BrClO_3Si$ ($M+H^+$) 367.0132, found 367.0142.

4-Bromo-5-chloro-6-methoxybenzene-1,3-diol (5)

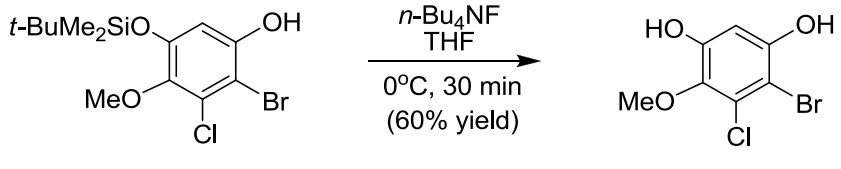

33 **5**

To a solution of 40 mg (0.108 mmol) of **33** in 2 mL of dry THF under argon at 0°C, was added 120 µL (0.12 mmol) of *n*-Bu_4NF (1 M solution in THF) and the solution was stirred at 0°C for 30 min. The reaction was diluted with 70 mL of diethyl ether, washed with 10 mL of water followed by 10 mL of brine, and the organic layer was dried over anhydrous $MgSO_4$. The solvent was concentrated and the crude product was column chromatographed on silica gel using a mixture of ethyl acetate and hexane (2:1) as an eluent to give 15 mg of **5** in 60% yield. IR

(neat) υ 3321 (bs), 3260, 2917, 1589, 1421, 1241, 984, 800; ^{1}H NMR δ 6.65 (s, 1 H), 3.87 (s, 3 H); ^{13}C NMR δ 150.5, 150.0, 138.7, 127.5, 101.8, 101.7, 61.5; HRMS calcd for $C_7H_7BrClO_3$ ($M+H^+$) 252.9267, found 252.9279.

2-Bromo-3-chloro-4,5-dibenzyloxyphenol (35)

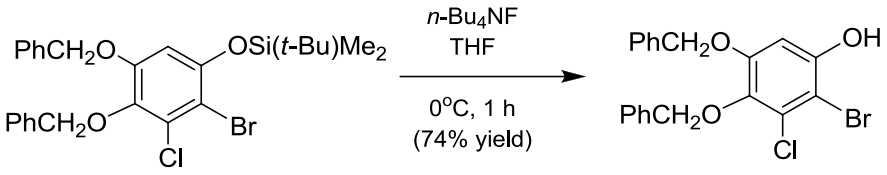

34 **35**

To a solution of 0.10 g (0.188 mmol) of **34**[26] in 3 mL of tetrahydrofuran (THF) at 0°C, was added 210 µL of *n*-Bu_4NF (1 M in THF) and stirred under argon at 0°C for 30 minutes. The solution was diluted with 100 mL of diethyl ether, washed with 10 mL of water followed by 10 mL of brine, and the organic layer was dried over anhydrous $MgSO_4$. The dry organic layer was concentrated and the crude product was column chromatographed on silica gel using a mixture of hexane and diethyl ether (10:1) as an eluent to give 56 mg of **35** as white solids in 74% yield. Mp.= 108 – 110 °C; ^{1}H NMR δ 7.40 - 7.20 (m, 10 H), 6.66 (s, 1 H), 5.07 (s, 2 H), 4.96 (s, 2 H); ^{13}C NMR δ 153.1, 149.9, 139.8, 137.0, 136.1, 129.2, 128.8, 128.5, 128.44, 128.40, 127.6, 102, 100.6, 75.4, 71.3; HRMS calcd for $C_{20}H_{17}BrClO_3$ ($M+H^+$) 419.0044, found 419.0051.

5-Bromo-6-chlorobenzene-1,2,4-triol (6)

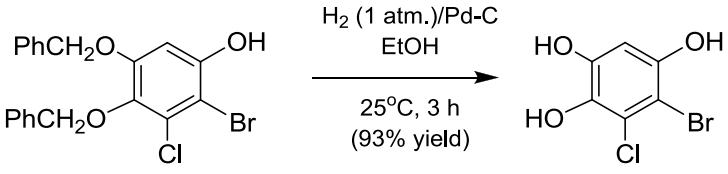

35 **6**

To a solution of 25 mg (0.06 mmol) of **35** in 1 mL of ethanol, was added 2.5 mg of 10% palladium/carbon and was stirred under 1 atmosphere of hydrogen (a balloon filled with

hydrogen was connected to the round bottom flask) at 25°C for 3 h. The reaction mixture was filtered through Celite and concentrated to dryness to give 13 mg of **6** in 93% yield. The triol **6** was stored in a dry box under nitrogen atmosphere: Mp. >350 °C; IR (neat) υ 3382 (bs, OH stretch), 2932, 2843, 1614, 1437, 1285, 1170, 1070 cm^{-1}; UV (in methanol) λ 209.6 (ε_{max} = 30300), 291.8 (1250; likely derived from a partial oxidation of the polyphenol functions), 332.5 (4640), 397.1 (1785) nm; ^1H NMR (CD_3OD) δ 6.66 (s, 1 H, Ar), 5.58 (bs, 1 H, OH), 5.27 (bs, 1 H, OH), 5.21 (bs, 1 H, OH); ^{13}C NMR (CD_3OD) δ 149.4, 147.6, 137.4, 123.1, 103.2, 100.6; HRMS calcd for $C_6H_5BrClO_3$ ($M+H^+$) 238.9105, found 238.9111.

2-Amino-4-(hydroxymethyl)phenol (7)[23] & 2-amino-4-methylphenol (8)[24]

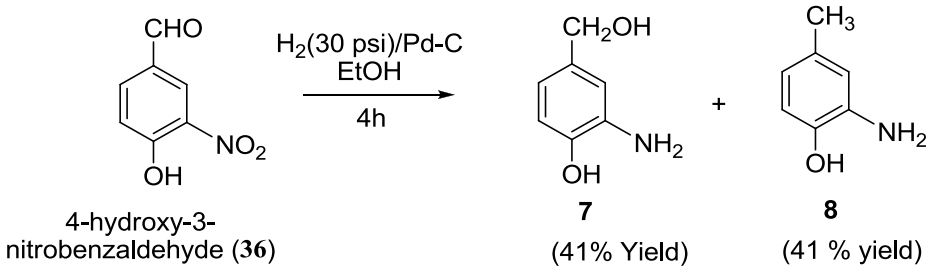

4-hydroxy-3-nitrobenzaldehyde (**36**)

7 (41% Yield)

8 (41 % yield)

To a solution of 0.30 g (1.8 mmol) of **36** in 30 mL of ethanol was added 0.15 g of 10% palladium over carbon and shaken on a hydrogenator under 30 psi atmosphere of hydrogen for 4 h. The reaction mixture was filtered through Celite, and the Celite was carefully rinsed with 30 mL ethyl acetate. The filtrate was concentrated and the crude was column chromatographed on silica gel using a mixture of dichloromethane and methanol (9:1) as eluent to give 0.1 g of **7**[23] and 91 mg of **8**[24], both in 41% yield. **Compound 7**: IR (neat) υ 3387 (sharp, m), 3313 (sharp, m), 3047 (broad), 2802, 1605, 1515, 1454, 1364, 1286, 1221, 1155, 1008, 816 cm^{-1}; ^1H NMR (D_2O) δ 6.88 (d, *J* = 1.2 Hz, 1 H), 6.85 (d, *J* = 8 Hz, 1 H), 6.77 (dd, *J* = 8, 1.2 Hz, 1 H), 4.49 (s, 2 H); ^{13}C NMR (DMSO-d_6) δ 144.9, 136.1, 133.4, 114.9, 113.8, 113.4, 63.3.**Compound 8:** IR (neat) υ 3370 (sharp, m), 3301 (sharp, m), 2921, 1601, 1519, 1458, 1388, 1286, 878, 800 cm^{-1}; ^1H NMR δ 6.62 (d, *J* = 7.6 Hz, 1 H), 6.58 (d, *J* = 1.6 Hz, 1 H), 6.48 (dd, *J* = 7.6, 1.6 Hz, 1 H), 2.21 (s, 3 H); ^{13}C NMR δ 141.9, 134.4, 131.2, 120.0, 118.1, 115.4, 20.9.

1-(3,5-Di-*tert*-butyl-4-hydroxyphenyl)-2-methylpropan-1-one (10)[30]

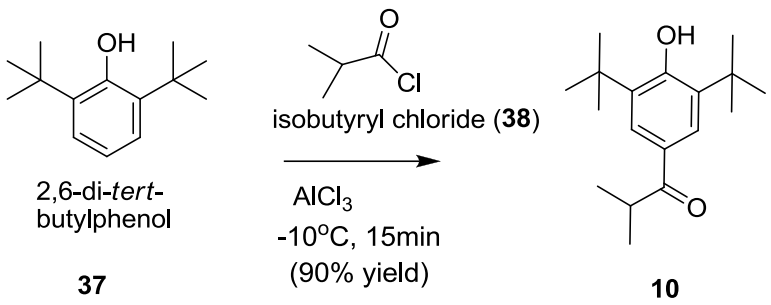

To 1 g (7.5 mmol) of anhydrous $AlCl_3$ under argon was added 1mL (9.5 mmol) of isobutyryl chloride (**38**) at -10°C followed by 1.2 g (5.8 mmol) of 2,6-di-*tert*-butylphenol (**37**). To the reaction mixture, 1 mL (9.5 mmol) of isobutyryl chloride was again added and shaken vigorously for 15 minutes till light pink paste was formed. The reaction was quenched with 50 mL of ice cold water and extracted thrice with 50 mL of ethyl ether. The combined organic layers were washed with 20 mL brine, dried over anhydrous $MgSO_4$ and concentrated to give 1.4208 g of (**10**)[30] in 90% yield. Thin layer chromatography (TLC) and NMR analysis indicated that the compound was pure and was used in the next step without further purification. ^{1}H NMR δ 7.89 (S, Ar, 2 H), 5.71 (s, OH, 1 H), 3.55 (m, 1 H), 1.48 (s, *t*-Bu, 18 H), 1.25 (d, J = 6.6 Hz, CH_3, 6 H); ^{13}C NMR δ 204.1, 158.4, 135.9, 127.9, 126.2, 34.91, 34.6, 30.3, 19.7.

2-Bromo-1-(3,5-di-*tert*-butyl-4-hydroxyphenyl)-2-methylpropan-1-one (11)[31]

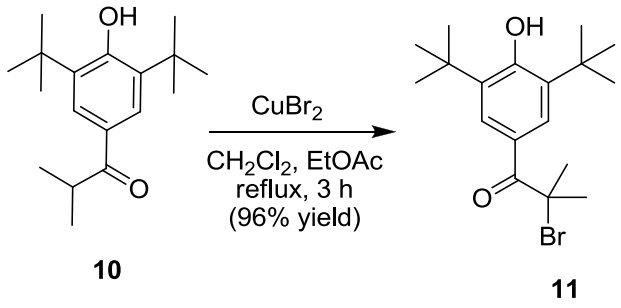

To a solution of 0.19 g (0.69 mmol) of **10** in a mixture of 0.5 mL of dry CH_2Cl_2 and 1 mL of dry ethyl acetate under argon, was added 0.37 g (1.68 mmol) of cupric bromide and heated to

reflux for 3 hours at 70°C. The reaction was filtered and concentrated to give 0.23 g of (**11**)[31] as yellow colored solid in 96% yield. Thin layer chromatography (TLC) and NMR analysis indicated that the compound was pure and was used in the next step without further purification. ^{1}H NMR δ 8.17 (s, Ar, 2 H), 5.75 (s, OH, 1 H), 2.06 (s, CH_3, 6 H), 1.48 (s, *t*-Bu, 18 H); ^{13}C NMR δ 195.7 (C=O), 158.2, 135.6, 128.8, 125.6, 60.6, 34.7, 32.4, 30.4.

2,6-Di-*tert*-butyl-4-(1-hydroxy-2-methylpropan-2-yl)phenol (12)[31]

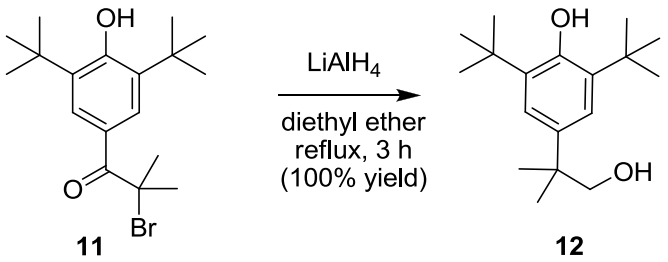

11 **12**

To a solution of 0.23 g (0.65 mmol) of **11** in 3 mL of dry ethyl ether at 0°C under argon, was added 55 mg (1.46 mmol) of $LiAlH_4$ on vigorous stirring and refluxed at 55°C for 3 hours. The reaction was carefully quenched by the addition of 20 mL of water followed by the addition of 2 mL of 1M H_2SO_4. The reaction was then extracted with 100 mL of diethyl ether. The organic layer was washed with 20 mL of brine, dried over anhydrous $MgSO_4$, and solvent evaporated to give 180 mg of **12**[47] as white solid in quantitative yield. Thin layer chromatography (TLC) and NMR analysis indicated that the compound was pure and was used in the next step without further purification. ^{1}H NMR δ 7.19 (s, Ar, 2 H), 5.13 (s, Ar-OH, 1 H), 3.57 (d, J = 6.6 Hz, 2 H), 1.45 (s, *t*-Bu, 18 H), 1.33 (s, CH_3, 6H); ^{13}C NMR δ 152.2, 136.4, 135.6, 123.0, 73.6, 40.1, 34.8, 30.5, 25.7.

2-(3,5-Di-*tert*-butyl-4-hydroxyphenyl)-2-methylpropanal (13)

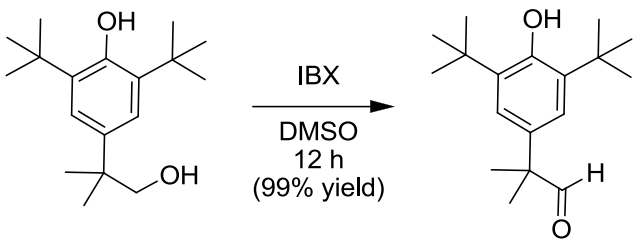

12 **13**

To a solution of 0.17 g (0.61 mmol) of **12** in 3 mL of dimethyl sulfoxide (DMSO), was added 0.21 g (0.73 mmol) of *o*-iodoxybenzoic acid (IBX) and stirred under argon at 25 ^{o}C for 12 h. The reaction was diluted with 200 mL of CH_2Cl_2, washed with 30 mL of water followed by 30 mL of brine, dried over anhydrous $MgSO_4$, and concentrated to give 0.17 g of **13** in quantitative yield. Thin layer chromatography (TLC) and NMR analysis indicated that the compound was pure and was used in the next step without further purification. IR (neat) υ 3603 (OH), 2952, 2900, 2700 (C-H aldehyde), 1714 (C=O aldehyde), 1435, 1360, 1230, 1141, 1120, 903, 826, 744; ^{1}H NMR δ 9.45 (s, 1 H, CHO), 7.06 (s, 2 H, Ar), 5.22 (s, 1 H, OH), 1.44 (s, 24 H, Me); ^{13}C NMR δ 202.8 (C=O), 153.1, 136.2 (2 C), 131.4, 123.6 (2 C), 50.4, 34.8, 30.4 (*t*-Bu), 22.7; MS negative mode: m/z 275.6 (M-1); positive mode: m/z 299.4 ($M+Na^{+}$).

2-(3,5-Di-*tert*-butyl-4-hydroxyphenyl)-2-methylpropanal oxime (15)

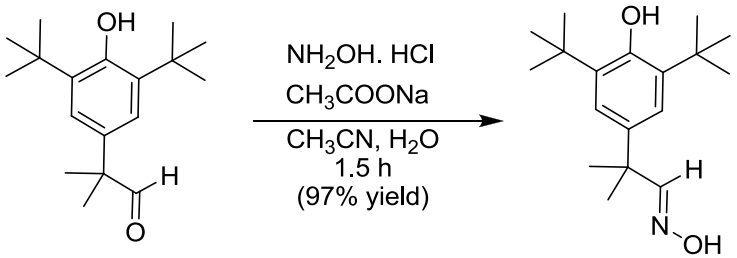

13 **15**

To a solution of 40 mg (0.14 mmol) of **13** in 3 mL of acetonitrile and water (2:1), were added 25 mg (0.35 mmol) of NH_2OH•HCl and 60 mg (0.43 mmol) of sodium acetate, and the

solution was stirred at 25°C for 1.5 h. The reaction mixture was concentrated, diluted with 20 mL of water, and extracted three times with diethyl ether (60 mL total). The combined extract was concentrated to give 41 mg of **15** in 97% yield. Thin layer chromatography (TLC) and NMR analysis indicated that the compound was pure. ^{1}H NMR δ 7.49 (s, 1 H, CH=N), 7.12 (s, 2 H, Ar), 1.47 (s, 6 H, Me), 1.44 (s, 18 H, *t*-Bu); ^{13}C NMR δ 158.7 (C=N), 152.5, 135.9, 135.7, 122.9 (2 C), 41.0, 34.7, 30.5 (6 C), 26.9; MS m/z 314 ($M+Na^{+}$).

4-[(2-Benzylamino)-1,1-dimethylethyl]-2,6-di-*tert*-butylphenol (16)

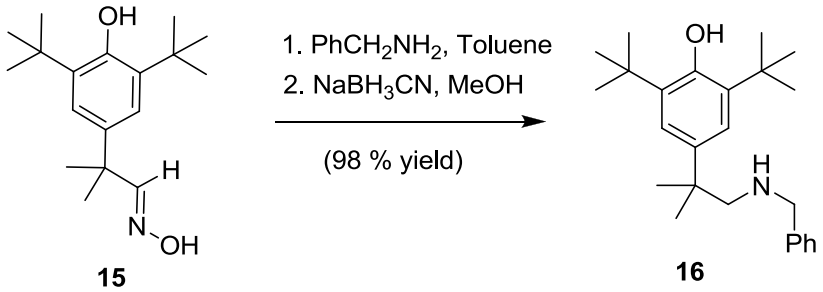

15 **16**

To a solution of 50 mg (0.18 mmol) of **15** in 3 mL of toluene was added 19 µL (0.18 mmol) of benzylamine and heated to reflux using a Diel's Stark apparatus for 12 h. Toluene was evaporated under rotovapor, the crude was dissolved in 2 mL of methanol, and 18 mg (0.29 mmol) of $NaCNBH_3$ was added. The resulting solution was stirred for 2 h, diluted with 20 mL of water, and extracted twice with ethyl acetate (100 mL total). The combined extract was washed with 10 mL of water and 10 mL of brine, dried over anhydrous $MgSO_4$, and concentrated to give 68 mg of **16** in 98% yield. Thin layer chromatography (TLC) and NMR analysis indicated that the compound was pure. ^{1}H NMR δ 7.35 – 7.18 (m, 5 H, Ph), 7.13 (s, 2 H, Ar), 5.08 (broad s, 1 H), 3.72 (s, 2 H, CH_2N), 2.68 (s, 2 H, CH_2N), 1.43 (s, 18 H, *t*-Bu), 1.33 (s, 6 H, Me); ^{13}C NMR δ 151.92, 140.4, 137.8, 135.4, 128.5, 128.1, 127.0, 122.7, 61.5, 54.2, 38.6, 34.7, 30.6, 27.9; MS m/z 368.5 (M+1).

2,4-Di-*tert*-butyl-6-(3-methyl-2-butenyl)phenol (17) and 6,8-di-*tert*-butyl-2,2-dimethyl-3,4-dihydro-2H-chromene (18)

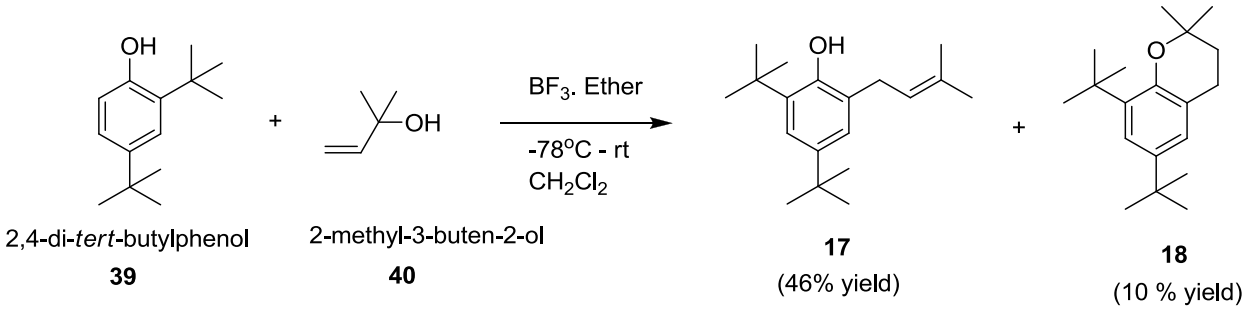

2,4-di-*tert*-butylphenol **39**

2-methyl-3-buten-2-ol **40**

17 (46% yield)

18 (10 % yield)

To a solution of 0.20 g (1.44 mmol) of **40** in 3 mL of dichloromethane at -78°C under argon, were added 0.18 mL (1.44 mmol) of BF_3•ether followed by 0.21 g (0.96 mmol) of **39**. The solution was warmed to 25 °C and stirred for 1 h. The reaction mixture was diluted with 200 mL of diethyl ether, washed with 20 mL of aqueous $NaHCO_3$ followed by 20 mL of brine, the organic layer was dried over anhydrous Na_2SO_4, concentrated, and column chromatographed on silica gel using 1% diethyl ether in hexane as eluent to give 0.12 g of **17** and 26 mg of **18** in 46% and 10% yield, respectively. **Compound 17**: ^{1}H NMR δ 7.22 (d, J = 3 Hz, 1 H, Ar), 6.99 (d, J = 3 Hz, 1 H, Ar), 5.34 (t,hept, J = 7, 1 Hz, 1 H, =CH), 3.37 (d, J = 7 Hz, 2 H, CH_2), 1.85 (s, 3 H, Me), 1.80 (s, 3 H, Me), 1.43 (s, 9 H, t-Bu), 1.31 (s, 9 H, *t*-Bu); ^{13}C NMR δ 151.5, 142.3, 135.9, 135.7, 126.0, 125.0, 122.6, 122.3, 35.1, 34.4, 31.9 (3 C), 31.7, 30.0 (3C), 26.0, 18.2; MS negative mode: m/z 273.8 (M-1). **Compound 18**: ^{1}H NMR δ 7.14 (d, J = 3 Hz, 1 H, Ar), 6.93 (d, J = 3 Hz, 1 H, Ar), 2.79 (t, J = 7 Hz, 2 H, CH_2), 1.79 (t, J = 7 Hz, 2 H, CH_2), 1.39 (s, 9 H, *t*-Bu), 1.36 (s, 6 H, Me), 1.30 (s, 9 H, *t*-Bu); ^{13}C NMR δ 150.3, 141.0, 136.9, 124.2, 121.8, 119.9, 73.9, 35.2, 34.3, 33.0, 31.9, 30.0, 27.3, 23.5; MS positive mode: m/z 275.2 (M+1).

1.6 References

1. Becker, N.; Petric, D.; Zgomba, M.; Boase, C.; Madon, M.; Dahl, C.; Kaiser, A. In *Mosquitoes and their control*; Second ed.; Springer: **2010**, p v.

2. Kunamneni, A.; Plou, F. J.; Ballesteros, A.; Alcalde, M. Laccases and their applications: a patent review. *Recent Pat. Biotechnol.* **2008**, *2*, 10-24.

3. Piontek, K.; Antorini, M.; Choinowski, T. Crystal structure of a laccase from the fungus *Trametes versicolor* at 1.90 Å resolution containing a full complement of coppers. *Journal of Biological Chemistry* **2002**, *277*, 37663-37669.

4. Mayer, A. M.; Staples, R. C. Laccase: new functions for an old enzyme. *Phytochemistry* **2002**, *60*, 551-565.

5. Thurston, C. F. The structure and function of fungal laccases. *Microbiology (Reading, U. K.)* **1994**, *140*, 19-26.

6. Geiger, J. P.; Nicole, M.; Nandris, D.; Rio, B. Root-rot diseases of *Havea brasiliensis*. I. Physiological and biochemical aspects of host aggression. *Eur. J. Forest Pathol.* **1986**, *16*, 22-37.

7. Dittmer, N. T.; Suderman, R. J.; Jiang, H.; Zhu, Y.-C.; Gorman, M. J.; Kramer, K. J.; Kanost, M. R. Characterization of cDNAs encoding putative laccase-like multicopper oxidases and developmental expression in the tobacco hornworm, *Manduca sexta*, and the malaria mosquito, *Anopheles gambiae*. *Insect Biochem. Mol. Biol.* **2004**, *34*, 29-41.

8. Kramer, K. J.; Kanost, M. R.; Hopkins, T. L.; Jiang, H.; Zhu, Y. C.; Xu, R.; Kerwin, J. L.; Turecek, F. Oxidative conjugation of catechols with proteins in insect skeletal systems. *Tetrahedron* **2001**, *57*, 385-392.

9. Arakane, Y.; Muthukrishnan, S.; Beeman, R. W.; Kanost, M. R.; Kramer, K. J. Laccase 2 is the phenol oxidase gene required for beetle cuticle tanning. *Proc. Natl. Acad. Sci. U. S. A.* **2005**, *102*, 11337-11342.

10. Piontek, K.; Antorini, M.; Choinowski, T. Crystal structure of a laccase from the fungus *Trametes versicolor* at 1.90 Å resolution containing a full complement of coppers. *Journal of Biological Chemistry* **2002**, *277*, 37663-37669.

11. Xu, F.; Deussen, H.-J. W.; Lopez, B.; Lam, L.; Li, K. Enzymatic and electrochemical oxidation of *N*-hydroxy compounds. Redox potential, electron-transfer kinetics, and radical stability. *Eur. J. Biochem.* **2001**, *268*, 4169-4176.

12. Baldrian, P. Fungal laccases - occurrence and properties. *FEMS Microbiol. Rev.* **2006**, *30*, 215-242.

13. Garzillo, A. M. V.; Colao, M. C.; Caruso, C.; Caporale, C.; Celletti, D.; Buonocore, V. Laccase from the white-rot fungus *Trametes trogii*. *Appl. Microbiol. Biotechnol.* **1998**, *49*, 545-551.

14. Johannes, C.; Majcherczyk, A. Laccase activity tests and laccase inhibitors. J. Biotech. 2000, 78, 193-199.

15. Paterson, R. R. M.; Meon, S.; Zainal Abidin, M. A.; Lima, N. Prospects for inhibition of lignin degrading enzymes to control Ganoderma white rot of oil palm. Curr. Enzyme Inhibition 2008, 4, 172-179.

16. Lyashenko, A. V.; Bento, I.; Zaitsev, V. N.; Zhukhlistova, N. E.; Zhukova, Y.; Gabdoulkhakov, A. G.; Morgunova, E. Y.; Voelter, W.; Kachalova, G. S.; Stepanova, E. V.; Koroleva, O. V.; Lamzin, V. S.; Tishkov, V. I.; Betzel, C.; Lindley, P. F.; Mikhailov, A. M. X-ray structural studies of the fungal laccase from Cerrena maxima. J. Biol. Inorg. Chem. 2006, 11, 963-973.

17. Messerschmidt, A. In *Multi-Copper Oxidases*; Messerschmidt, A., Ed.; World Scientific: Singapore, **1997**, p 23-80.

18. Solomon, E. I.; Augustine, A. J.; Yoon, J. O_2 reduction to H_2O by the multicopper oxidases. *Dalton Trans.* **2008**, *30*, 3921-3932.

19. Nation, J. L. In *Encyclopedia of Entamology*; Second ed.; Capinera, J. L., Ed.; Springer: **2008**, p 2015.

20. Arakane, Y., Lomakin, J., Beeman, R.W., Muthukrishnan, S., Gehrke, S.H., Kanost, M.R., Kramer, K.J., Molecular and functional analyses of amino acid decarboxylases involved in cuticle tanning in Tribolium castaneum. *J. Biol.Chem*. **2009**, 284, 16584-16594.

21. Quaratino, D.; Federici, F.; Petruccioli, M.; Fenice, M.; Fenice, A. D. A.; D'Annibale, A. Production, purification and partial characterisation of a novel laccase from the white-rot fungus *Panus tigrinus* CBS 577.79. *Antonie van Leeuwenhoek* **2007**, *91*, 57-69.

22. Touzeau, F.; Arrault, A.; Guillaumet, G.; Scalbert, E.; Pfeiffer, B.; Rettori, M.-C.; Renard, P.; Merour, J.-Y. Synthesis and biological evaluation of new 2-(4,5-dihydro-1*H*-imidazol-2-yl)-3,4-dihydro-2*H*-1,4-benzoxazine derivatives. *J. Med. Chem.* **2003**, *46*, 1962-1979.

23. Kikugawa, Y.; Tsuji, C.; Miyazawa, E.; Sakamoto, T. A new intramolecular migration of the imino group of *O*-aryl ketoximes to the aryl group under the Beckmann condition. *Tetrahedron Lett.* **2001**, *42*, 2337-2339.

24. Lyashenko, A. V.; Bento, I.; Zaitsev, V. N.; Zhukhlistova, N. E.; Zhukova, Y. N.; Gabdoulkhakov, A. G.; Morgunova, E. Y.; Voelter, W.; Kachalova, G. S.; Stepanova, E. V.; Koroleva, O. V.; Lamzin, V. S.; Tishkov, V. I.; Betzel, C.; Lindley, P. F.; Mikhailov, A. M. X-ray structural studies of the fungal laccase from *Cerrena maxima*. *J. Biol. Inorg. Chem.* **2006**, *11*, 963-973.

25. Giardina, P.; Faraco, V.; Pezzella, C.; Piscitelli, A.; Vanhulle, S.; Sannia, G. Laccases: a never-ending story. *Cell. Mol. Life Sci.* **2010**, *67*, 369-385.

26. Hua, D. H.; Huang, X.; Chen, Y.; Battina, S. K.; Tamura, M.; Noh, S. K.; Koo, S. I.; Namatame, I.; Tomoda, H.; Perchellet, E. M.; Perchellet, J.-P. Total syntheses of (+)-chloropuupehenone and (+)-chloropuupehenol and their analogues and evaluation of their bioactivities. *J. Org. Chem.* **2004**, *69*, 6065-6078.

27. Barakat, M. Z.; El-Wahab, M. F. A.; El-Sadr, M. M. Some reactions with *N*-bromosuccinimide. *J. Am. Chem. Soc.* **1955**, *77*, 1670-1672.

28. Ferrar, P. H.; Walker, J. R. L. Inhibition of diphenol oxidases: a comparative study. *Journal of Food Biochemistry* **1996**, *20*, 15-30.

29. Semensi, V.; Sugumaran, M. Effect of MON-0585 on sclerotization of *Aedes aegypti* cuticle. *Pestic. Biochem. Physiol.* **1986**, *26*, 220-230.

30. Suda, H.; Kanoh, S.; Hasegawa, H.; Motoi, M. Acylation of sterically hindered phenols in the presence of anhydrous aluminum chloride. *Kanazawa Daigaku Kogakubu Kiyo* **1982**, *15*, 71-74.

31. Schwartz, L. H.; Flor, R. V. Lithium aluminum hydride reduction of phenacyl halides. Aryl rearrangement pathway. *J. Org. Chem.* **1969**, *34*, 1499-1500.

32. Lai, J. T. Totally hindered phenols. 2,6-di-*tert*-butyl-4-(1,1-dialkyl-1-acetamide)phenols and their persistent phenoxy radicals. *Tetrahedron Lett.* **2001**, *42*, 557-560.

33. Prasain, K.; Nguyen, T. D. T.; Gorman, M. J.; Barrigan, L. M.; Peng, Z.; Kanost, M. R.; Syed, L. U.; Li, J.; Zhu, K. Y.; Hua, D. H. Redox potentials, laccase oxidation, and antilarval activities of substituted phenols. *Bioorganic & Medicinal Chemistry* **2012**, *20*, 1679-1689.

34. Xu, F. Oxidation of phenols, anilines, and benzenethiols by fungal laccases: Correlation between activity and redox potentials as well as halide inhibition. *Biochemistry* **1996**, *35*, 7608-7614.

35. Xu, F.; Shin, W.; Brown, S. H.; Wahleithner, J. A.; Sundaram, U. M.; Solomon, E. I. A. Biochim. Biophys. Acta 1996, 1292, 303.

36. Tadesse, M. A.; D'Annibale, A.; Galli, C.; Gentili, P.; Sergi, F. Org. Biomol. Chem. 2008, 6, 868.

37. D'annibale, A.; Celletii, D.; Felici, M.; DiMattia, E.; Giovannozzi-Sermanni, G. Substrate specificity of laccase from *Lentinus edodes*. *Acta Biotechnol.* **1996**, *16*, 257-270.

38. Skvortsova, L. I.; Kiryushov, V. N.; Aleksandrova, T. P.; Karunina, O. V. Voltammetry determination of dihydroxybenzenes at a mechanically renewed electrode made from a graphite-epoxy composite. *Journal of Analytical Chemistry* **2008**, *63(3)*, 258-264.

39. Masagutov, R. M.; Tolstikov, G. A.; Kirichenko, G. N.; Grigor'eva, N. G.; Tsypysheva, L. G. *Neftekhimiya* **1985**, 25, 481. (synthesis MON)

40. Spafford, H.; Jardine, A.; Carver, S.; Tarala, K.; van Wees, M.; Weinstein, P. *J. Am. Mosquito Control Assoc.* **2007**, 23, 304.

41. Madhavi, V.; Lele, S. S. Laccase: Properties and applications. *BioResources* **2009**, *4*, 1694-1717.

42. Xu, F. Effect of redox potential and hydroxide inhibition on the pH activity profile of fungal laccases. *The Journal of Biological Chemistry* **1997**, *272*, 924-928.

43. Murao, S.; Hinode, Y.; Matsumura, E.; Numata, A.; Kawai, K.; Jin, H.; Oyama, H.; Shin, T. A novel laccase inhibitor, *N*-hydroxyglycine, produced by *Penicillium citrinum* YH-31. *Biosci. Biotech. Biochem.* **1992**, *56*, 987-988.

44. Voda K., Boh B., Vrtacnik M., Pohleven F. Effect of the antifungal activity of oxygenated aromatic essential oil compounds on the white-rot Trametes versicolor and the brown-rot Coniophora puteana. *International Biodeterioration & Biodegradation*. **2003**, 51, 51-59.

Chapter 2. Distribution of CP2 and TP70 in mouse brain region and various tissues of mice.

2.1 Introduction

Alzheimer's disease (AD), the most common type of dementia, was first described in 1906 by Alois Alzheimer, a German neurologist. "Dementia" is an umbrella term describing a variety of diseases and conditions that develop when nerve cells in the brain (called neurons) die or no longer function normally. The death or malfunction of neurons causes changes in one's memory, behavior, motor functions and ability to think clearly. In AD, these changes in the brain eventually impair an individual's ability to carry out such basic bodily functions as walking and swallowing. AD is ultimately fatal.[1,2]

More than 35 million people worldwide and 5.5 million in the United States suffer AD. With the general increase in longevity of the U.S. population, the incidence of AD has risen to the point where it is now the sixth-leading cause of death in the US and the fifth-leading cause of death for individuals age 65 and older. By 2025, the number of people 65 and older with AD is estimated to reach 7.1 million.[3] No treatment is available to slow or stop the disease. Four medications approved by the U.S. Food and Drug Administration that temporarily improve symptoms are Donepezil (Aricept®), rivastigmine (Exelon®), galantamine (Razadyne®) and memantine (Namenda®). However, these drugs do not ameliorate the underlying disease process and may help only for a few months to a few years. The development of new anti-AD drugs are highly warranted.[4]

Previous study in our laboratory has found that a tricyclic pyrone (TP) compound, CP2 (code name; **Figure 2.1**) showed the prevention of cell death from MC65 cells assay associated with intracellular amyloid beta oligomers (AβO) and inhibits Aβ aggregation *in vitro* and reduced amyloid plaques and soluble AβO *in vivo*.[5,6] Recently, further exploration of similar analogs by modifying C13 position in CP2, TP70 (code name; **Figure 2.1**) was identified to

possess strong cell protective properties against intracellularly induced Aβ toxicity, inhibitory activities against Acyl-CoA: cholesterol acyltransferase (ACAT), and enhancing properties of ATP-binding cassette subfamily A member 1 (ABCA1) cholesterol transporter gene with nanomolar efficacy.[7]

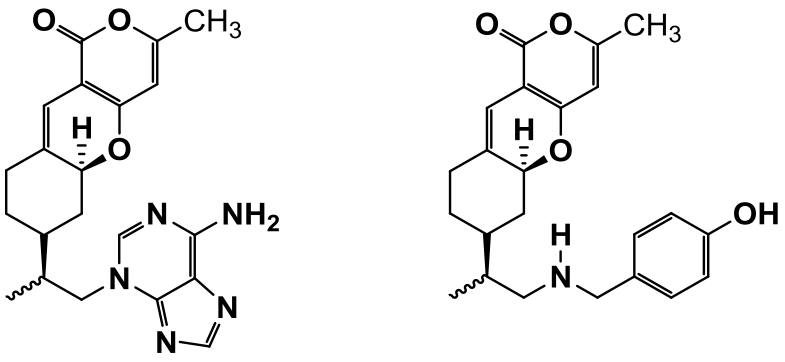

Figure 2.1 Chemical structure of CP2 and TP70.

My research project involved the synthesis of CP2 and TP70 in gram scale reactions for *in vivo* studies and studies of the pharmacokinetics (PK) and bioavailability. After that, quantifications of CP2 and TP70 in mouse brain regions and various tissues of mice were determined using high-performance liquid chromatography (HPLC). These studies are essential to define the pharmacokinetics and metabolisms of these drugs in mice which can be used to design the optimal dose of compounds for *in vivo* efficacy study.

Oral feeding or intravenous (iv) administration of CP2 and neuronal cultures and mouse brain region collection were conducted by Dr. Eugenia Trushina and Dr. Liang Zhang at Mayo Clinic. Oral or intravenous (iv) route of TP70 and tissues collection were done by Dr. Ximin Simon Xie group, AfaSci Research Laboratory. In this chapter, the distribution of CP2 in neuronal cultures and mouse brain region and the time course distribution of TP70 in different tissues and plasma of mice are presented and discussed.

2.2 Background

AD can be classified in two forms: (1) the rare, early onset familial form of AD (FAD) is caused by mutations in the amyloid precursor protein (APP) and presenilin 1 and 2 (PS1 and PS2) genes that lead to the accumulation of Aβ; and (2) a common sporadic non-familial AD, which results in the generation of Aβ42. APP is a transmembrane glycoprotein and is found in many tissues and organs, including the brain and spinal cord (central nervous system). Its primary function is not known, though it has been implicated as a regulator of synapse formation, neural plasticity and iron export. Presenilins are a family of related multi-pass transmembrane proteins that function as a part of the gamma-secretase intramembrane protease complex. Vertebrates have two presenilin genes, called *PSEN1* (located on chromosome 14 in humans) that encodes presenilin 1 (PS1) and *PSEN2* (on chromosome 1 in humans) that codes for presenilin 2 (PS-2). Notably, patients with either sporadic or familial AD share common clinical and neuropathological markers including Aβ plaques, accumulation of neurofibrillar tangles and massive neuronal cell loss. [9-13]

The mechanism of AD is yet to be known, however, it is believed that AD develops as a result of multiple factors rather than a single cause. Extracellular β-amyloid (Aβ) peptide plaques and intracellular neurofibrillary tangles (NFTs) are two main pathological features of AD which distinguishes AD from other neurodegenerative diseases.[8-9] Aβ peptide are natural products of metabolism consisting of 36 to 43 amino acid. Aβ peptide originates from proteolysis of the APP by sequential enzymatic actions of two enzymes, β-secretase and γ-secretase. Neurofibrillary tangles are mainly composed of intracellular hyperphosphorylated taus in the form of paired helical filaments. Tau is a microtubule stabilizing protein. When tau is hyperphosphorylated, it dissociates from microtubes causing their disassembly or loss of essential functions.[10] In addition, hyperphosphorylated tau tends to aggregate and sequester additional normal tau from binding microtubes. According to the amyloid cascade hypothesis, Aβ is the main culprit triggering a whole cascade of events, including formation of NFTs, eventually leading to neurodegeneration and loss of brain function in AD patients.[4,11] Other risk factors associated with the development of AD are age, food, cholesterol, head injury, and family's genetic, and behavioral history.[12-14]

Recent studies suggested that the intraneuronal accumulation of Aβ are the primary toxic species and might be the first step of amyloid cascade leading to the AD.[14-15] Also it has been suggested that intracellular Aβ induces a higher toxicity, being at least 10,000 times more toxic than extracellular Aβ.[16-17] Therefore, drugs targeting Aβ and downstream events could be one of the primary therapeutic targets in AD. Previous studies[5-6] in our lab demonstrated that tricyclic pyrone CP2 ameliorates cell death associated with binding to Aβ42 oligomers, reducing the levels of intracellular Aβ, and disaggregating Aβ42 oligomers and protofibrils. Furthermore, it was found that long-term CP2 treatment not only restores memory but also improves motor function in AD mouse models. (These experiments were performed by Dr. Eugenia Trushina's group at Mayo Clinic, the data are not shown here and the results are being formulated into a manuscript to be submitted).

New findings from epidemiological, molecular and biochemical strongly support the involvement of cholesterol metabolism in the control of both the generation and/or accumulation of Aβ.[18] For example, the identification of ε4 gene, an AD biomarker, of apolipoprotein E (APOE) as the most common genetic risk factor for late-onset AD.[19-20] Moreover, the neurons with tangles were found to have higher level of cholesterol compared to the healthy neurons.[21-22] ATP-binding cassette subfamily A member 1 (ABCA1), cholesterol transporters through cell membrane, is also shown to mediate the secretion of Aβ from the cells.[23] Acetyl-coenzyme A acetyltransferases (ACAT) is essential for the regulation of intracellular cholesterol homeostasis and distribution of cholesterol throughout the body by converting free cholesterol to neutral cholesteryl ester for storage. The inhibition of ACAT will reduce the formation of cholesterol ester and increasing the level of free cholesterol inside the cells, which then induce cholesterol efflux by increasing the cholesterol transporter gene ABCA1.[24] Therefore, ACAT inhibitors are good candidates for regulating of amyloid pathology by regulating cholesterol homeostasis.[25-27] The lead compounds CP2 and TP70 possess inhibitory activity against ACAT along with the upregulation of ABCA1 gene promoting the efflux of cholesterol, increasing the efficiency of cholesterol transporters, restoring axonal trafficking, and enhancing hippocampal synaptic activity. Like CP2, TP70 also protects the neuronal cell death. In addition, both CP2 and TP70 were found to have high oral bioavailability, excellent blood brain barrier permeability and low

toxicity. These synergistic cellular actions could be potential mechanisms underlying the protective effects *in vivo*.

Increasing evidence suggests that mitochondria are involved in aging which is the major risk factor for AD. Even though the primary cause for mitochondrial dysfunction with age is still controversial, studies in several species reveal a wide spectrum of alterations in mitochondria and mitochondrial DNA (mtDNA) with aging, including (1) increased disorganization of mitochondrial structure, (2) decline in mitochondrial oxidative phosphorylation function, (3) accumulation of mtDNA mutation, (4) increased mitochondrial production of reactive oxygen species (ROS), and (5) increased extent of oxidative damage to DNA, proteins, and lipids. Mitochondria are the most complex and metabolically active organelles in the cell. [28-30]

Recent studies[31-35] also have linked the Aβ with mitochondrial dysfunction. The mechanism of mitochondria dysfunction in AD is controversial. These studies suggests that Aβ enters mitochondria and interacts with mitochondria protein, disrupts the electron transfer process, and generate reactive oxygen species contributing to the loss of synaptic function and plasticity, which are increasingly recognized as major mechanisms responsible for memory loss in AD. In the nervous system, a synapse is a structure that permits a neuron (or nerve cell) to pass an electrical or chemical signal to another cell (neural or otherwise). Therefore, understanding the role of mitochondrial abnormalities in the pathogenesis is important to develop the efficient tools for early diagnosis, and for the design of new therapeutic strategies aimed to preserve/ameliorate mitochondrial function.

Cerebellum is two-size mounds of folded tissue located at the top of the brain stem and back bottom of the brain, the cerebellum is the guru of skilled and coordinated movement. Hippocampus located deep within the brain, it processes new memories for long term storage. It is among the first functions to falter in AD. The cerebral cortex is the outermost layered structure of neural tissue of the cerebrum (brain), in humans and other mammals. It covers the cerebrum, and divides into two cortices, along the sagittal plane, covering the left and right cerebral hemispheres. The cortex plays a key role in memory, attention, perceptual awareness, thought, language, and consciousness. It consists of up to six horizontal layers, each

with a different composition in terms of neurons and connectivity. The human cerebral cortex is 2 to 4 millimeters (0.079 to 0.157 in) thick. It is referred to as grey matter as it consists of cell bodies and capillaries and contrasts with the underlying white matter, which mainly composes of the white myelinated sheaths of neuronal axons (**Figure 2.2**).

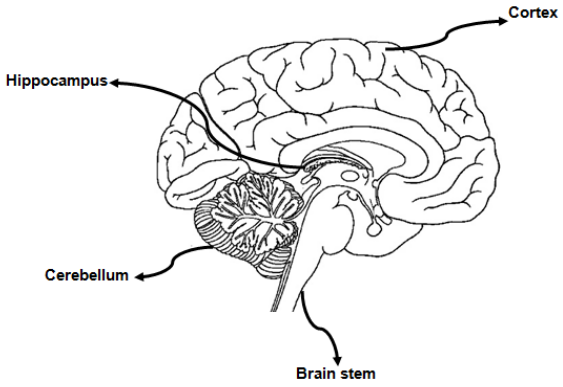

Figure 2.2 Location of cerebellum, hippocampus and cortex in human brain anatomy.

Pharmacokinetics (PK) is the study of drug disposition in the body and focuses on the changes in drug plasma concentration. For any given drug and dose, the plasma concentration of the drug will rise and fall according to the rates of three processes: absorption, distribution, and elimination. Absorption of a drug refers to the movement of drug into the bloodstream, with the rate dependent on the physical characteristics of the drug and its formulation. Elimination of a drug from the blood relies on two processes biotransformation or metabolism of a drug to one or more metabolites, primary in the liver; and the excretion of the parent drug or its metabolites, primary by the kidneys.

Drug distribution in pharmacology is a branch of pharmacokinetics which refers to the movement of a drug to and from the blood and various tissues of the body (for example, fat, muscle, and brain tissue). After a drug is absorbed into the bloodstream, it rapidly circulates through the body. As the blood recirculates, the drug moves from the bloodstream into the body's tissues. Each organ or tissue can receive different doses of the drug and the drug can remain in the different organs or tissues for a varying amount of time. The distribution of a drug

between tissues is dependent on vascular permeability, regional blood flow, cardiac output and perfusion rate of the tissue, and the ability of the drug to bind tissue and plasma proteins and its lipid solubility. The pH partition plays a major role as well. The drug is easily distributed in highly perfused organs such as the liver, heart and kidneys. It is distributed in small quantities through less perfused tissues like muscle, fat and peripheral organs. The drug can move from the plasma to the tissue until the equilibrium is established (for unbound drug present in plasma). Understanding how drugs behave in a biological system is a subject of prime importance in the treatment of various diseases.

For systemic drug administration in research, the drugs are generally administered in mice through three main routes that include oral gavage, intravenous injection, and intraperitoneal injection. In oral gavage, the drug in the form of solution is administered directly into the lower esophagus or stomach by the use of feeding needle. The feeding needle has a bulb tip which prevents the rupture of delicate tissues during the drug administration. The maximum volume that can be fed by oral gavage is 10 mL/Kg body weight of the mice. Intraperitoneal (IP) injection of drug is one of the most frequently performed drug administration methods in mice. In this method the drug in the form of the solution is injected into the peritoneal cavity, a space that surrounds the abdominal organs. A small and thin needle is inserted into the abdominal cavity in the lower right quadrant to avoid the puncture of cecum and urinary bladder with the needle. For IP injection the volume of drug solution should not exceed 2 mL in an adult mouse. Intravenous (IV) injection is used to administer the drug solution directly in the blood through veins. The vein in the tail of a mouse functions in thermoregulation and dilates on the rise in body temperature. Thus application of heat to the tail of the mouse causes venodilation making the veins easily accessible for IV administration. The maximum volume of drugs administration through IV should not exceed 0.5 mL in an adult mouse. The drugs administered through oral gavage and IP injections first diffuse into the blood stream. The blood then transports and distributes the drugs in various tissues in the body.

Elimination half-life ($t_{1/2}$) is time required to reduce the plasma drug concentration by 50%. It can be calculated from the elimination rate constant, but it is usually determined from the plasma drug concentration curve. **Figure 2.3** shows a standardized drug plasma

concentration curve over time after oral or iv administration of a typical drug.[37] The Y-axis is a linear scale of drug plasma concentration, often in μg/mL or mg/L, and the X-axis is a time scale, usually in hours. Parameters of the plasma drug concentration curve are the maximum concentration (C_{max}), the time needed to reach the C_{max} (T_{max}). A measure of the total amount of drug during the time course is given by the area under the curve (AUC). These parameters are useful for comparing the bioavailability of different pharmaceutical formulations or of drugs given by different routes of administration. To determine bioavailability, F, the AUC of the oral administration AUC_{po}, is divided by the AUC of the intravenous administered drug, AUC_{iv}.

$$\text{Bioavailability (F)} = AUC_{po} / AUC_{iv}$$

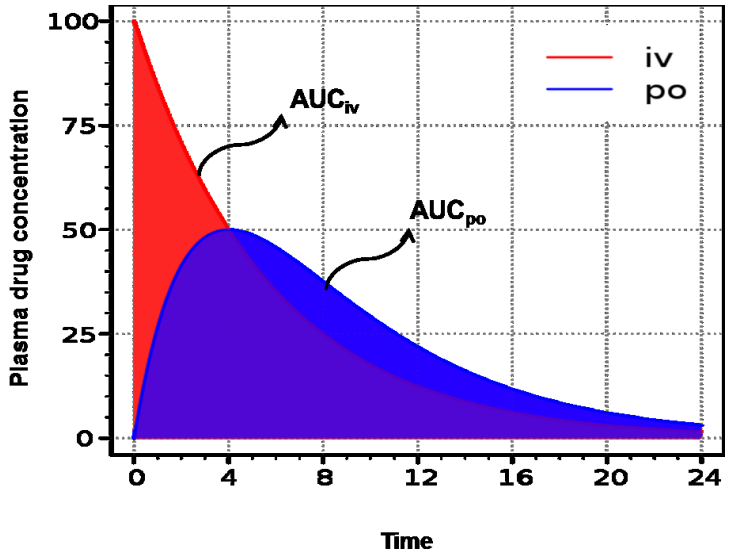

Figure 2.3 A standardized drug plasma concentration curve over time after oral administration (po) or intravenous (iv) of a typical drug.[37]

Bioavailability is defined as the fraction (F) of the administered dose of a drug that reaches the systemic circulation in an active form. The oral bioavailability of a particular drug is determined by dividing the AUC of an orally administered dose of the drug by the AUC of an intravenously administered dose of the same drug. Intravenous administration of a drug provides the greatest possible bioavailability, and this method is defined to yield a bioavailability of 1 (or 100%). The bioavailability of drugs administered via other routes can be determined in the same

manner as the bioavailability of drugs administered orally. The bioavailability of orally administered drugs is of particular concern because it can be reduced by many pharmaceutical and biologic factors. Pharmaceutical factors include the rate and extent of tablet disintegration and drug dissolution. Biological factors include the effect of food, which can sequester or inactivate a drug, the effect of gastric acid, which can inactivate a drug; and the effects of gut and liver enzymes, which can metabolize a drug during its absorption and first pass through the liver.

The following two steps are often used to calculate the area under the curve (AUC)[38]: (i) Calculate area of each trapezoid; and (ii) Sum all trapezoid areas to get AUC.

The equation to calculate the area of trapezoid is when the curve in an increasing trend:

$$Area_{trapezoid} = \frac{1}{2}\,(C_1 + C_2)(t_2 - t_1)$$

The following equation is applied when the curve in a decreasing trend:

$$Area_{log} = \frac{(C_1 - C_2)}{(lnC_1 - lnC_2)}\,(t_2 - t_1)$$

C denotes drug concentration.

t denotes time.

The subscript refers to the sample number.

2.3 Results and discussions

2.3.1 CP2 distribution in neuronal cells and mouse brain region collection.

CP2 in the cells or in the tissues was determined by plotting a calibration graph with the ratios peak areas of CP2 to BTA vs. molar ratios of CP2 to BTA as mentioned in the experimental section of this chapter. The calibration graph for CP2 is shown in **Figure 2.4**.

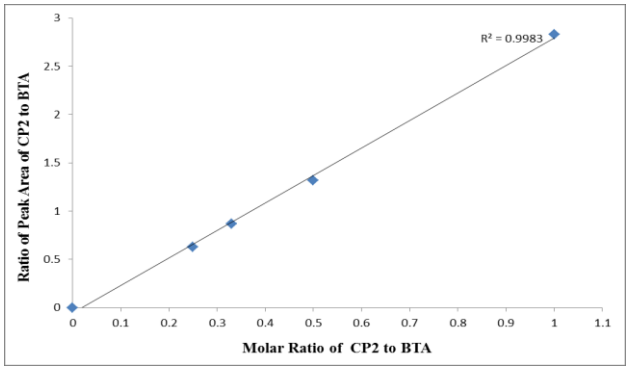

Figure 2.4 Correlation of ratios peak areas of pure CP2 and authentic BTA from HPLC chromatogram and molar ratios of pure CP2 and authentic BTA injected.
Solutions of 100 µL of various concentrations of pure CP2 and authentic BTA were injected into an HPLC, the peak areas corresponding to CP2 and BTA were integrated from the HPLC chromatogram, and the ratios of the peaks were obtained. The results of the ratios of HPLC peak areas and the ratios from CP2 and BTA concentrations were plotted, and a linear correlation line was obtained from the graph.

The amount of CP2 in the cell or tissues extract was calculated by determining the peak areas ratio of CP2 to BTA and determining the number of moles CP2 from the correlation graphs, as the number of moles BTA added to the cell and tissue extract was known. HPLC chromatograms of the cells and tissues extract injected with a known amount of BTA showed a peak at 17 minutes which had the same retention time compared to the authentic CP2 as shown

in **Figure 2.5**. The representative mass spectrum of eluant corresponding to the peak at 17 minutes is highlighted in **Figure 2.6**.

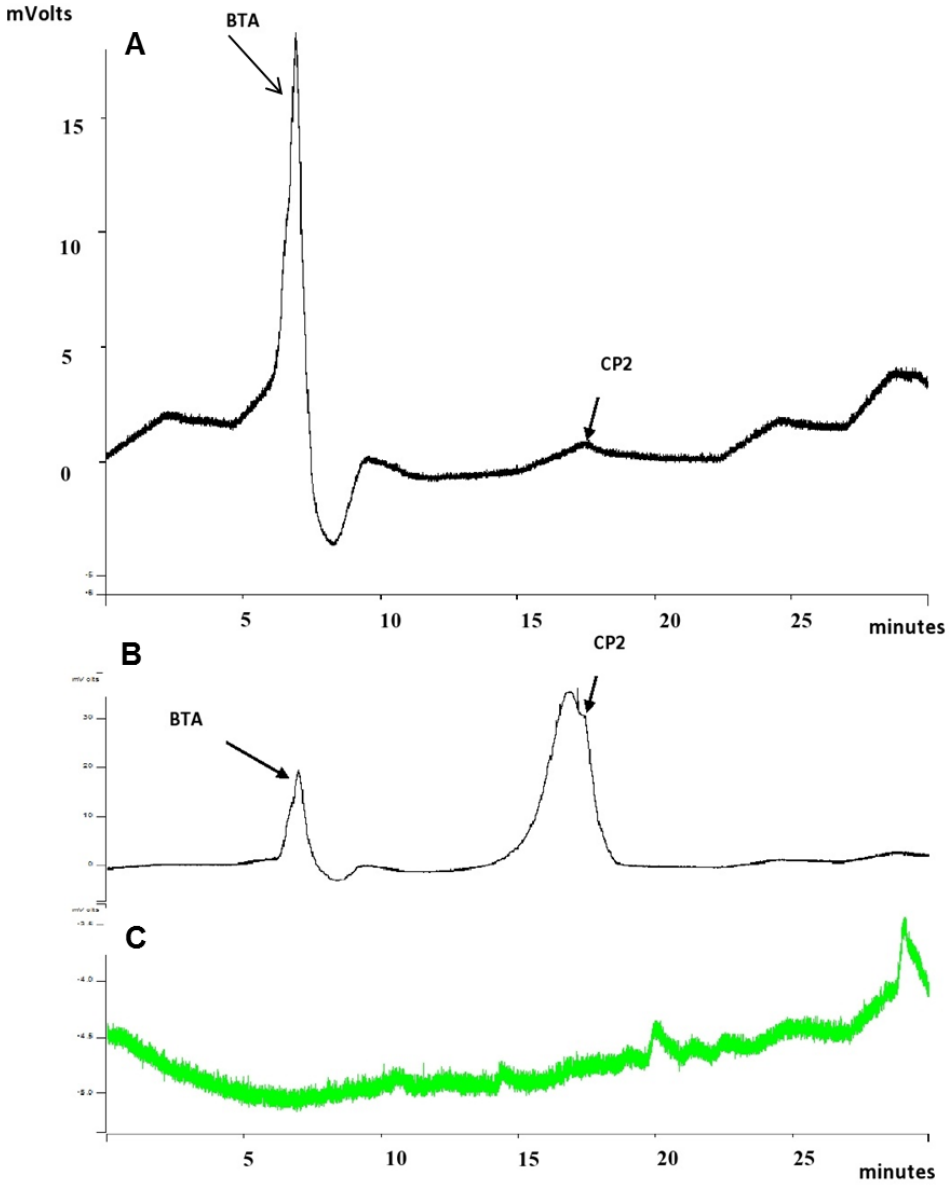

Figure 2.5 Representative HPLC chromatograms. **A** is the HPLC chromatogram of the brain extract with known amount of BTA. **B** is the HPLC chromatogram of 1:1 mol ratio of BTA and pure CP2. **C** is the HPLC chromatogram of the control (brain tissue without CP2). The peak at 17 minutes retention time in A had the same mass as pure CP2 which was confirmed by mass spectrometry.

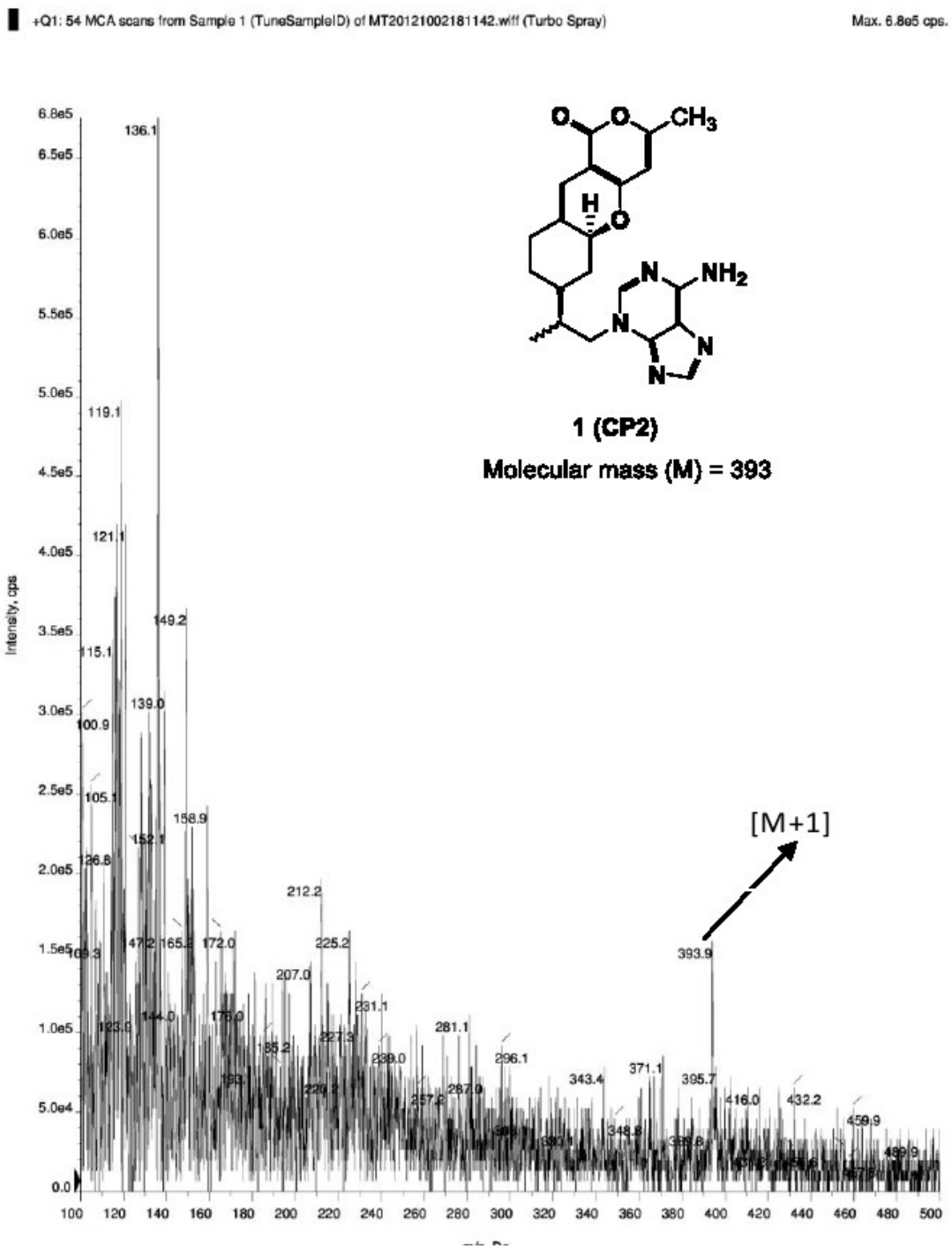

Figure 2.6 Mass spectrum of the eluant corresponding to the peak at 17 minutes (of **Figure 2.5A**) and is identical to pure CP2.

The results of CP2 distribution in subcellular fractions: crude nuclear, heavy mitochondria (HM) and light mitochondria (LM) are shown in **Figure 2.7**. CP2 was found at mitochondria and shown to accumulate mostly in the heavy mitochondria fraction followed by light mitochondria fraction and least to accumulate in the crude nuclear fraction.

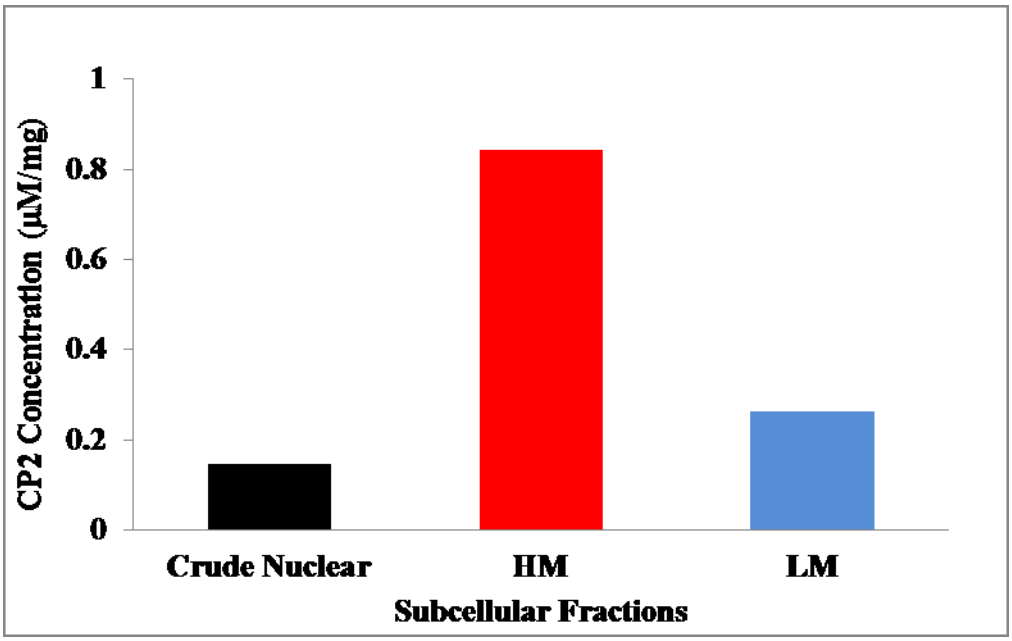

Figure 2.7 CP2 concentration (µM/mg) in subcellular fractions: crude nuclear, heavy mitochondria and light mitochondria.

After knowing that CP2 targets the mitochondria in cells, the next question we would like to address was that how much CP2 accumulated within each vital organ in mice. Therefore, specific brain region including cerebellum, hippocampus, cortex and whole brain were harvested from two of the adult mice wild type (WT, C75/Blc) and APP/PS1 (A/P, transgenic). Each tissue was isolated into three fractions: heavy mitochondria, light mitochondria and the crude nuclear. The distribution of CP2 (nM/mg) of tissue fractionation and brain regions in transgenic (A/P, APP/PS1) and wild type (WT, C75/Blc) mouse are highlighted in **Figure 2.8** and **Figure 2.9.**

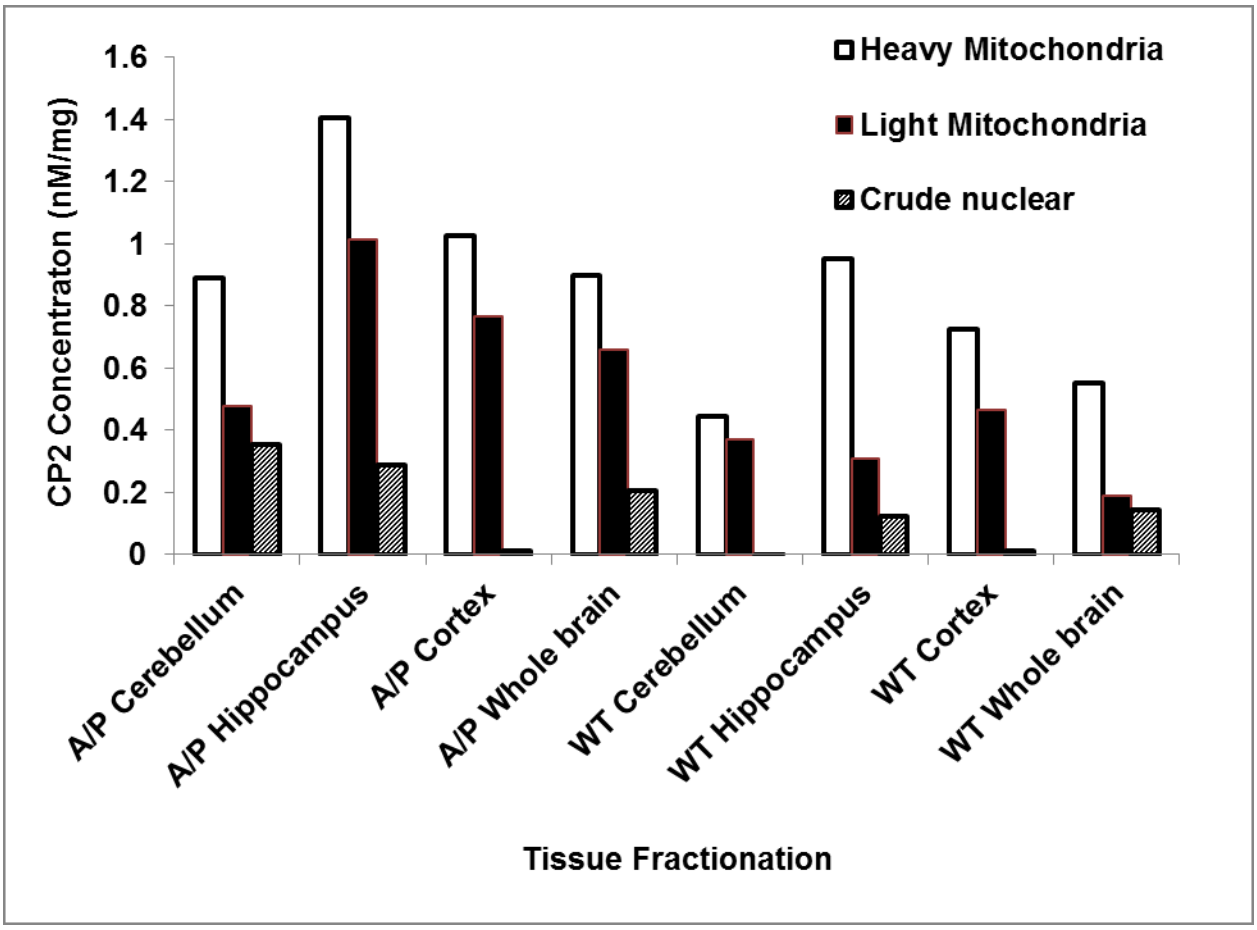

Figure 2.8 CP2 concentrations (nM/mg) in APP/PS1 (A/P, transgenic) mouse and wild type (WT, C75/Blc) mouse brain tissue fractionation.

In both A/P and WT mouse, the brain tissue with the largest CP2 concentration was the heavy mitochondria, whereas crude nuclear had the smallest amount of CP2. Light mitochondria had less amount of CP2 than heavy mitochondria but more than the crude nuclear fraction. The hippocampus is a brain area critical for learning and memory, is especially vulnerable to damage at early stages of AD. Interestingly, hippocampus area is the brain region which has the greatest amounts of CP2 concentration in both A/P and WT mouse. The distribution of CP2 in the mouse brain regions suggests its efficacy to penetrate the blood brain barrier, which is generally difficult in cases of many drugs.

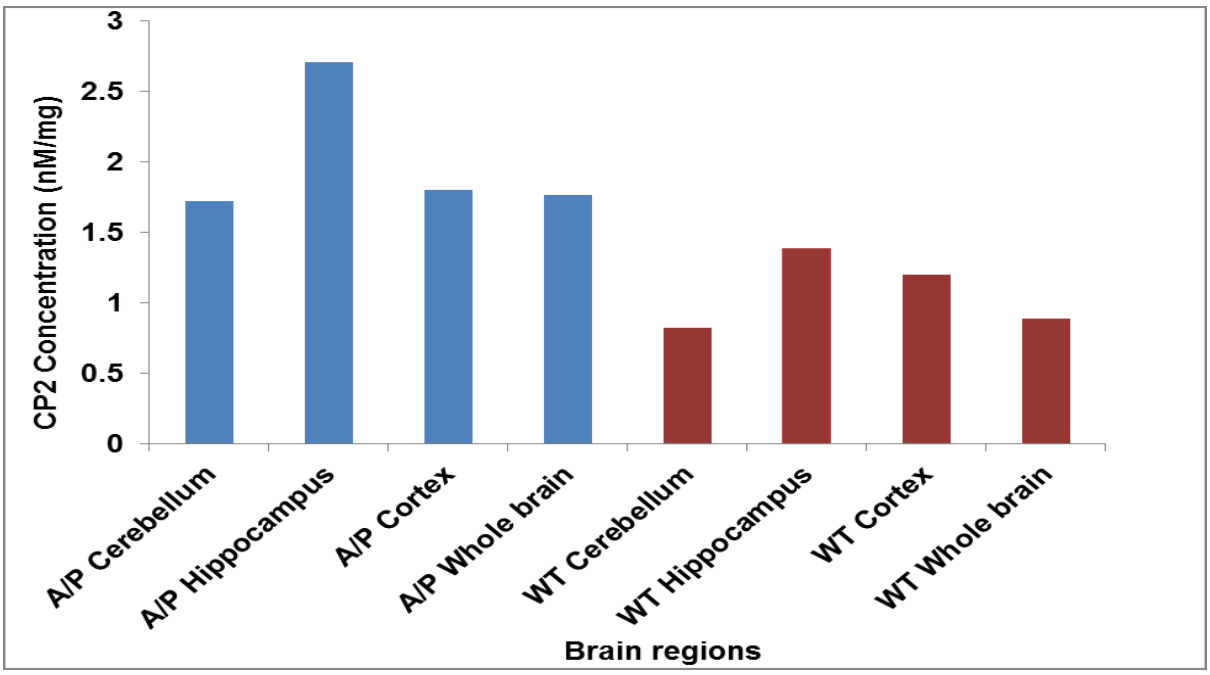

Figure 2.9 CP2 concentrations (μM/mg) in different brain regions of APP/PS1 (A/P, transgenic) mice and wild type (WT, C75/Blc) mice.

Inside the mitochondrion is a group of proteins that carry electrons along four chain reactions (Complexes I-IV), resulting in energy production. This chain is known as the electron transport chain (ETC). Mitochondria are essential organelles for neuronal survival and function since it produces more than 90% of the cellular adenosine triphosphate (ATP) in neurons. Extensive literature exists supporting a causative role of mitochondrial dysfunction in neurodegenerative disease pathogenesis including the AD. Complex I, the first step in ETC, was known as the most common site for mitochondrial abnormalities.

Notably, our latest results revealed that CP2 direct inhibits complex I of mitochondria leading to restriction in energy production, increasing in AMP/ATP ratio, upregulating of activated protein kinase (AMPK), inhibition of GSK-3β and reduction of hyperphosphorylated tau. Moreover, our data suggests that 13 months of treatment CP2 restores axonal trafficking leading to improve cognitive and behavior phenotype in multiple animal models of FAD. (These experiments were done by Dr. Eugenia Trushina's group at Mayo Clinic, the data are not shown here and the results are being formulated into a manuscript to be submitted).

2.3.2 Distribution of TP70 in various organs.

To examine the tissue distribution of TP70 in different organs, a dose of 25 mg/Kg of TP70, was administered to the male, 3-month old WT C57BL/6NHsd (Harlan) mice by iv administration. TP70 in various tissues was determined by plotting a calibration graph with the ratios of peak areas of TP70 to 4-methoxyphenol vs. molar ratios of TP70 to 4-methoxyphenol as mentioned in the experimental section of this chapter. The calibration graph for TP70 is shown in **Figure 2.10**.

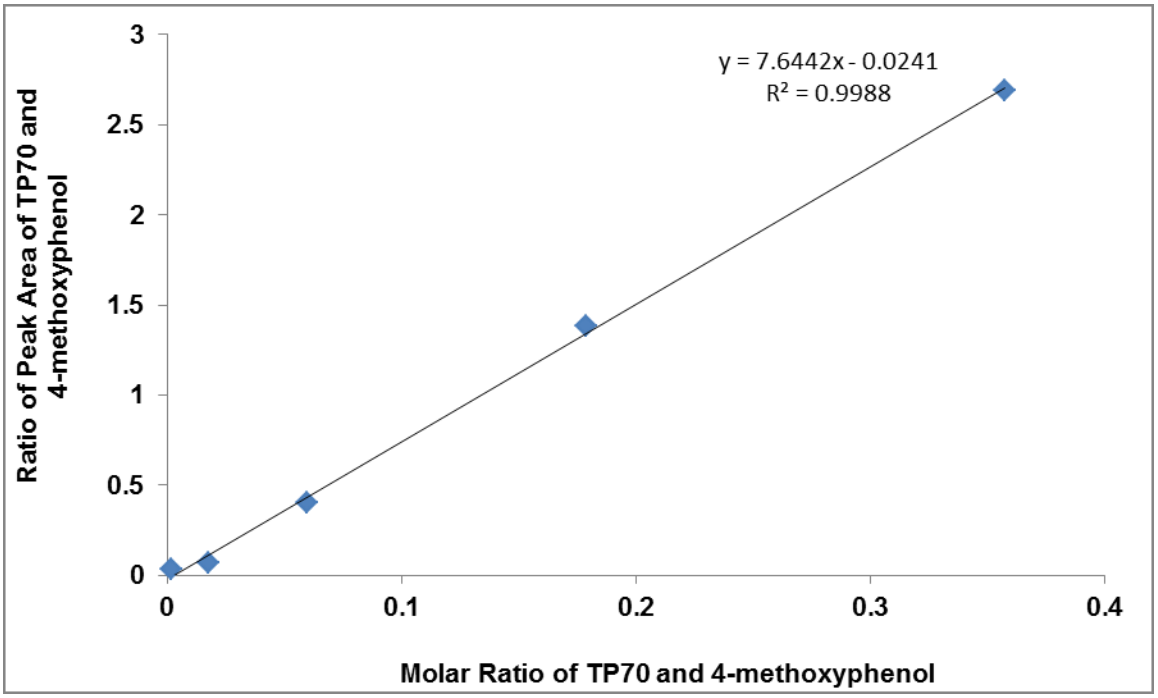

Figure 2.10 Correlation of ratios peak areas of authentic 4-methoxyphenol and pure TP70 from HPLC chromatogram and molar ratios of TP70 and 4-methoxyphenol injected.

Solutions of 100 µL of various concentration of authentic TP70 and pure 4-methoxyphenol were injected into an HPLC, the peak areas corresponding to TP70 and 4-methoxyphenol were integrated from the HPLC chromatogram, and the ratios of the peaks were obtained. The results of the ratios of HPLC peak areas and the ratios from TP70 and pure 4-methoxyphenol concentrations were plotted, and a linear correlation line was obtained from the graph.

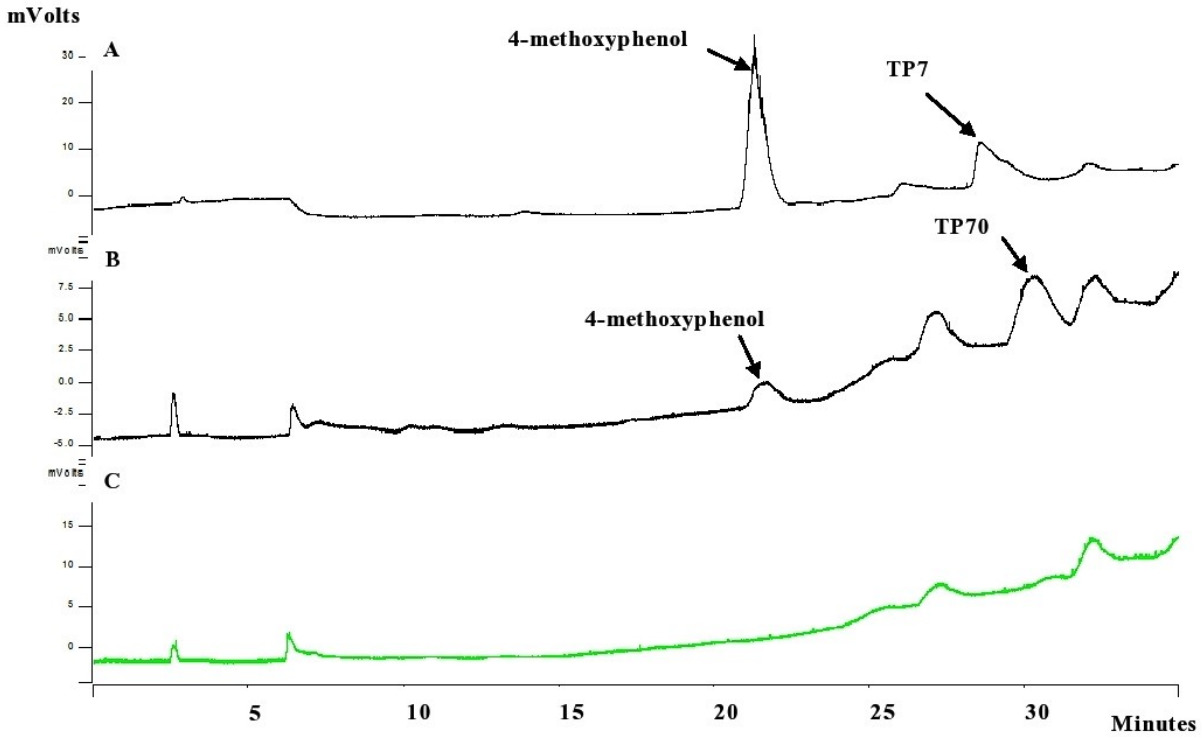

Figure 2.11 Representative HPLC chromatograms. **A** is the HPLC chromatogram of 1:1 mol ratio of 4-methoxyphenol and pure TP70. **B** is the HPLC chromatogram of the lungs extract with a known amount of 4-methoxyphenol. **C** is the HPLC chromatogram of the control (lungs without TP70). The peak at 30 minutes retention time in B has the same mass as pure TP70 which was confirmed by mass spectrometry.

The amount of TP70 in the tissues extract was calculated by determining the peak areas ratio of TP70 to 4-methoxyphenol and determining the number of moles of TP70 from the correlation graphs, as the number of moles of 4-methoxyphenol added to the tissue extract was known. HPLC chromatograms of the tissues extract injected with a known amount of 4-methoxyphenol showed a peak at 30 minutes which had the same retention time compared to the authentic TP70 as shown in **Figure 2.11**. The representative mass spectrum of eluant corresponding to the peak at 30 min is highlighted in **Figure 2.12**.

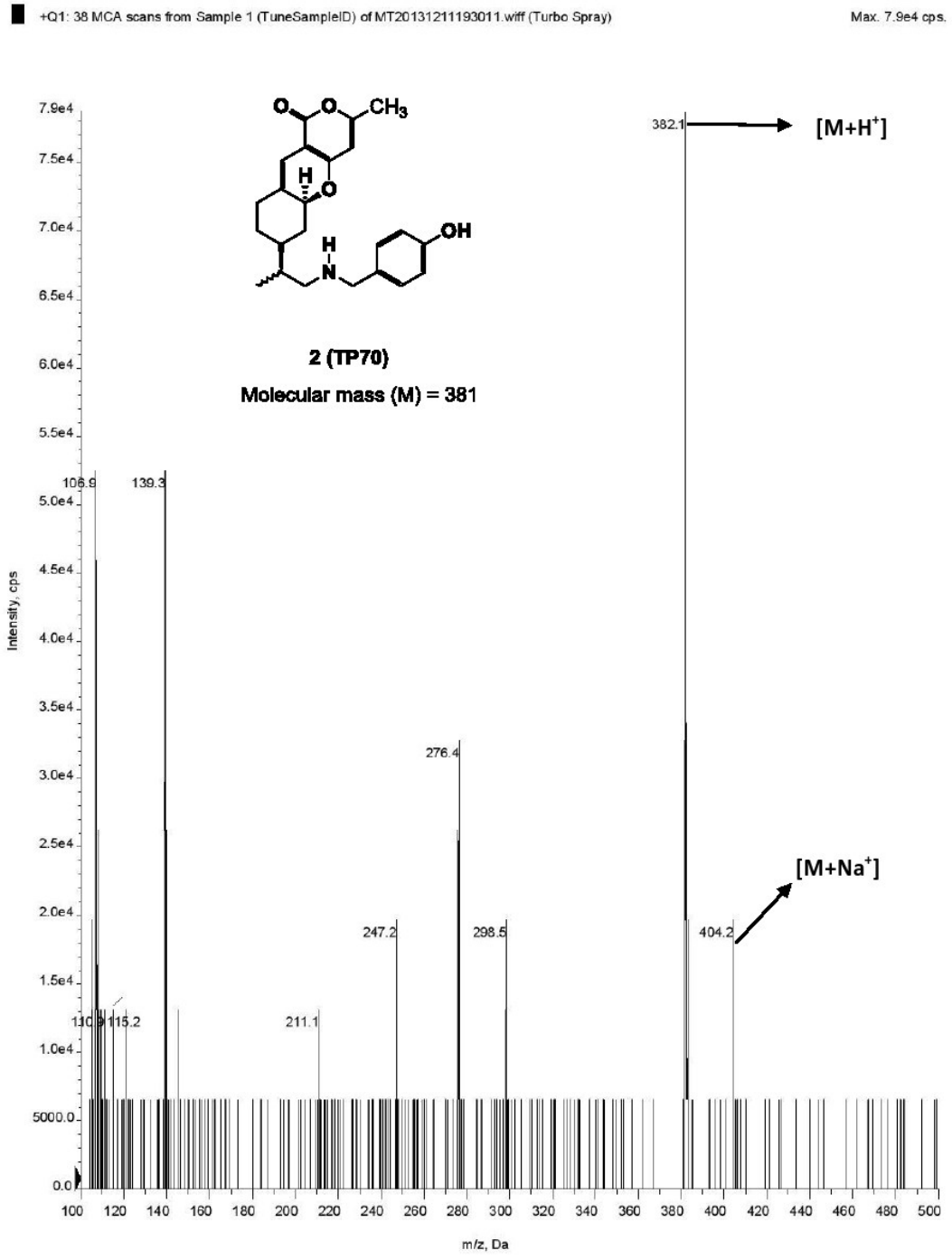

Figure 2.12 Mass spectrum of the eluant corresponding to the peak at 30 minutes (of **Figure 1.11B**) which is identical to pure TP70.

The summarization amounts of TP70 in various organs for distribution study and the half-life values are shown in **Table 2.1** and **Figure 2.13.**

Table 2.1 Results of PK study of TP70 (25 mg/Kg body weight; iv route; n = 3) and distribution in various organs.

Time (hr)	Average concentrations of TP70 (mg/L)						
	Brain	Heart	Liver	Lungs	Kidneys	Intestine	Spleen
0.5	18.6 ± 1.9	10.9 ± 0.65	13.4 ± 2.8	11.8 ± 1	16.7 ± 1.4	12.3 ± 3.3	11.3 ± 0.4
1	12.5 ± 1	0.9 ± 0.38	18.4 ± 4.9	5.3 ± 2.3	11.2 ± 1.3	8.8 ± 1.9	7.8 ± 1.6
2	8.5 ± 0.2	0.2 ± 0.04	5.7 ± 1.8	3.8 ± 1.3	9.9 ± 2	3.5 ± 2.2	2.5 ± 1.98
4	3.6 ± 0.4	0.03	4.9 ± 1.4	2.8 ± 0.7	7.2 ± 3.7	2.4 ± 0.28	0.8 ± 0.43
6	2.5 ± 0.4	0.01	2 ± 0.8	0.6 ± 0.5	6 ± 1.4	0.2 ± 0.25	0.15 ± 0.08
24	1.12 ± 0.08	0	0	0	0.8 ± 0.6	0	0
$t_{1/2}$ (hr)	**1.36**	**0.6**	**2**	**1.57**	**4.2**	**1.5**	**1.3**
Total mass of TP70 (µg)	**12**	**1.2**	**10.1**	**0.9**	**7.1**	**2.6**	**1.1**

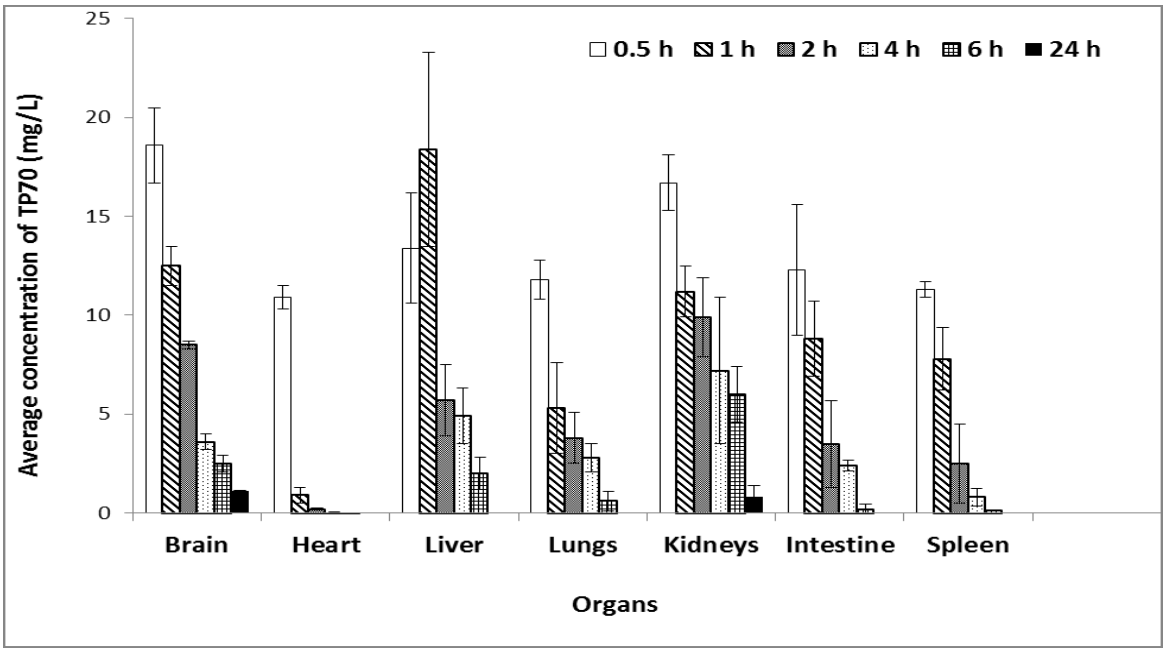

Figure 2.13 Results of PK study of TP70 (25 mg/Kg body weight; iv route; n = 3) and distribution in various organs. Each bar represents the average concentration of TP70 measured from 3 mice and is provided with (±) standard error.

In 0.5 h from the iv administration of the drug, TP70 was detected in the major organs including brain, heart, liver, lungs, intestine, spleen and kidneys. Brain had the highest distribution of TP70 with the respective concentration of 18.6 (mg/L) which implies the good penetration of the drug through the blood brain barrier. Kidneys, liver, intestine, lungs, spleen and heart were found to have 16.7 (mg/L), 13.4 (mg/L), 12.3 (mg/L), 11.8 (mg/L), 11.3 (mg/L) and 10.9 (mg/L), respectively. The amount of TP70 gradually decreases from 0.5 h to 6 h in most of the organs with the except of heart which has the concentration of TP70 dramatically change from 0.5 h to 1 h. In 24 h time of the drug administration, the amount of TP70 decreases to 1.12 (mg/L) in brain and 0.8 (mg/L) in kidneys, whereas heart, lungs, intestine, spleen and liver had no detectable amount of TP70 in 24 hours. These results indicate that TP70 accumulates in the brain in effective quantity and with half-life of 1.36 hours in brain.

The average weight of each mouse is 25 g; therefore, the ideal amount of TP70 administered to each mouse is 625 (μg). After organs extraction and quantification, total mass of TP70 distributed in brain, heart, liver, lungs, kidneys, intestine and spleen is 35 (μg). This result indicate that TP70 can be absorbed, distributed to major tissues, and metabolized in various tissues or excreted out from the body of mice.

2.3.3 Pharmacokinetic (PK) and bioavailability of TP70 in plasma from the intravenous (iv) and oral gavage (po) administration.

Table 2.2 and **Figure 2.14** summarize results of PK and bioavailability of TP70 in plasma from the iv and po administration.

Table 2.2 Results of PK study of TP70 (25 mg/Kg body weight; oral gavage and iv routes; n = 3) in plasma.

Time (min)	Average concentration of TP70 in plasma (mg/L)	
	po route	**iv route**
5	0	16.6 ± 6.1
15	2.8 ± 0.09	10.2 ± 4
30	3.9 ± 0.14	8.2 ± 3.5
60	6.9 ± 0.17	3.7 ± 0.8
120	4.2 ± 0.19	2.02 ± 0.6
240	2.4 ± 1.37	1.8 ± 0.5
360	1.2 ± 0.23	0.9 ± 0.3
AUC (mg.min/L)	678	989
F	0.68	1
$t_{1/2}$ (h)	2.05	1.06

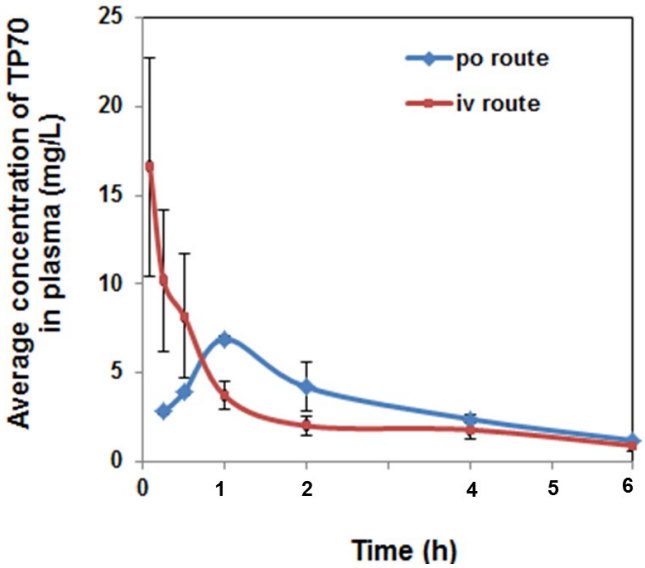

Figure 2.14 Results of PK study of TP70 (25 mg/Kg body weight; oral gavage and iv routes; n = 3) in plasma. Each bar represents the average concentration of TP70 measured from 3 mice and is provided with (±) standard error.

In 5 minutes from the iv administration of the drug, TP70 was detected in plasma with the concentration of 16.6 (mg/L); however, no drug was found in plasma in 5 min when using the po route. For the iv route, at first the drug concentration reduce quickly from 16.6 (mg/L) at 5 min to 3.7 (mg/L) at 1h; then, it is slowly decreasing to 0.9 mg/L after 6 h of the drug administration. In contrast, there is a quick increase from 15 min to 1 h with the TP70 concentration of 2.8 (mg/L) and 6.9 (mg/L) when po administration. After reaching the highest concentration of TP70 at 1 h, TP70 was found decrease steadily from 1 h to 6 h. These results show that TP70 has good clearance property along with the values of area under the curve (AUC) and bioavailability (F) point out that the drug can be administered for efficacy evaluation *in vivo*.

2.4 Conclusion

Distribution of CP2 in neuronal cultures and mouse brain region collection were studied. The results show that CP2 targets mitochondria and has the highest concentration in hippocampus which is one of the first regions of the brain to suffer the damage in Alzheimer's disease. Identification of the early molecular mechanisms underlying AD is of great important in order to develop efficient methods for diagnosis and therapeutic intervention.

Pharmacokinetics and bioavailability of compound TP70 were determined. Area under the curve and bioavailability value F were calculated, and data show that TP70 has a good PK profile and bioavailability. Pharmacodynamics study should be carried out.

2.5 Experimental

2.5.1 Synthesis of CP2.[5-6]

CP2 was synthesized in four steps (**Scheme 2.1**). 4-Hydroxy-6-methyl-2-pyrone and (S)-perilaldehyde which are commercial available were refluxed for 24 hours in the presence of L-Proline and ethyl acetate to afford a single diastereoisomer tricyclic pyrone **46** in 78 % yield. Selective hydroxylation of the terminal double bond in **46** was carried out by hydroboration followed by oxidation to yield alcohol **47** in 68 % yield. Mesylation of the alcohol **47** was achieved by treating alcohol with triethyl amine and methanesulfonyl chloride to afford **48** in 95 % yield. Mesylate **48** and adenine were taken together and heated in distilled dimethylacetamide (DMA) at 150 ^{o}C for 8 hours. Column chromatographic separation using methylene chloride, ethyl acetate and methanol gave CP2 in 20% yield.

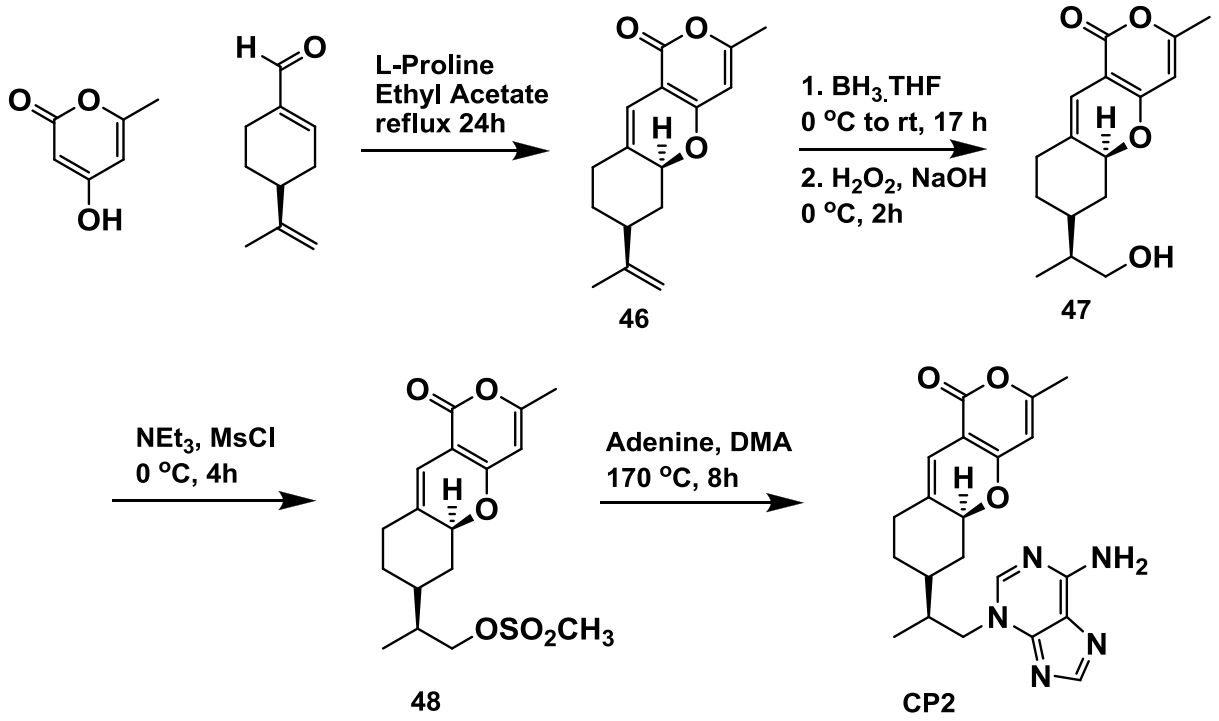

Scheme 2.1 Synthesis of CP2.

(5a*S*,7*S*)-7-Isopropenyl-3-methyl-1*H*,7*H*-5a,6,8,9-tetrahydro-1-oxopyrano[4,3-b][1] benzopyran (46)

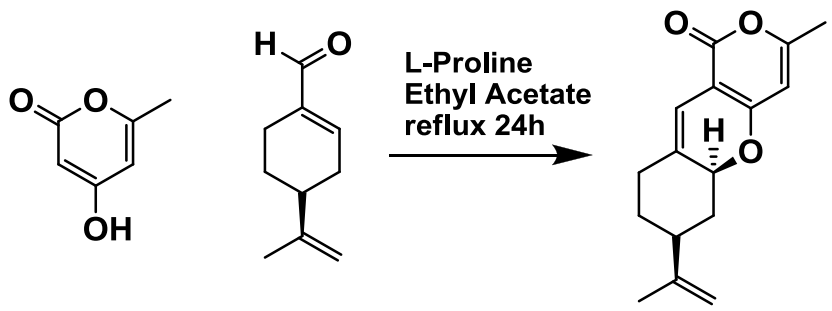

46

To a solution of 20.0 g (158 mmol) of 4-hydroxy-6-methyl-2-pyrone in 0.8 L of ethyl acetate under argon at room temperature was added 24.0 g (0.158 mol) of (S)-(-)- perilaldehyde and 7.0 g (60.0 mmol) of L-proline. The reaction mixture was heated to reflux for 24 h. The progress of the reaction was monitored using TLC using hexane and ethyl acetate as a developing solvent. The reaction mixture was washed with water and brine. The water layer was extracted two times with ethyl acetate. The combined organic layer was dried with anhydrous sodium sulfate, filtered and concentrated. Purification was carried out by crystallization using ethyl acetate as a solvent to give a yellow solid of **46** in 78% yield. $[\alpha]^{22}_{D}$ = +31.90 (*c* 0.75, $CHCl_3$); ^{1}H NMR ($CDCl_3$) δ 6.1 (s, 1H, C10H), 5.72 (s, 1H, C4H), 5.1 (dd, *J* = 11, 5 Hz, 1H, C5a H), 4.75 (m, 1H, =CH), 4.73 (m, 1H, =CH), 2.48 (ddd, *J* = 14, 4, 2.4 Hz, 1H), 2.22-2.02 (m, 3H), 2.19 (s, 3H, C4-Me), 1.88-1.72 (m, 2H), 1.74(s, 3H, MeC=), 1.31 (ddd, *J* = 25, 12.8, 4 Hz, 1H); ^{13}C NMR ($CDCl_3$) δ 163.4, 162.6, 161.7, 147.9, 132.3, 109.8, 109.6, 99.9, 97.5, 79.4, 43.6, 40.0, 32.5, 32.1, 20.9, 20.3.; MS FAB, m/z 259 ($M + H^+$).

(5a*S*,7*S*)-7-[(1*R*) and (1*S*)-2-Hydroxy-1-methylethyl]- 3-methyl-1*H*,7*H*-5a,6,8,9- tetrahydro-1-oxopyrano[4,3-b][1]benzopyran (47)

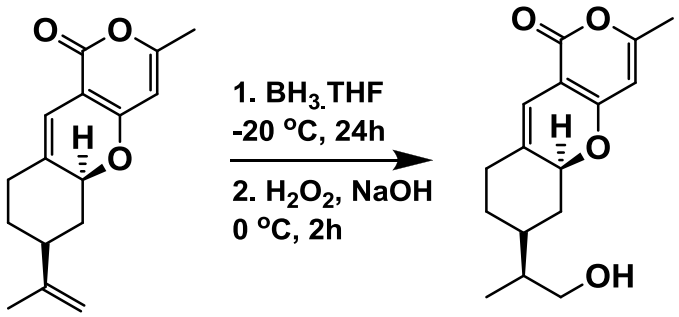

46 47

To a cold solution (0 ºC) of 5.0 g (19.0 mmol) of **46** in 200 mL of distilled THF under argon, was added 11.6 mL (11.6 mmol) of BH_3•THF complex (1.0 M in THF). After stirring the solution at 0 ºC for 3 h, gradually warmed up to room temperature and stirred for another 15 h. Cooled to 0 ºC and 20 mL of 0.1 % aqueous NaOH and 15 mL of 30% hydrogen peroxide were added. The solution was stirred for 2 h, diluted with $NaHCO_3$, and extracted three times with ethyl acetate. The combined organic layer was washed with 100 mL of brine, dried ($MgSO_4$), concentrated, and column chromatographed on silica gel using a gradient mixture of hexane and ethyl acetate as eluents to give 3.27 g (68% yield; based on reacted **46**) of **47** as a mixture of two diastereomers at C12 (1:1; based on ^{13}C NMR spectrum) and 0.5 g (10 % recovery) of **46**. ^1H NMR ($CDCl_3$) δ 6.08 (s, 1H, C4H), 5.71 (s, 1H, C10H), 5.07 (t, *J* = 5.2 Hz, 1H, C5aH), 3.62 – 3.52 (m, 2H, CH_2O), 2.46 (m,1H), 2.19 (s, 3H, Me), 2.13 – 1.99 (m, 2H), 1.73 – 1.51 (m, 3H), 1.19 – 1.12 (m, 2H), 0.92 (d, *J* = 7 Hz, 3H, Me); ^{13}C NMR ($CDCl_3$) (two diastereomers) δ 163.5, 162.8, 161.6, 133.0, 109.0, 100.0, 97.4, 79.7, 79.6, 65.6, 39.9, 39.8, 39.4, 37.2, 37.1, 36.9, 32.4, 32.3, 31.1, 30.4, 28.5, 20.1, 13.2 (Me for a diastereomer), 13.1 (Me for another diastereomer).

(5a*S*,7*S*)-3-Methyl-7-[(1*R*) and (1*S*)- 2-(methanesulfonyloxy)-1-methylethyl]-1*H*,7*H*-5a,6,8,9-tetrahydro-1-oxopyrano[4,3-b][1]benzopyran (48)

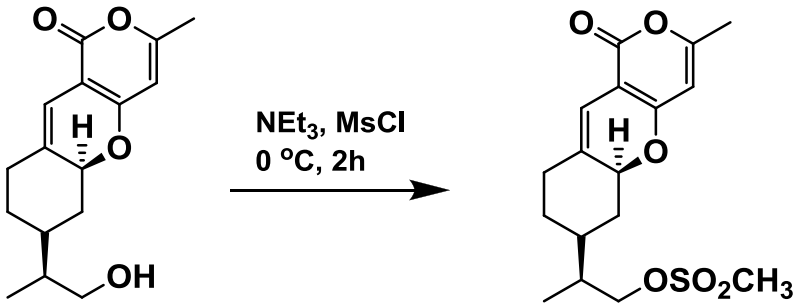

47 **48**

To a cold (0 ºC) solution of 7 g (25.0 mmol) of **47** in 200 mL of distilled methylene chloride under argon, were added 10.7 mL (76.0 mmol) of distilled triethylamine and 3 mL (40.0 mmol) of methanesulfonyl chloride. The solution was stirred for 4 h at room temperature, diluted with $NaHCO_3$, and extracted three times with methylene chloride. The combined dichloromethane layer was washed with brine, dried ($MgSO_4$), concentrated, and column chromatographed on silica gel using a gradient mixture of hexane and ethyl acetate as eluents to give 6.65 g (95% yield) of **48** as a mixture of two diastereomers (1:1; based on ^{13}C NMR spectrum). ^{1}H NMR ($CDCl_3$) δ 6.08 (s, 1H, C4H), 5.71 (s, 1H, C10H), 5.06 (m, 1H, CHO), 4.18 – 4.08 (m, 2H, CH_2O), 3.03 (s, 3H, MeS), 2.49 (d, J = 2.8 Hz, 1H), 2.19 (s, 3H, Me), 2.14 – 1.11 (m, 7H), 0.98 (d, J = 6.8 Hz, 3H, Me); ^{13}C NMR ($CDCl_3$) δ 163.2, 162.4, 161.7, 132.1, 109.6, 105.2, 99.8, 79.2, 79.1, 72.3, 38.9, 37.5, 37.4, 37.3, 37.2, 36.9, 32.2, 32.1, 30.8, 28.6, 20.2, 13.3 (Me for a diastereomer), 13.2 (Me for another diastereomer).

(5a*S*,7*S*)-7-[(1*R*) and (1*S*)- 2-(*N*3-adenyl)-1-methylethyl]-3-methyl-1*H*,7*H*-5a,6,8,9-tetra hydro-1-oxopyrano[4,3-b][1]benzopyran (CP2)

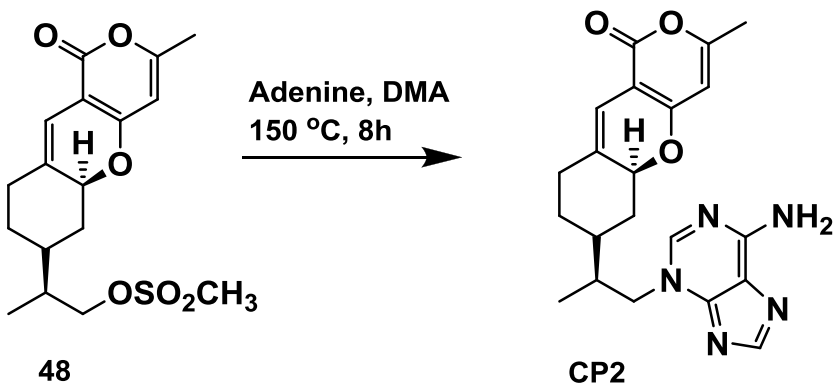

48 CP2

In a round bottom flask fitted with a reflux condenser, taken 6.0 g of mesylate **48** (16.9 mmol) and 2.5 g of adenine (18.6 mmol) together and vacuum dried, purge argon and added 150 mL of distilled DMA and heated at 170 - 180 °C for 8 h. TLC showed no starting material. The reaction was cooled to 25 °C and vacuum distilled to remove DMA. Column chromatographed on silica using a gradient mixture of methylene chloride, ethyl acetate and methanol as eluent to afford CP2 in 20% yield. ^{1}H NMR ($CDCl_3$) δ 8.07 (s, C8 H of adenine), 7.98 and 7.97 (2 s, 1H, C2H of adenine; 2 diastereomers), 6.10 (s, 1H, C10H), 5.72 and 5.71 (2s, 1H, C4H), 5.02 (m, 1H, C5aH), 4.50 (dd, *J* = 14, 7 Hz, 1H, CHN), 4.08 (2dd, *J* = 14, 8 Hz, 1H, CHN; 2 diastereomers), 2.46 (m, 2H), 2.20 and 2.19 (2s, 3H, Me; 2 diastereomers), 2.10 – 1.22 (a series of m, 6H), 0.91 (d, *J* = 47.0 Hz, 3H, Me). ^{13}C NMR ($CDCl_3$) (2 diastereomers) δ 163.2 and 163.1, 162.4, 161.7, 154.4,154.0, 150.7, 142.3, 131.7 and 131.6, 121.0, 199.8, 99.7, 97.3, 79.0, 78.8, 54.5 and 54.4, 38.9, 38.1 and 38.0, 37.1 and 36.9, 36.1, 32.0 and 31.9, 30.7, 27.6, 20.1, 13.3 and 13.2.

2.5.2 Synthesis of TP70.

TP70 was synthesized as shown in **Scheme 2.2**. Hydroboration-amination of compound **46** by treating with BH_3•THF in dry tetrahyrofuran (THF) at 0 ^oC for 2 hours and then warming up to room temperature for another 12 hours followed by refluxing with hydroxylamine-*O*-sulfonic acid (HSA) furnished tricyclic pyrone amine **49** in 50% yield. Treatment of tricyclic pyrone amine **49** with 4-hydroxybenzaldehyde in methanol followed by sodium cyanoborohydride and acetic acid afforded TP70 in 56% yield.

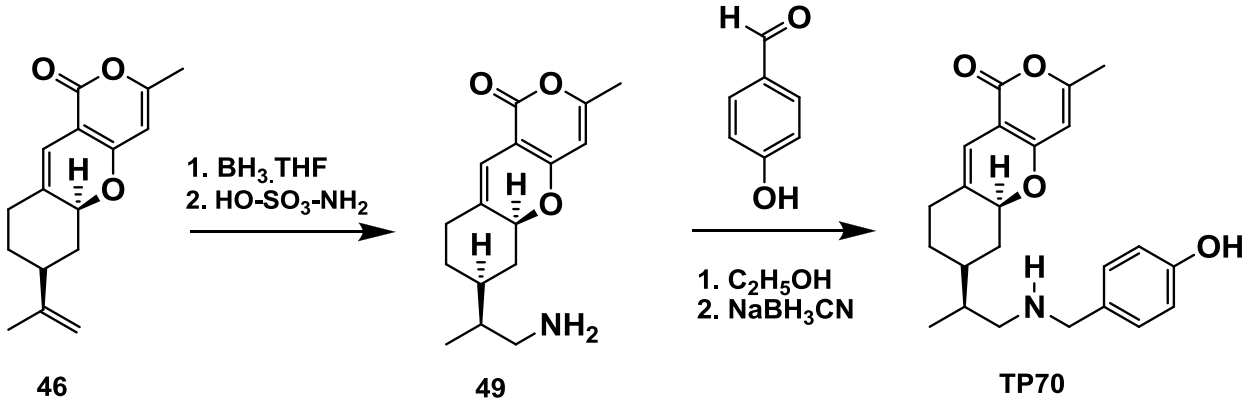

Scheme 2.2 Synthesis of TP70.

(5a*S*,7*S*)-7-[(1*R*) and (1*S*)-2-Amino-1-methylethyl)-3-methyl-1*H*,7*H*-5a,6,8,9-tetrahydro-1- oxopyrano[4,3-b][1]benzopyran (49)

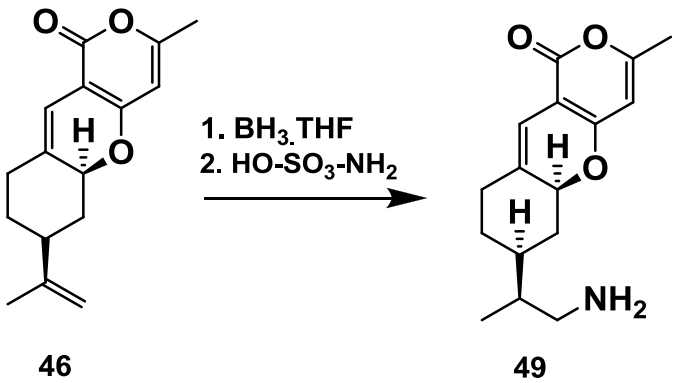

A solution of 10 mL (10.0 mmol) of BH_3•THF complex (1.0 M in THF) was added dropwise to a cold (0 ^oC) solution of 5.0 g (19.4 mmol) of compound **46** in 100 mL of THF, under argon. After stirring the solution at 0 ^oC for 2 h and 25 ^oC for 12 h, the borane solution was added to 3.3 g (29.2 mmol) of hydroxylamine-*O*-sulfonic acid via a cannula followed by the addition of 20 mL of chloroform. The reaction mixture was heated to reflux for 7 h, cooled to 25 ^oC, diluted with 300 mL of ethyl acetate, and extracted with 2 N HCl (100 mL x 2). The combined HCl layer was washed three times with ethyl acetate (100 mL each), basified carefully with 5% sodium carbonate until pH = 9 ~ 10, and extracted three times with dichloromethane. The combined dichloromethane layer was washed with brine, dried (anhydrous Na_2SO_4), and concentrated to give 2.7 g (50% yield) of compound **49**, whose ^1H and ^{13}C NMR spectra are identical to that reported previously from our group.[36]

(5a*S*,7*S*)-3-Methyl-7-[(1*R*) and (1*S*)-1-(4-hydroxybenzylamino)propan-2-yl]-1*H*,7*H*-5a,6,8,9-tetrahydro-1-oxopyrano[4,3-b][1]benzopyran (TP70)

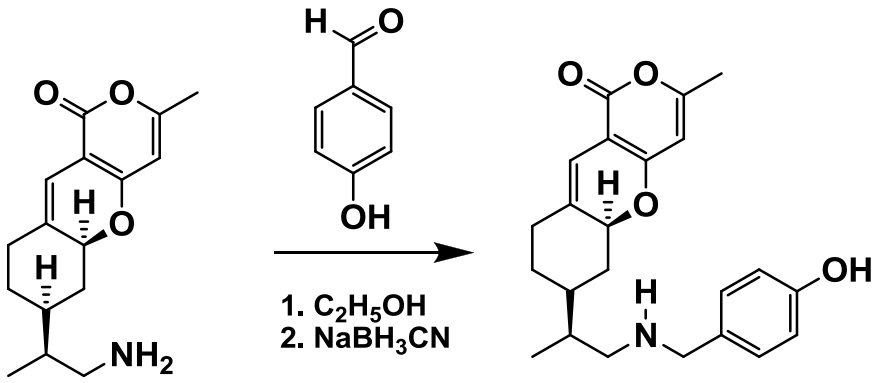

49 **TP70**

A solution of 3.2 g (11.6 mmol) of amine **49** and 1.1 g (8.8 mmol) of 4-methoxy benzaldehyde in 40 ml of dry MeOH was stirred under argon at 25 ^oC for 12 h. To it were added acetic acid (5 drops) and 2.47 g (39 mmol) of $NaBH_3CN$. After stirring for 1 h, the reaction solution was with 200 mL of 5% aqueous ammonium hydroxide and extracted three times with dichloromethane. The combined organic layers was washed with brine, dried ($MgSO_4$), concentrated, and crystallized in ethyl acetate to give 2.5 g (57% yield) of light-yellow solid **TP70** whose ^1H and ^{13}C NMR spectra are identical to that reported previously from our group.[7]

2.5.3 CP2 treatments in neuronal cultures and mouse brain region collection.

These following experiments were performed by Dr. Eugenia Trushina and Dr. Liang Zhang at Mayo Clinic.

Primary cortical neurons were isolated from mouse pups which have 15 – 17 embryonic day (E) and plated at a density of 6 x 10^6 cells per plate in 10-cm plate. The cells were cultured for 5 days before they were treated with 2 μM of CP2 for 24 hrs. To it, 0.01% of DMSO was used as vehicle in control cultures. Media were aspirated off from the culture at the end of the treatment and the cells were washed twice in ice-cold PBS buffer before collected in 0.6 mL of MIBA buffer for mitochondria isolation.

A dose of 50 mg/kg (mice body weight) of CP2 as trifluoroacetic acid (TFA) salt dissolved in water was fed to two of the adult mice wild type (WT, C75/Blc) and APP/PS1 (A/P, transgenic) up to two months before they were sacrificed. One other mice (WT) was served as the control. Mice were sacrificed by cervical dislocation. Specific brain region including cerebellum, hippocampus, cortex and whole brain were harvested from one hemisphere of the mice brain under the microscope in PBS buffer at room temperature and stored the isolated tissue on ice for mitochondria isolation.

Mitochondria isolation process

The tissue were suspended in MIBA buffer containing 10 mM Tris-HCl, pH 7.4, 1 mM EDTA, 0.2 M D-manitol, 0.05M sucrose, 0.5 mM sodium orthovanadate, 1 mM sodium fluoride, 1X complete protease inhibitors and phosphatase inhibitor. The tissue was homogenized with the aid of a Teflon pestle and lysis was confirmed microscopically. The crude nuclei were removed from the lysate by centrifugation at 500 rpm at 4 ^{o}C for 5 min. The remaining supernatant was centrifuged at 8,000 rpm for 10 min at 4 °C, yielding the heavy mitochondrial (HM, pellet) and the light mitochondrial/cytosolic (LM, supernatant) fraction. The HM pellet was washed twice with ice-cold MIBA buffer before it was resuspended in 0.3 mL of this buffer.

2.5.4 TP70 administration and plasma collection.

A dose of 25 mg/kg (mice body weight) of TP70 as trifluoroacetic acid (TFA) salt dissolved in 2% DMSO in 0.5% hydroxypropyl cellulose (HPC) was administered to the male, 3 months old WT C57BL/6NHsd (Harlan) mice by oral (po) or intravenous injection (iv). Cardiac blood collection was treated with ethylenediamine tetraacetic acid (EDTA). About 250 μL plasma was collected from each mouse. All the tissues and plasma collected were stored at -78 ^{0}C until further analysis was carried.

2.5.5 Extraction of CP2 and TP70 from the cells and the tissues.

To the mitochondria fraction solution were added 3 mL of deionized water and 10 mL of 9:1 mixture of ethyl acetate and 1-propanol. Sodium bicarbonate (10 mg) was added to the mitochondria fraction solution and sonicated for 3 minutes. The organic layer was separated from a separatory funnel. The aqueous layer was extracted twice with 10 mL of a 9:1 mixture of ethyl acetate and 1-propanol. The organic layers were combined, washed with 10 mL of brine, dried over anhydrous $MgSO_4$, and concentrated to dryness on a rotary evaporator. The residue was diluted with 1 mL of 1-propanol and filtered through a 0.2 μm filter disc (PTFE 0.2 μm, Fisherbrand) and analyzed using HPLC and mass spectrometry as described below.

In case of TP70, organs were weighed and cut into small pieces. The same procedure as CP2 extraction was then conducted.

2.5.6 Quantification of CP2 and TP70 using HPLC

HPLC analysis of CP2 and TP70 was carried out on a Varian Prostar 210 with a UV-Vis detector. A C18 reverse phase column from Xper-chrom Aegis (S. No: 104117, 250 x 10 mm, 10 micron) was used for both CP2 and TP-70. A flow rate of 10 mL/min and detection wavelength of 254 nm were used. A gradient elution of solvent A, containing deionized water and 0.01 % of trifluoroacetic acid, and solvent B, containing acetonitrile and 0.01 % of

trifluoroacetic acid, was applied for the analysis of CP2. A gradient elution of solvent A, containing deionized water and solvent B, containing methanol was applied for the analysis of TP70.

1,2,4,5-Benzenetetracarboxylic acid (BTA) or 4-methoxyphenol were used as an internal standard to quantify the amount of CP2 and TP70, respectively. BTA does not undergo amide formation reaction with CP2 at ambient temperature because (i) –OH group in carboxylic acid is a poor leaving group and (ii) BTA has a pKa ~ 3 that is lower as compared to the pKa of the amine on the adenine moiety (pKa ~ 9.8) of CP2 resulting in a very small amount of free amine (nucleophile) in the equilibrium as shown in **Scheme 2.3**. Moreover, the presence of 0.01% of trifluoroacetic acid (pKa = 0.52) in the solvents for HPLC regenerates BTA from its salt as.

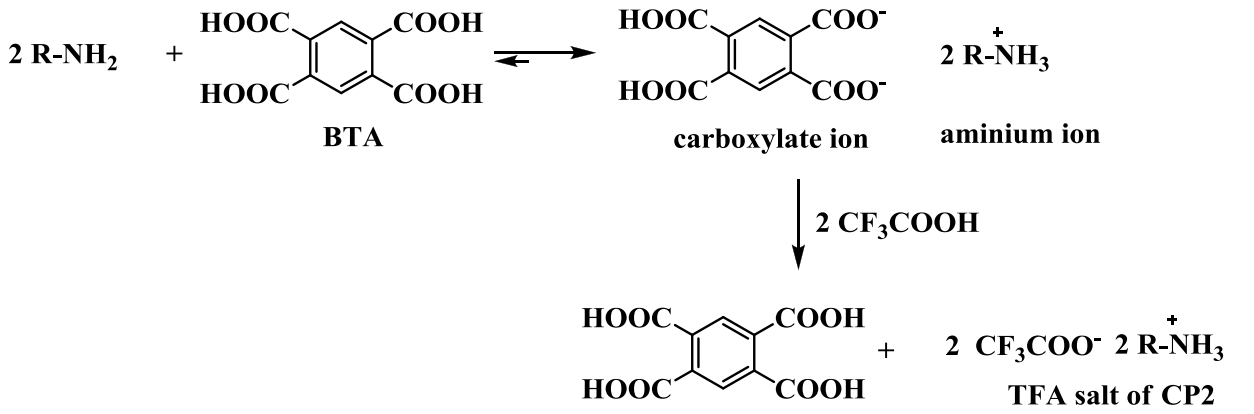

Scheme 2.3 Schematic representation of the regeneration of BTA from the salt of BTA with CP2.

Solutions of 100 µL of various concentrations of pure CP2 and BTA or TP70 and 4-methoxyphenol were injected into an HPLC instrument, the peak areas corresponding to CP2 and BTA or TP70 and 4-methoxyphenol were integrated from the HPLC chromatogram, and the ratios of the peaks were obtained. The results of the ratios of the HPLC peak areas and the ratios from CP2 and BTA or TP70 and 4-methoxyphenol concentrations were plotted, and a linear correlation line was obtained from the graph (**Figure 2.4** and **Figure 2.10**). Hence, using this correlation diagram, the ratio of HPLC peak areas of CP2 and BTA or TP70 and 4-methoxyphenol from cells or tissue extract, and added known amount of BTA to the cells or tissue extract, the amount of CP2 or TP70 in the cells or tissue extract was determined.

Moreover, the eluant corresponding to the peak that has the same retention time as that of CP2 or TP70 from the injection of the cells or tissue extract was collected, and their masses were determined using mass spectrometer. The mass spectrometer acquired from the collected peak of CP2 and TP70 from the cells or tissue extract were identical to that of pure CP2 and TP70 mass spectra. The eluent corresponding to CP2 or TP70 peak from the HPLC was collected and injected into the mass spectrometer. A mass of 394 corresponding to $[M+H^+]$ of CP2 was found in their mass spectra and the fragmentation pattern of this $[M+H^+]$ mass is similar to that of pure CP2 verifying the identity of CP2. A mass of 382 and 404 corresponding to $[M+H^+]$ and $[M+Na^+]$ of TP70 were found in their mass spectra which is identical to that of pure TP70 verifying the identity of TP70.

To determine the volume or weight of cells, total DNA or protein content within the tissues or cell is normally chosen to normalize the data obtaining from any assay. In the series of experiments had done for CP2, protein content within the cells or tissues is the most appropriate denominator, hence μM CP2 per mg of total protein found within the cell or tissue was chosen to normalize for the experiments. This is performed by Dr. Liang Zhang at Mayo Clinic. One may also normalize the result to wet weight of the tissue; however, since the mass of cells in cultures can not "weigh out" or obtain fixed volume after mitochondria isolation process, the most sensible approach would be using total protein content.

The concentration of TP70 in the organs was obtained by finding the number of moles of TP70 in the given volume of the organs (assuming that mass of organs = volume of organs ~ 1).

2.6 References

1. Wolfe, M. S. Introduction to special issue on Alzheimer's disease , *J. Med. Chem.*, **2012**, 55, 8977-8978.

2. http://www.alz.org/alzheimers_disease_what_is_alzheimers.asp

3. http://www.alz.org/downloads/facts_figures_2013.pdf

4. Reitz, C. Alzheimer's disease and the amyloid cascade hypothesis: a critical review. *Int. J. Alzheimer's disease*, **2012**, article ID 369808, 11 pp.

5. Maezawa, I.; Hong, H.-S.; Wu, H.-C.; Battina, S. K.; Rana, S.; Iwamoto, T.; Radke, G. A.; Pettersson, E.; Martin, G. M.; Hua, D. H.; Jin, L. W. A novel tricyclic pyrone compound ameliorates cell death associated with intracellular amyloid-beta oligomeric complexes. *J. Neurochem*. **2006**, 98, 57−67.

6. Hong, H. S.; Rana, S.; Barrigan, L.; Shi, A.; Zhang, Y.; Zhou, F.; Jin, L.-W.; Hua, D. H. Inhibition of Alzheimer's amyloid toxicity with a tricyclic pyrone molecule in vitro and in vivo. *J. Neurochem*. **2009**, 108, 1097−1108.

7. Pokrel, L.; Maezawa, I.; Nguyen, T. D.T.; Chang, K.; Jin, L. W; Hua, D. H. Inhibition of Acyl-CoA: Cholesterol Acyltransferase (ACAT), Overexpression of cholesterol transporter gene, and protection of amyloid β (Aβ) oligomers-induced neuronal cell death by tricyclic pyrone molecules. *J. Med. Chem*. **2012**, 55, 8969-8973.

8. Crowther R. A. Structural aspects of pathology in Alzheimer's disease. *Biochim. Biophys. Acta.* **1991**, 1096, 1-9.

9. De Felice F.G., Wu D., Lambert M.P. et al. Alzheimer's disease type neuronal tau hyperphosphorylation induced by Aβ oligomers. *Neurobiol. Aging*, **2008**, 29, 1334-1337.

10. Lee, V. M. Regulation of tau phosphorylation in Alzheimer's disease, *Annals of New York Academy of Sciences,* **1996**, 777, 107-113.

11. Hardy, J.; Selkoe, D. J. The amyloid hypothesis of Alzheimer's disease: progress and problems on the road to therapeutics, *Science*, **2002**, 297, 353-356.

12. Kivipelto, M.; Ngandu, T.; Fratiglioni, L.; Viitanen, M.; Kareholt, I.; Winblad, B.; Helkala, E. L.; Tuomilehto, J.; Soininen, H.; Nissinen, A. Obesity and vascular risk factors at midlife and the risk of dementia and Alzheimer disease, *Arch Neural*, **2005**, 62, 1556-1560.

13. Plassman, B. L.; Havlik, R. J.; Steffens, D. C.; Helms M. J.; Newman, T. N.; Drosdic, D.; Phillips, C.; Gau, B. A.; Welsh-Bohmer, K. A.; Burke, J. R.; Guralnik, J. M.;

Breitner, J. C. Documented head injury in early adulthood and risk of Alzheimer's disease and other demetias, *Neurology*, **2000**, 55, 1158-1166.

14. Wirth O., Multhaup G. and Bayer T. A. A modified β-amyloid hypothesis: intraneuronal accummulation of the β-amyloid peptide – the first step of a fatal casscade, *J. Neurochem*, **2004**, 91, 513-520.

15. Gouras G. K., Almeida C. G. and Takahashi R. H. Intraneuronal Aβ accummulation and origin of plaques in Alzheimer's disease, *Neurobiol. Aging*, **2005**, 26, 1235-1244.

16. Kienlen-Campard P., Miolet S., Tasiaux B. et al. Intracellular amyloid-β 1-42, but not extracellular soluable amyloid-β peptides, induces neuronal apoptosis. *J. Biol. Chem*. **2002**, 277, 666-615.

17. Zhang Y., Mc Laughlin R., Goodyer C. et al. Selective cytotoxicity of intracellular amyloid-β peptide 1-42 through p53 and Bax in cultured primary human neurons. *J. Cell Biol.*, **2002**, 156, 519-529.

18. Wolozin, B. Cholesterol and the biology of Alzheimer's disease. *Neuron*, **2004**, 41, 7−10.

19. Mahley, R. W.; Weisgraber, K. H.; Huang, Y. Apolipoprotien ε4: A causative factor and therapeutic target in neuropathology including Alzheimer's disease *PNAS*, **2006**, 103, 5644-5651.

20. Wisniewski, T.; Castano, E. M.; Golabek, A.; Vogel, T.; Frangione, B. Acceleration of Alzheimer's fibril formation by apolipoprotein E in vitro, *Am. J. Pathol.*, **1994**, 145, 1030-1035.

21. Distl, R.; Meske, V.; Ohm, T. G.; Tangle-bearing neurons contain more free cholesterol than adjacent tangle-free neurons, *Acta Neuropathol.*, **2001**, 101, 547-554.

22. Fukumoto, H.; Deng, A.; Irizarry, M. C.; Fitzgerald, M. L.; Rebeck, G. W. Induction of the cholesterol transporter ABCA1 in central nervous system cells by liver X receptor agonists increases secreted Abeta levels. *J. Biol. Chem*. **2002**, 277, 48508−48513.

23. Mayeux, R.; Sano, M.; Chen, J.; Tatemichi, T.; Stem, Y. Risk of dementia in first-degree relatives of patients with Alzheimer's disease and related disorders, *Arch Neurol,* **1991**, 48, 269-273.

24. Schmitz, G.; Robenek, H.; Beuck, M.; Krause, R.; Schurek, A.; Niemann, R. Ca^{+2} antagonists and ACAT inhibitors promote cholesterol efflux from macrophages by different mechanisms. I. Characterization of cellular lipid metabolism. *Arterioscler. Thromb. Vasc. Biol.* **1988**, 8, 46−56.

25. Puglielli, L.; Tanzi, R. E.; Kovacs, D. M. Alzheimer's disease: the cholesterol connection. *Nature Neurosci*. **2003**, 6, 345−351.

26. Huttunen, H. J.; Kovacs, D. M. ACAT as a drug target for Alzheimer's disease. *Neurodegener. Dis.* **2008**, 5, 212−214.

27. Hutter-Paier, B.; Huttunen, H. J.; Puglielli, L.; Eckman, C. B.; Kim, D. Y.; Hofmeister, A.; Moir, R. D.; Domnitz, S. B.; Frosch, M. P.; Windisch, M.; Kovacs, D. M. The ACAT inhibitor CP-113, 818 markedly reduces amyloid pathology in a mouse model of Alzheimer's disease. *Neuron,* **2004**, 44, 227−238.

28. Michael T. Lin and M. Flint Beal, Mitochondria dysfunction and oxidative stress in neurodegenerative diseases. *Nature*, **2006**, 787-795.

29. P.H. Reddy and M.F. Beal, Are mitochondria critical in the pathogenesis of Alzheimer's disease? *Brain Res Rev,* **2005***,* 49, 618–632.

30. X. Zhu, M.A. Smith, G. Perry and G. Aliev, Mitochondrial failures in Alzheimer's disease, *Am J Alzheimers Dis Other Demen.,* **2004,** 19**,** 345–352.

31. Crouch, P. J., Blake, R., Duce, J. A., et al. Copper-dependent inhibition of human cytochrome c oxidase by a dimeric conformer of amyloid-beta1–42. *Journal of Neuroscience*, **2005**, 25, 672–679.

32. Caspersen, C., Wang, N., Yao, J., Sosunov, A., Chen, X., Lustbader, J. W., et al. Mitochondrial Abeta: A potential focal point for neuronal metabolic dysfunction in Alzheimer's disease. *FASEB Journal*, **2005**, 19, 2040–2041.

33. Manczak, M., Park, B. S., Jung, Y., & Reddy, P. H. Differential expression of oxidative phosphorylation genes in patients with Alzheimer's disease: Implications for early mitochondrial dysfunction and oxidative damage. *Neuromolecular Medicine*, **2004**, 5, 147–162.

34. Lustbader, J. W., Cirilli, M., Lin, C., et al. ABAD directly links Abeta to mitochondrial toxicity in Alzheimer's disease. *Science*, **2004**, 304, 448–452.

35. Reddy, P. H., & Beal, M. F. Amyloid beta, mitochondrial dysfunction, and synaptic damage: Implications for cognitive decline in aging and Alzheimer's disease. *Trends in Molecular Medicine*, **2008**, 14, 45–53.

36. Hua, D. H.; Huang, X.; Tamura, M.; Chen, Y.; Woltkamp, M.; Jin, L.-W.; Perchellet, E. M.; Perchellet, J. P.; Chiang, P. K.; Namatame, I.; Tomoda, H. Synthesis and bioactivities of tricyclic pyrones, *Tetrahedron*, **2003**, 59, 4795-4803.

37. Michelle A. Clark **,** Richard Finkel, Jose A. Rey **,** Karen Whalen, *Lippincott's Illustrated Reviews: Pharmacology*, 3rd ed. ; Lippincott Williams and Wilkims, 2006.

38. Milo Gibaldi, *Biopharmaceutics and Clinical Pharmacokinetics*, 4th ed.; Lea and Febiger, 1991.

Chapter 3. Synthesis of unnatural aminal acids for the preparation of novel tripeptidyl anti-viral inhibitors.

3.1 Introduction

With the emergence of the GII.4 Sydney strain of norovirus in 2012, the search for a therapeutic drug has become even more essential than previously thought. Norovirus (NV) is detrimental to human way of life because contagious fecal particles can be transmitted several ways, like ingestion, direct contact, and through air, which are all easily permissible due to how interconnected our society is. Therefore, once a person becomes contaminated, the virus will spread easily and affect those, especially in enclosed quarters, like that of cruise ships, hospitals, and school dormitories. Often mislabeled as the stomach flu or food poisoning, this gastroenteritis-causing virus inflames the stomach and/or intestines while producing symptoms like diarrhea, fever, nausea, vomiting, body ache, et cetera.[1] No medication currently exists, so anyone affected experiences the symptoms for an average three days; however, the elderly, immune deficient and young children will have a harder time recovering. In fact, there are 70,000 hospitalizations and over 800 deaths annually[2], in the United States, alone. Current therapeutics, such as Tamiflu, utilizes a small synthesized organic compound that inhibits the release of viral molecules into the surrounding environment of the body by targeting one of the virus' surface proteins. However, this medicine can only be used specifically for the influenza virus strain. Therefore, it is important to create an anti-viral therapeutic to reduce casualties that occur from the various norovirus strains.

Previous study in our group[3] has discovered a novel, highly active tripeptidyl compound for broad-spectrum viral inhibition; however, oral bioavailability of this drug is poor. Our research group is currently synthesizing the tripeptidyl analogue in three separate parts. The amino acid utilizes the P1 and P2 parts for recognition of the norovirus cleavage site, while it includes P3 with the intention of bettering its bioavailability and aiding cell penetration (**Figure 3.1**). My work involved in the synthesis of the P3 unnatural amino acid for the preparation of a

novel tripeptidyl compound. The main focus is on increasing the hydrophilicity of the amino acid by incorporating polar hydroxyl groups which will help increase the oral bioavailability of the drug. It has been found that several viruses, in fact, have conserved specificity for cleavage sites at the P1 and P2 sites, making this amino acid analogue a possible broad-spectrum therapeutic, capable of inhibiting the norovirus, SARS, HAV, and rhinovirus' proteases.

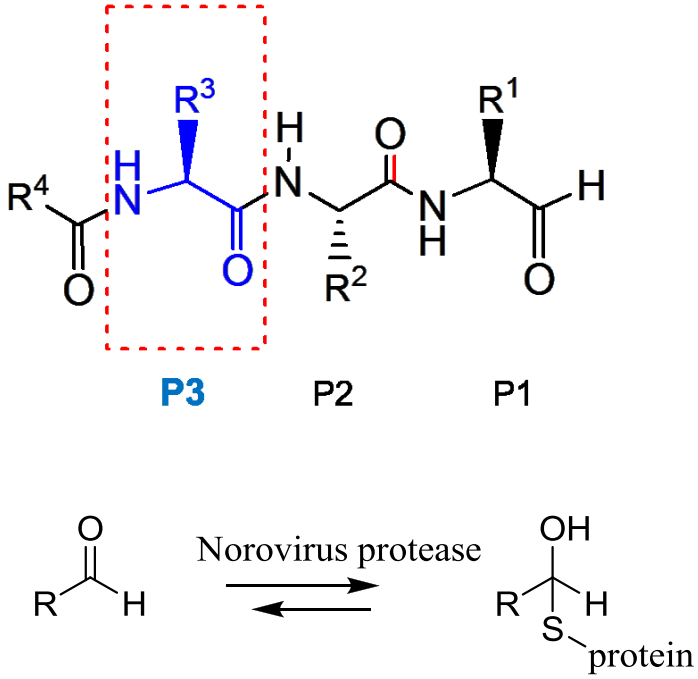

Figure 3.1 Generic tripeptidal protease inhibitor structure and the reversibility of the aldehyde warhead and cysteine residue at the active site of norovirus.

3.2 Background

Noroviruses (NVs) are a non-enveloped, single stranded RNA with a positive sense genome belonging to the family of Calcivirdae. It is 7.5 kBp and approximately 60 kDa. Its mutation rate is very high, occurring on average of every two to three years. The genome has been found to contain three open reading frames (ORFs) as shown in **Figure 3.2**.[4]

Figure 3.2 Norovirus Genome.

Overall, there are five norovirus genogroups (GI, GII, GIII, GIV and GV), and they all vary slightly because the virus does not contain a proofreading mechanism, unlike that found in human DNA replication. Viruses most commonly infecting humans belong to GI and GII. In the non-structural proteins of the ORF1 (open reading frame 1), the norovirus genome contains the 3C-like protease (3CL). This protease is important to the virus' survival because it cleaves the non-structural proteins to form mature proteins, and therefore, an active virus that can be packaged and sent to infect other cells.

According to previous studies[5,6] the protease's active site has conserved specificity among several strains of norovirus, which makes it an effective target spot for an anti-viral inhibitor. The 3CL protease normally cleaves the replicated peptide strand to produce functional proteins; therefore, by identifying the specific amino acid residues at the active site, the norovirus protease cannot cut necessary portions as the drug will competitively block that spot. The most important residue for the substrate specificity is a glutamine amino acid residue, and therefore, the P1 site of the inhibitor is a surrogate glutamine containing an aldehyde warhead that allows a nucleophilic attack by the thiol function of cysteine residue in norovirus 3CL

protease. The P2 site, which is a leucine residue, is also important for recognition of the virus active site because it fits in the pocket created by the protease's catalytic dyad.

Our efforts to create a new anti-NV drug focus primarily on the inhibition of NV 3C-like protease ($NV3CL^{pro}$). We recently reported a novel class of tripeptidal anti-Noroviral compounds which strongly inhibit $NV3CL^{pro}$ in enzyme and cell based assay.[3] Compound **50** and **51** were found to be two of the most active compounds with IC_{50} 0.14 μM; EC_{50} 0.04 μM and IC_{50} 0.21 μM; EC_{50} 0.06 μM, respectively. Compound **50** has an aldehyde warhead, a P1 glutamine surrogate, a P2 leucine, a P3 L-1-napthylalanine and an *N*-terminal Cbz cap (**Figure 3.3**). Compound **51** has similar structure to compound **50** except of the P3 has the benzyl funtionality group. The warhead is the part of the molecule that is forming covalent bond with the enzyme (aldehyde function or ketoamide function). Compound **50** and **51** also possess strong inhibitory against other viral strains in the caliciviridae, picornavirus, and coronaviridae viral families especially human rhino virus (HRV) and SARs. The compounds also show minimal cell cytotoxicity. These encouraging results prompted us to conduct an ongoing study to improve activity and bioavailability for the lead compounds which will be discussed in the following section.

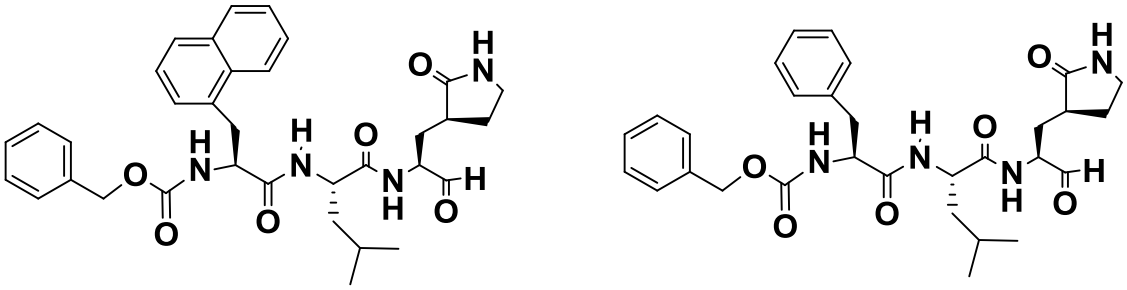

Figure 3.3 Chemical structure of compound **50** and **51**.

3.3 Synthesis of P3 unnatural amino acids for the preparation of novel tripeptidyl compounds.

We hypothesize that incorporating a polar hydroxyl group in the P3 part would help increase hydrogen bonding between the enzyme active site and the drug leading to a stronger binding and ultimately will help oral bioavailability of the drug. In fact, computation docking of compound **50** with SARs protease enzyme (pdb file SARS-CoV-3CL) revealed that adding the *meta* hydroxyl group on the P3 L-1-napthylalanine of compound **50** can provide additional hydrogen bonding between the acid moiety of glutamic acid (Glu) and the OH (**Figure 3.4**). The docking results were supported by a single-crystal X-ray analysis of a complex of SARs-$3CL^{pro}$ and **50** (unpublished results)**.** This helps improve the binding affinity and reducing the partition coefficient value.

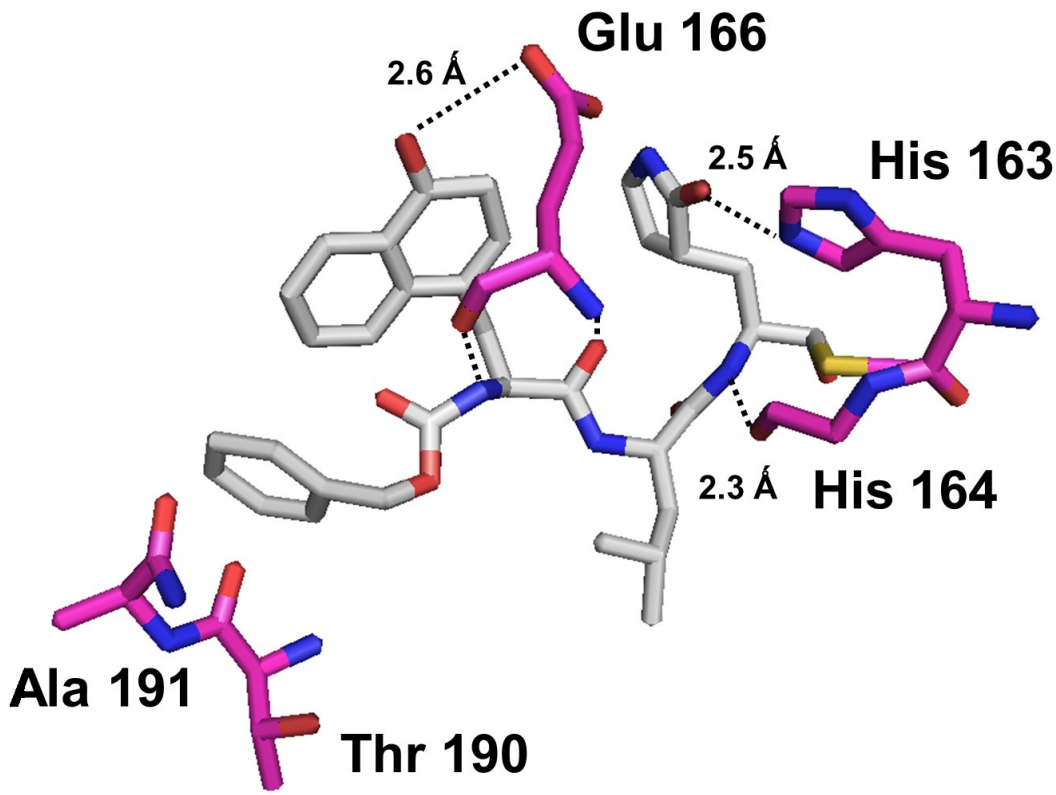

Figure 3.4 Computational docking of compound **50** derivative (Napthylalanine-C3-OH) in complex with SARs protease enzyme (pdb file SARS-CoV-3CL).

Therefore, the P3 unnatural amino acid (**Figure 3.5**) for the preparation of a novel tripeptidyl compound is synthesized as shown in **Scheme 1**.

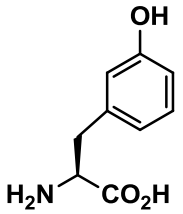

Figure 3.5 Chemical structure of P3 [((*S)*-3-hydroxyphenylalanine)][7] unnatural amino acid.

Following the reported procedure[7], protection of 3-hydroxybenzaldehyde by using *tert*-butyldimethylsilyl chloride in the presence of triethylamine and DMAP in dichloromethane at 25^{o}C for 2 hours to give **52** in 90% yield. Aldehyde **52** was reduced by using sodium borohydride ($NaBH_4$) in ethanol at 0 ^{o}C for 1 hour to obtain alcohol **53** in 93% yield. Bromination of compound **53** by using triphenylphosphine (PPh_3) and NBS in CH_2Cl_2 at 25^{o}C for 5 hours to give **54** in 70% yield. Reaction of diethyl acetamidomalonte (**55**) with **54** in absolute ethanol in the presence of one equivalent of sodium ethoxide (NaOEt) led to the disubstituted malonyl diester **56** in 63% yield. Diester **56** was saponified to afford the mono ester **57** in a 32% yield. Decarboxylation of neat mono ester **57** occurred at 160 ^{o}C in vacuum within 10 minutes to give racemic **58a** and **58b** which was then resolved by using enzyme Subtilisin in DMSO to obtain **59a** in 12 % yield**.** The acetamide protecting group of compound **59a** will be removed by acid hydrolysis to give **60** (*S*)-3-hydroxyphenylalanine. The final step was not done due to only a small amount of compound **59a** was afforded which was not enough to continue for the final step.

Scheme 3.1 Synthesis of P3 unnatural amino acid.

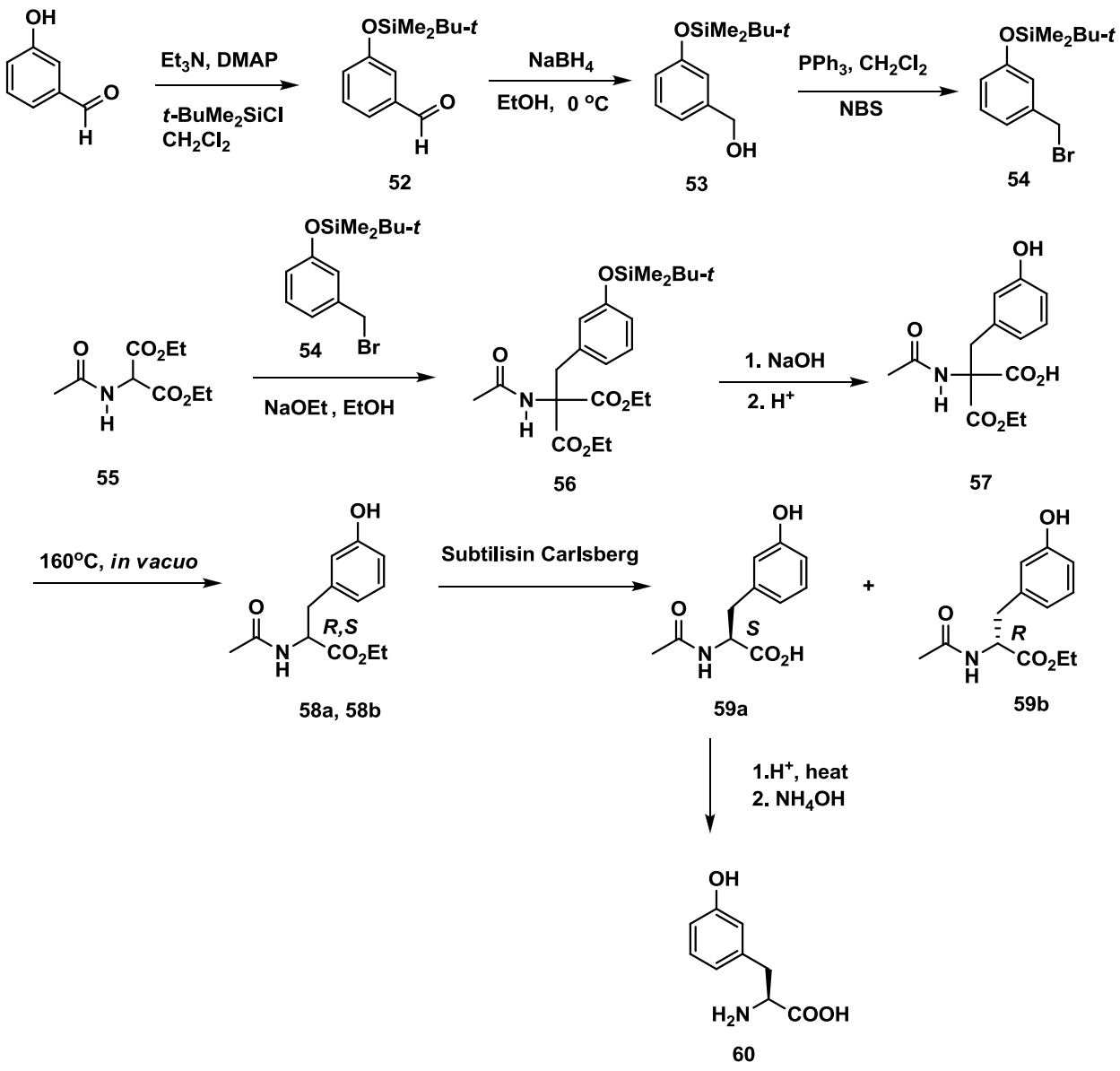

3.4 Conclusion

An unnatural amino acid was synthesized using the above method for the creation a novel tripeptidyl compound. This simple synthesis method can also be used as a model method for the synthesis of other unnatural amino acids for preparation of novel tripeptidyl anti-viral inhibitors. After incorporating the synthesized P3 into P1 and P2 amino acids to form the tripeptidyl compound, a biological evaluation will be completed to test for bioactivity. Moreover, structure-activity relationship study will show if our estimations are correct and if we are headed in the right direction of improving our tripeptidyl compounds. In addition, this compound will be also tested against other similarly structured viruses to determine whether our novel tripeptidyl compound can act as a broad-spectrum viral protease inhibitor.

3.5 Experimental section

3-(tert-Butyldimethylsilanyloxy)benzaldehyde (52)

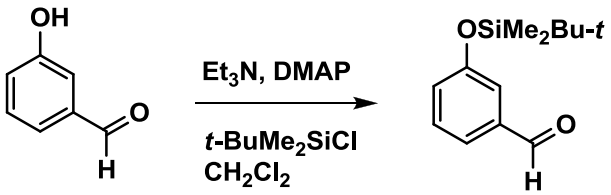

52

To a solution of 5.0 g (41 mmol) of 3-hydroxybenzaldehyde in 100 mL of distilled dichloromethane at 0 ^{o}C under argon, were added 11.5 mL of triethylamine, 0.75 g (6 mmol) of 4-dimethylaminopyridine (DMAP), and 12.4 g (0.82 mol) of *tert*-butyldimethylsilyl chloride and the solution was stirred at 25 ^{o}C for 2 hours. The reaction was diluted with 150 mL of diethyl ether and washed with 100 mL of saturated aqueous NH_4Cl solution, 20 mL of water, and 20 mL of brine. The organic layer was dried over anhydrous $MgSO_4$, concentrated, and column

chromatographed on silica gel using a mixture of hexane and diethyl ether as an eluent to give 8.72 g of product **52** (90.2% yield). ^{1}H NMR ($CDCl_3$) δ 9.96 (s, 1H), 7.48 (m, 1H), 7.42 (t, J = 7.81 Hz, 1H), 7.34 (m, 1H), 7.09 – 7.15 (m, 1H), 1.01 (s, 9H), 0.24 (s, 6H).

3-tert-Butyldimethylsilyloxybenzyl alcohol (53)

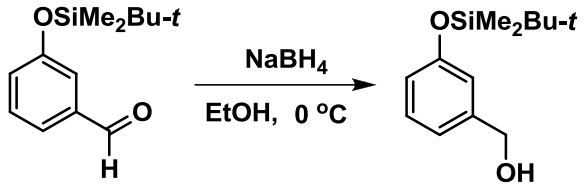

52 **53**

To the solution **52** (9.41 g, 39.8 mmol) in 100 mL of ethanol, sodium borohydride ($NaBH_4$, 0.75g, 19.9 mmol) was added at 0 °C. The mixture was stirred at 0 °C for 1 hour. The reaction solution was diluted with 200 mL of ether, washed with 50 mL aqueous. The aqueous layer was extracted 2 times with ether (100 mL each time). The combined organic layers were washed with brine, dried over anhydrous sodium sulfate, and concentrated to give 8.79 g of product **53** (92.6% yield). ^{1}H NMR ($CDCl_3$) δ 7.22 (t, 1H, J = 7.81 Hz), 6.96 (d, 1H, J = 7.81 Hz), 6.87 (s, 1H, J = 1.5 Hz), 6.75 - 6.80 (m, 1H), 4.65 (d, 2H, J = 5.5 Hz), 1.00 (s, 9H), 0.21 (s, 6H).

3-(tert-Butyldimethylsilyloxy)Benzyl Bromide (54)

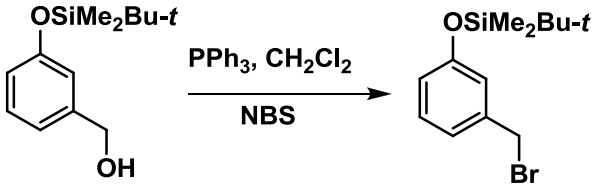

53 **54**

To a solution of compound **53** (8.79 g, 36.9 mmol), triphenylphosphine PPh_3 (14.5g, 55.4 mmol) in distilled CH_2Cl_2 (100 mL), *N*-bromosuccinimide (NBS, 9.86 g, 55.4 mmol) was added at 0 °C. The reaction was stirred under argon at room temperature for 5 hours. The

reaction was diluted with 50 mL water and extracted with CH_2Cl_2 (150 mL x 2). The combined organic layers were washed with brine, dried over sodium sulfate, filtered, and concentrated. The oily concentrate was column chromatographed on silica gel using a gradient mixture of hexane and diethyl ether as eluants to give 7.85 g of product **54** (70.8% yield). ^{1}H NMR ($CDCl_3$) δ 7.20 (t, 1H, *J* = 7.81 Hz), 6.96 (d, 1H, *J* = 7.7 Hz), 6.88 (t, 1H, *J* = 1.95 Hz), 6.75 – 6.80 (m, 1H), 4.45 (s, 2H), 0.99 (s, 9H), 0.20 (s, 6H). ^{13}C NMR (CDCl3), δ 156, 139.3, 129.9, 122.1, 121.0, 120.4, 33.6, 25.9, 18.4, –4.2. MS (electronspray ionization) *m/z* 325 ($M+Na^+$).

Diethyl 2-acetamido-2-(3-(*tert*-butyldimethylsilyloxy)benzyl)malonate (56)

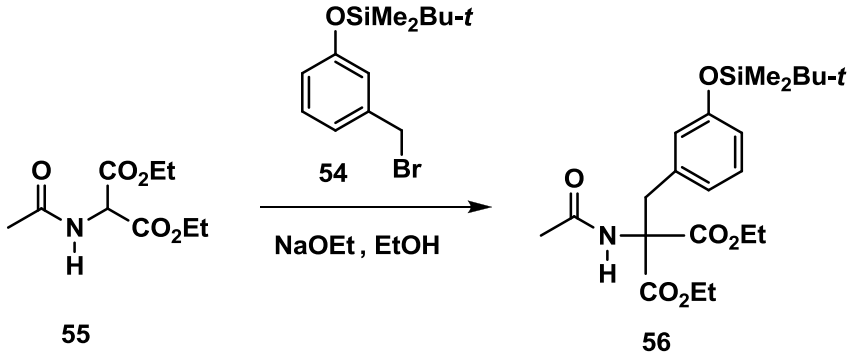

Sodium (77.4 mg, 3.37 mmol) was dissolved in absolute ethanol (10 mL). After the mixture was cooled down to 0 ^{o}C, diethyl acetamidomalonate **55** (0.73 g, 3.37 mmol) was added under argon. Compound **54** (1 g, 3.33 mmol) in absolute ethanol (10mL) was added after 5 minutes stirring at 0 ^{o}C. The reaction mixture was refluxed for 6 hours. Once cooled to room temperature, the solution was concentrated, and the crude was column chromatographed on silica gel using a gradient mixture of hexane and diethyl ether as eluants to give 0.94 g of product **56** (64% yield). ^{1}H NMR ($CDCl_3$) δ 7.11 (t, *J* = 7.81 Hz, 1H), 6.72 (d, *J* = 7.81 Hz, 1H), 6.60 (d, *J* = 7.03 Hz, 1H), 6.56 (br. s, 1H), 6.51 (s, 1H), 4.20 - 4.34 (m, 4H), 3.59 (s, 2H), 2.03 (s, 3H), 1.25 - 1.34 (m, 6H), 0.98 (s, 9H), 0.18 (s, 6H).

2-acetamido-3-ethoxy-2-(3-hydroxybenzyl)-3-oxopropanoic acid (57)

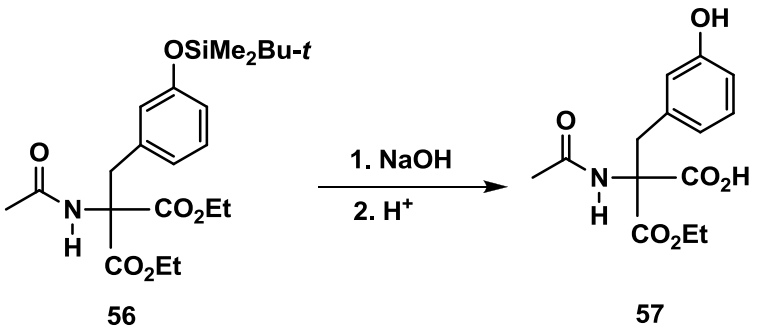

56 57

To a solution of compound **56** (0.7 g, 1.6 mmol) in 1 mL dioxane, was added NaOH (0.13 g, 3.2 mmol) in 1mL of 1:9 H_2O:dioxane solution. After 15 hours stirring at room temperature, the reaction mixture was acidified with 1 N HCl (pH = 3 – 4), and extracted with ethyl acetate. Organic layers were dried with sodium sulfate, filtered and concentrated to give 0.16 g of compound **57** (45% yield). ^{1}H NMR (DMSO-d_6) δ 8.99 - 9.08 (s, 1H), 6.87 - 6.94 (m, 1H), 6.58 - 6.63 (m, 1H), 6.45 - 6.49 (m, 1H), 6.39 - 6.44 (m, 1H), 3.84 - 4.08 (m, 4H), 1.78 (s, 3H), 1.09 (t, 3H).

Ethyl-2-acetamido-3-(3-hydroxyphenyl)propanoate (58a, 58b)

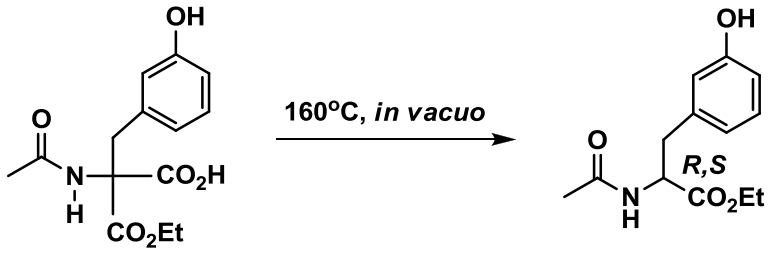

57 58a, 58b

Compound **57** (0.15 g, 0.52 mmol) was decarboxylated at 160°C under vacuo in 10 minutes. After cooling to room temperature, the crude was column chromatographed on silica gel using a gradient mixture of hexane and ethyl acetate as eluants to give 40 mg mixture of **58a, 58b** (30.5% yield). ^{1}H NMR ($CDCl_3$) δ 7.15 (t, *J* = 7.81 Hz, 1H), 6.71 - 6.77 (m, 1H), 6.65 -

6.68 (m, 1H), 6.31 (s, 1H), 6.05 (d, *J* = 7.42 Hz, 1H), 4.86 (td, *J* = 6.05, 7.81 Hz, 1H), 4.19 (q, *J* = 7.03 Hz, 2H), 3.02 - 3.14 (m, 2H), 2.02 (s, 3H), 1.25 (t, *J* = 7.22 Hz, 3H).

(*S*)-ethyl-2-acetamido-3-(3-hydroxyphenyl)propanoate (59a)

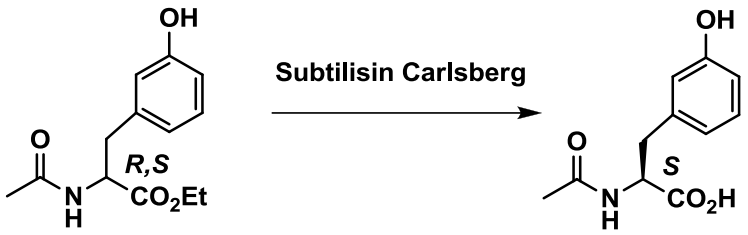

58a, 58b **59a**

To a solution of of **58a, 58b** (40 mg, 0.16 mmol) in 1 mL of dimethyl sulfoxide (DMSO) was added deionized water (0.5 mL), and 1 N KCl (0.14 mL). Subtilisin Carlsberg (1 mg) was dissolved in deionized water (0.5 mL) and 0.1. N KCl solution (80 μL). The enzyme solution (0.3 mL) was added to the reaction and the mixture was stirred at 39 ^{o}C for 1 hour. 0.15 mL and 50 μL of the enzyme solution was added to the reaction after stirring for 1 hour and 3 hours, respectively. The reaction was diluted with deionized water (10 mL). The aqueous layer was acidified with 1 N HCl to pH = 3, extracted three times with ethyl acetate (10 mL each time). Combined organic layers were washed with water, brine, dried with sodium sulfate, filtered and concentrated to give 4.2 mg of compound **59a** (12 % yield). ^{1}H NMR (DEUTERIUM OXIDE) δ 7.11 - 7.20 (m, 1H), 6.73 - 6.79 (m, 1H), 6.69 - 6.73 (m, 1H), 6.65 - 6.70 (m, 1H), 4.36 - 4.43 (m, 1H), 3.03 - 3.11 (m, 1H), 2.76 - 2.86 (m, 1H), 1.84 (s, 3H). MS (electronspray ionization) *m/z* 246 ($M+Na^{+}$).

3.6 References

1. Rocha-Pereira, J.; Nascimento, M. S. J., *Targeting Norovirus: Strategies for the Discovery of New Antiviral Drugs*. InTech: Rijeka, 2012; p 121-150.
2. Center for Disease Control and Prevention. (2013). *Norovirus.* Retrieved from: http://www.cdc.gov/norovirus/about/overview.html.
3. Allan M. Prior, Yunjeong Kim, Sahani Weerasekaraa, Meghan Morozea, Kevin R. Allistonc, Roxanne Adeline Z. Uyc, William C. Groutas, Kyeong-Ok Chang, Duy H. Hua. Design, synthesis, and bioevaluation of viral 3C and 3C-like protease inhibitors, Bioorganic & Medicinal Chemistry Letters **2013,** 23, 6317–6320.
4. Rocha-Pereira, J.; Jochmans, D.; Dallmeier, K.; Leyssen, P.; Cunha, R.; Costa, I.; Nascimento, M. S.; Neyts, J., *Biochem Biophys Res Commun* **2012,** 427, (4), 796-800.
5. Kim, Y., Lovell, S., Tiewc, K., Mandadapuc, S.R., Allistonc, K.R., Battailed, K.P.,…Changa, K. (2012). Broad-spectrum antivirals against 3C or 3C-like proteases of picornaviruses, noroviruses, and coronaviruses. *Journal of Virology, 86*(21), 11754-11762. Doi:10.1128/JVI.01348-12.
6. Hussey, R.J.., Coates, L., Gill, R.S., Erskine, P.T., Coker, S., Mitchell, E., …Shoolingin-Jordan, P.M. (2010). A structural study of norovirus 3C protease specificity: binding of a designed active site-directed peptide inhibitor. *Biochemistry, 50*(2), 240-249. doi:10.1021/bi1008497.
7. Rodriguez, M., Bernad. N., Galas, M.C., Lignon, M.F., Laur, J., Aumelas, A., and Martinez, J. (1991). Synthesis and biological activities of cholecystokinin analogues substituted in position 30 by 3-(1-napthyl)-L-alanine [Nal(1)] or 3-(2-naphthyl)-L-alanine [Nal(2)]. *Eur J Med Chem., 26*, 245-253.

Appendix A - ^{1}H NMR, ^{13}C NMR, IR and MS SPECTRA

Appendices: 1H NMR, 13C NMR, and IR Spectra

Compound 20 ^{1}H NMR

Acquisition Time (sec)	1.9945	***Comment***	STANDARD 1H OBSERVE			***Date***	May 14 2009
Date Stamp	May 14 2009	***File Name***	C:\USERS\KESHAR\DESKTOP\NMR\BOOK 4\KP-4-91-DPPURE.FID\FID				
Frequency (MHz)	199.98	***Nucleus***	1H	***Number of Transients***	36	***Original Points Count***	5984
Points Count	8192	***Pulse Sequence***	s2pul	***Receiver Gain***	40.00	***Solvent***	CHLOROFORM-d
Spectrum Offset (Hz)	1002.0226	***Spectrum Type***	STANDARD	***Sweep Width (Hz)***	3000.30	***Temperature (degree C)***	AMBIENT TEMPERATURE

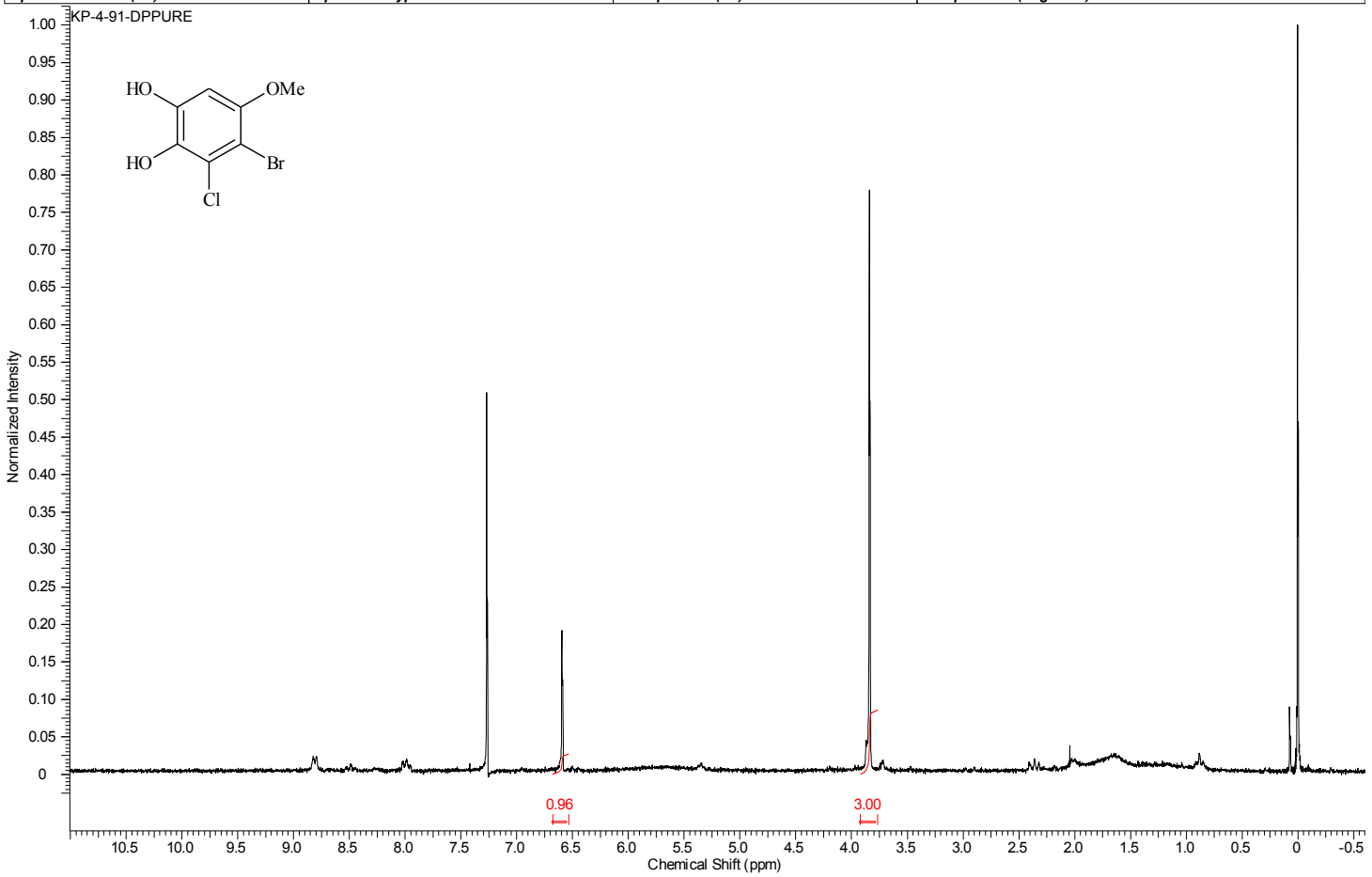

Compound 20 ^{13}C NMR

6/27/2012 3:30:36 PM

Acquisition Time (sec)	1.3005	***Comment***	Std proton	***Date***	Jul 13 2009	***Date Stamp***	Jul 13 2009
File Name	C:\USERS\KESHAR\DESKTOP\NMR\OTHERS\KP-4-78-C13\FID					***Frequency (MHz)***	100.53
Nucleus	13C	***Number of Transients***	188	***Original Points Count***	31375	***Points Count***	32768
Pulse Sequence	s2pul	***Receiver Gain***	30.00	***Solvent***	acetone	***Spectrum Offset (Hz)***	11069.2324
Spectrum Type	STANDARD	***Sweep Width (Hz)***	24125.45	***Temperature (degree C)***	25.000		

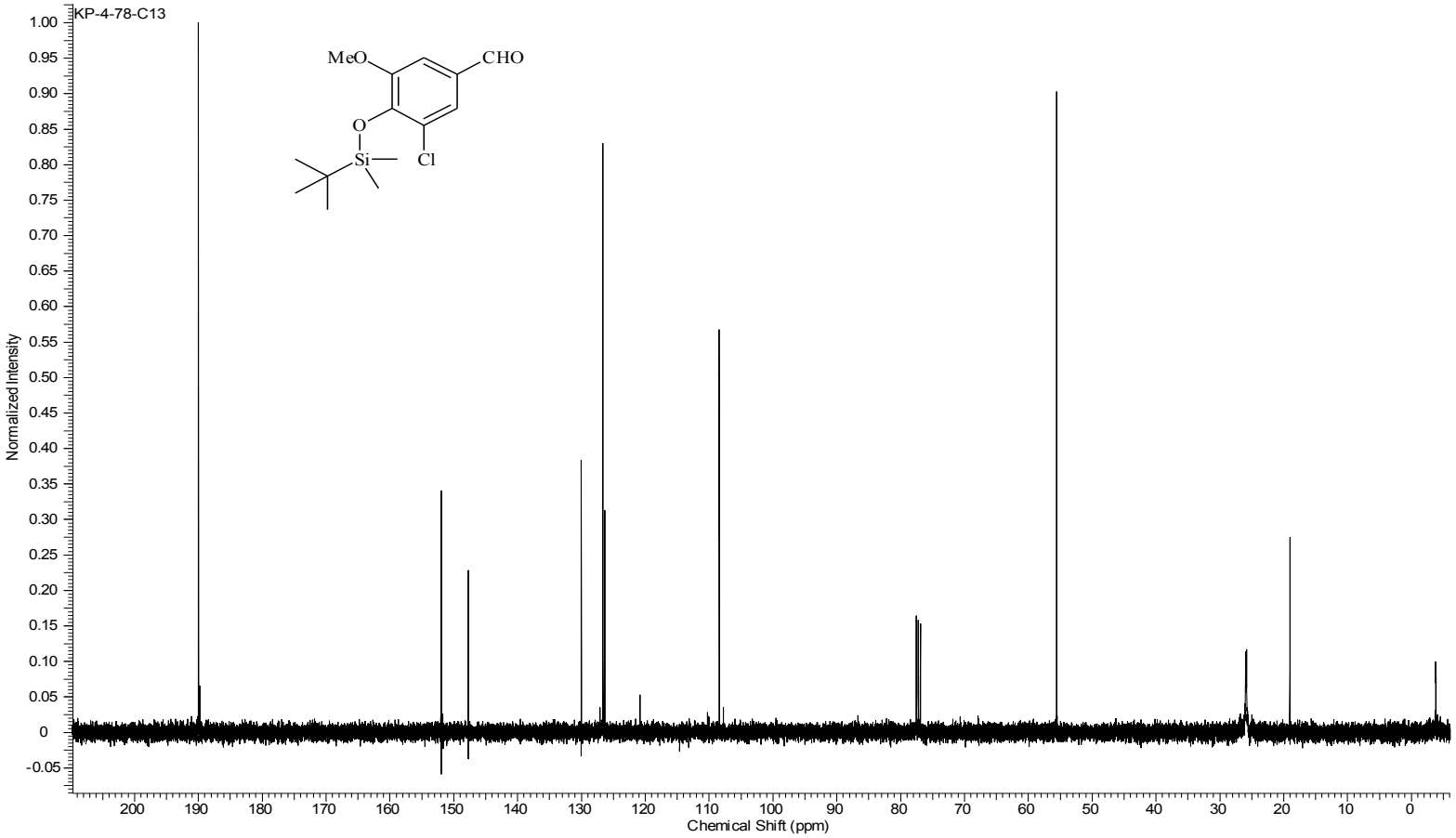

Compound 21 ^{1}H NMR

Acquisition Time (sec)	2.0487	***Comment***	Std proton	***Date***	Aug 15 2009	***Date Stamp***	Aug 15 2009
File Name	C:\USERS\KESHAR\KP-4-115-FR-1-Proton						
Frequency (MHz)	399.75	***Nucleus***	1H	***Number of Transients***	36	***Original Points Count***	13103
Points Count	16384	***Pulse Sequence***	s2pul	***Receiver Gain***	44.00	***Solvent***	CHLOROFORM-d
Spectrum Offset (Hz)	2403.9280	***Spectrum Type***	STANDARD	***Sweep Width (Hz)***	6395.91	***Temperature (degree C)***	25.000

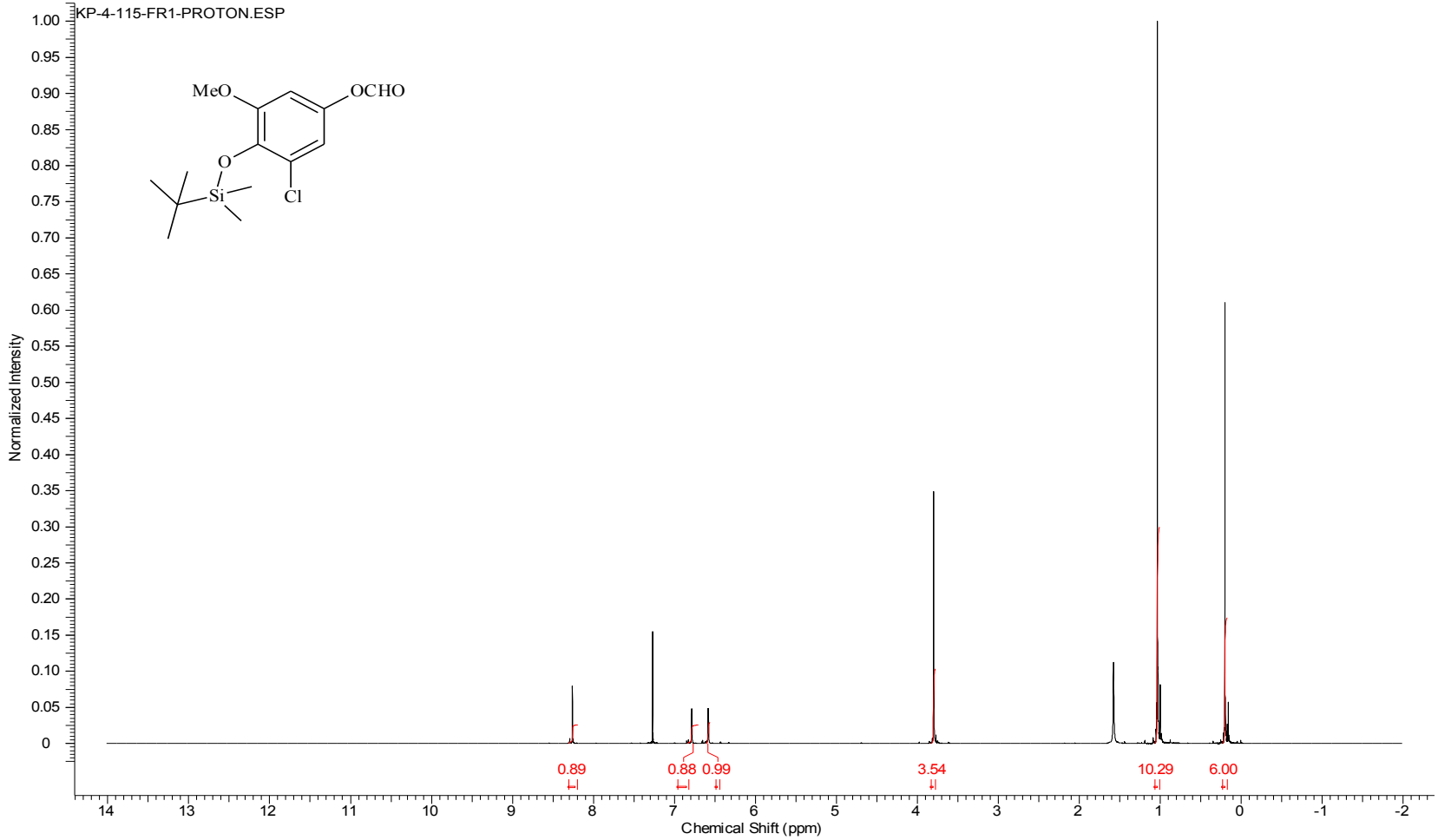

Compound 21 ^{13}C NMR

Acquisition Time (sec)	1.3005	***Comment***	Std proton	***Date***	Jul 16 2009	***Date Stamp***	Jul 16 2009
File Name	C:\USERS\KESHAR\DESKTOP\NMR\OTHERS\KP-4-115-FR1-C13\FID					***Frequency (MHz)***	100.53
Nucleus	13C	***Number of Transients***	88	***Original Points Count***	31375	***Points Count***	32768
Pulse Sequence	s2pul	***Receiver Gain***	30.00	***Solvent***	CHLOROFORM-d		
Spectrum Offset (Hz)	10551.5918	***Spectrum Type***	STANDARD	***Sweep Width (Hz)***	24125.45	***Temperature (degree C)***	25.000

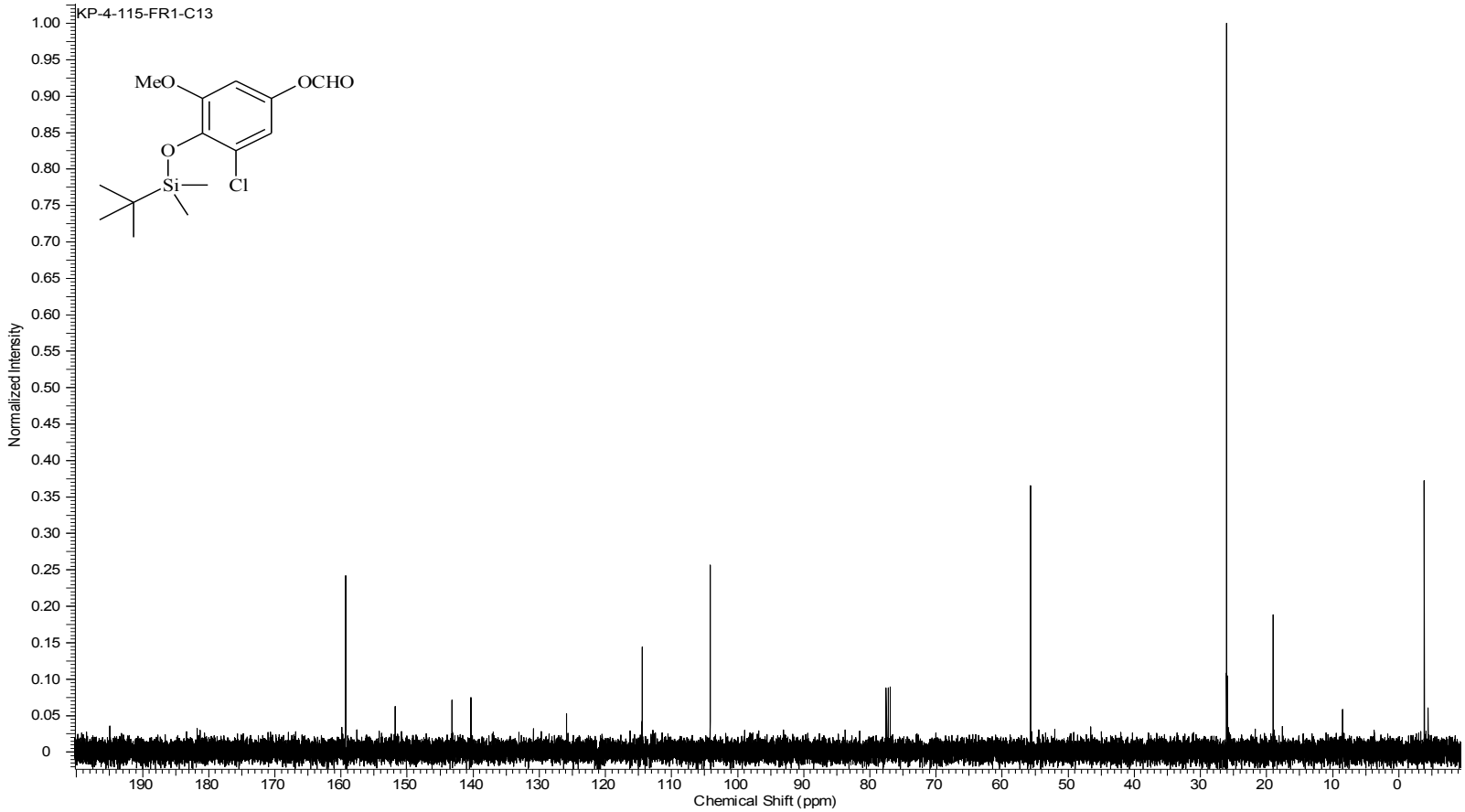

Compound 22 ^{1}H NMR

Acquisition Time (sec)	1.9945	***Comment***	STANDARD 1H OBSERVE			***Date***	Aug 16 2009
Date Stamp	Aug 16 2009	***File Name***	C:\USERS\KESHAR\DESKTOP\NMR\BOOK 4\KP-4-117-DP.FID\FID				
Frequency (MHz)	199.98	***Nucleus***	1H	***Number of Transients***	36	***Original Points Count***	5984
Points Count	8192	***Pulse Sequence***	s2pul	***Receiver Gain***	40.00	***Solvent***	CHLOROFORM-d
Spectrum Offset (Hz)	1002.3889	***Spectrum Type***	STANDARD	***Sweep Width (Hz)***	3000.30	***Temperature (degree C)***	AMBIENT TEMPERATURE

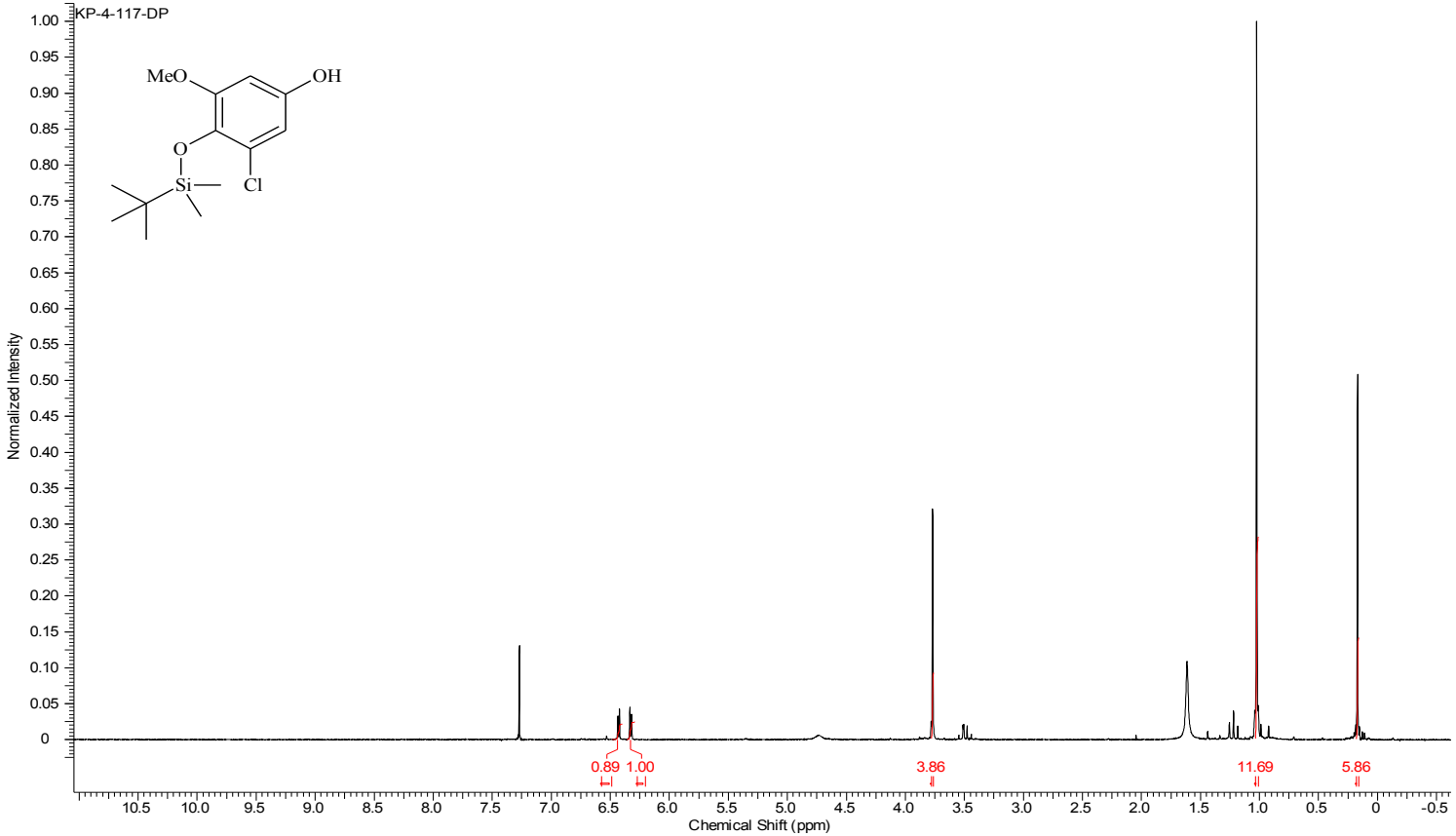

Compound 22 ^{13}C NMR

Acquisition Time (sec)	1.4976	***Comment***	13C OBSERVE	***Date***	Sep 12 2009	***Date Stamp***	Sep 12 2009
File Name	C:\USERS\KESHAR\DESKTOP\NMR\LACCASE\KP-4-80-FR2-C13\FID					***Frequency (MHz)***	50.29
Nucleus	13C	***Number of Transients***	4016	***Original Points Count***	18720	***Points Count***	32768
Pulse Sequence	s2pul	***Receiver Gain***	40.00	***Solvent***	CHLOROFORM-d		
Spectrum Offset (Hz)	4879.6978	***Spectrum Type***	STANDARD	***Sweep Width (Hz)***	12500.00	***Temperature (degree C)***	AMBIENT TEMPERATURE

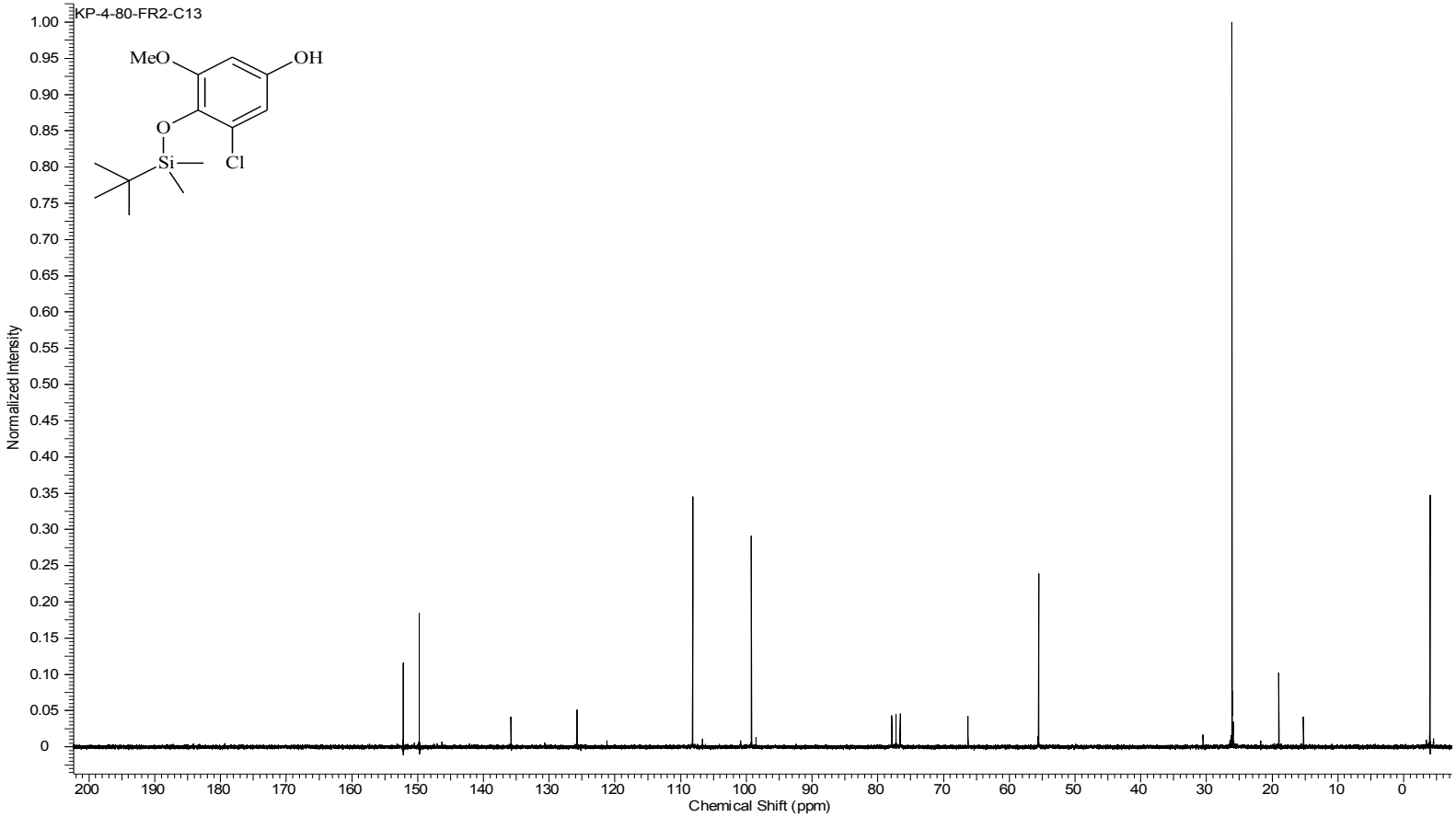

Compound 19 ^{1}H NMR

Acquisition Time (sec)	1.9945	***Comment***	STANDARD 1H OBSERVE			***Date***	Sep 17 2009
Date Stamp	Sep 17 2009	***File Name***	C:\USERS\KESHAR\DESKTOP\NMR\BOOK 5\KP-5-31-QUINONE.FID\FID				
Frequency (MHz)	199.98	***Nucleus***	1H	***Number of Transients***	56	***Original Points Count***	5984
Points Count	8192	***Pulse Sequence***	s2pul	***Receiver Gain***	40.00	***Solvent***	CHLOROFORM-d
Spectrum Offset (Hz)	1002.3889	***Spectrum Type***	STANDARD	***Sweep Width (Hz)***	3000.30	***Temperature (degree C)***	AMBIENT TEMPERATURE

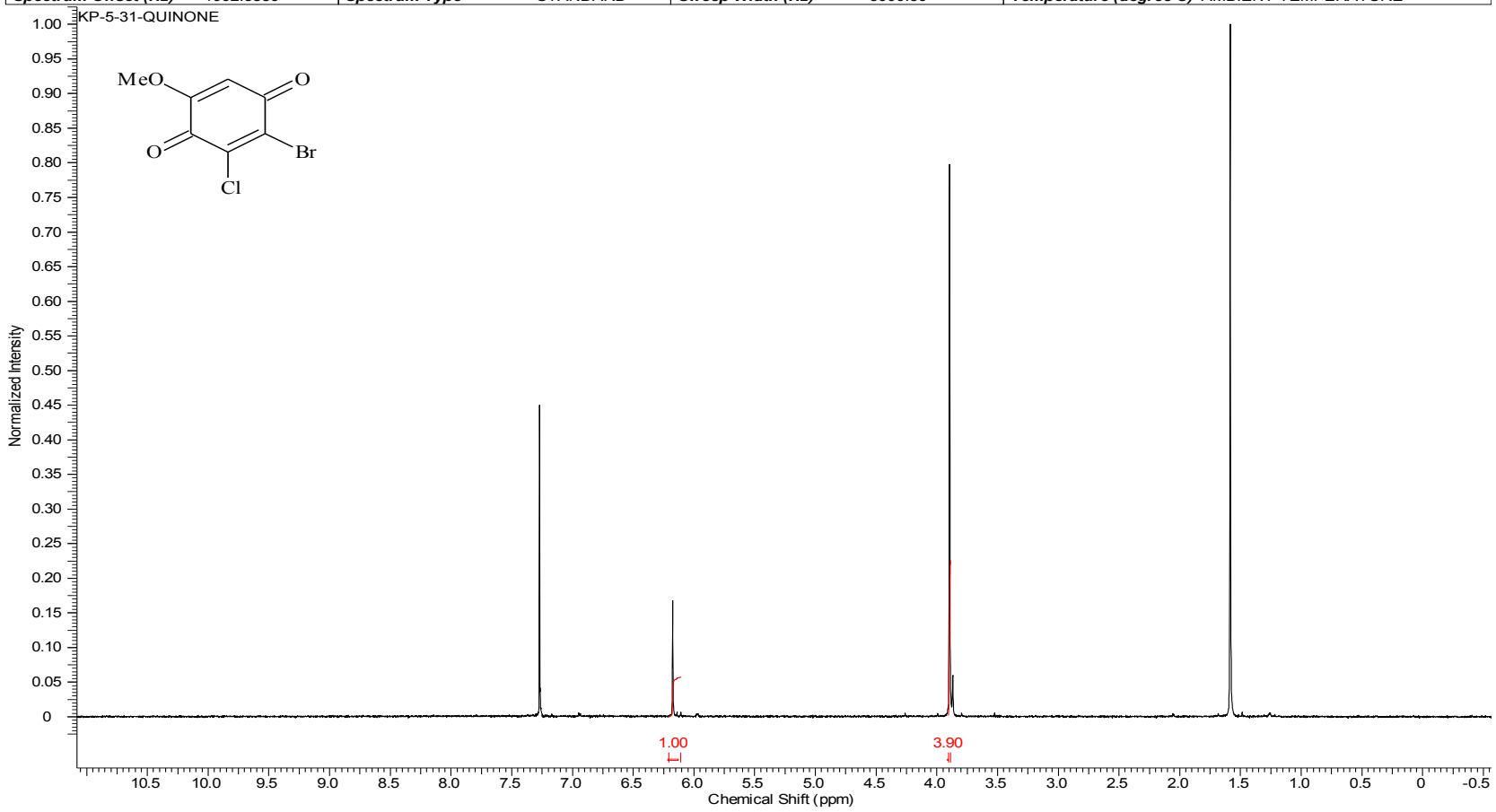

Compound 19 ^{13}C NMR

6/27/2012 1:52:28 PM

Acquisition Time (sec)	1.3005	***Comment***	Std proton	***Date***	Oct 7 2009	***Date Stamp***	Oct 7 2009
File Name	C:\USERS\KESHAR\DESKTOP\NMR\LACCASE\KP-4-119-C13\FID					***Frequency (MHz)***	100.53
Nucleus	13C	***Number of Transients***	9152	***Original Points Count***	31375	***Points Count***	32768
Pulse Sequence	s2pul	***Receiver Gain***	30.00	***Solvent***	CHLOROFORM-d		
Spectrum Offset (Hz)	10554.7441	***Spectrum Type***	STANDARD	***Sweep Width (Hz)***	24125.45	***Temperature (degree C)***	25.000

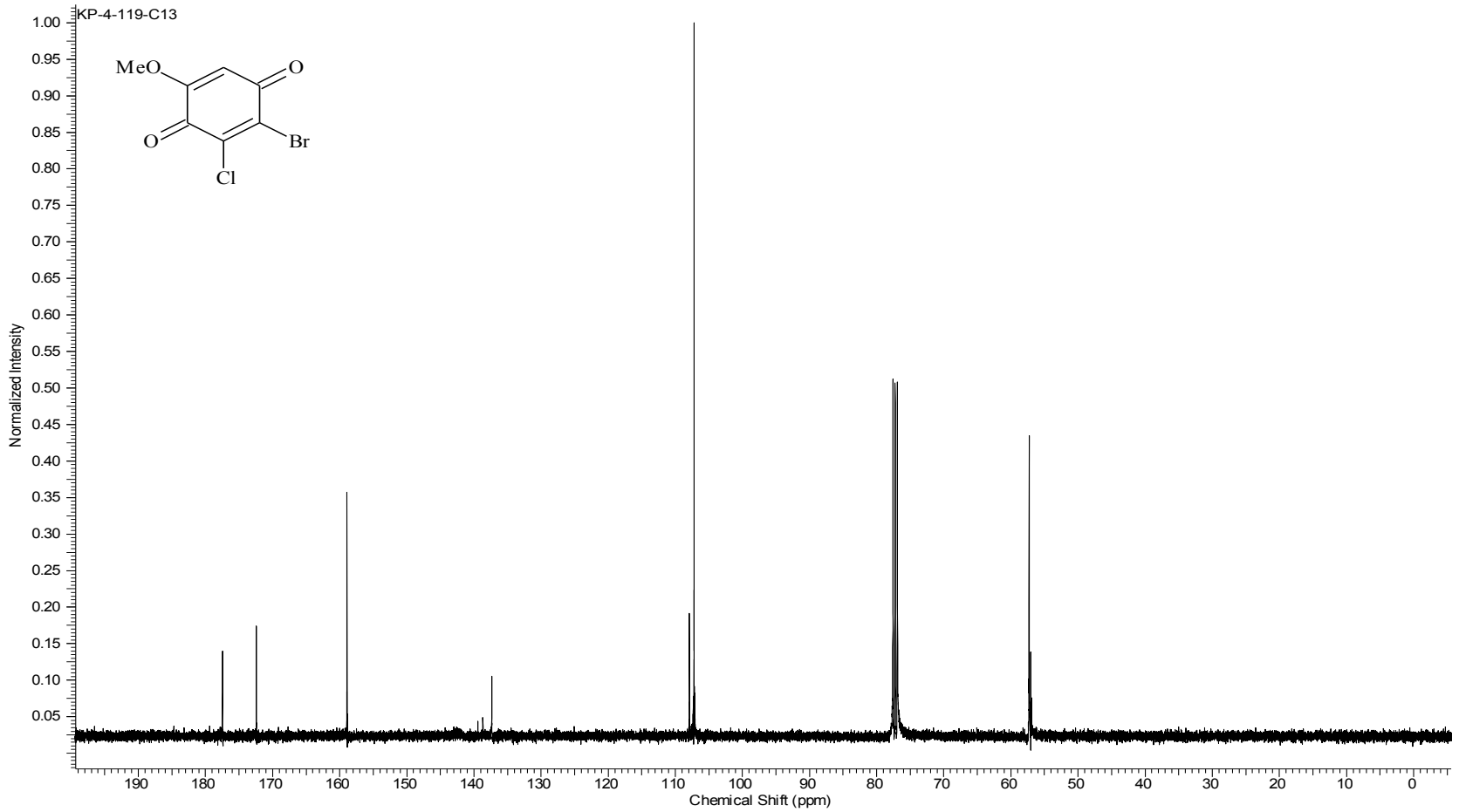

Compound 19 IR

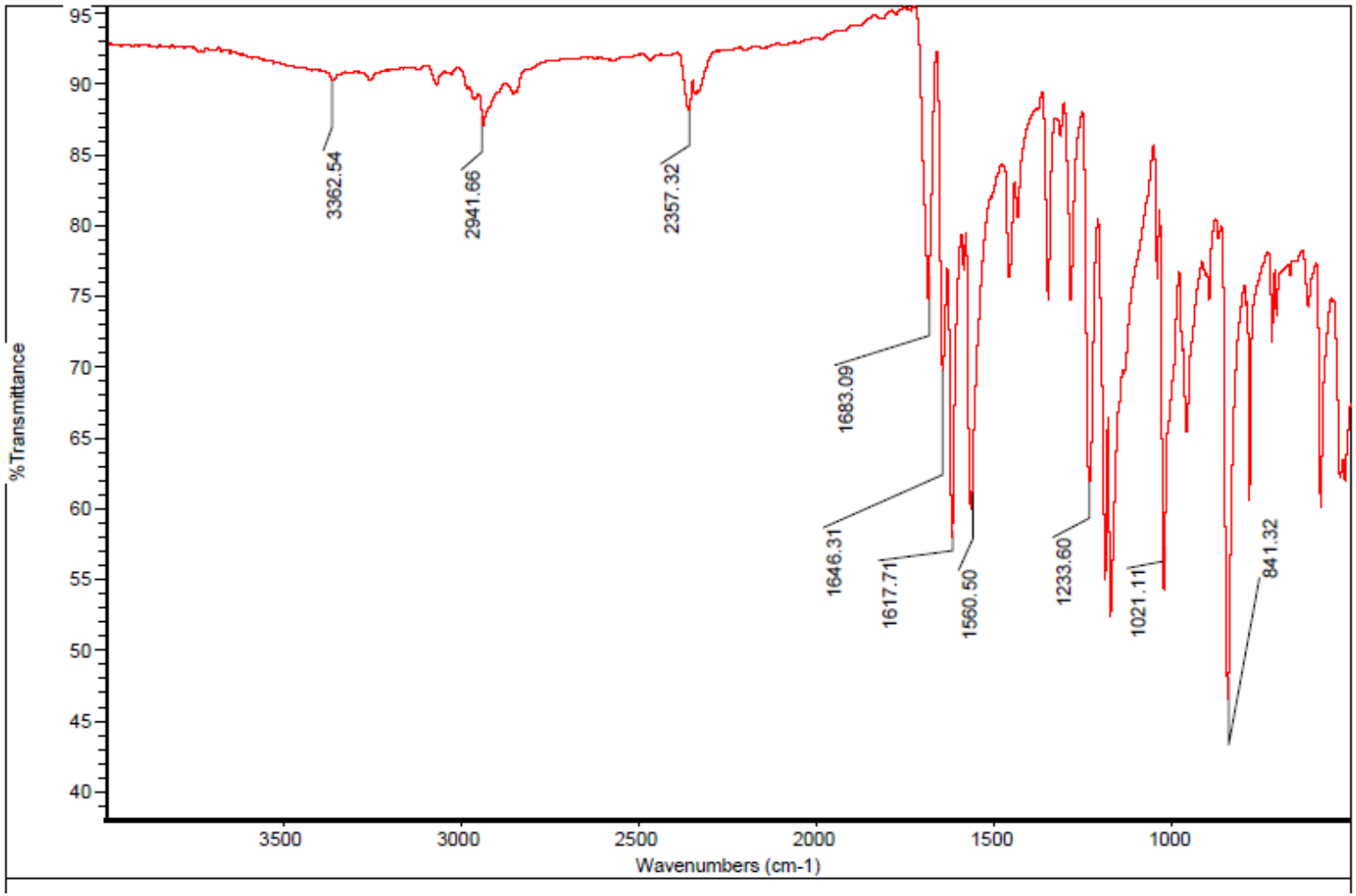

Compound 23 ^{1}H NMR

Acquisition Time (sec)	2.0487	***Comment***	Std proton	***Date***	Aug 15 2009	***Date Stamp***	Aug 15 2009
File Name	C:\USERS\KESHAR\DESKTOP\NMR\BOOK 4\KP-4-82-FRAC1.FID\FID					***Frequency (MHz)***	399.75
Nucleus	1H	***Number of Transients***	24	***Original Points Count***	13103	***Points Count***	16384
Pulse Sequence	s2pul	***Receiver Gain***	54.00	***Solvent***	CHLOROFORM-d		
Spectrum Offset (Hz)	2403.5376	***Spectrum Type***	STANDARD	***Sweep Width (Hz)***	6395.91	***Temperature (degree C)***	25.000

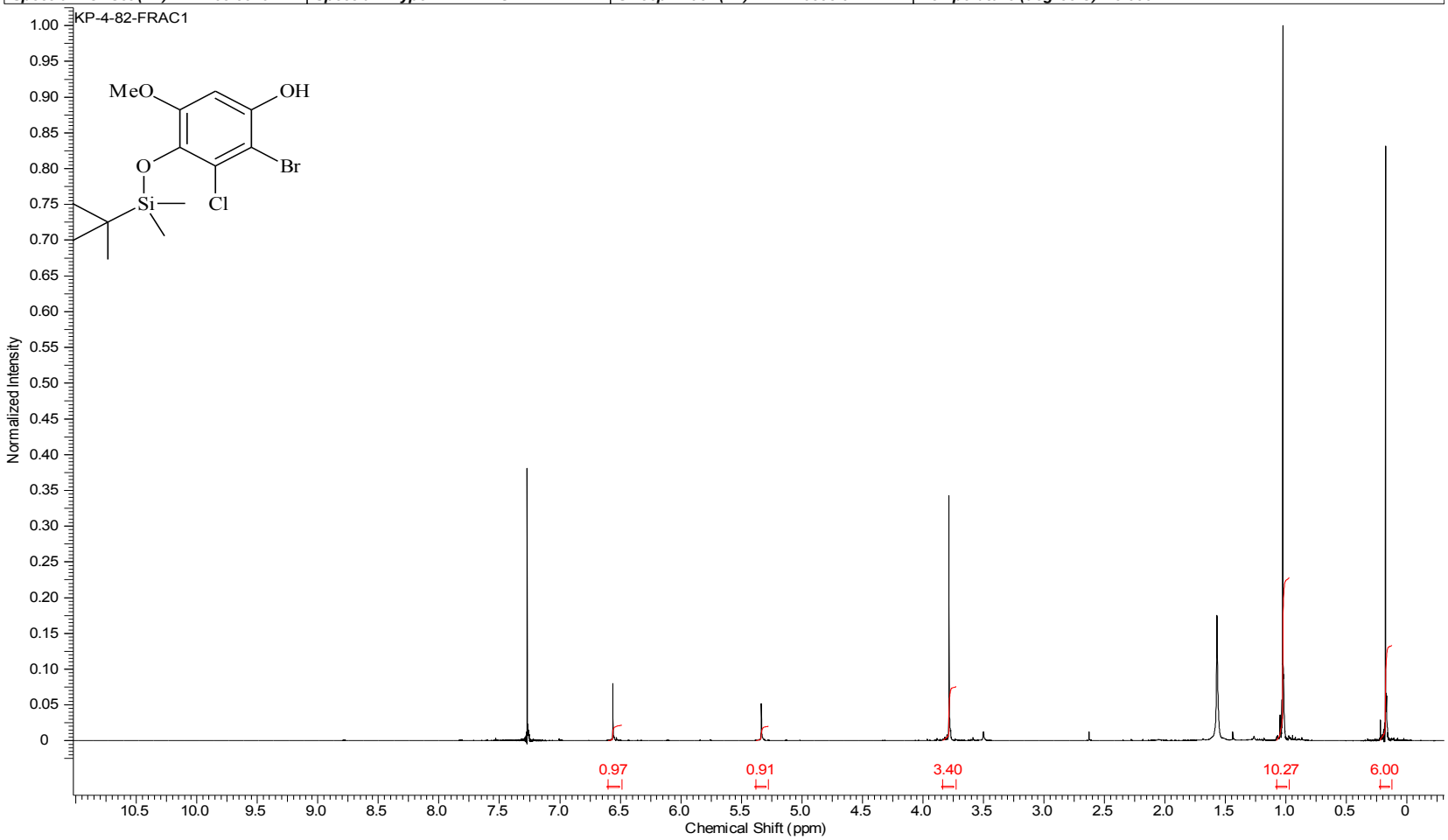

Compound 23 ^{13}C NMR

Acquisition Time (sec)	1.3005	***Comment***	Std proton	***Date***	Oct 7 2009	***Date Stamp***	Oct 7 2009
File Name	C:\USERS\KESHAR\KP-4-115-FR2-Carbon					***Frequency (MHz)***	100.53
Nucleus	13C	***Number of Transients***	2112	***Original Points Count***	31375	***Points Count***	32768
Pulse Sequence	s2pul	***Receiver Gain***	30.00	***Solvent***	CHLOROFORM-d		
Spectrum Offset (Hz)	10554.9160	***Spectrum Type***	STANDARD	***Sweep Width (Hz)***	24125.45	***Temperature (degree C)***	25.000

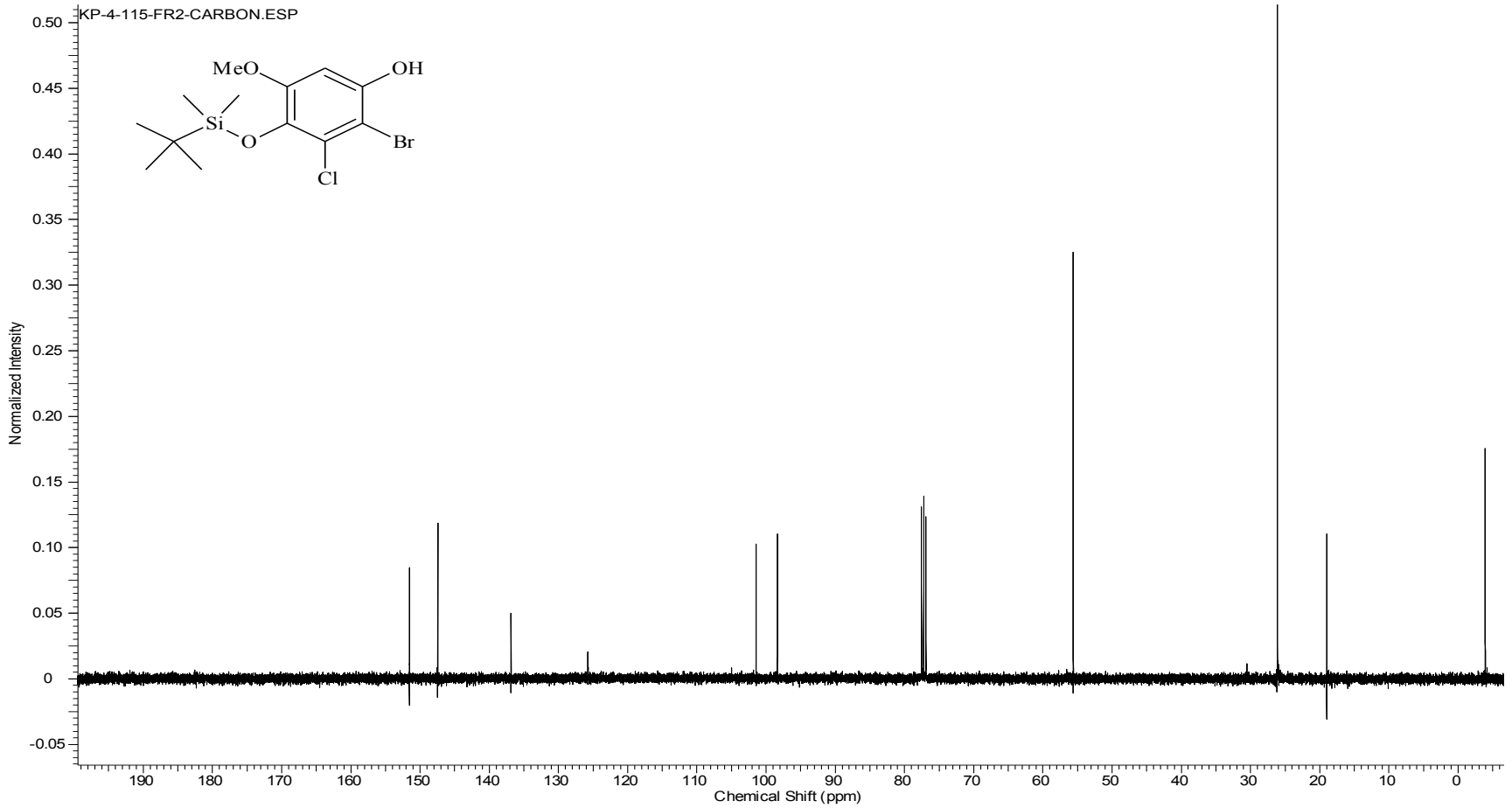

Compound 4 ^{1}H NMR

Acquisition Time (sec)	1.9945	***Comment***	STANDARD 1H OBSERVE			***Date***	Oct 1 2009
Date Stamp	Oct 1 2009	***File Name***	C:\USERS\KESHAR\DESKTOP\NMR\BOOK 5\KP-5-PARADIPHENOL.FID\FID				
Frequency (MHz)	199.98	***Nucleus***	1H	***Number of Transients***	16	***Original Points Count***	5984
Points Count	8192	***Pulse Sequence***	s2pul	***Receiver Gain***	30.00	***Solvent***	CHLOROFORM-d
Spectrum Offset (Hz)	1002.3889	***Spectrum Type***	STANDARD	***Sweep Width (Hz)***	3000.30	***Temperature (degree C)***	AMBIENT TEMPERATURE

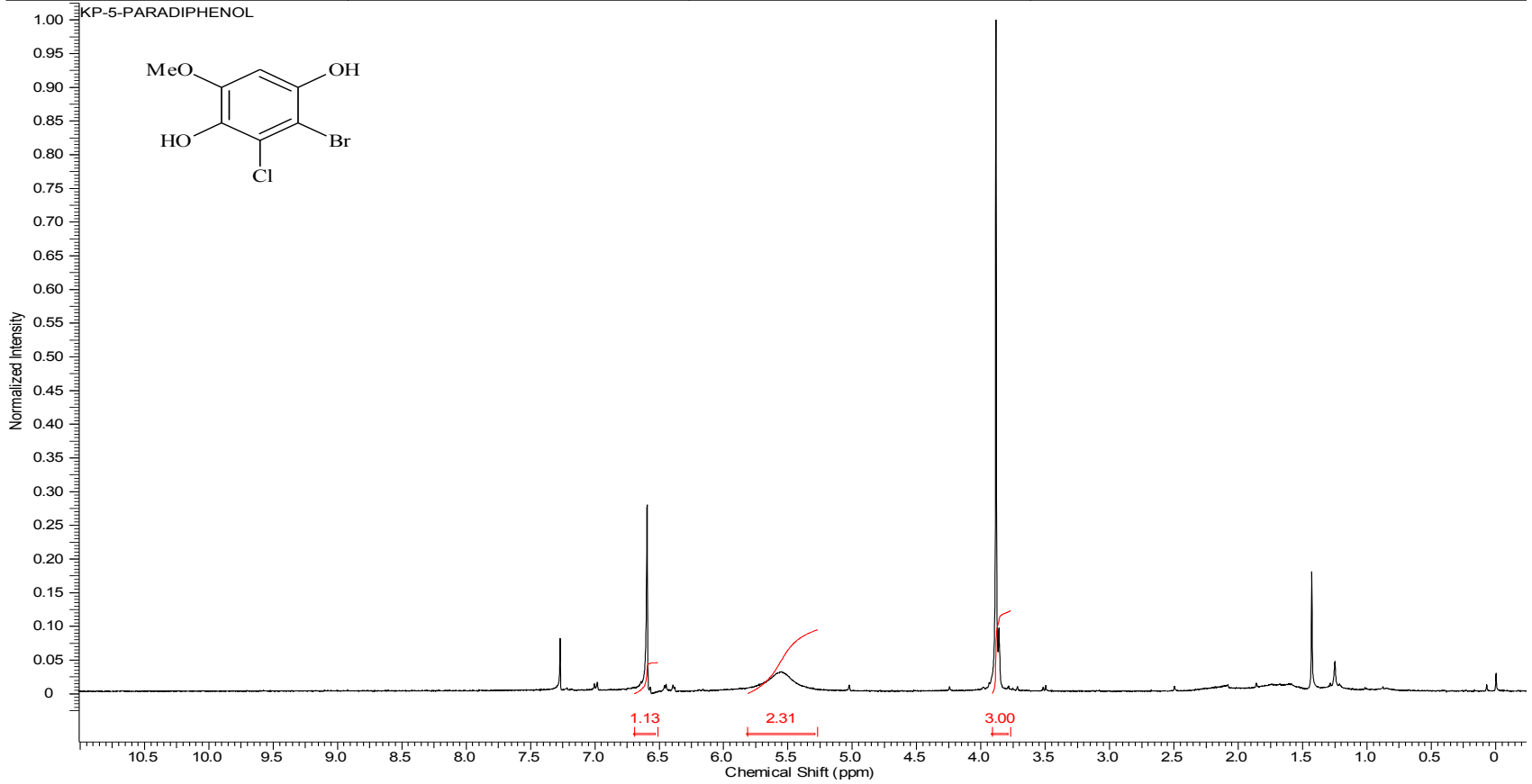

Compound 4 ^{13}C NMR

Acquisition Time (sec)	1.4976	***Comment***	13C OBSERVE	***Date***	Oct 8 2009	***Date Stamp***	Oct 8 2009
File Name	C:\USERS\BOOK 6\KP-LI6-C13-DIPHENOL.FID\FID						
Frequency (MHz)	50.29	***Nucleus***	13C	***Number of Transients***	3680	***Original Points Count***	18720
Points Count	32768	***Pulse Sequence***	s2pul	***Receiver Gain***	40.00	***Solvent***	DMSO-d6
Spectrum Offset (Hz)	4915.7617	***Spectrum Type***	STANDARD	***Sweep Width (Hz)***	12500.00	***Temperature (degree C)***	AMBIENT TEMPERATURE

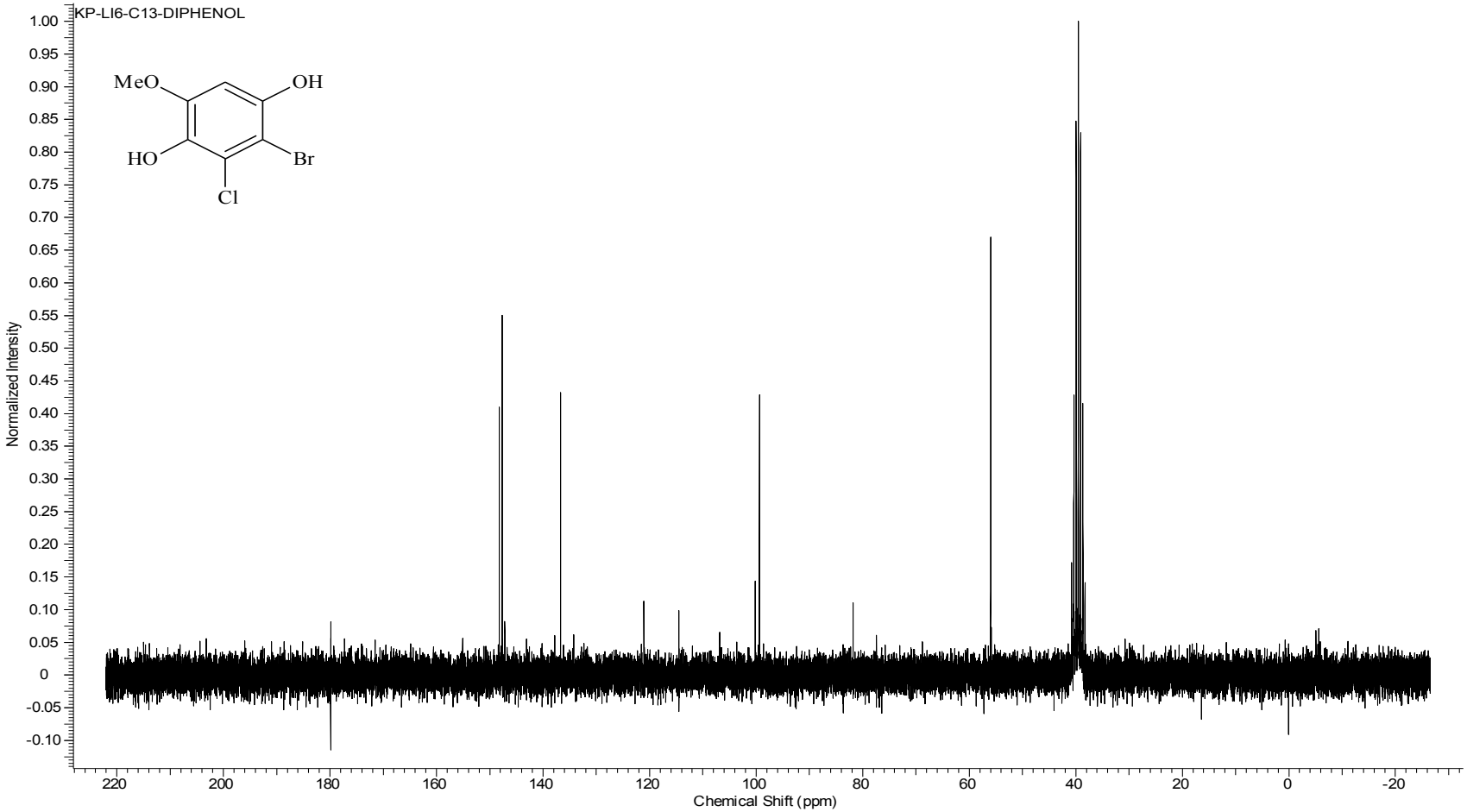

Compound 4 IR

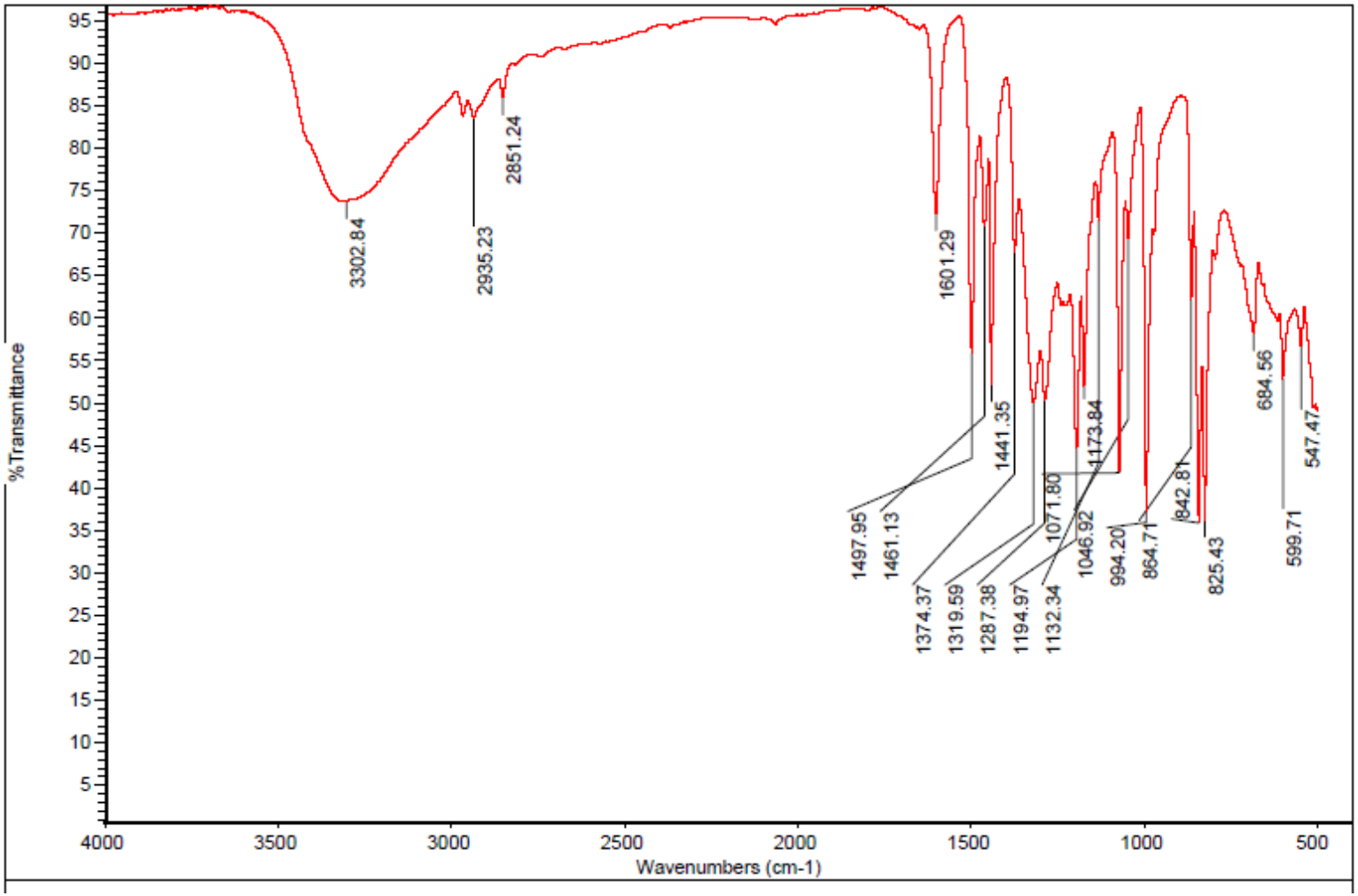

Compound 2 ^{1}H NMR

Acquisition Time (sec)	1.9945	***Comment***	STANDARD 1H OBSERVE			***Date***	Jul 19 2007
Date Stamp	Jul 19 2007	***File Name***	C:\USERS\KESHAR\KP-4-22-Proton				
Frequency (MHz)	199.98	***Nucleus***	1H	***Number of Transients***	64	***Original Points Count***	5984
Points Count	8192	***Pulse Sequence***	s2pul	***Receiver Gain***	28.00	***Solvent***	Acetone
Spectrum Offset (Hz)	999.5056	***Spectrum Type***	STANDARD	***Sweep Width (Hz)***	3000.30	***Temperature (degree C)***	AMBIENT TEMPERATURE

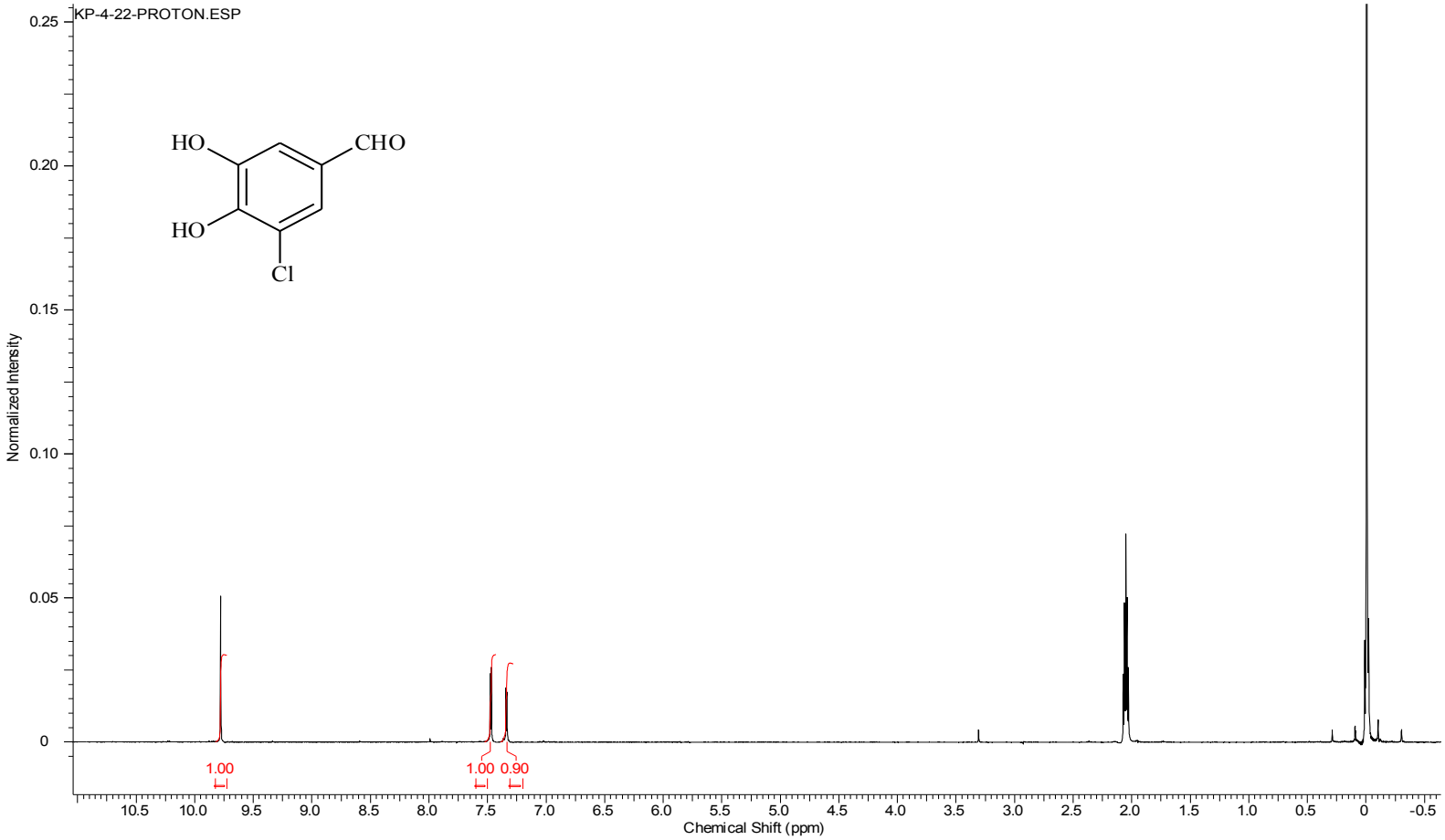

Compound 2 ^{13}C NMR

Acquisition Time (sec)	1.4976	***Comment***	13C OBSERVE	***Date***	Aug 1 2007	***Date Stamp***	Aug 1 2007
File Name	C:\USERS\KESHAR\KP-4-22-Carbon					***Frequency (MHz)***	50.29
Nucleus	13C	***Number of Transients***	11897	***Original Points Count***	18720	***Points Count***	32768
Pulse Sequence	s2pul	***Receiver Gain***	40.00	***Solvent***	Acetone	***Spectrum Offset (Hz)***	4962.9824
Spectrum Type	STANDARD	***Sweep Width (Hz)***	12500.00	***Temperature (degree C)***	AMBIENT TEMPERATURE		

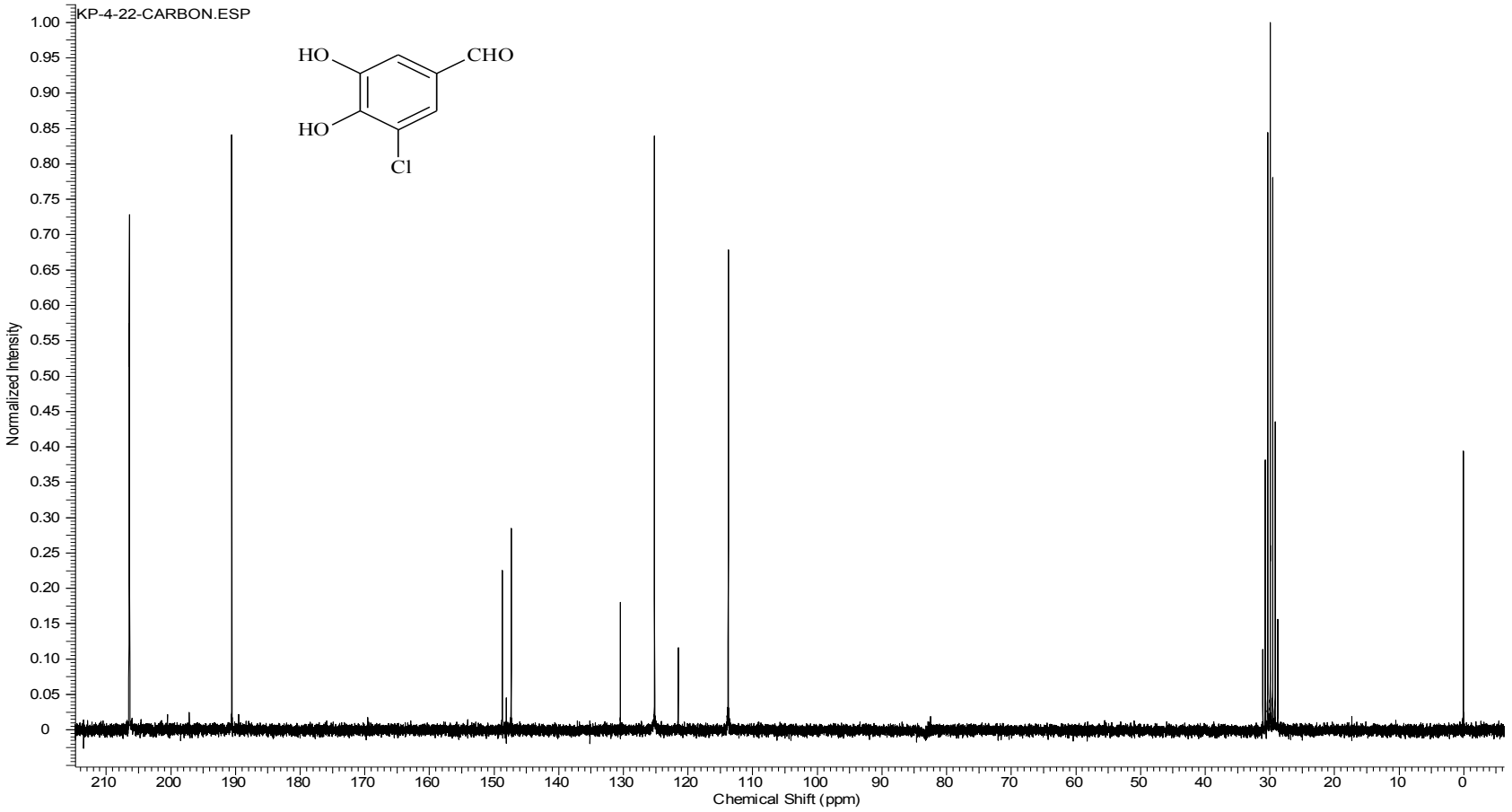

Compound 24 ^{1}H NMR

Acquisition Time (sec)	1.9945	***Comment***	STANDARD 1H OBSERVE			***Date***	Jul 20 2007
Date Stamp	Jul 20 2007	***File Name***	C:\USERS\KESHAR\DESKTOP\NMR\HUIPING\HZ-9-82-AC.FID\FID				
Frequency (MHz)	199.98	***Nucleus***	1H	***Number of Transients***	32	***Original Points Count***	5984
Points Count	8192	***Pulse Sequence***	s2pul	***Receiver Gain***	28.00	***Solvent***	CHLOROFORM-d
Spectrum Offset (Hz)	1002.0226	***Spectrum Type***	STANDARD	***Sweep Width (Hz)***	3000.30	***Temperature (degree C)***	AMBIENT TEMPERATURE

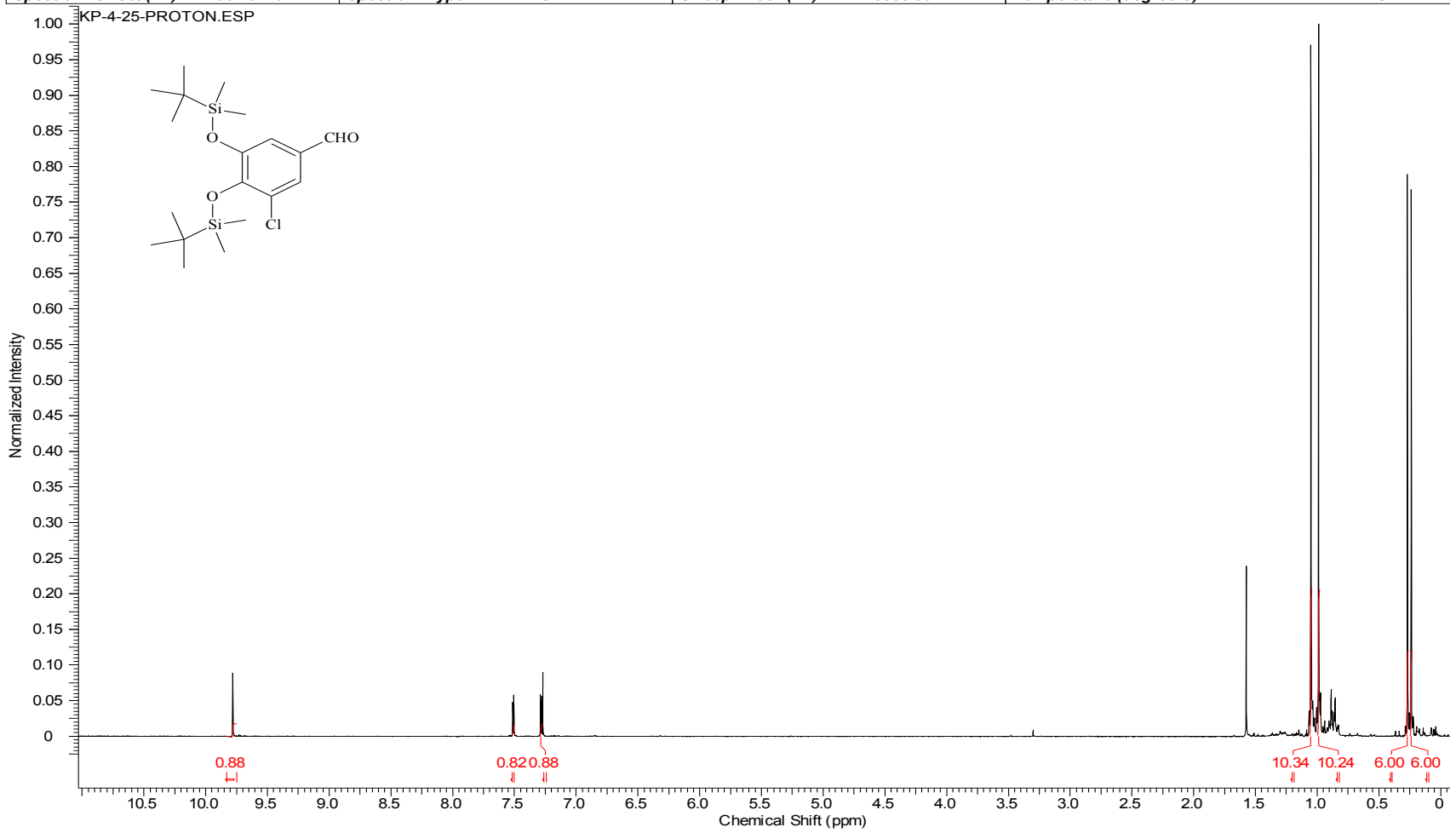

Compound 24 ^{13}C NMR

Acquisition Time (sec)	1.2800	***Comment***	13C OBSERVE			***Date***	Aug 2 09
Date Stamp	Aug 2 09	***File Name***	C:\USERS\KESHAR\DESKTOP\KP-4-25-FRAC2\FID			***Frequency (MHz)***	100.56
Nucleus	13C	***Number of Transients***	96	***Original Points Count***	32000	***Points Count***	32768
Pulse Sequence	s2pul	***Receiver Gain***	60.00	***Solvent***	CHLOROFORM-d		
Spectrum Offset (Hz)	9502.9023	***Spectrum Type***	STANDARD	***Sweep Width (Hz)***	25000.00	***Temperature (degree C)***	27.000

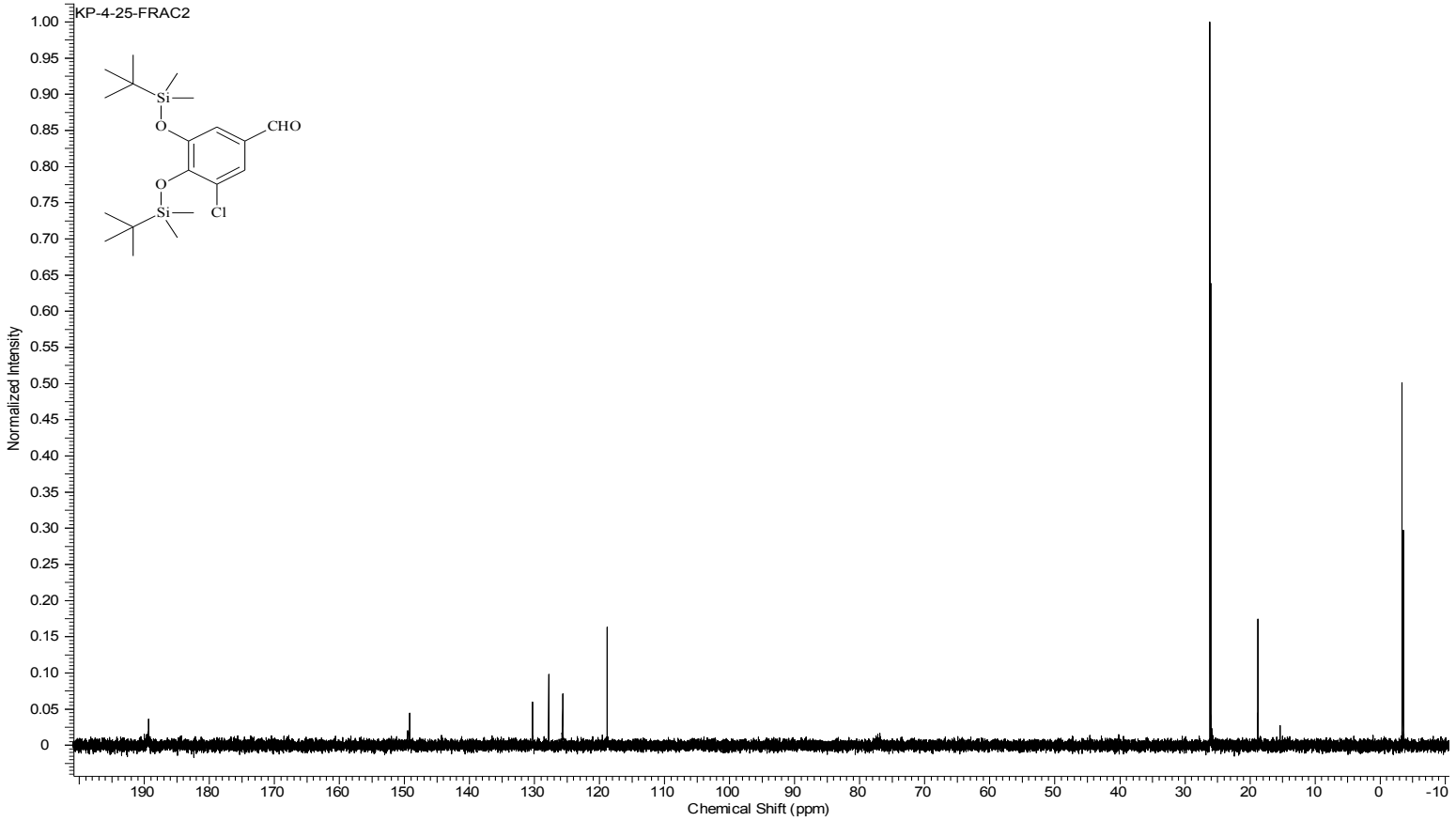

Compound 25 ^{1}H NMR

Acquisition Time (sec)	2.0486	***Comment***	Std proton	***Date***	Jul 21 2007	***Date Stamp***	Jul 21 2007
File Name	C:\USERS\KESHAR\KP-5-Formate					***Frequency (MHz)***	399.78
Nucleus	1H	***Number of Transients***	4	***Original Points Count***	17199	***Points Count***	32768
Pulse Sequence	s2pul	***Receiver Gain***	44.00	***Solvent***	DEUTERIUM OXIDE		
Spectrum Offset (Hz)	3241.8862	***Spectrum Type***	STANDARD	***Sweep Width (Hz)***	8395.42	***Temperature (degree C)***	25.000

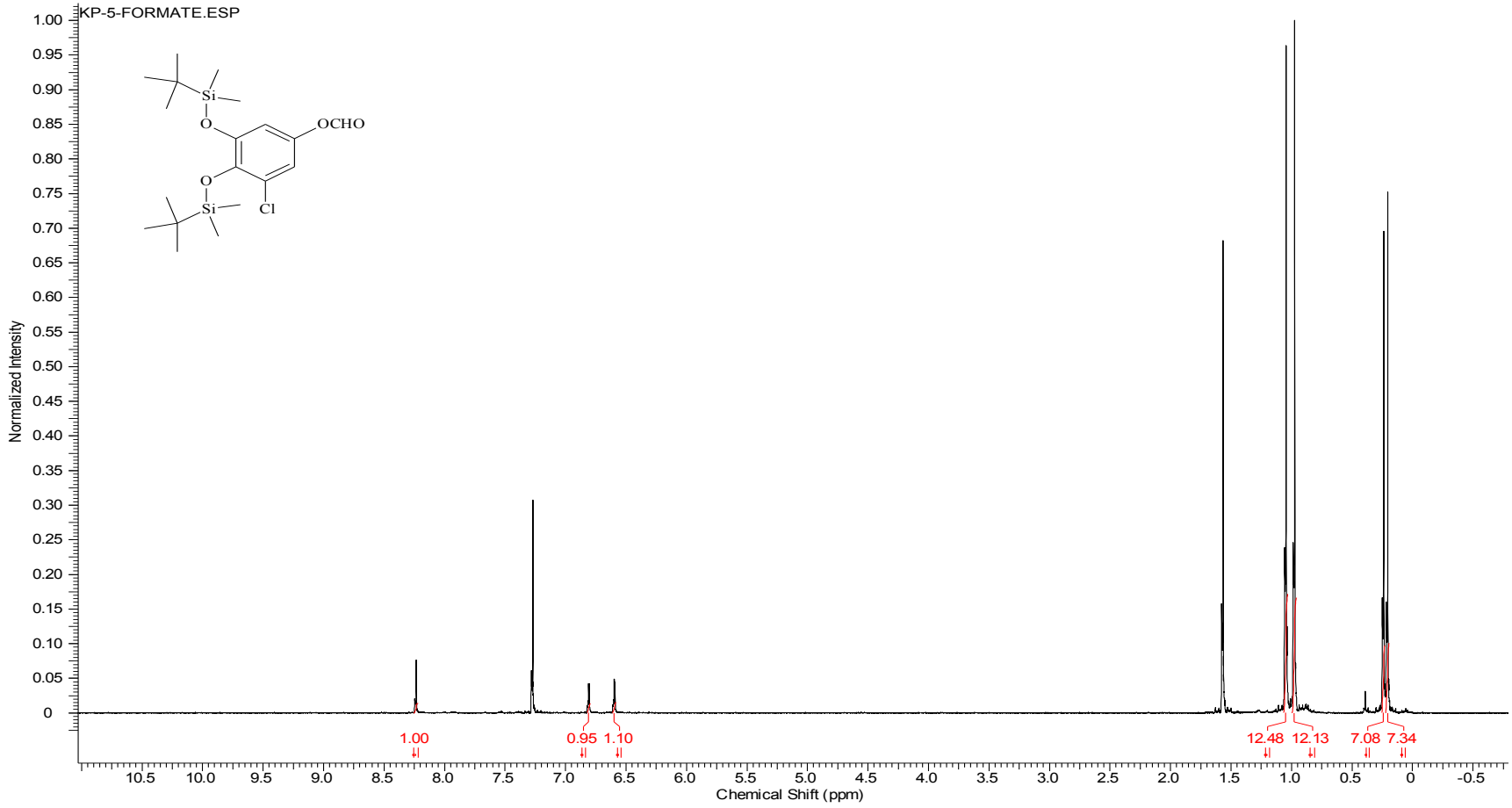

Compound 25 ^{13}C NMR

Acquisition Time (sec)	1.2800	***Comment***	13C OBSERVE			***Date***	Aug 4 09
Date Stamp	Aug 4 09	***File Name***	C:\USERS\KESHAR\DESKTOP\KP-4-FORMATE\FID			***Frequency (MHz)***	199.9
Nucleus	13C	***Number of Transients***	128	***Original Points Count***	32000	***Points Count***	32768
Pulse Sequence	s2pul	***Receiver Gain***	60.00	***Solvent***	CHLOROFORM-d		
Spectrum Offset (Hz)	9512.8496	***Spectrum Type***	STANDARD	***Sweep Width (Hz)***	25000.00	***Temperature (degree C)***	25

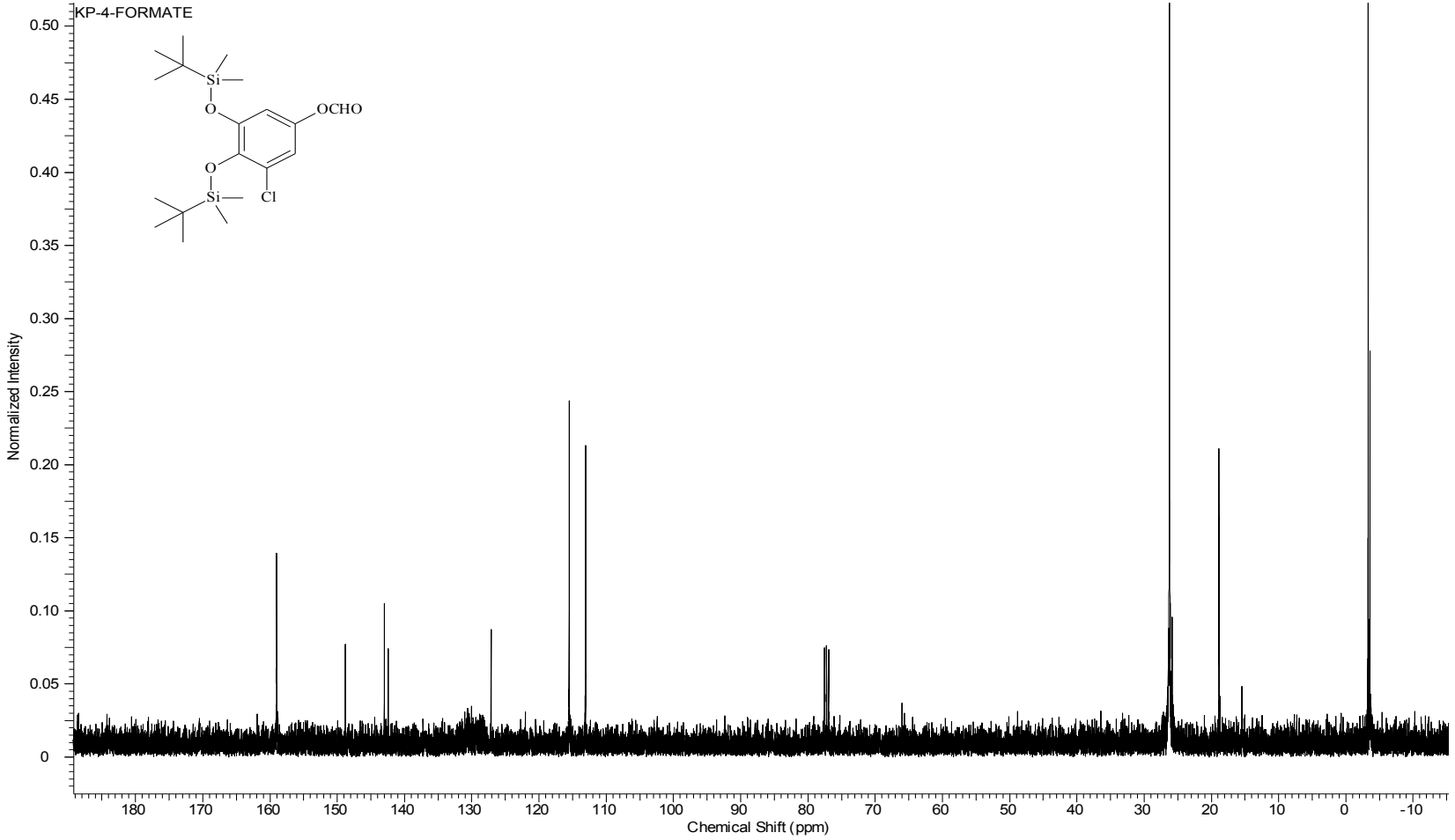

Compound 26 ^{1}H NMR

Acquisition Time (sec)	1.9945	***Comment***	STANDARD 1H OBSERVE			***Date***	Aug 2 2008
Date Stamp	Aug 2 2008	***File Name***	C:\USERS\KESHAR\DESKTOP\NMR\BOOK 1\KP-1-86-DP.FID\FID				
Frequency (MHz)	199.98	***Nucleus***	1H	***Number of Transients***	32	***Original Points Count***	5984
Points Count	8192	***Pulse Sequence***	s2pul	***Receiver Gain***	34.00	***Solvent***	CHLOROFORM-d
Spectrum Offset (Hz)	1001.2900	***Spectrum Type***	STANDARD	***Sweep Width (Hz)***	3000.30	***Temperature (degree C)***	AMBIENT TEMPERATURE

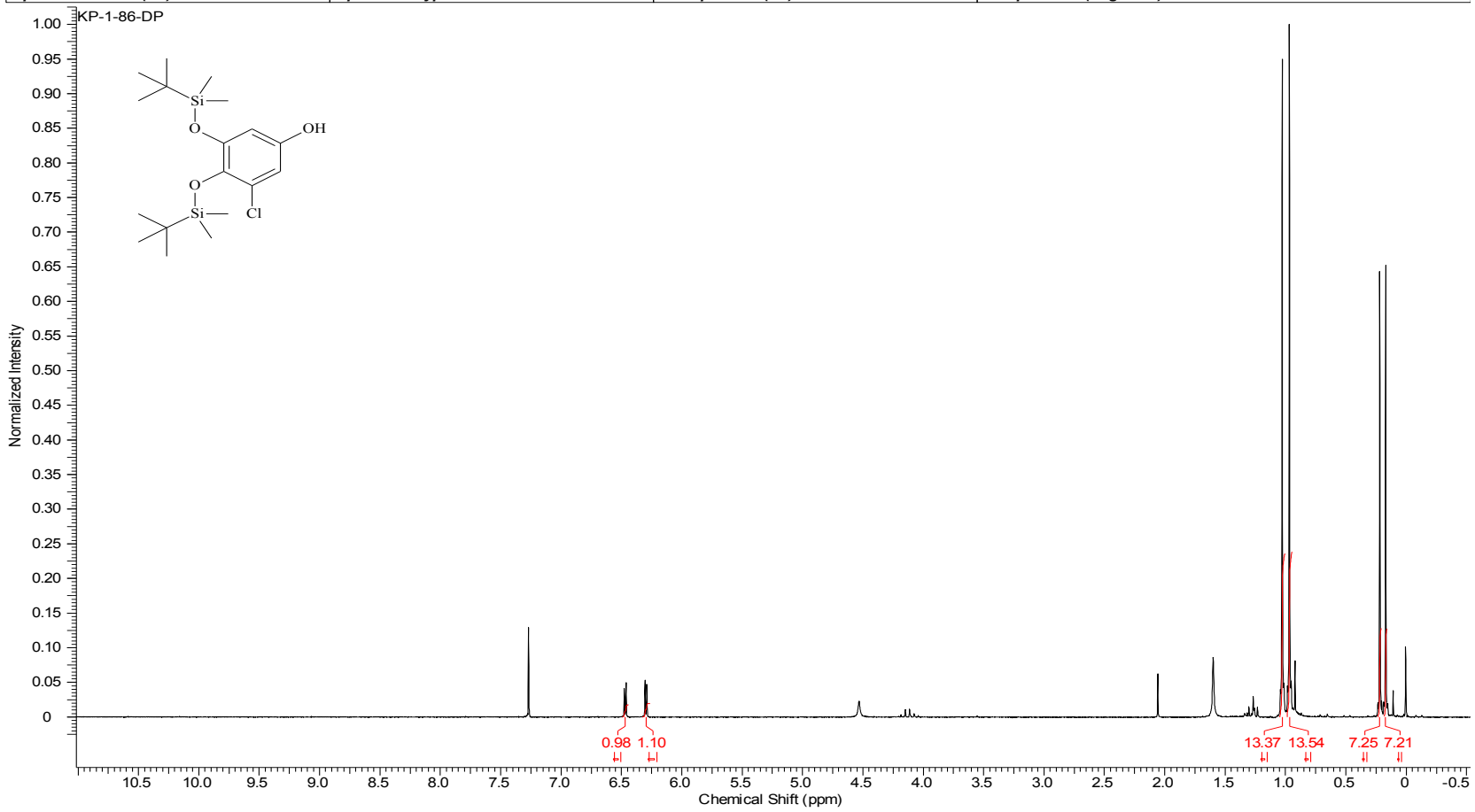

Compound 26 ^{13}C NMR

Acquisition Time (sec)	1.2800	***Comment***	13C OBSERVE			***Date***	Jan 7 2009
Date Stamp	Jan 7 2009	***File Name***	C:\USERS\KESHAR\DESKTOP\KP-4-76-SM-C13\FID			***Frequency (MHz)***	199.9
Nucleus	13C	***Number of Transients***	128	***Original Points Count***	32000	***Points Count***	32768
Pulse Sequence	s2pul	***Receiver Gain***	60.00	***Solvent***	CHLOROFORM-d		
Spectrum Offset (Hz)	9513.0752	***Spectrum Type***	STANDARD	***Sweep Width (Hz)***	25000.00	***Temperature (degree C)***	25

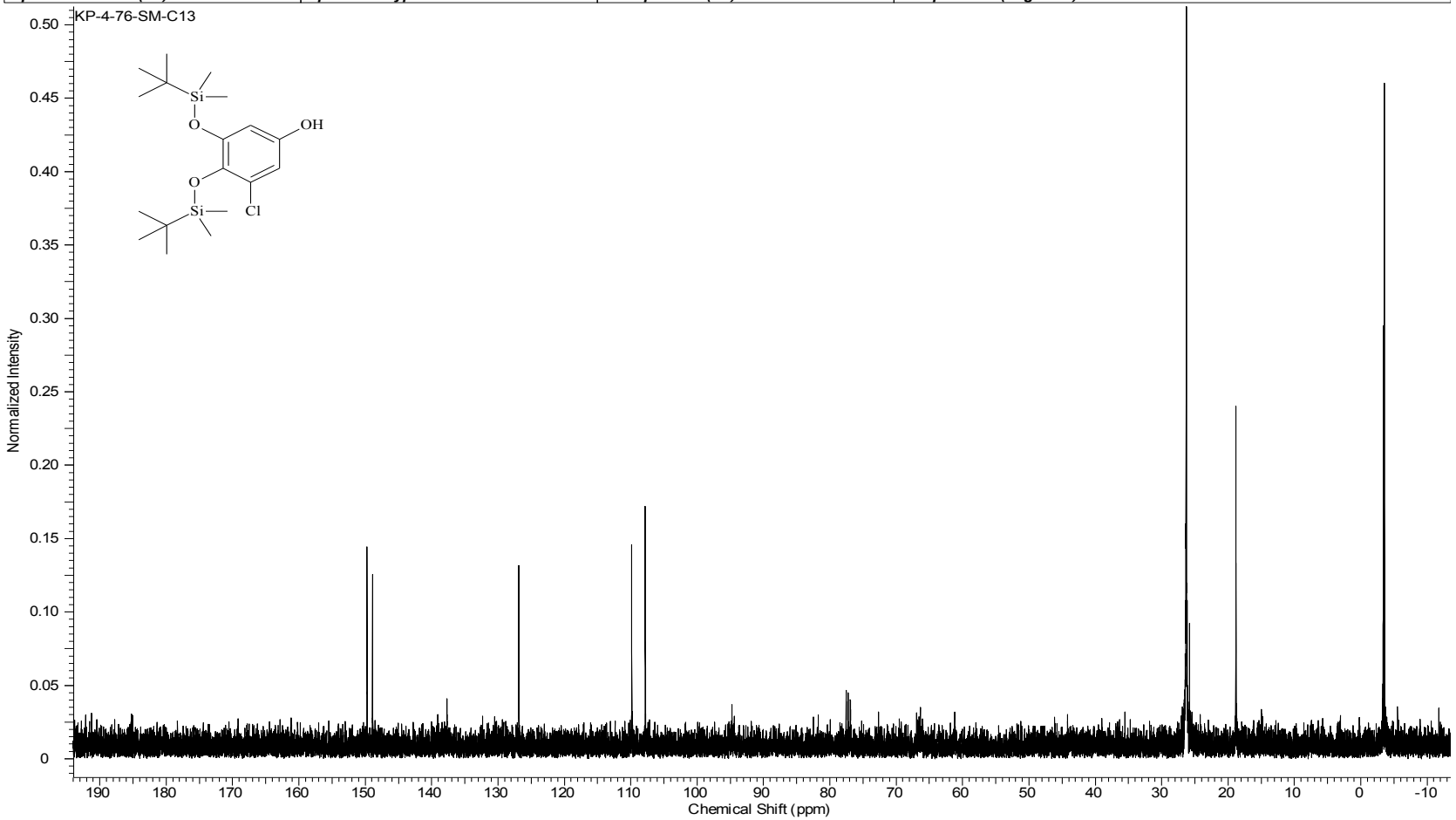

Compound 27 ^{1}H NMR

Acquisition Time (sec)	1.9945	***Comment***	STANDARD 1H OBSERVE			***Date***	Aug 6 2008
Date Stamp	Aug 6 2008	***File Name***	C:\USERS\KESHAR\DESKTOP\NMR\BOOK 1\KP-1-86-DPCOLUMN.FID\FID				
Frequency (MHz)	199.98	***Nucleus***	1H	***Number of Transients***	64	***Original Points Count***	5984
Points Count	8192	***Pulse Sequence***	s2pul	***Receiver Gain***	39.00	***Solvent***	CHLOROFORM-d
Spectrum Offset (Hz)	1001.6563	***Spectrum Type***	STANDARD	***Sweep Width (Hz)***	3000.30	***Temperature (degree C)***	AMBIENT TEMPERATURE

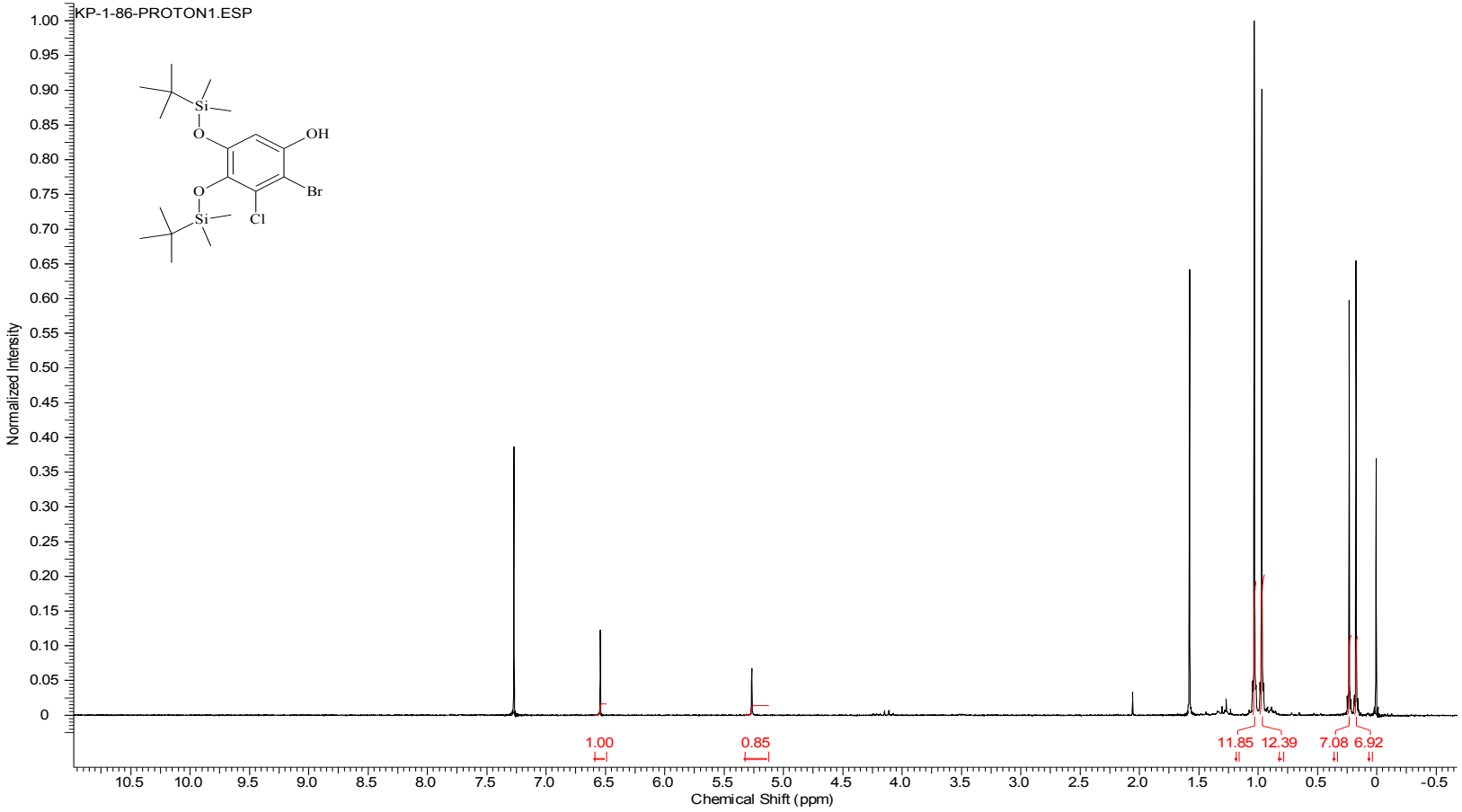

Compound 27 ^{13}C NMR

Acquisition Time (sec)	1.4976	***Comment***	13C OBSERVE	***Date***	Sep 6 200	***Date Stamp***	Sep 6 2009
File Name	C:\USERS\KESHAR\DESKTOP\NMR\LACCASE\KP-4-76-SM-BR\FID					***Frequency (MHz)***	50.29
Nucleus	13C	***Number of Transients***	320	***Original Points Count***	18720	***Points Count***	32768
Pulse Sequence	s2pul	***Receiver Gain***	40.00	***Solvent***	CHLOROFORM-d		
Spectrum Offset (Hz)	4880.4648	***Spectrum Type***	STANDARD	***Sweep Width (Hz)***	12500.00	***Temperature (degree C)***	AMBIENT TEMPERATURE

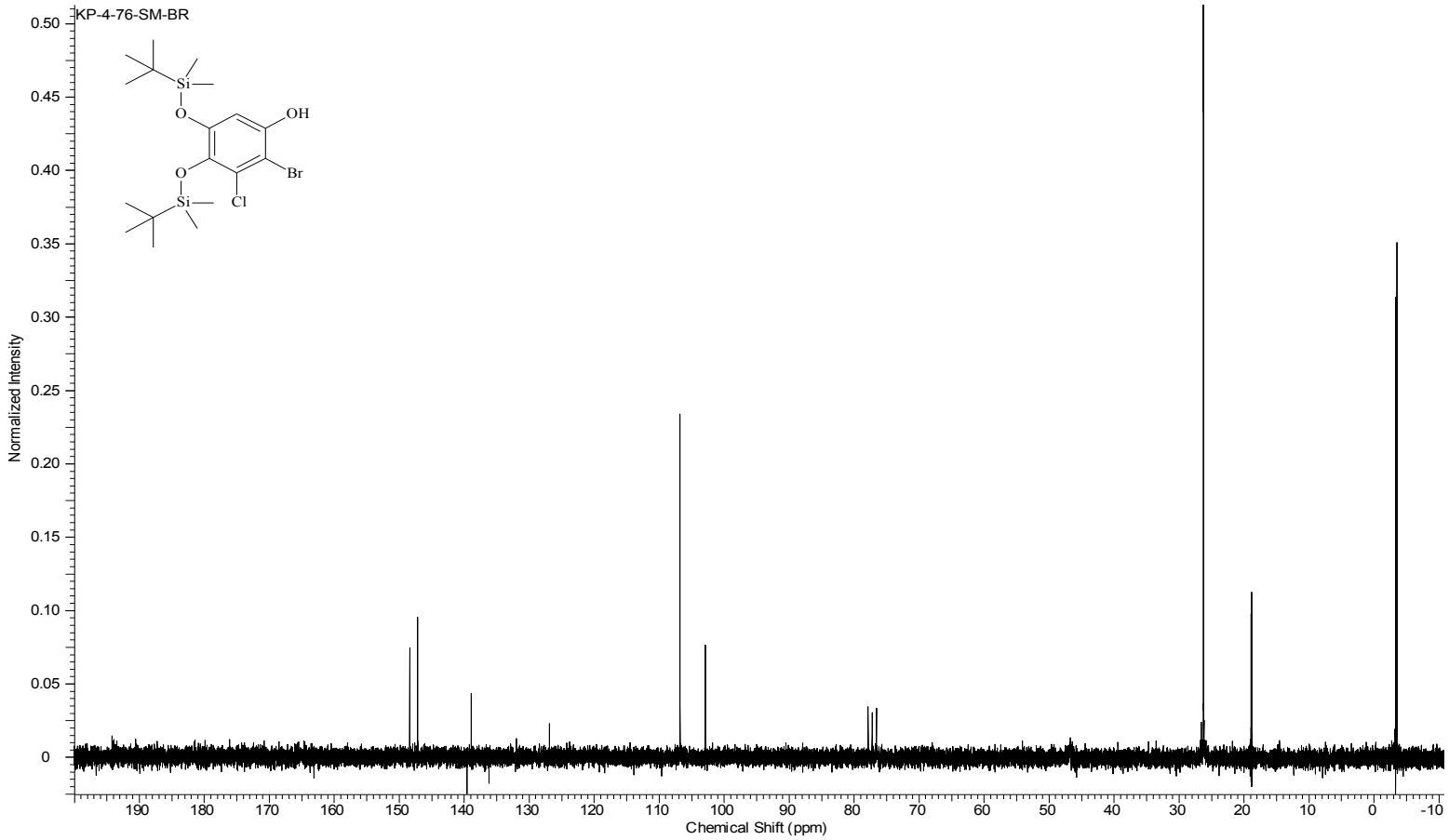

Compound 28 ^{1}H NMR

Acquisition Time (sec)	1.9945	***Comment***	STANDARD 1H OBSERVE			***Date***	Apr 21 2009
Date Stamp	Apr 21 2009	***File Name***	C:\USERS\KESHAR\DESKTOP\NMR\BOOK 4\KP-4-76-CRUDE.FID\FID				
Frequency (MHz)	199.98	***Nucleus***	1H	***Number of Transients***	100	***Original Points Count***	5984
Points Count	8192	***Pulse Sequence***	s2pul	***Receiver Gain***	40.00	***Solvent***	CHLOROFORM-d
Spectrum Offset (Hz)	1002.3816	***Spectrum Type***	STANDARD	***Sweep Width (Hz)***	3000.30	***Temperature (degree C)***	AMBIENT TEMPERATURE

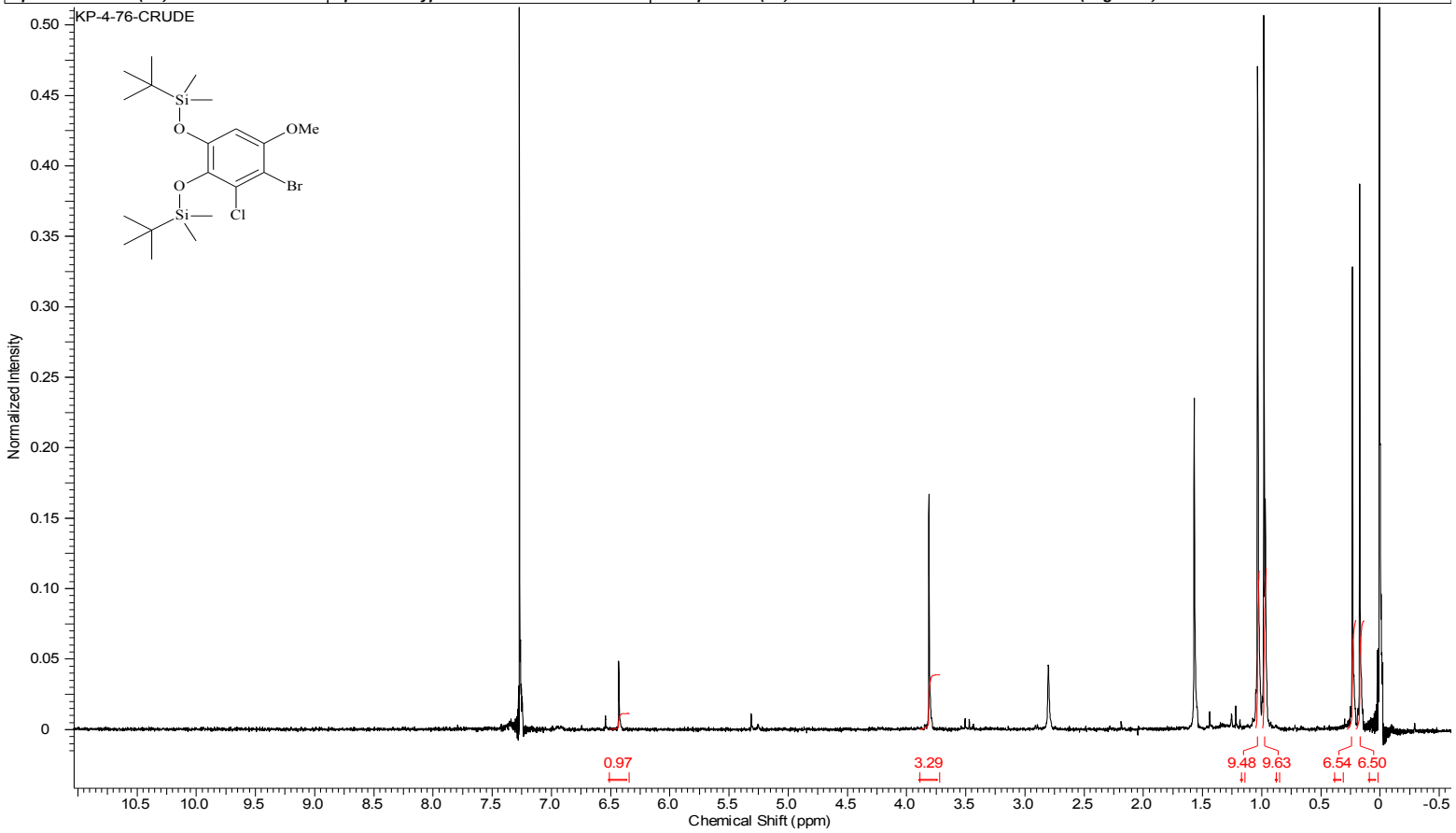

Compound 28 ^{13}C NMR

Acquisition Time (sec)	1.3005	***Comment***	Std proton	***Date***	Oct 8 2009	***Date Stamp***	Oct 8 2009
File Name	C:\USERS\KESHAR\KP-4-76-C13					***Frequency (MHz)***	100.53
Nucleus	13C	***Number of Transients***	1408	***Original Points Count***	31375	***Points Count***	32768
Pulse Sequence	s2pul	***Receiver Gain***	30.00	***Solvent***	CHLOROFORM-d		
Spectrum Offset (Hz)	10554.9160	***Spectrum Type***	STANDARD	***Sweep Width (Hz)***	24125.45	***Temperature (degree C)***	25.000

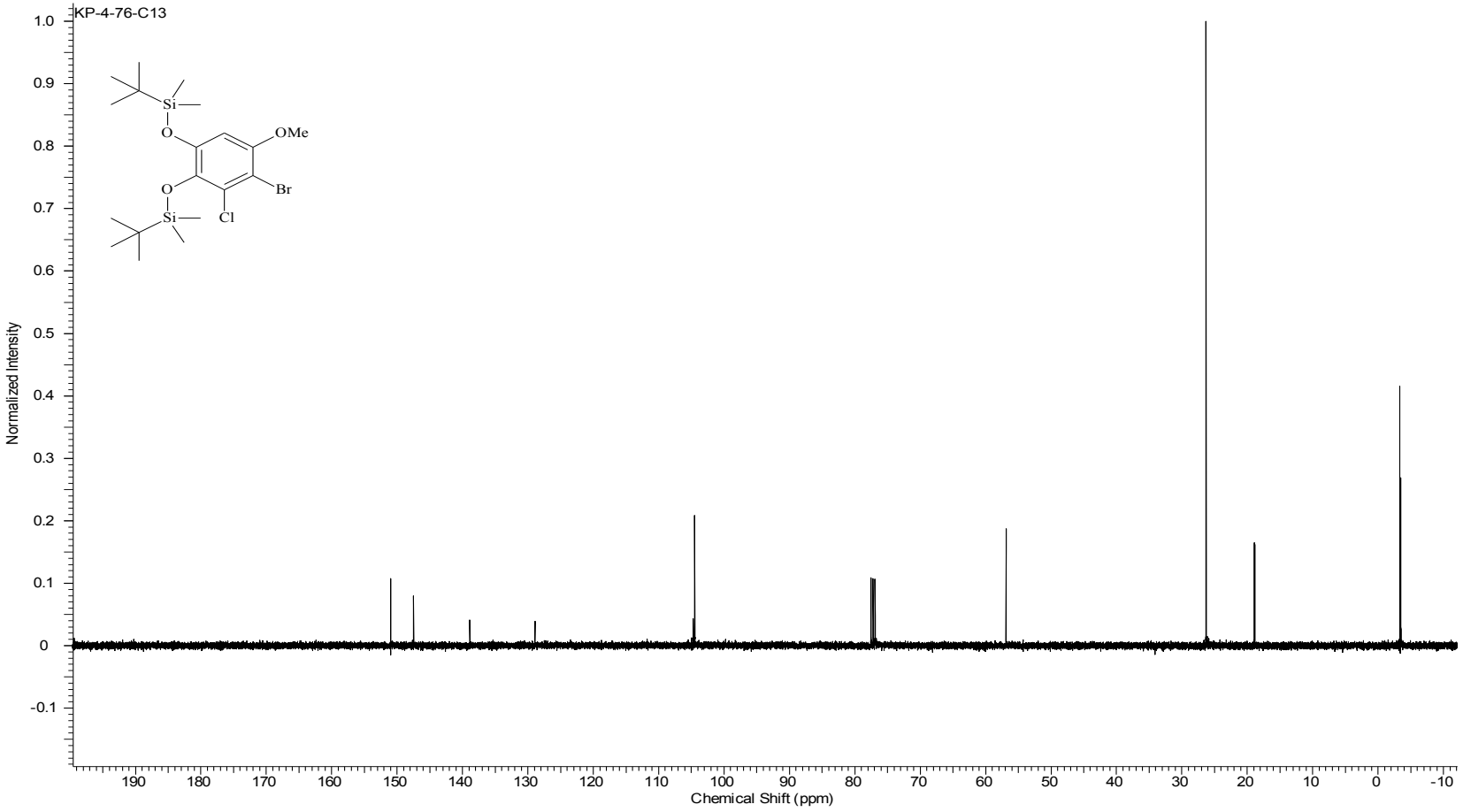

Compound 3 ^{1}H NMR

Acquisition Time (sec)	1.9945	***Comment***	STANDARD 1H OBSERVE			***Date***	May 14 2009
Date Stamp	May 14 2009	***File Name***	C:\USERS\KESHAR\DESKTOP\NMR\BOOK 4\KP-4-91-DPPURE.FID\FID				
Frequency (MHz)	199.98	***Nucleus***	1H	***Number of Transients***	36	***Original Points Count***	5984
Points Count	8192	***Pulse Sequence***	s2pul	***Receiver Gain***	40.00	***Solvent***	CHLOROFORM-d
Spectrum Offset (Hz)	1002.0226	***Spectrum Type***	STANDARD	***Sweep Width (Hz)***	3000.30	***Temperature (degree C)***	AMBIENT TEMPERATURE

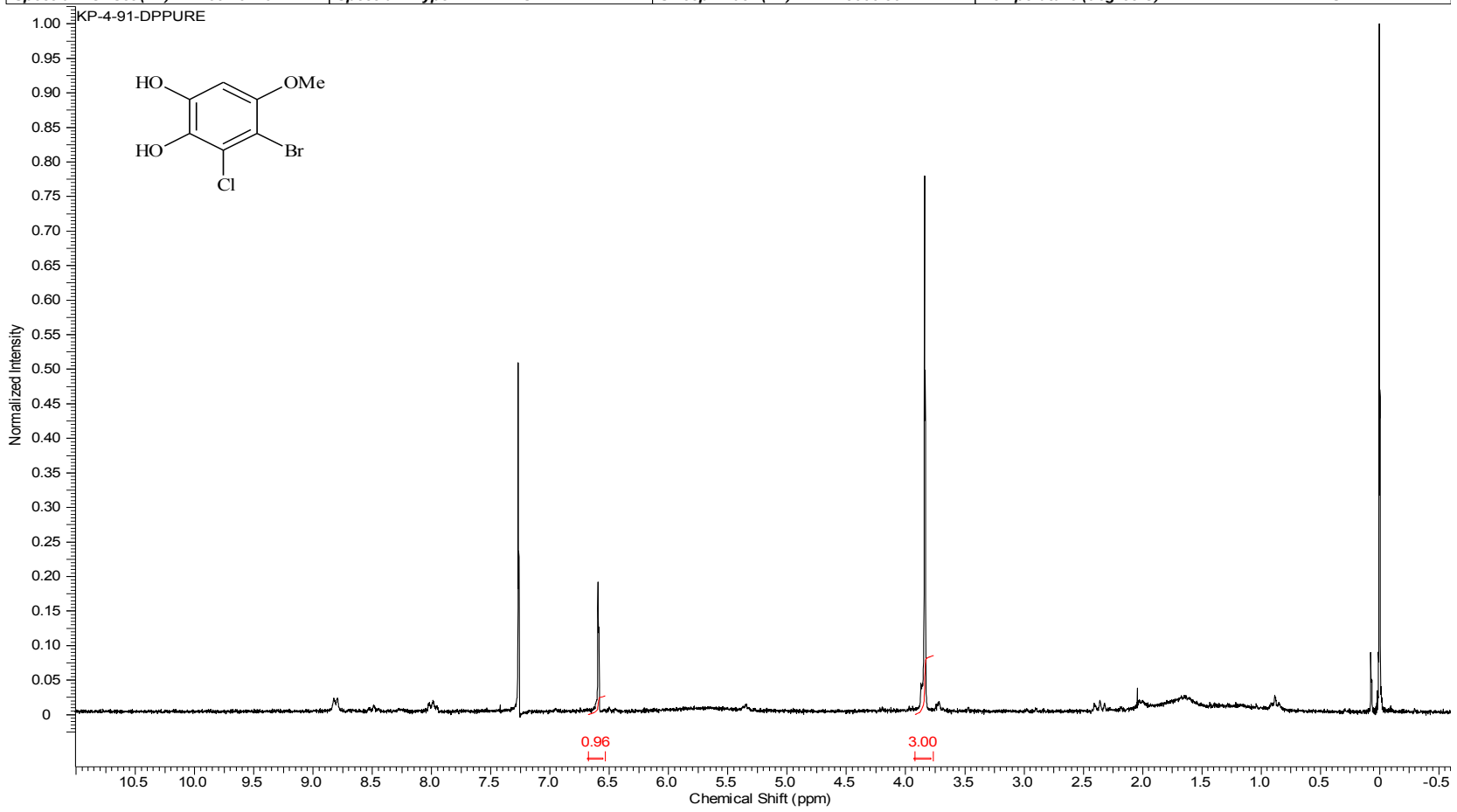

Compound 3 ^{13}C NMR

Acquisition Time (sec)	1.4976	***Comment***	13C OBSERVE	***Date***	Oct 22 2009	***Date Stamp***	Oct 22 2009
File Name	C:\USERS\KESHAR\DESKTOP\NMR\LACCASE\KP-4-91-C13\FID					***Frequency (MHz)***	50.29
Nucleus	13C	***Number of Transients***	17867	***Original Points Count***	18720	***Points Count***	32768
Pulse Sequence	s2pul	***Receiver Gain***	40.00	***Solvent***	CHLOROFORM-d		
Spectrum Offset (Hz)	4880.8467	***Spectrum Type***	STANDARD	***Sweep Width (Hz)***	12500.00	***Temperature (degree C)***	AMBIENT TEMPERATURE

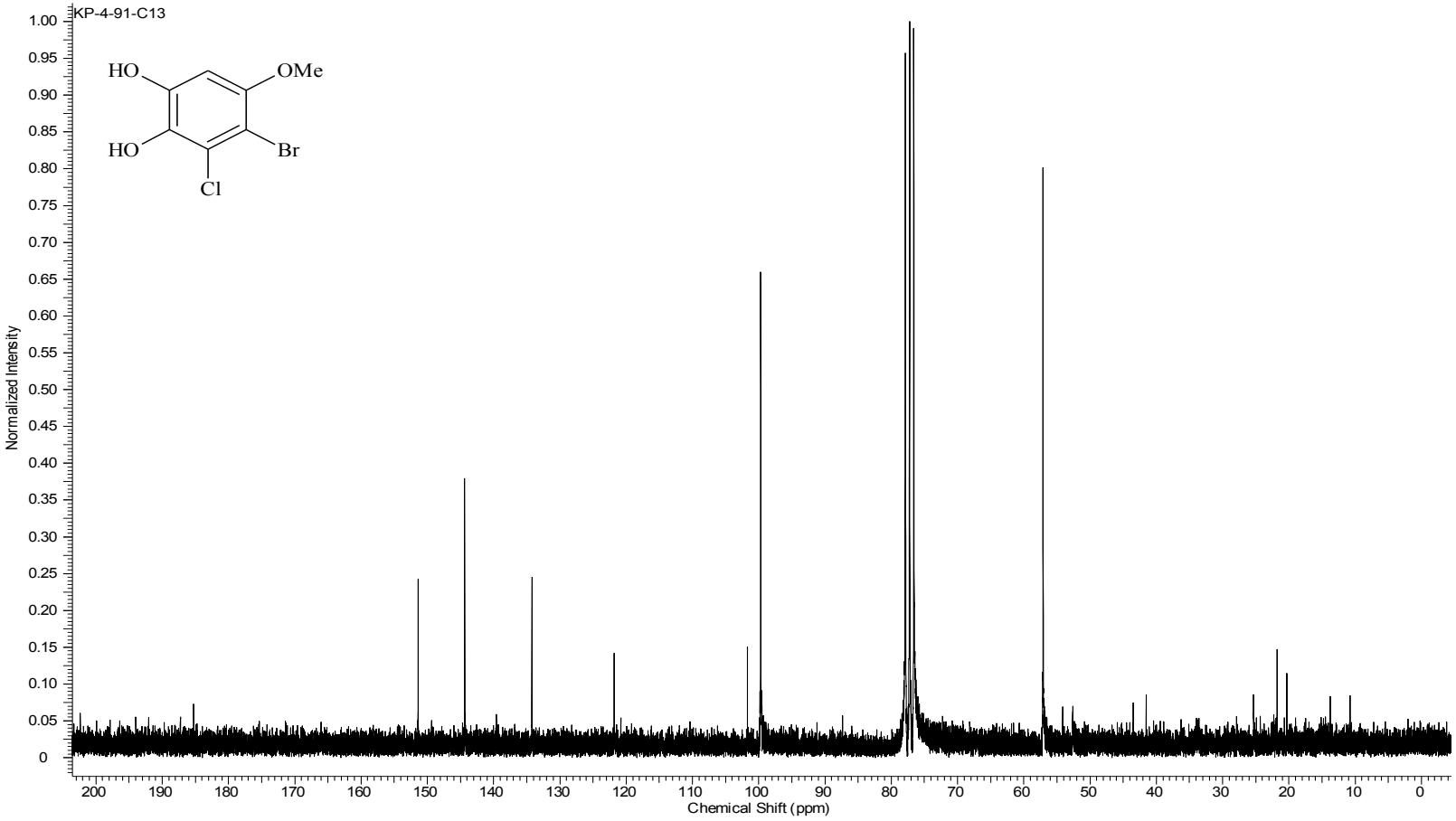

Compound 3 IR

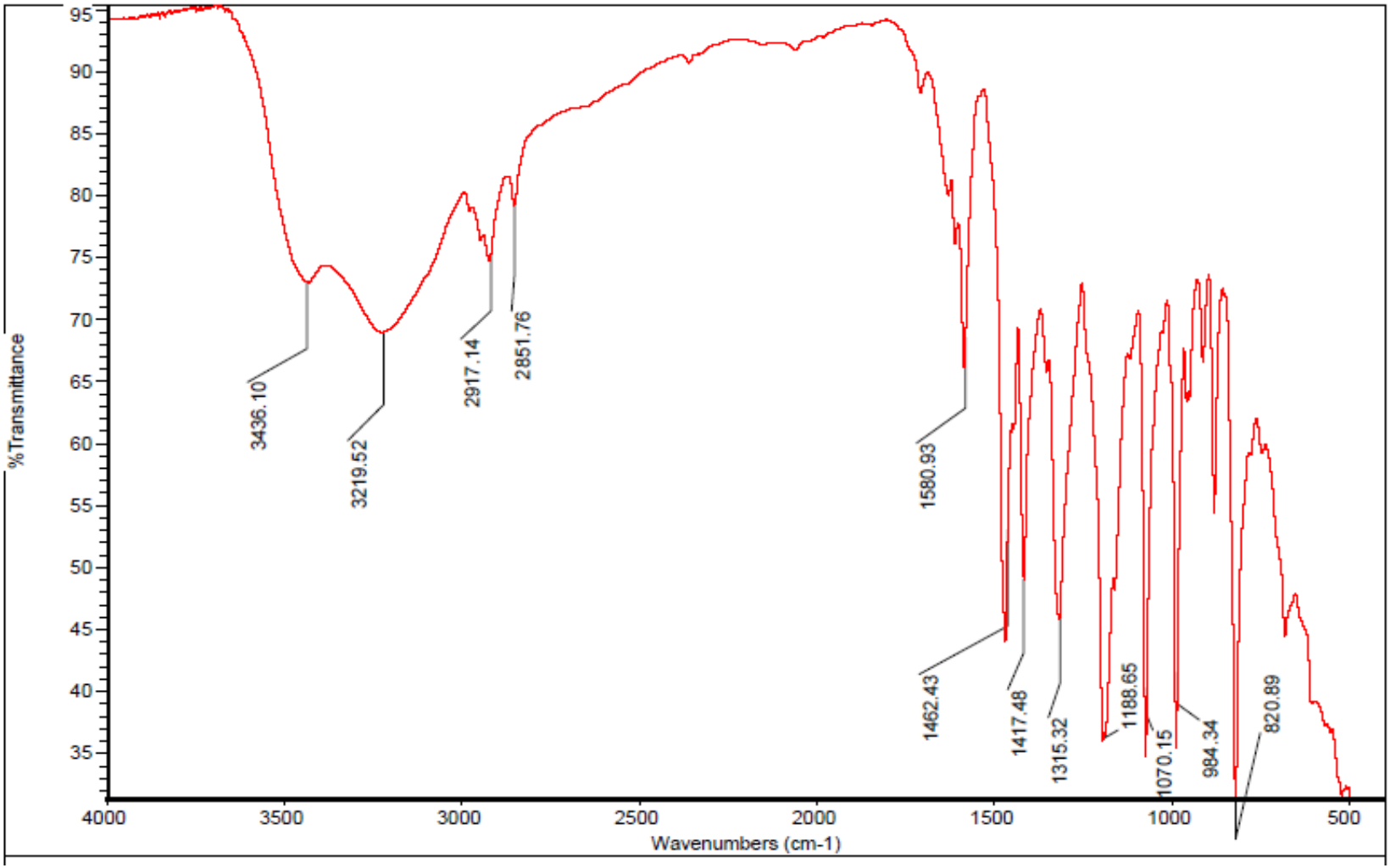

Compound 29 ^{1}H NMR

Acquisition Time (sec)	1.9945	***Comment***	STANDARD 1H OBSERVE			***Date***	Aug 4 2009
Date Stamp	Aug 4 2009	***File Name***	C:\USERS\KESHAR\DOCUMENTS\PHD THESIS SUPPORT JUNE 28\NMR\LACCASE\KP-4-97-SM\FID				
Frequency (MHz)	199.98	***Nucleus***	1H	***Number of Transients***	64	***Original Points Count***	5984
Points Count	8192	***Pulse Sequence***	s2pul	***Receiver Gain***	18.00	***Solvent***	CHLOROFORM-d
Spectrum Offset (Hz)	1003.0914	***Spectrum Type***	STANDARD	***Sweep Width (Hz)***	3000.30	***Temperature (degree C)***	AMBIENT TEMPERATURE

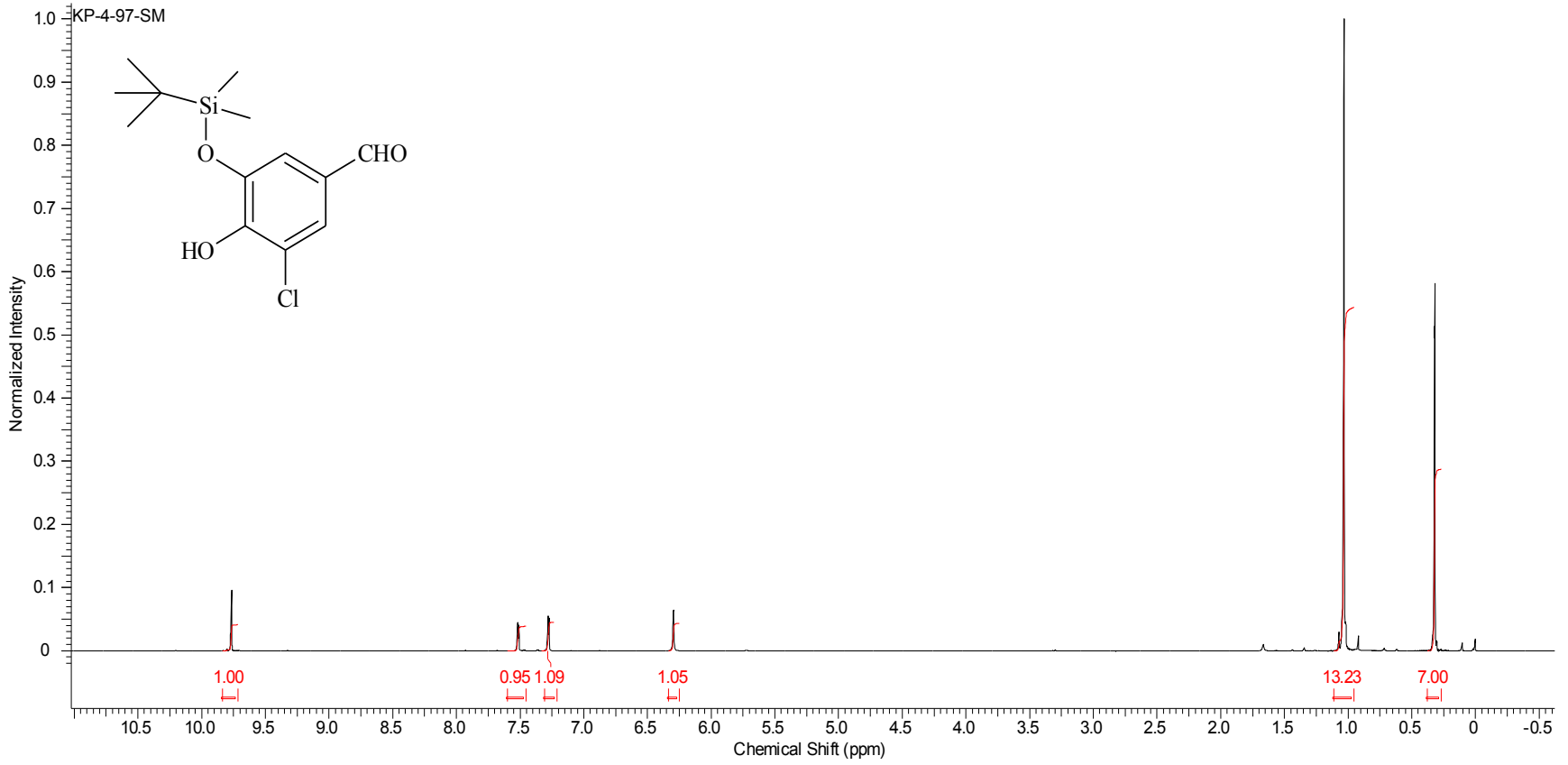

Compound 29 ^{13}C NMR

Acquisition Time (sec)	1.3005	***Comment***	Std proton	***Date***	Aug 17 2009	***Date Stamp***	Aug 17 2009
File Name	C:\USERS\KESHAR\DOCUMENTS\PHD THESIS SUPPORT JUNE 28\NMR\LACCASE\KP-4-97-SM-C13\FID						
Frequency (MHz)	100.53	***Nucleus***	13C	***Number of Transients***	640	***Original Points Count***	31375
Points Count	32768	***Pulse Sequence***	s2pul	***Receiver Gain***	30.00	***Solvent***	CHLOROFORM-d
Spectrum Offset (Hz)	10554.5117	***Spectrum Type***	STANDARD	***Sweep Width (Hz)***	24125.45	***Temperature (degree C)***	25.000

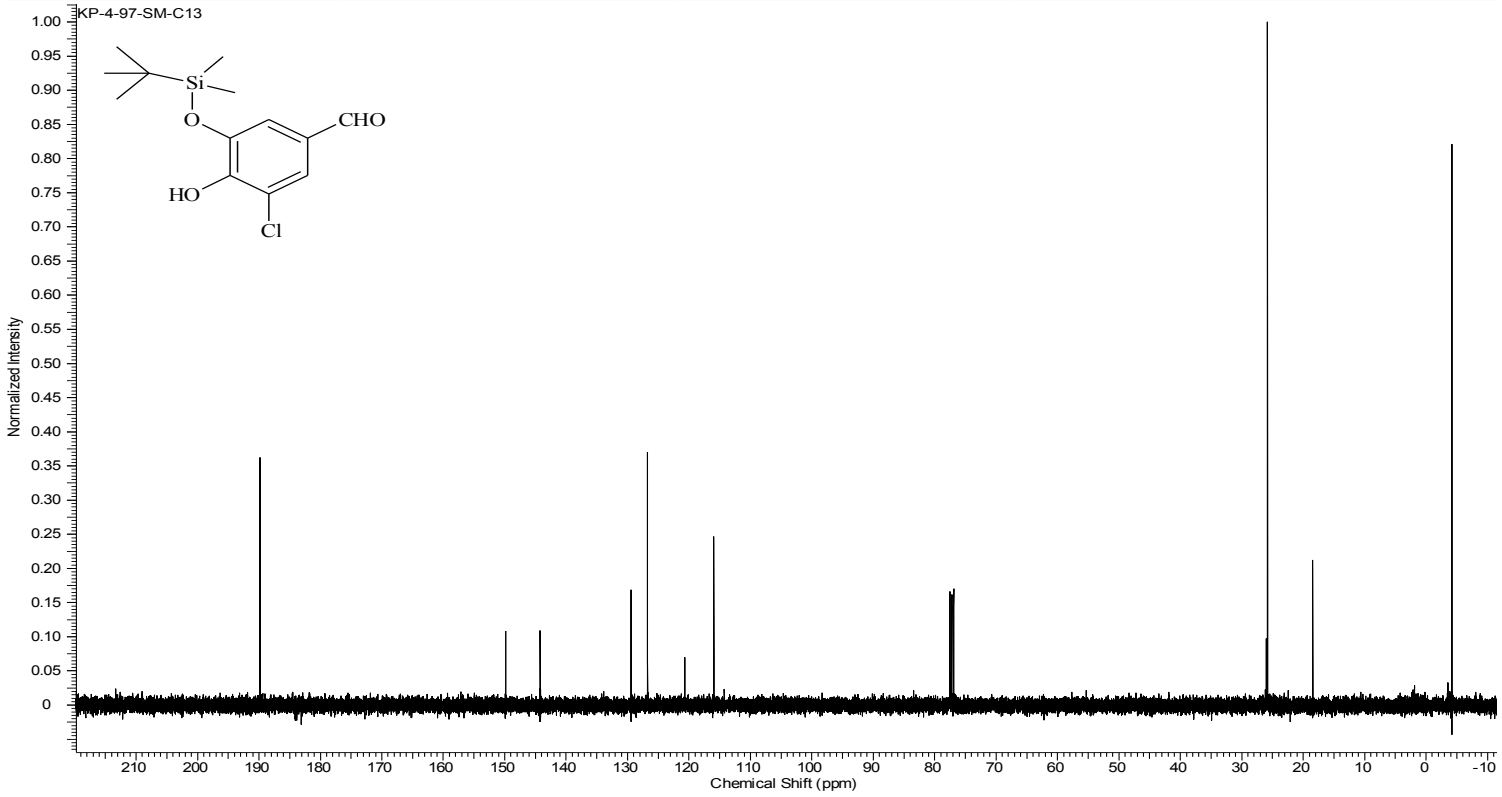

Compound 30 ^{1}H NMR

Acquisition Time (sec)	1.9945	***Comment***	STANDARD 1H OBSERVE			***Date***	Sep 18 2009
Date Stamp	Sep 18 2009	***File Name***	C:\USERS\KESHAR\DESKTOP\NMR\BOOK 5\KP-5-32-DP.FID\FID				
Frequency (MHz)	199.98	***Nucleus***	1H	***Number of Transients***	44	***Original Points Count***	5984
Points Count	8192	***Pulse Sequence***	s2pul	***Receiver Gain***	40.00	***Solvent***	CHLOROFORM-d
Spectrum Offset (Hz)	1002.3889	***Spectrum Type***	STANDARD	***Sweep Width (Hz)***	3000.30	***Temperature (degree C)***	AMBIENT TEMPERATURE

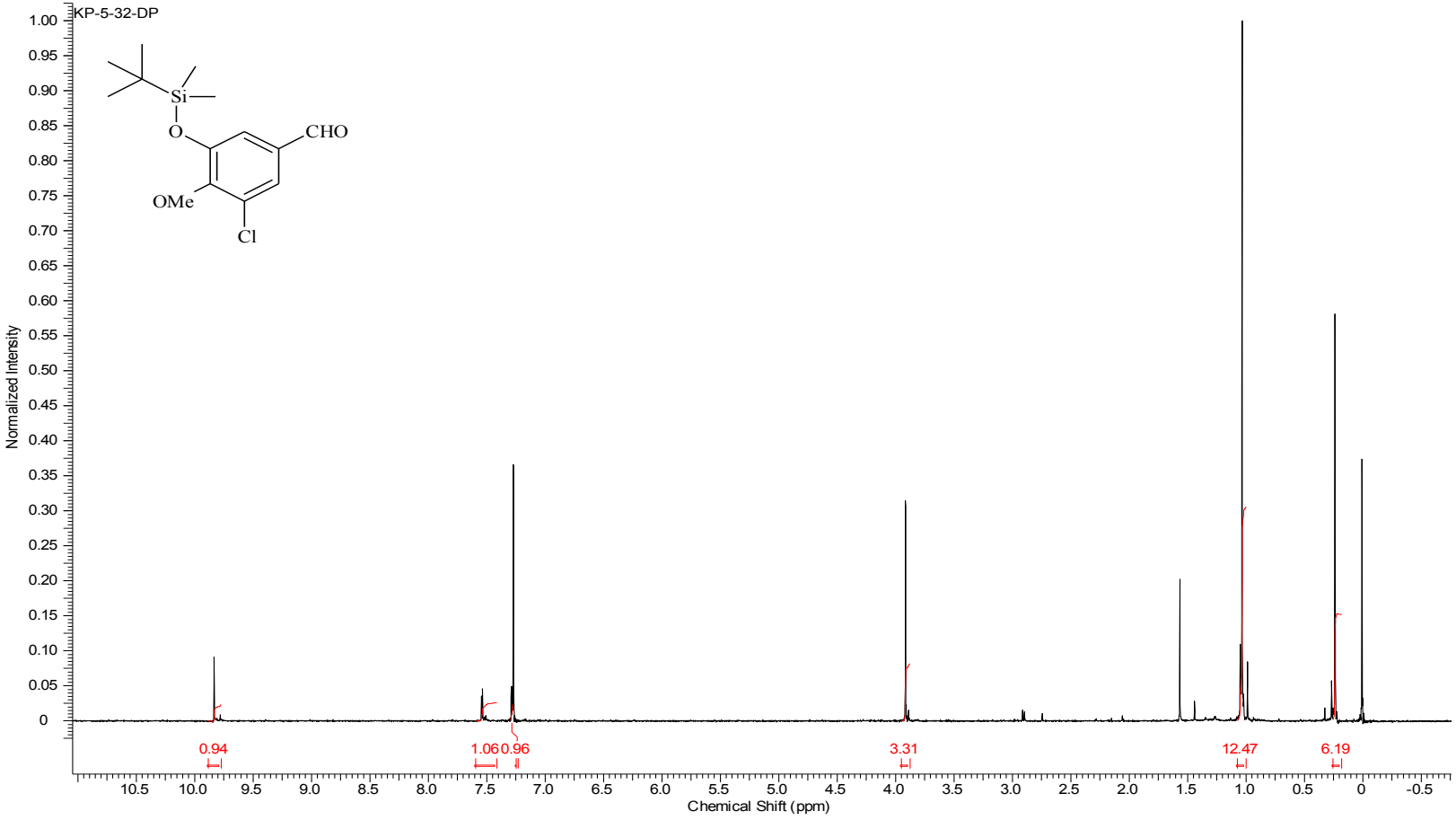

Compound 30 ^{13}C NMR

Acquisition Time (sec)	1.4976	***Comment***	13C OBSERVE	***Date***	Aug 17 2009	***Date Stamp***	Aug 17 2009
File Name	C:\USERS\KESHAR\DESKTOP\NMR\LACCASE\KP-4-97-SM-C13P\FID					***Frequency (MHz)***	50.29
Nucleus	13C	***Number of Transients***	752	***Original Points Count***	18720	***Points Count***	32768
Pulse Sequence	s2pul	***Receiver Gain***	40.00	***Solvent***	CHLOROFORM-d		
Spectrum Offset (Hz)	4880.0840	***Spectrum Type***	STANDARD	***Sweep Width (Hz)***	12500.00	***Temperature (degree C)***	AMBIENT TEMPERATURE

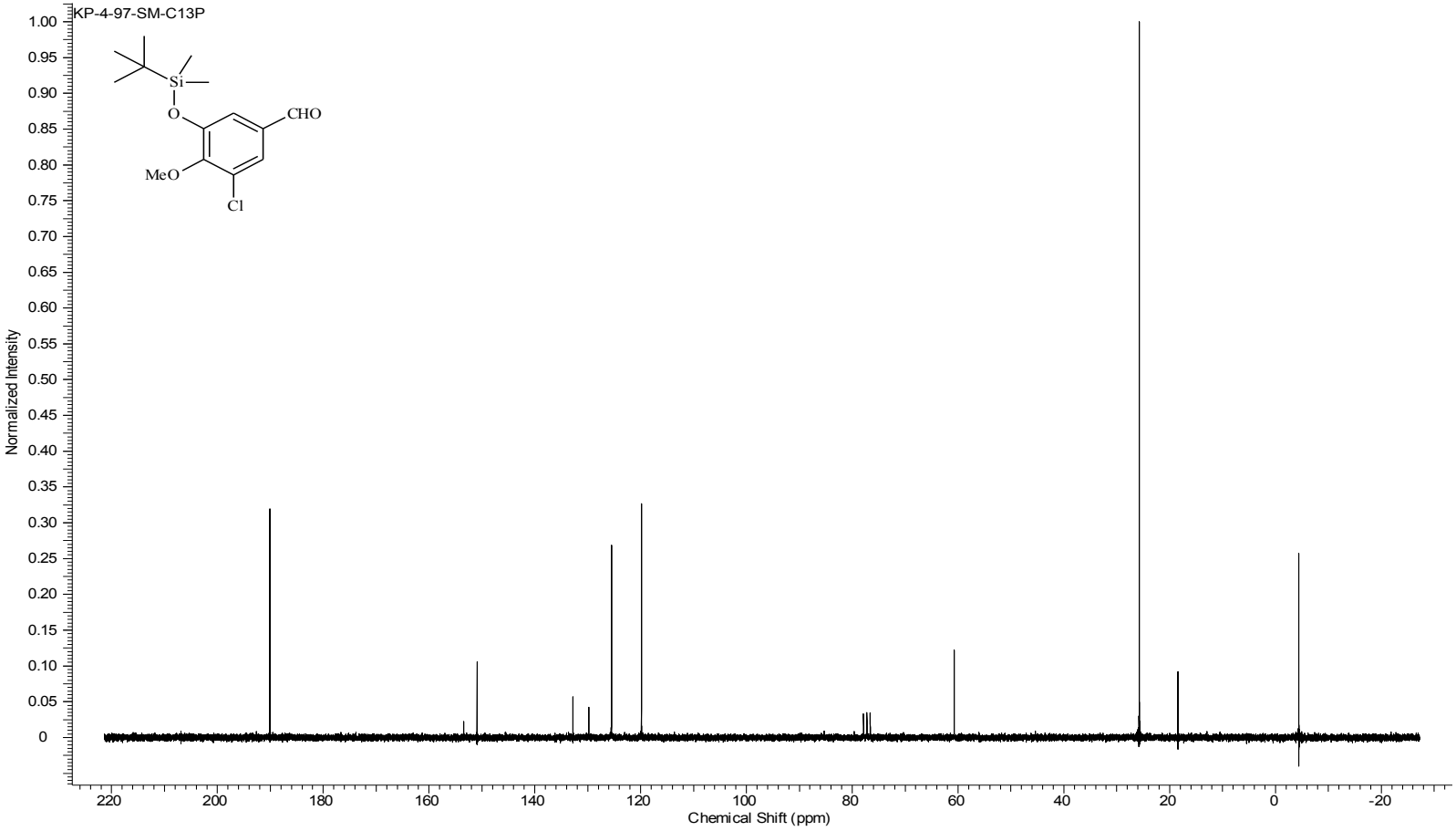

Compound 31 ^{1}H NMR

Acquisition Time (sec)	1.9945	***Comment***	STANDARD 1H OBSERVE			***Date***	Aug 27 2007
Date Stamp	Aug 27 2007	***File Name***	C:\USERS\KESHAR\KP-4-97-Fr1-Proton				
Frequency (MHz)	199.98	***Nucleus***	1H	***Number of Transients***	64	***Original Points Count***	5984
Points Count	8192	***Pulse Sequence***	s2pul	***Receiver Gain***	28.00	***Solvent***	CHLOROFORM-d
Spectrum Offset (Hz)	1002.3890	***Spectrum Type***	STANDARD	***Sweep Width (Hz)***	3000.30	***Temperature (degree C)***	AMBIENT TEMPERATURE

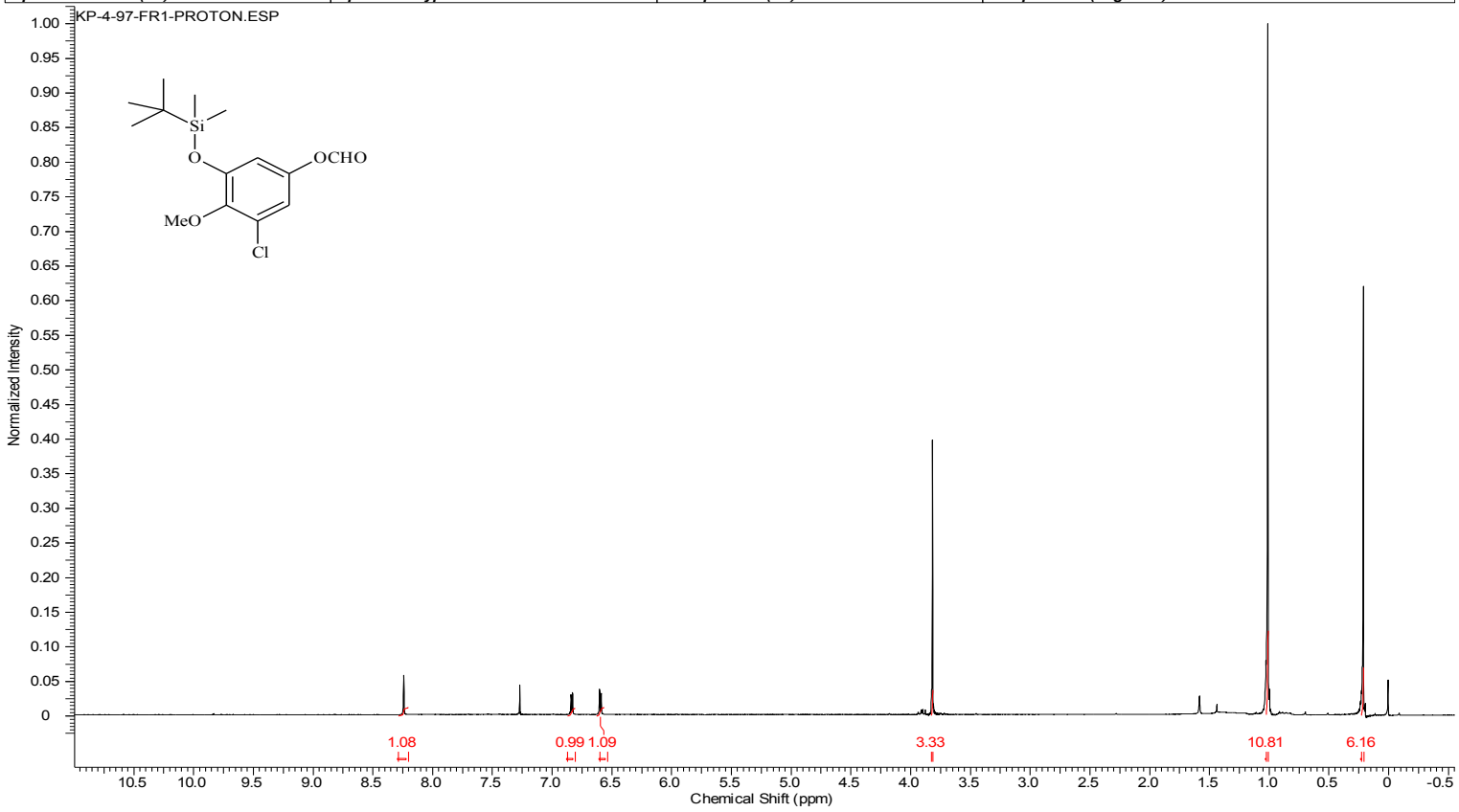

Compound 31 ^{13}C NMR

Acquisition Time (sec)	1.4976	***Comment***	13C OBSERVE	***Date***	Sep 1 2009	***Date Stamp***	Sep 1 2009
File Name	C:\USERS\KESHAR\DOCUMENTS\PHD THESIS SUPPORT JUNE 28\NMR\LACCASE\KP-4-97-FR-1-C13\FID					***Frequency (MHz)***	50.29
Nucleus	13C	***Number of Transients***	12208	***Original Points Count***	18720	***Points Count***	32768
Pulse Sequence	s2pul	***Receiver Gain***	40.00	***Solvent***	CHLOROFORM-d	***Spectrum Offset (Hz)***	4881.2285
Spectrum Type	STANDARD	***Sweep Width (Hz)***	12500.00	***Temperature (degree C)***	AMBIENT TEMPERATURE		

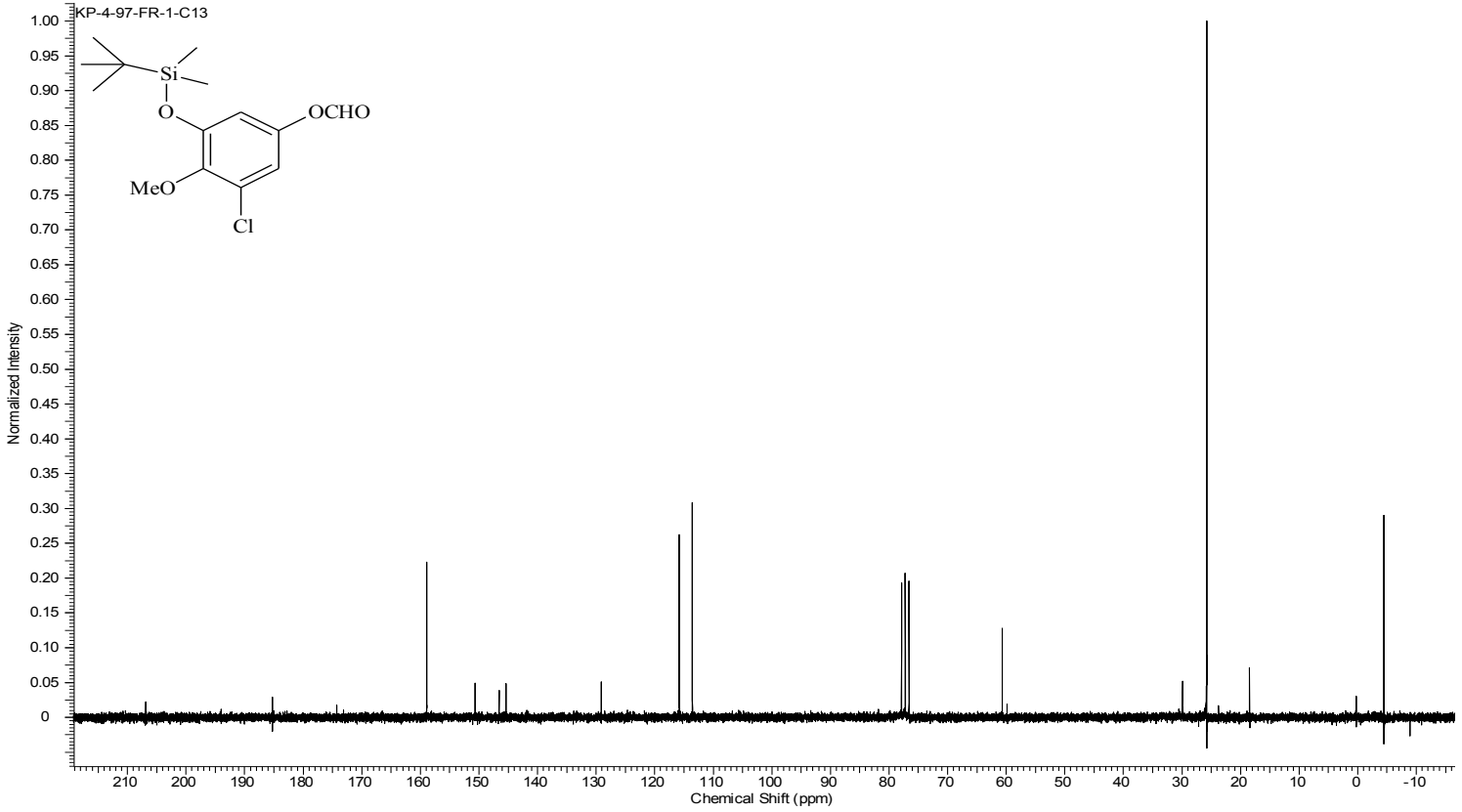

Compound 32 ^{1}H NMR

Acquisition Time (sec)	1.9945	***Comment***	STANDARD 1H OBSERVE			***Date***	Aug 27 2009
Date Stamp	Aug 27 2009	***File Name***	C:\USERS\KESHAR\DESKTOP\NMR\LACCASE\KP-4-97-FR2\FID				
Frequency (MHz)	199.98	***Nucleus***	1H	***Number of Transients***	64	***Original Points Count***	5984
Points Count	8192	***Pulse Sequence***	s2pul	***Receiver Gain***	34.00	***Solvent***	CHLOROFORM-d
Spectrum Offset (Hz)	1001.6563	***Spectrum Type***	STANDARD	***Sweep Width (Hz)***	3000.30	***Temperature (degree C)***	AMBIENT TEMPERATURE

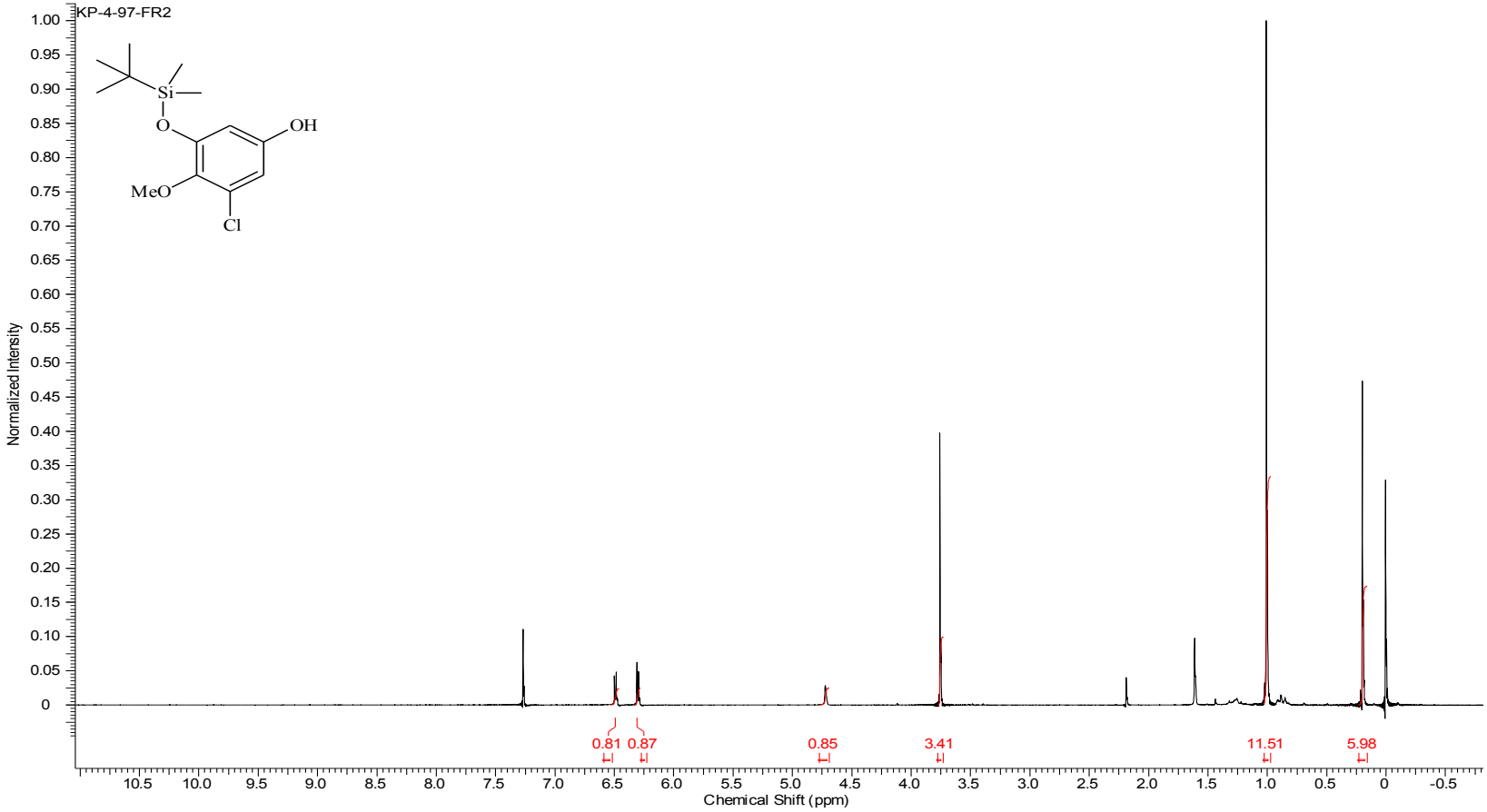

Compound 32 ^{13}C NMR

Acquisition Time (sec)	1.3005	***Comment***	Std proton	***Date***	Aug 29 2009	***Date Stamp***	Aug 29 2009
File Name	C:\USERS\KESHAR\DESKTOP\NMR\LACCASE\KP-4-97-FRAC2-C13\FID					***Frequency (MHz)***	100.53
Nucleus	13C	***Number of Transients***	1856	***Original Points Count***	31375	***Points Count***	32768
Pulse Sequence	s2pul	***Receiver Gain***	30.00	***Solvent***	CHLOROFORM-d		
Spectrum Offset (Hz)	10557.2520	***Spectrum Type***	STANDARD	***Sweep Width (Hz)***	24125.45	***Temperature (degree C)***	25.000

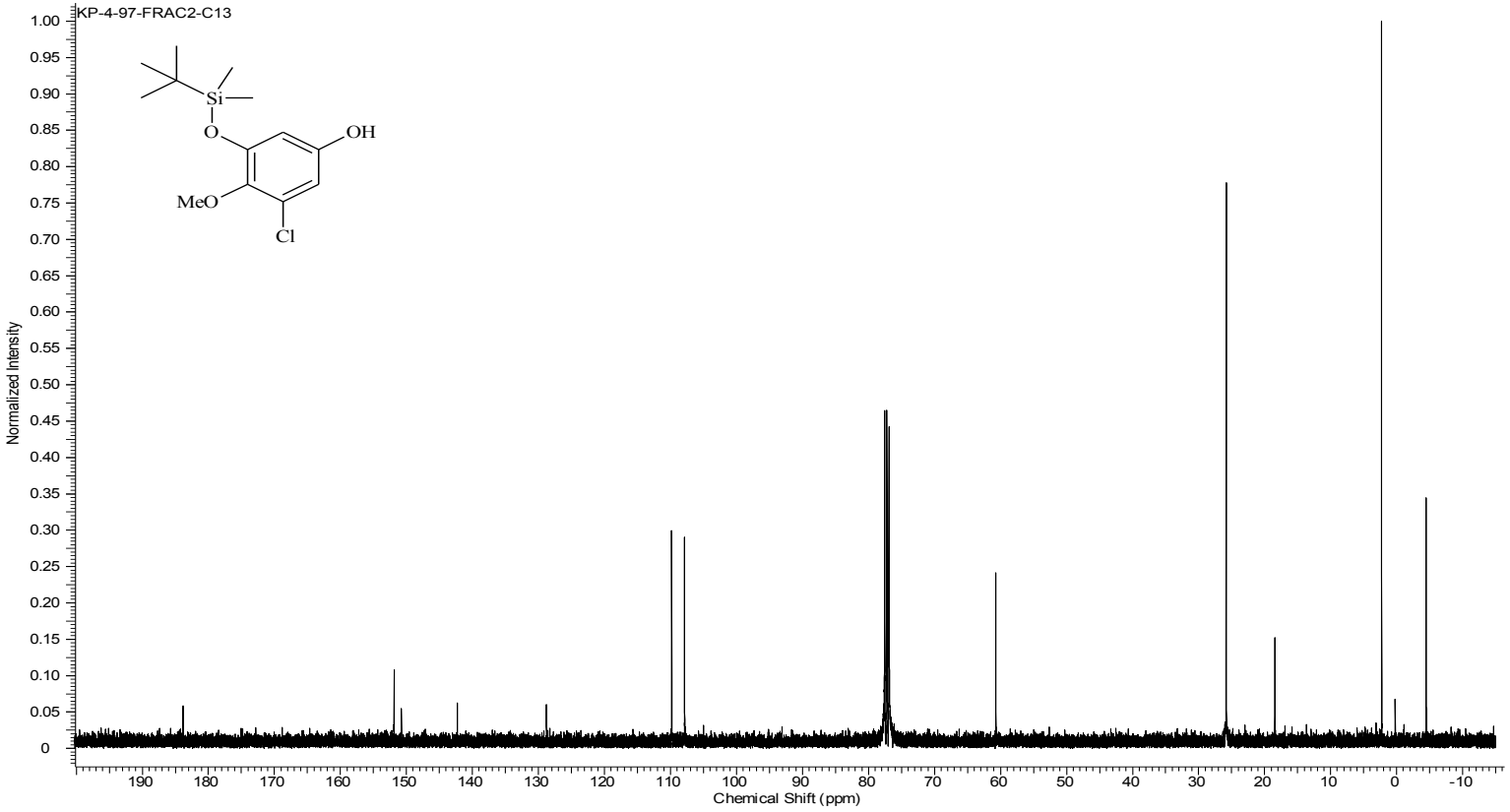

Compound 33 ^{1}H NMR

Acquisition Time (sec)	2.0487	***Comment***	Std proton	***Date***	Aug 26 2009	***Date Stamp***	Aug 26 2009
File Name	C:\USERS\KESHAR\KP-5-11-FR1-Proton						
Frequency (MHz)	399.75	***Nucleus***	1H	***Number of Transients***	44	***Original Points Count***	13103
Points Count	16384	***Pulse Sequence***	s2pul	***Receiver Gain***	60.00	***Solvent***	CHLOROFORM-d
Spectrum Offset (Hz)	2403.9280	***Spectrum Type***	STANDARD	***Sweep Width (Hz)***	6395.91	***Temperature (degree C)***	25.000

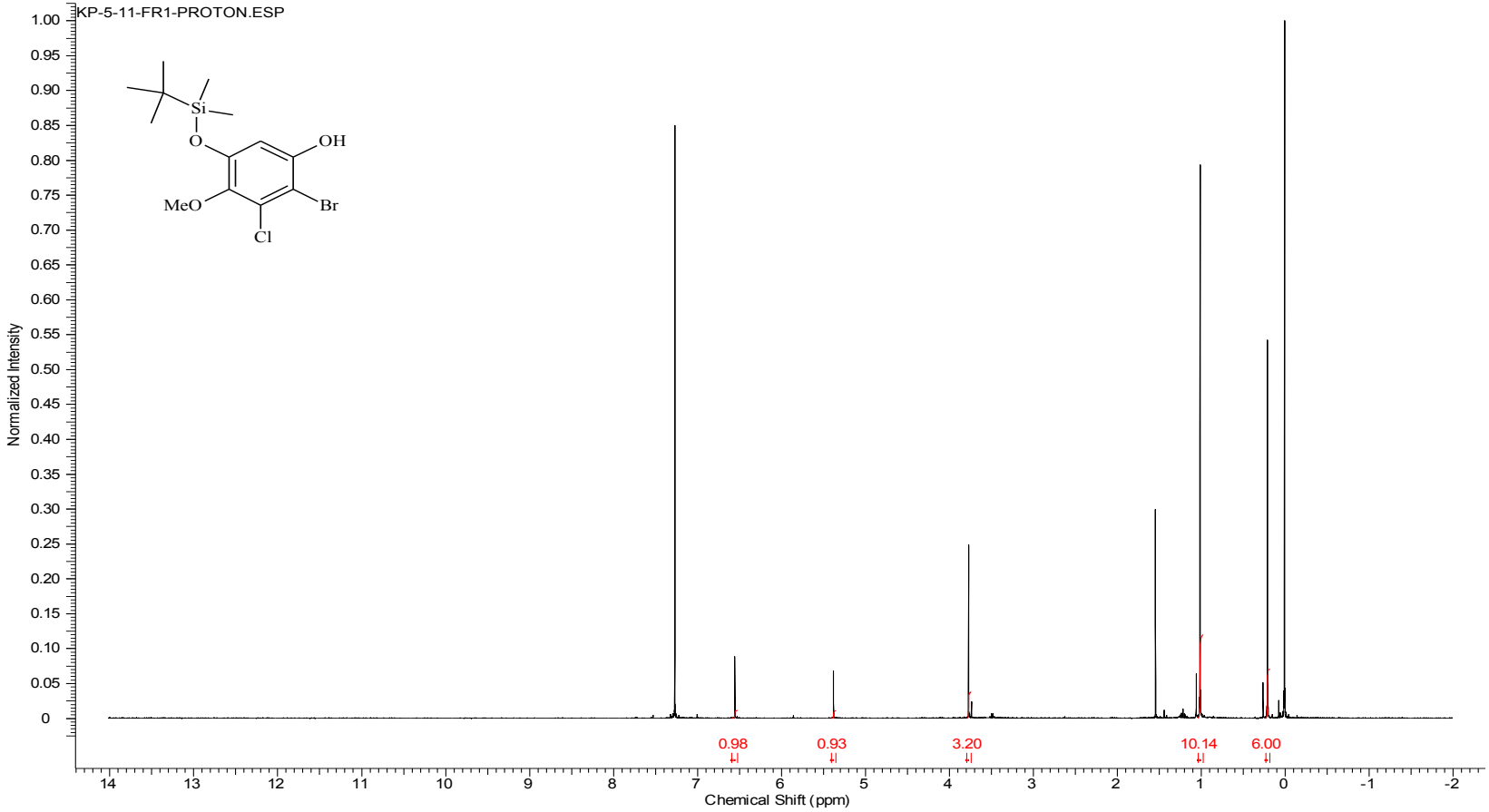

Compound 33 ^{13}C NMR

Acquisition Time (sec)	1.3005	***Comment***	Std proton	***Date***	Sep 4 2009	***Date Stamp***	Sep 4 2009
File Name	C:\USERS\KESHAR\DESKTOP\NMR\LACCASE\KP-5-19-SM-C13\FID					***Frequency (MHz)***	100.53
Nucleus	13C	***Number of Transients***	15226	***Original Points Count***	31375	***Points Count***	32768
Pulse Sequence	s2pul	***Receiver Gain***	30.00	***Solvent***	CHLOROFORM-d		
Spectrum Offset (Hz)	10555.8564	***Spectrum Type***	STANDARD	***Sweep Width (Hz)***	24125.45	***Temperature (degree C)***	25.000

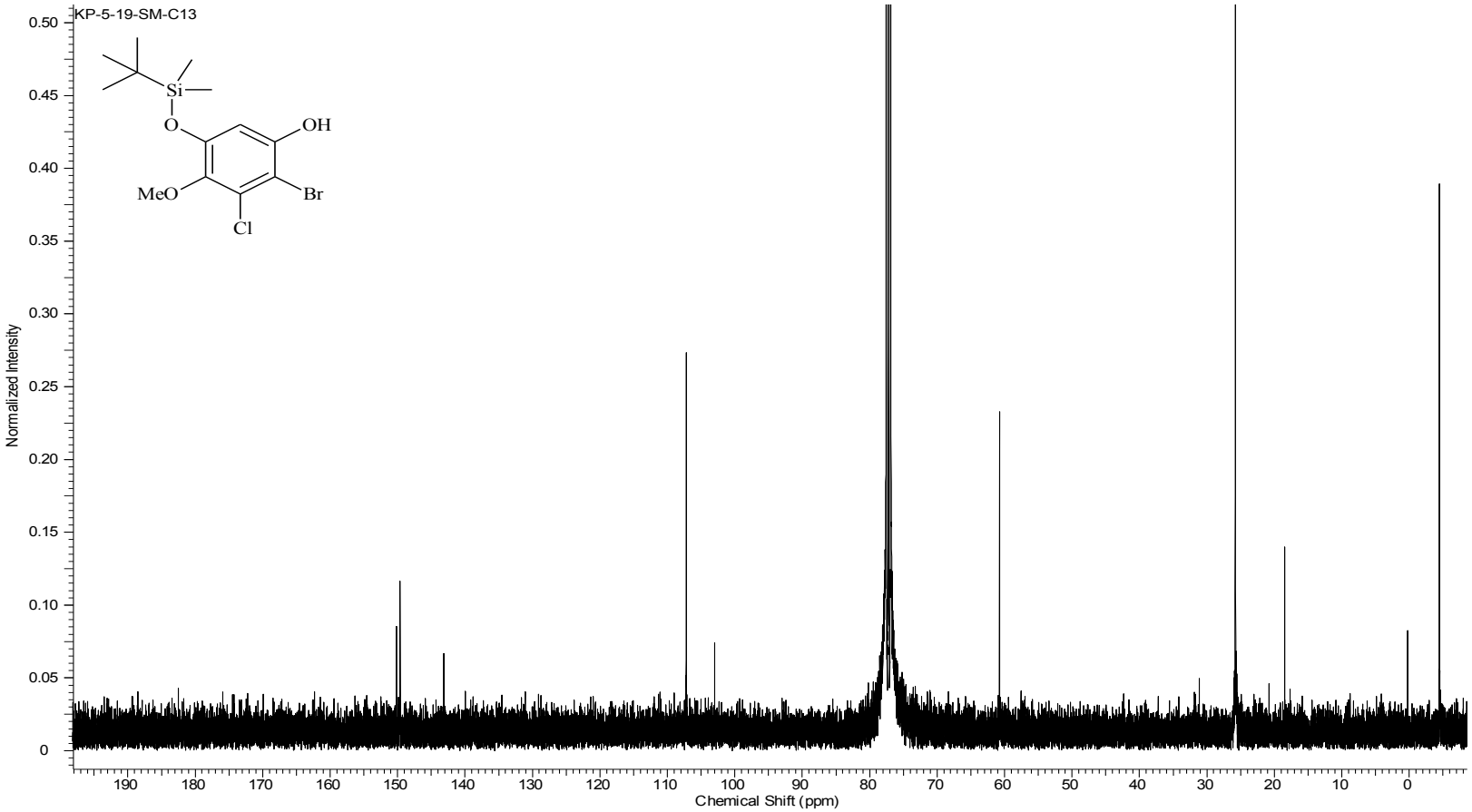

Compound 5 ^{1}H NMR

Acquisition Time (sec)	2.0487	***Comment***	Std proton	***Date***	Aug 27 2009	***Date Stamp***	Aug 27 2009
File Name	C:\USERS\KESHAR\KP-5-19-Proton						
Frequency (MHz)	399.75	***Nucleus***	1H	***Number of Transients***	20	***Original Points Count***	13103
Points Count	16384	***Pulse Sequence***	s2pul	***Receiver Gain***	42.00	***Solvent***	CHLOROFORM-d
Spectrum Offset (Hz)	2403.5376	***Spectrum Type***	STANDARD	***Sweep Width (Hz)***	6395.91	***Temperature (degree C)***	25.000

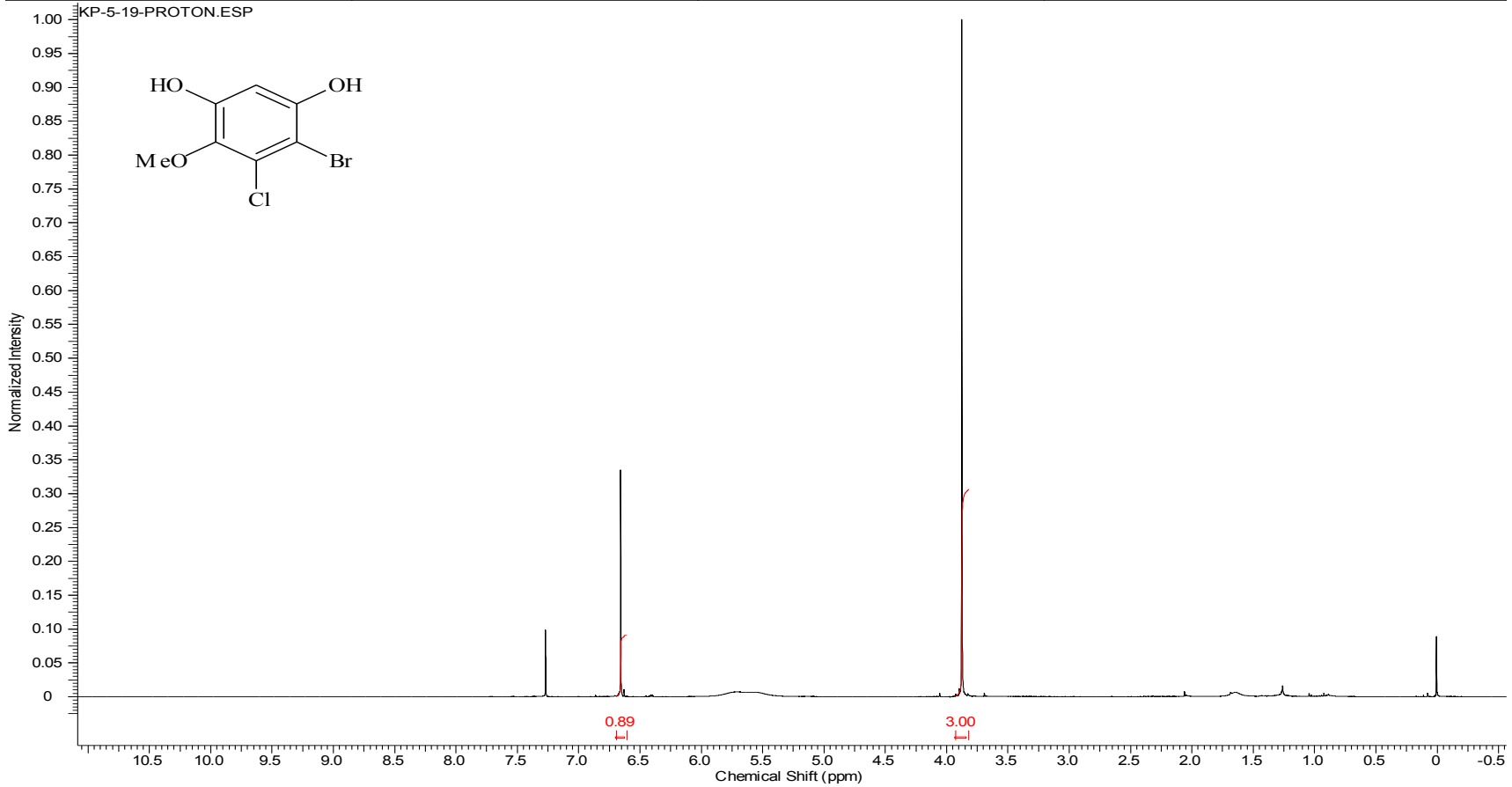

Compound 5 ^{13}C NMR

Acquisition Time (sec)	1.3005	***Comment***	Std proton	***Date***	Oct 23 2009	***Date Stamp***	Oct 23 2009
File Name	C:\USERS\KESHAR\DESKTOP\NMR\LACCASE\KP-5-19-DP-C13\FID					***Frequency (MHz)***	100.53
Nucleus	13C	***Number of Transients***	5696	***Original Points Count***	31375	***Points Count***	32768
Pulse Sequence	s2pul	***Receiver Gain***	30.00	***Solvent***	CHLOROFORM-d		
Spectrum Offset (Hz)	10554.3848	***Spectrum Type***	STANDARD	***Sweep Width (Hz)***	24125.45	***Temperature (degree C)***	25.000

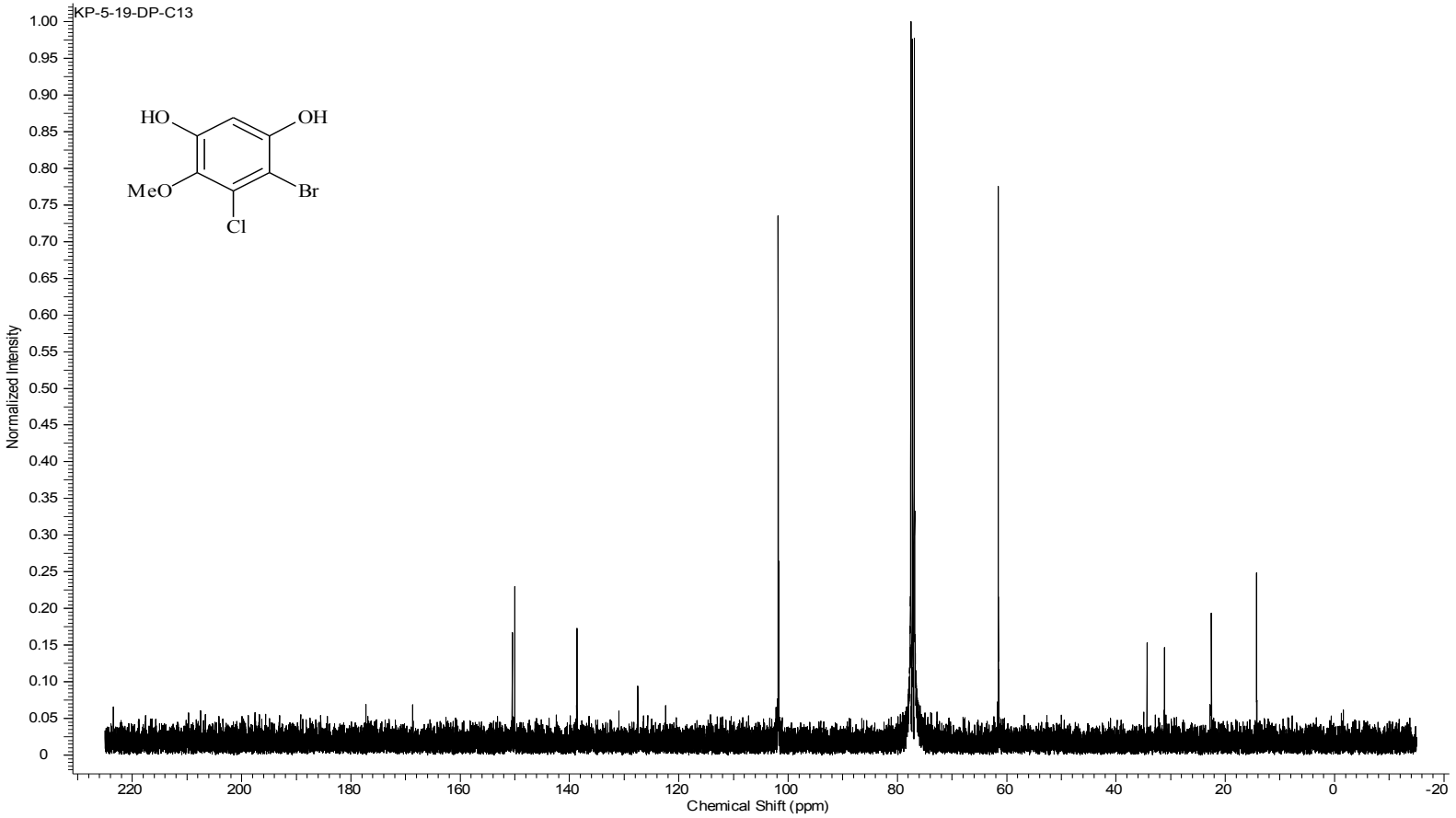

Compound 5 IR

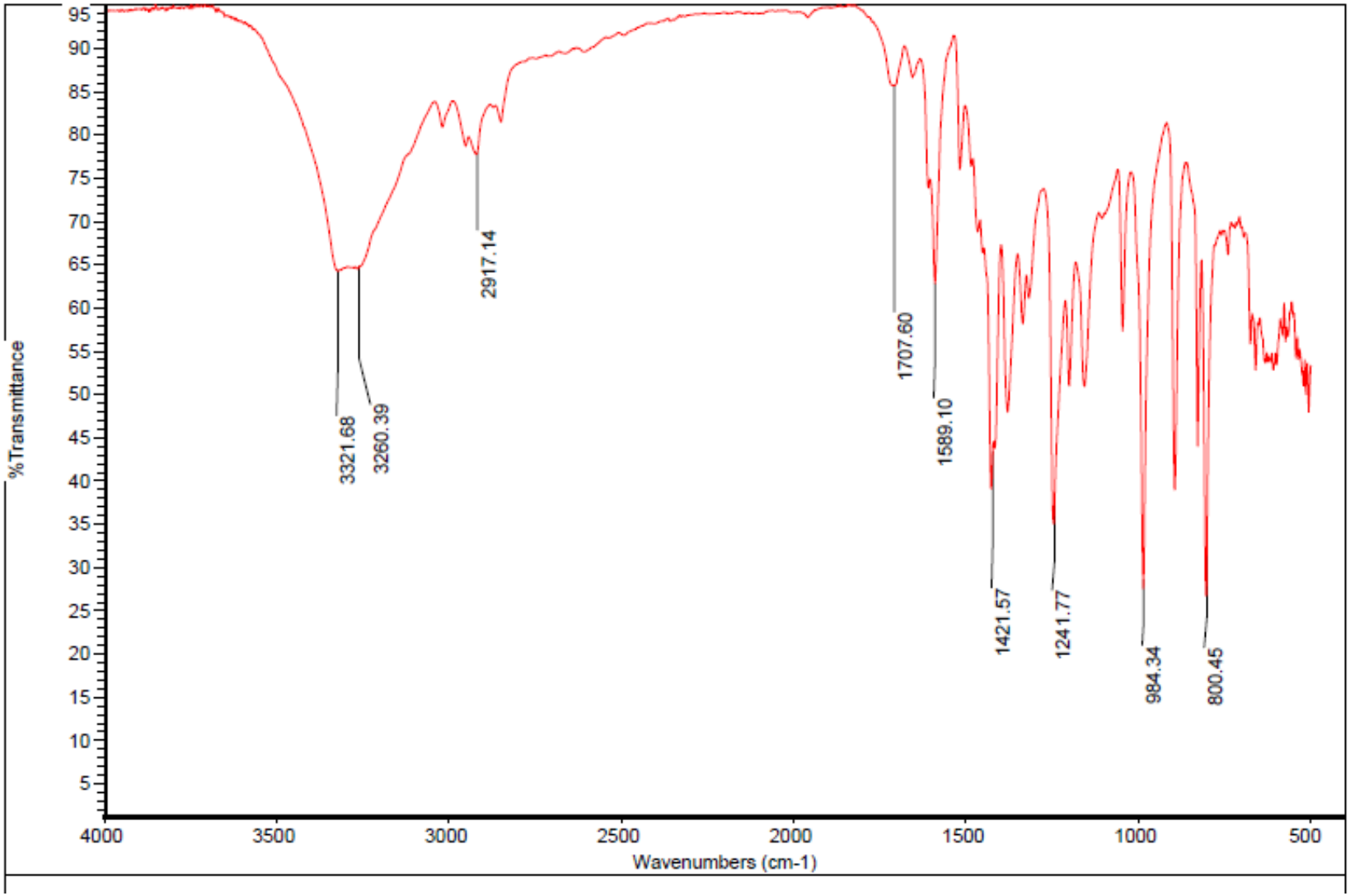

Compound 35 ^{1}H NMR

Acquisition Time (sec)	1.9945	***Comment***	STANDARD 1H OBSERVE			***Date***	May 19 2009
Date Stamp	May 19 2009	***File Name***	C:\USERS\KESHAR\DESKTOP\NMR\BOOK 4\KP-4-95-CRUDE.FID\FID				
Frequency (MHz)	199.98	***Nucleus***	1H	***Number of Transients***	64	***Original Points Count***	5984
Points Count	8192	***Pulse Sequence***	s2pul	***Receiver Gain***	40.00	***Solvent***	CHLOROFORM-d
Spectrum Offset (Hz)	1002.3890	***Spectrum Type***	STANDARD	***Sweep Width (Hz)***	3000.30	***Temperature (degree C)***	AMBIENT TEMPERATURE

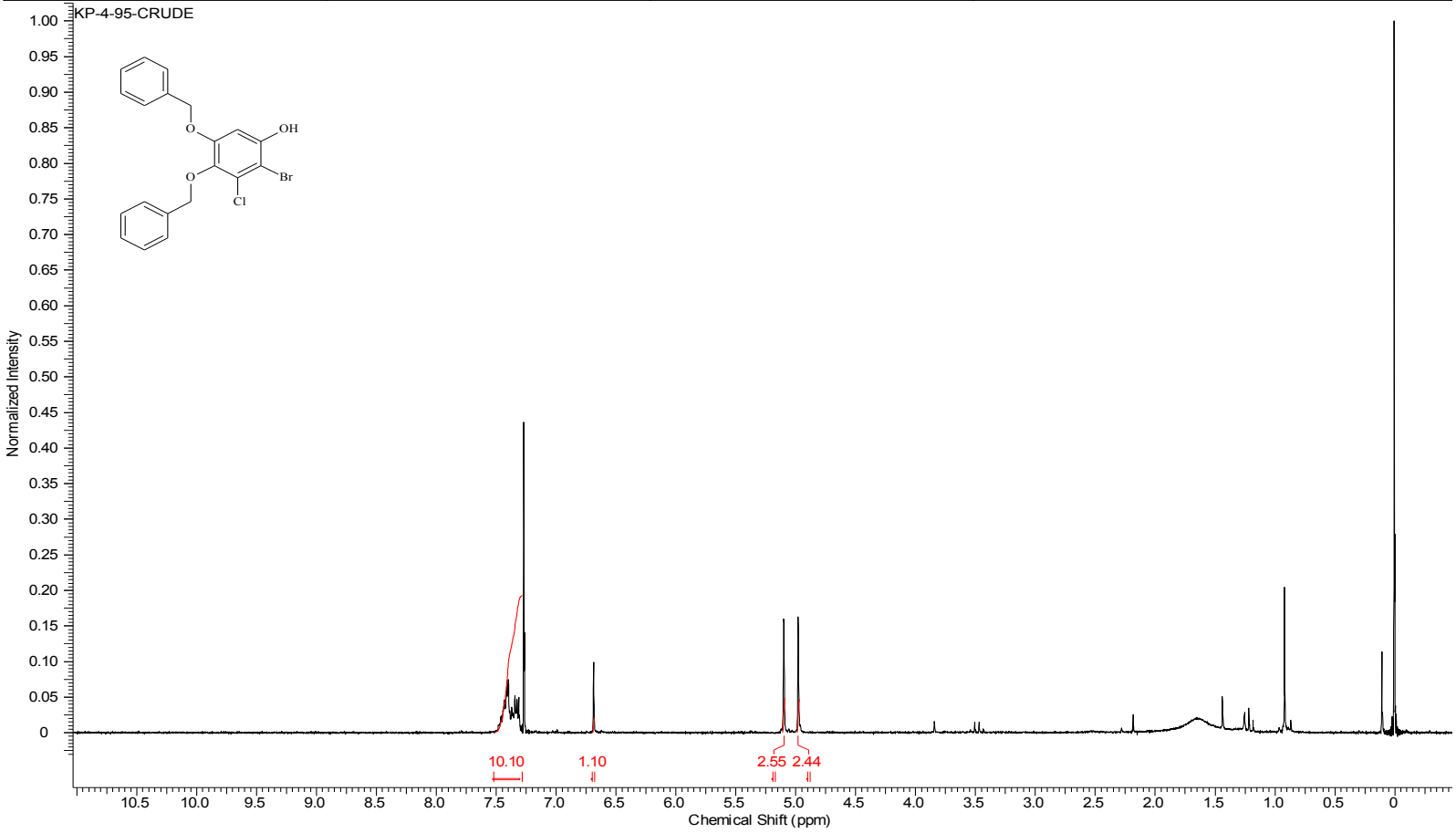

Compound 35 ^{13}C NMR

Acquisition Time (sec)	1.4976	***Comment***	13C OBSERVE			***Date***	Jul 8 2009
Date Stamp	Jul 8 2009	***File Name***	E:\KESHAR NMR REMAIN\SR-10-96-PURE-13C.FID\FID			***Frequency (MHz)***	50.29
Nucleus	13C	***Number of Transients***	1872	***Original Points Count***	18720	***Points Count***	32768
Pulse Sequence	s2pul	***Receiver Gain***	40.00	***Solvent***	CHLOROFORM-d		
Spectrum Offset (Hz)	4878.5532	***Spectrum Type***	STANDARD	***Sweep Width (Hz)***	12500.00	***Temperature (degree C)***	AMBIENT TEMPERATURE

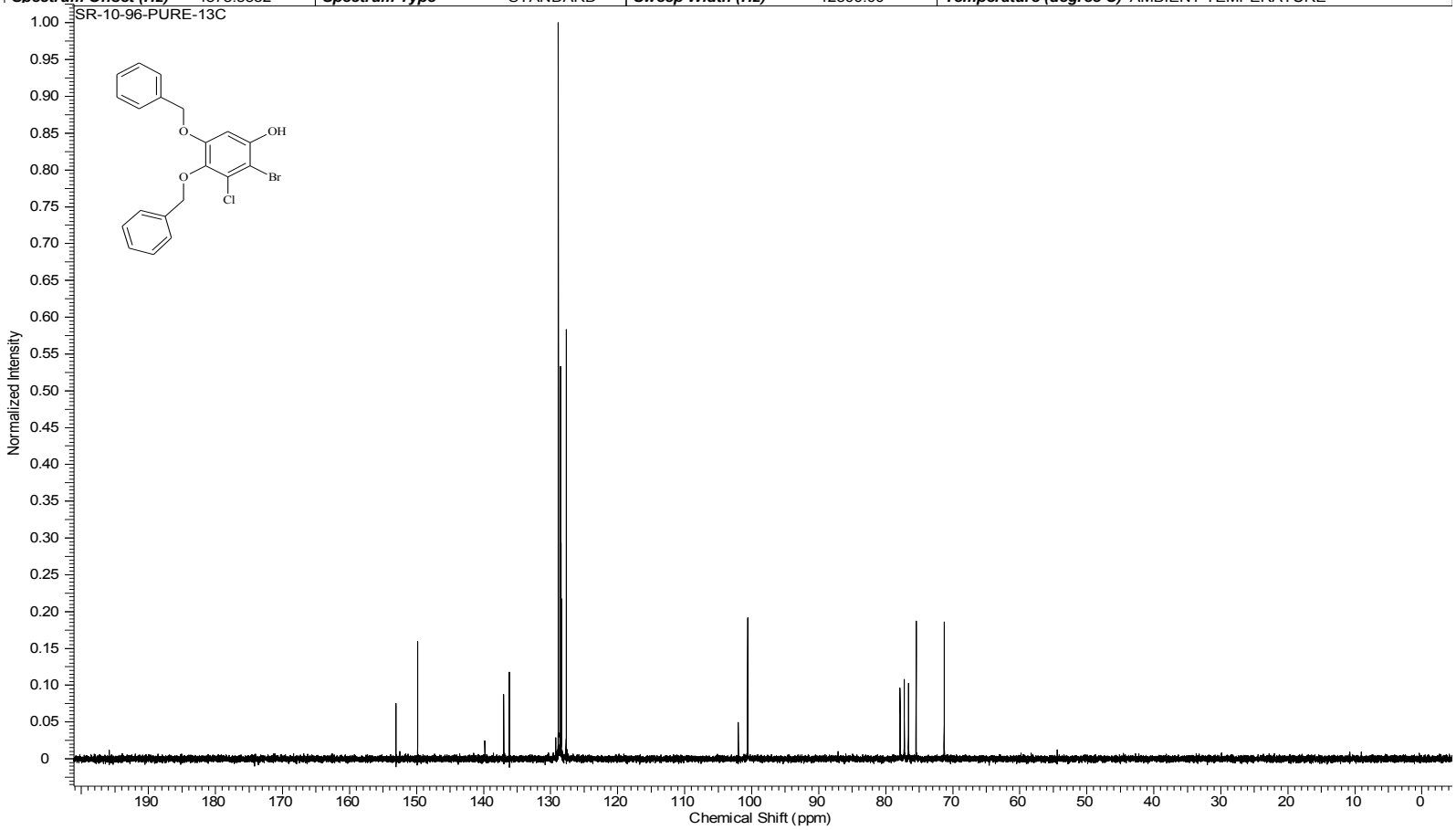

Compound 6 ^{1}H NMR

Acquisition Time (sec)	2.0487	***Comment***	Std proton	***Date***	Jul 7 2009	***Date Stamp***	Jul 7 2009
File Name	C:\USERS\KESHAR\DESKTOP\NMR\OTHERS\KP-5-13-CRUDE\FID					***Frequency (MHz)***	399.75
Nucleus	1H	***Number of Transients***	4	***Original Points Count***	13103	***Points Count***	16384
Pulse Sequence	s2pul	***Receiver Gain***	46.00	***Solvent***	CHLOROFORM-d		
Spectrum Offset (Hz)	2403.9280	***Spectrum Type***	STANDARD	***Sweep Width (Hz)***	6395.91	***Temperature (degree C)***	25.000

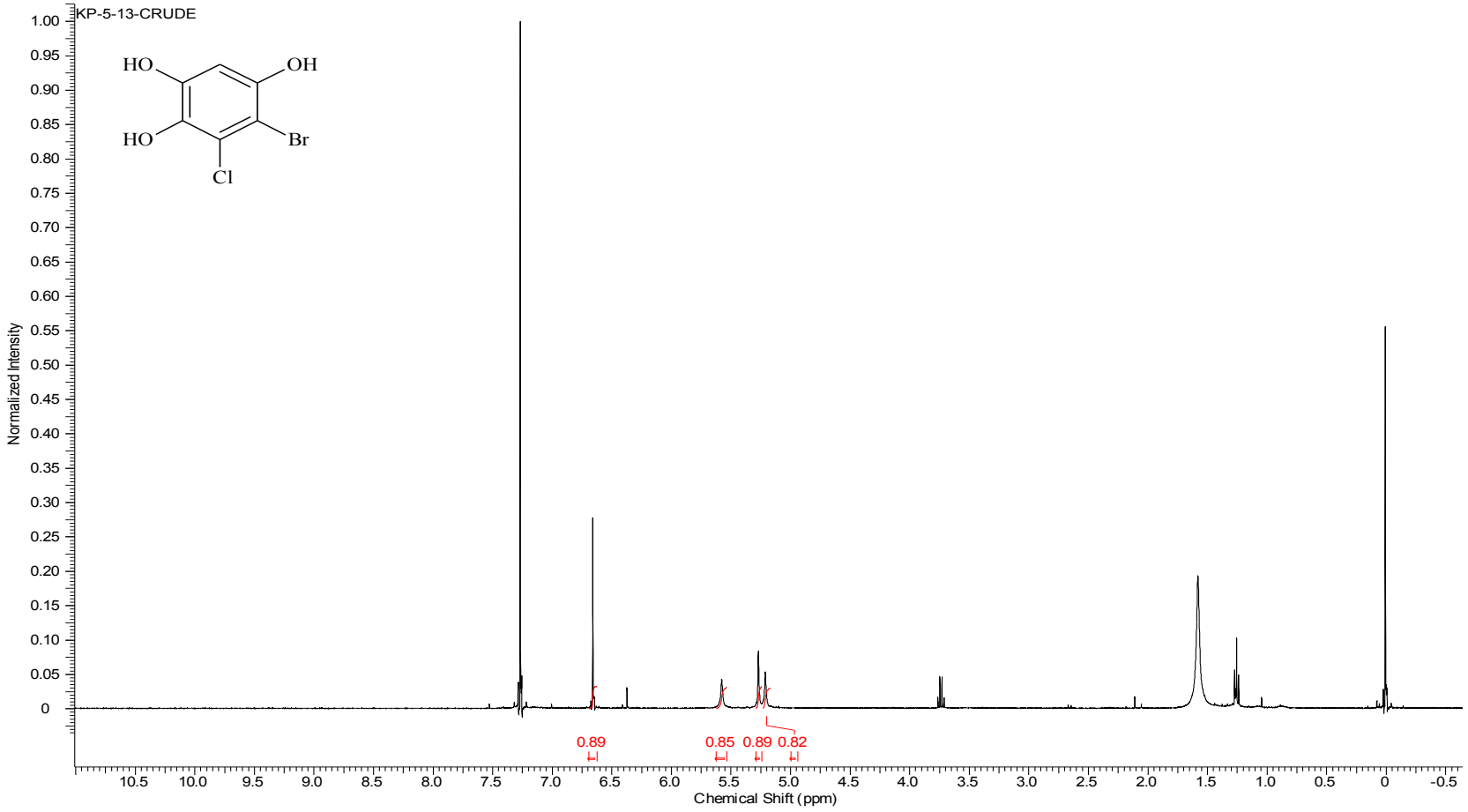

Compound 6 ^{13}C NMR

Acquisition Time (sec)	1.4976	***Comment***	13C OBSERVE	***Date***	Jul 22 2009	***Date Stamp***	Jul 22 2009
File Name	E:\KESHAR NMR REMAIN\SR-10-97-REPEAT-C13-METHANOL-D4.FID\FID					***Frequency (MHz)***	50.29
Nucleus	13C	***Number of Transients***	7048	***Original Points Count***	18720	***Points Count***	32768
Pulse Sequence	s2pul	***Receiver Gain***	40.00	***Solvent***	METHANOL-d4	***Spectrum Offset (Hz)***	4978.7695
Spectrum Type	STANDARD	***Sweep Width (Hz)***	12500.00	***Temperature (degree C)***	AMBIENT TEMPERATURE		

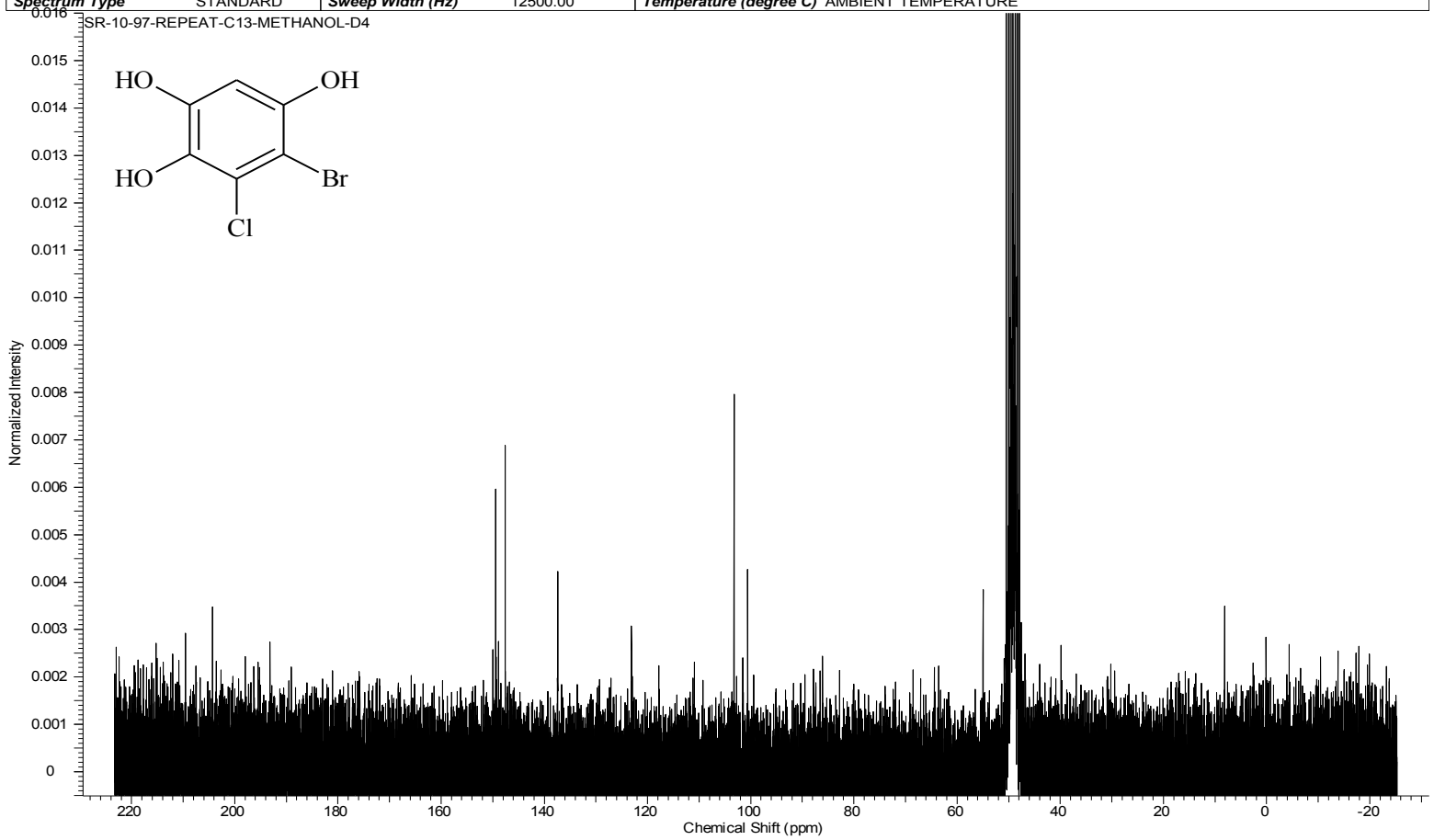

Compound 6 IR

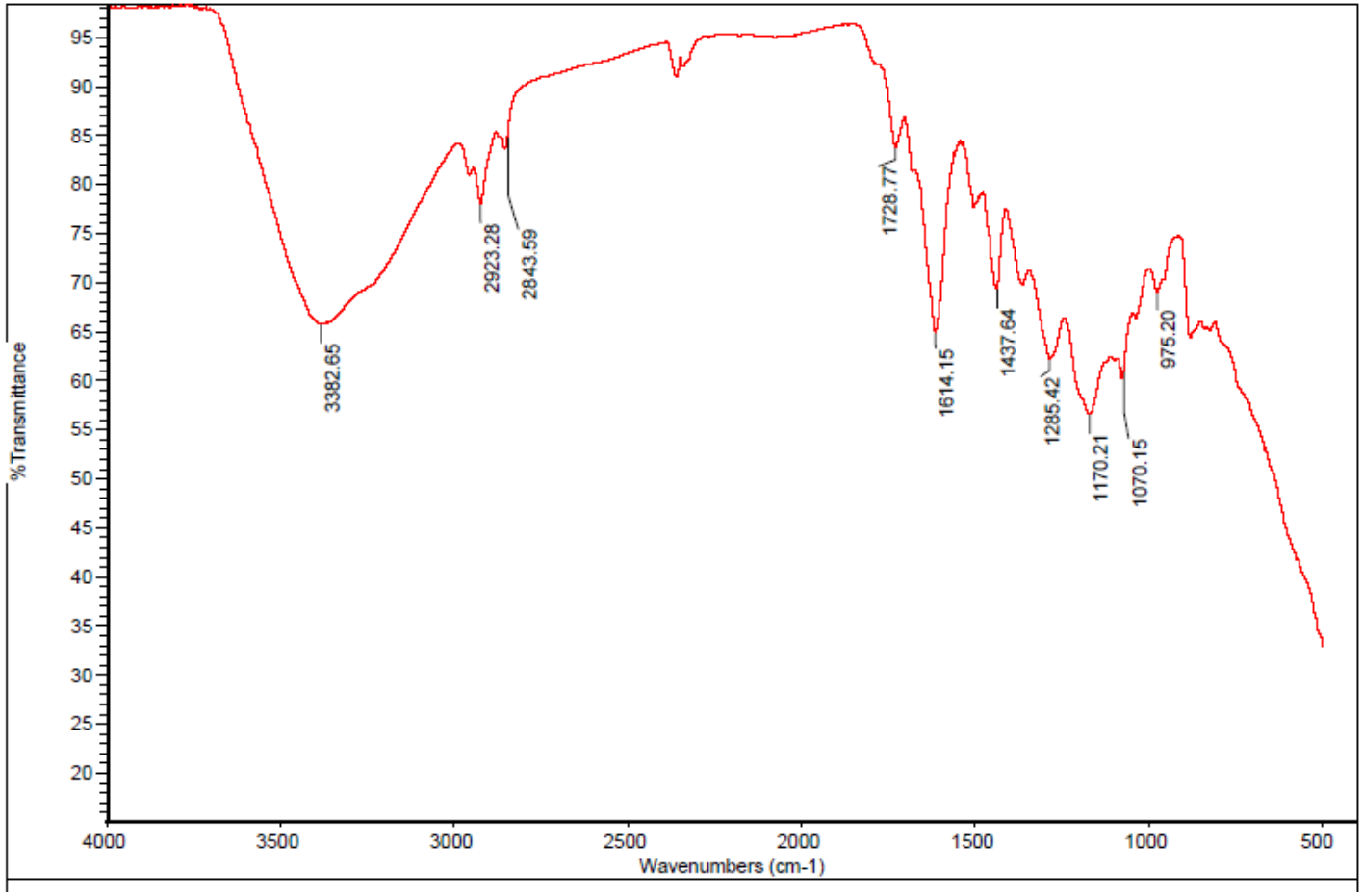

Compound 7 ^{1}H NMR

Acquisition Time (sec)	2.0487	***Comment***	Std proton	***Date***	Jun 2 2008	***Date Stamp***	Jun 2 2008
File Name	C:\USERS\KESHAR\DESKTOP\NMR\OTHERS\KP-1-16-FRAC-13-29.FID\FID					***Frequency (MHz)***	399.76
Nucleus	1H	***Number of Transients***	32	***Original Points Count***	13103	***Points Count***	16384
Pulse Sequence	s2pul	***Receiver Gain***	50.00	***Solvent***	DEUTERIUM OXIDE		
Spectrum Offset (Hz)	2455.7793	***Spectrum Type***	STANDARD	***Sweep Width (Hz)***	6395.91	***Temperature (degree C)***	25.000

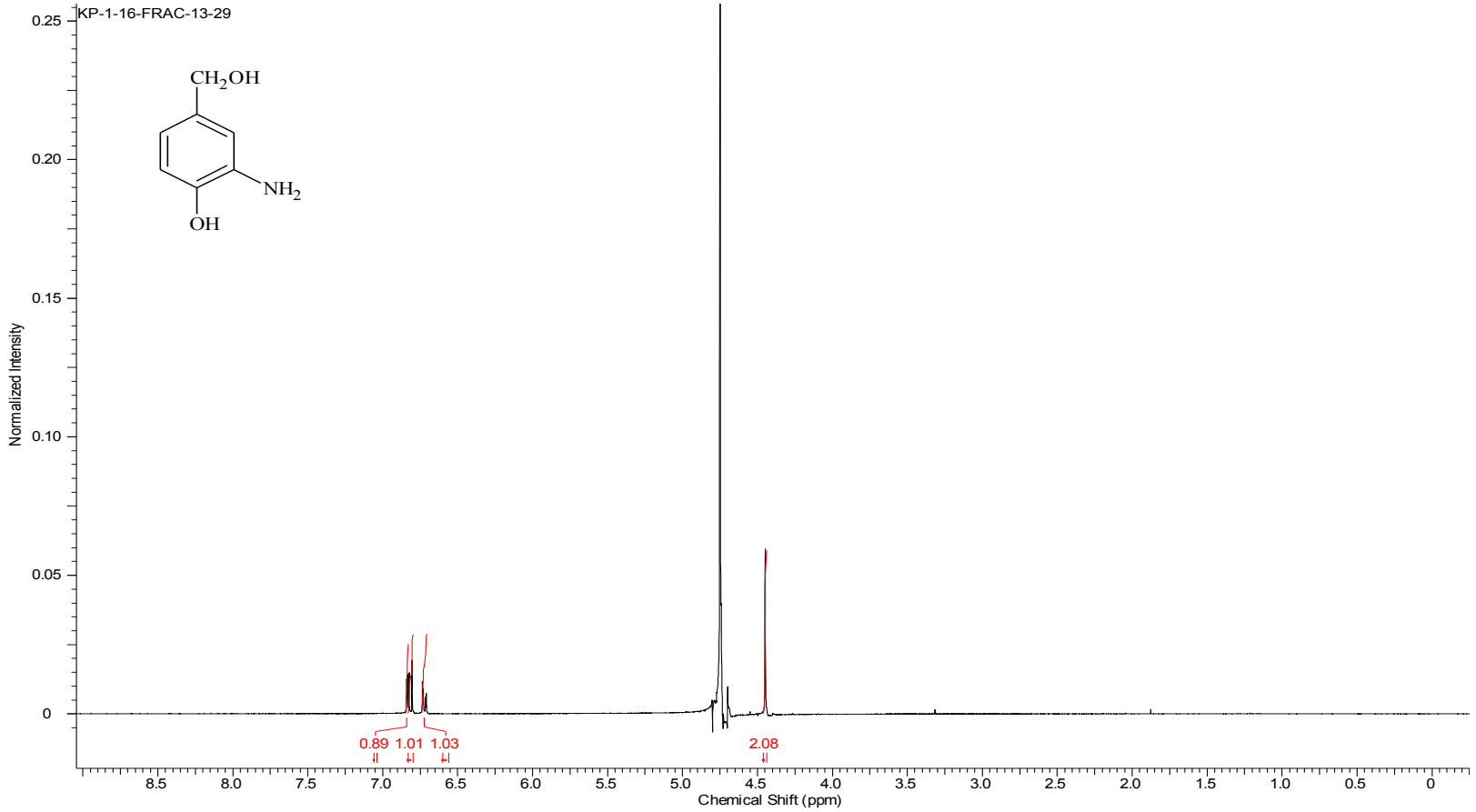

Compound 7 ^{13}C NMR

Acquisition Time (sec)	1.3005	***Comment***	Std proton	***Date***	Jul 17 2009	***Date Stamp***	Jul 17 2009
File Name	C:\USERS\KESHAR\KP-1-16-FR2-C13\FID					***Frequency (MHz)***	100.53
Nucleus	13C	***Number of Transients***	26396	***Original Points Count***	31375	***Points Count***	32768
Pulse Sequence	s2pul	***Receiver Gain***	30.00	***Solvent***	DMSO-d6	***Spectrum Offset (Hz)***	10486.7480
Spectrum Type	STANDARD	***Sweep Width (Hz)***	24125.45	***Temperature (degree C)***	25.000		

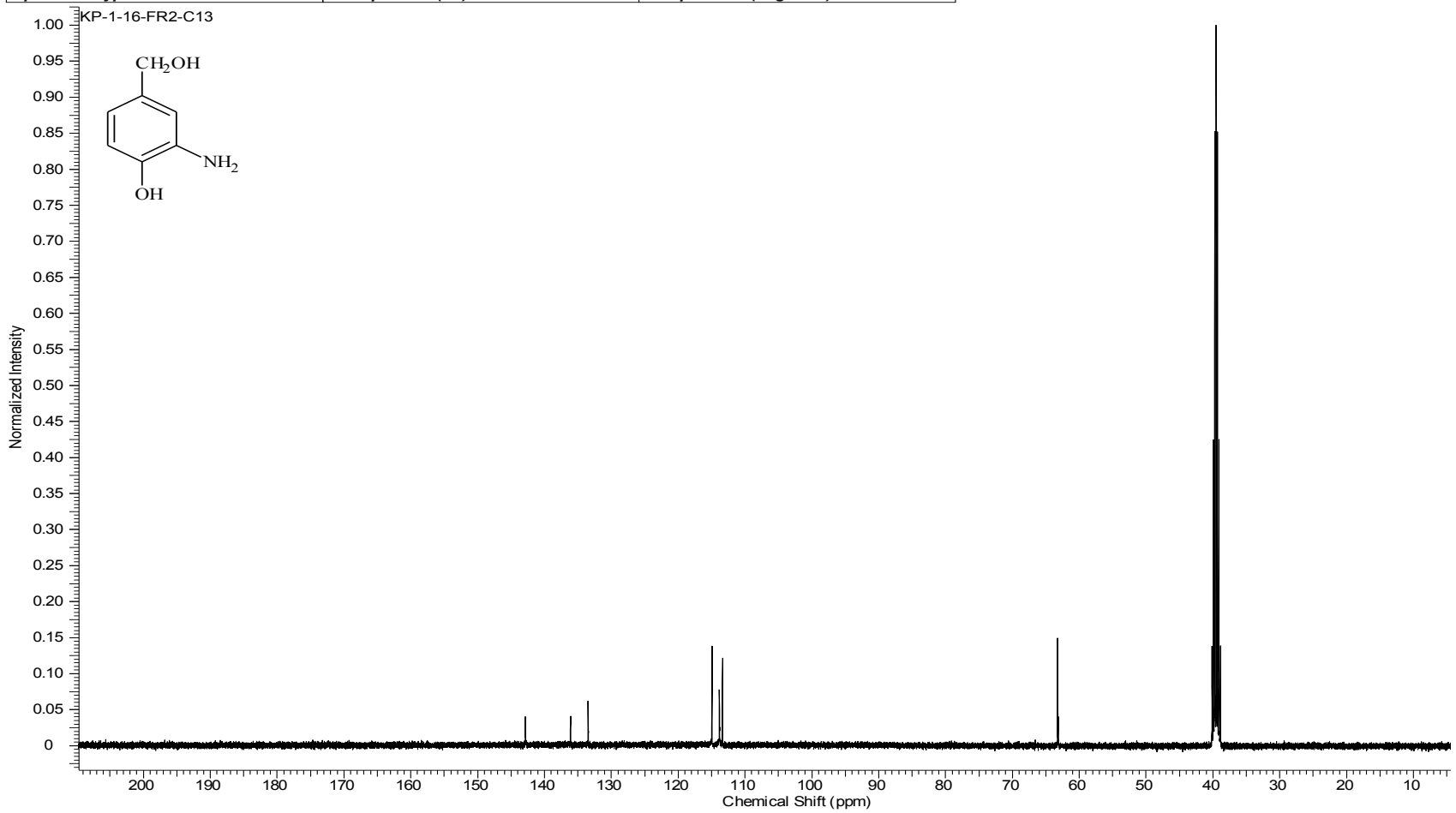

Compound 7 IR

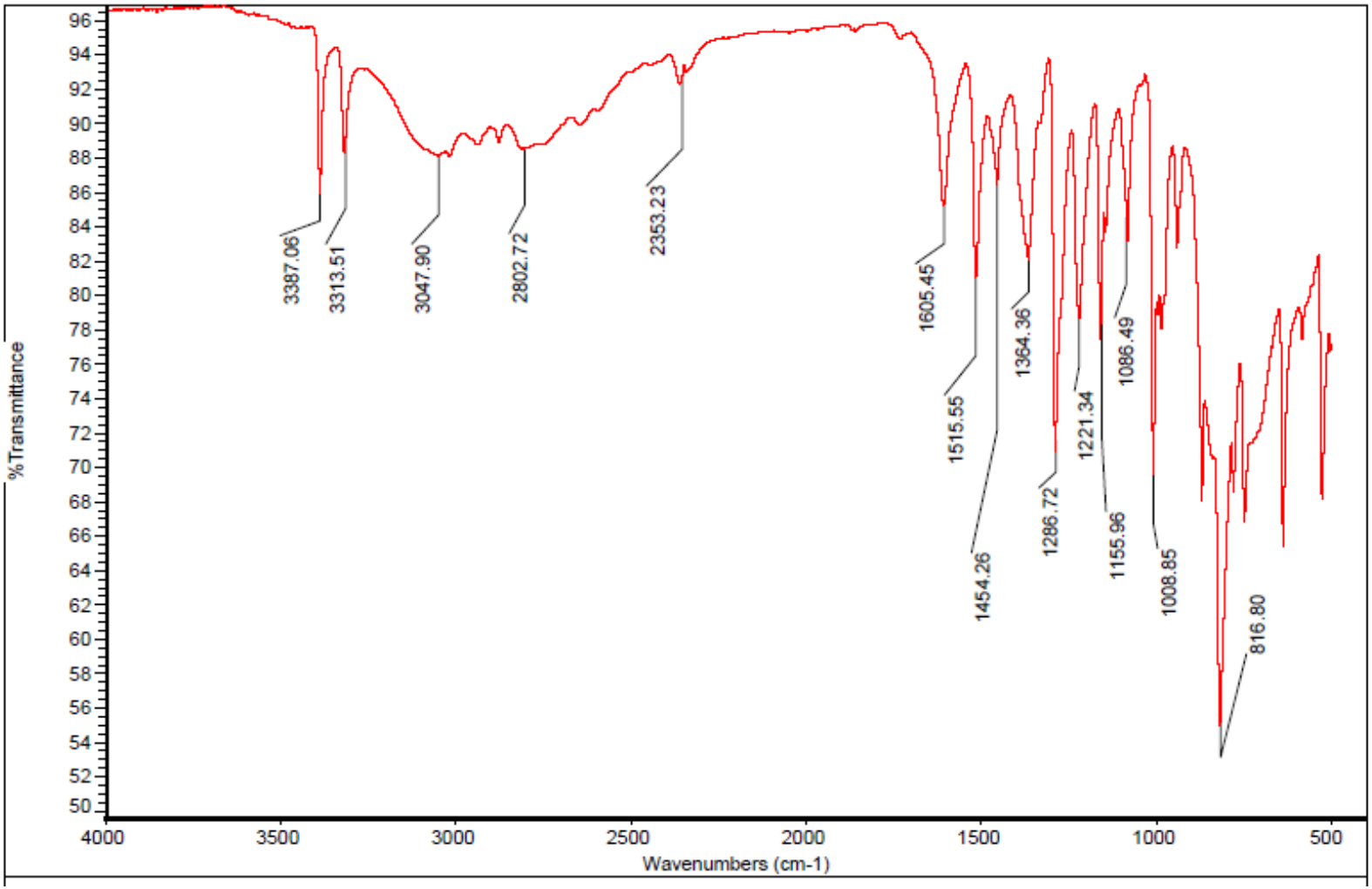

Compound 8 ^{1}H NMR

Acquisition Time (sec)	2.0487	***Comment***	Std proton	***Date***	Jun 2 2008	***Date Stamp***	Jun 2 2008
File Name	C:\USERS\KESHAR\DESKTOP\NMR\BOOK 1\KP-1-16-FRAC-4-9.FID\FID					***Frequency (MHz)***	399.76
Nucleus	1H	***Number of Transients***	32	***Original Points Count***	13103	***Points Count***	16384
Pulse Sequence	s2pul	***Receiver Gain***	56.00	***Solvent***	CHLOROFORM-d		
Spectrum Offset (Hz)	2418.0771	***Spectrum Type***	STANDARD	***Sweep Width (Hz)***	6395.91	***Temperature (degree C)***	25.000

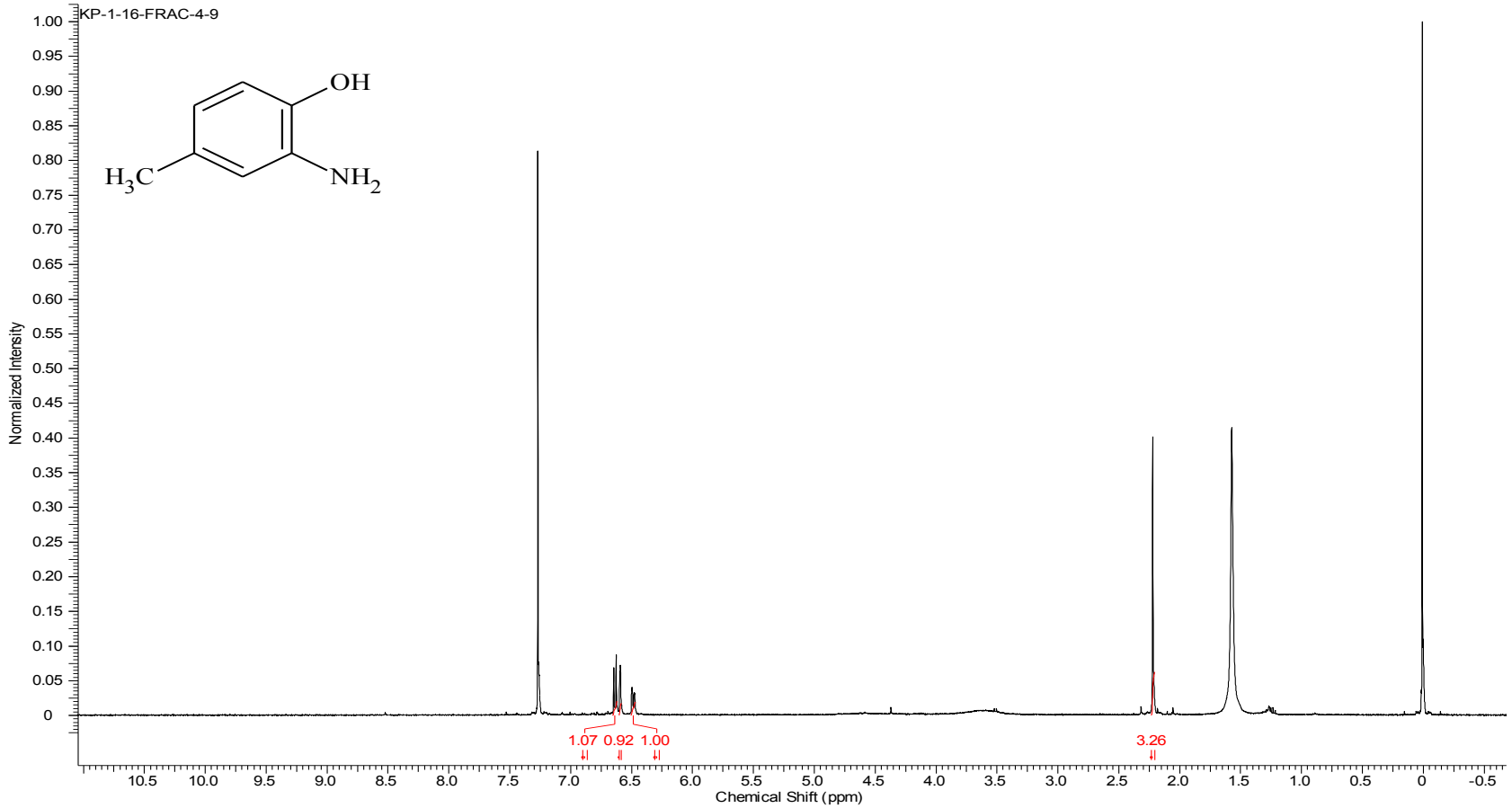

Compound 8 ^{13}C NMR

Acquisition Time (sec)	1.3005	***Comment***	Std Carbon experiment			***Date***	Jun 28 2012
Date Stamp	Jun 28 2012	***File Name***	C:\USERS\KESHAR\DESKTOP\KP-1-16-FRAC1-C13.FID\FID				
Frequency (MHz)	100.58	***Nucleus***	13C	***Number of Transients***	1664	***Original Points Count***	31413
Points Count	32768	***Pulse Sequence***	s2pul	***Receiver Gain***	20.00	***Solvent***	CHLOROFORM-d
Spectrum Offset (Hz)	10556.1475	***Spectrum Type***	STANDARD	***Sweep Width (Hz)***	24154.59	***Temperature (degree C)***	25.000

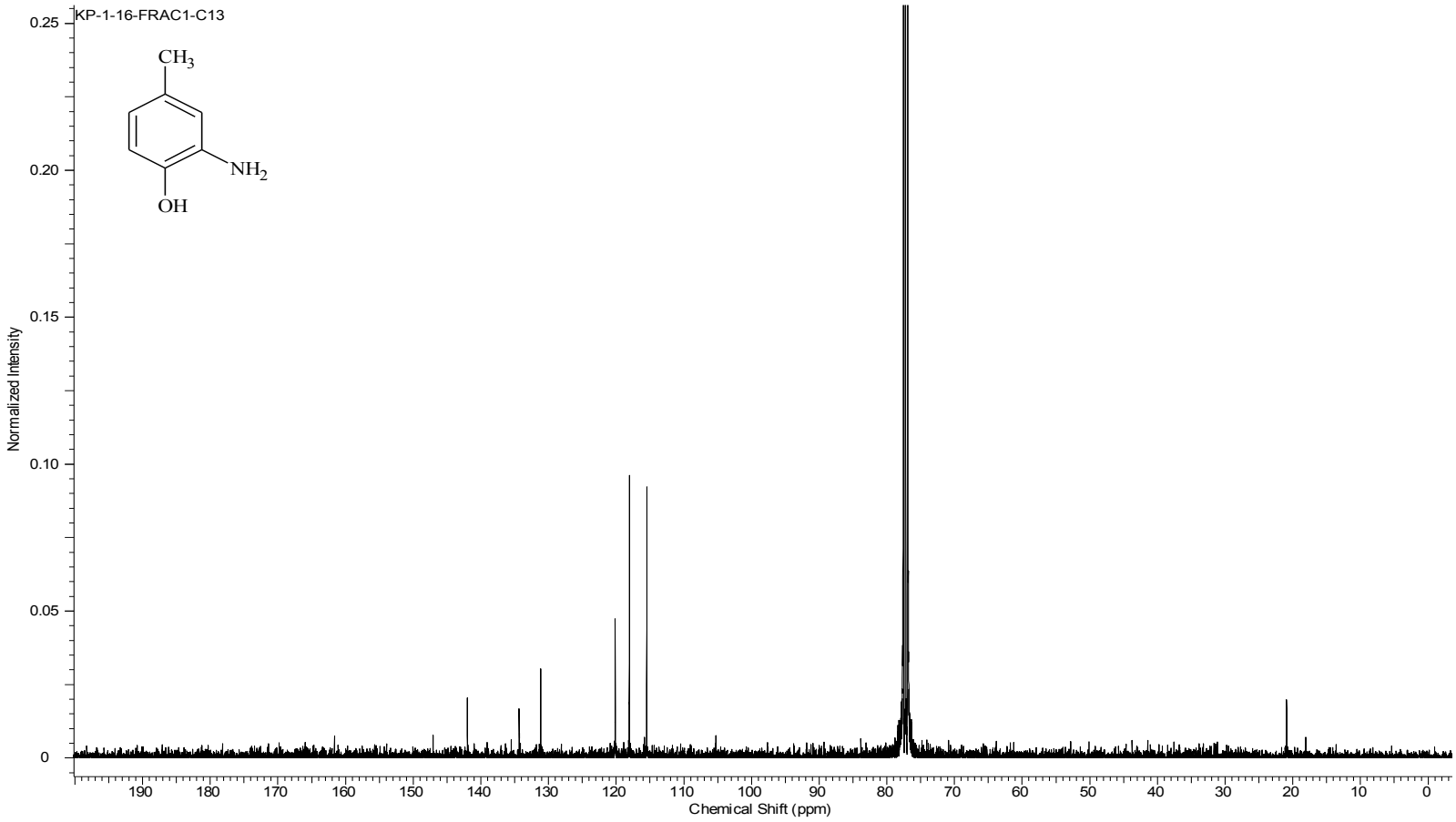

Compound 8 IR

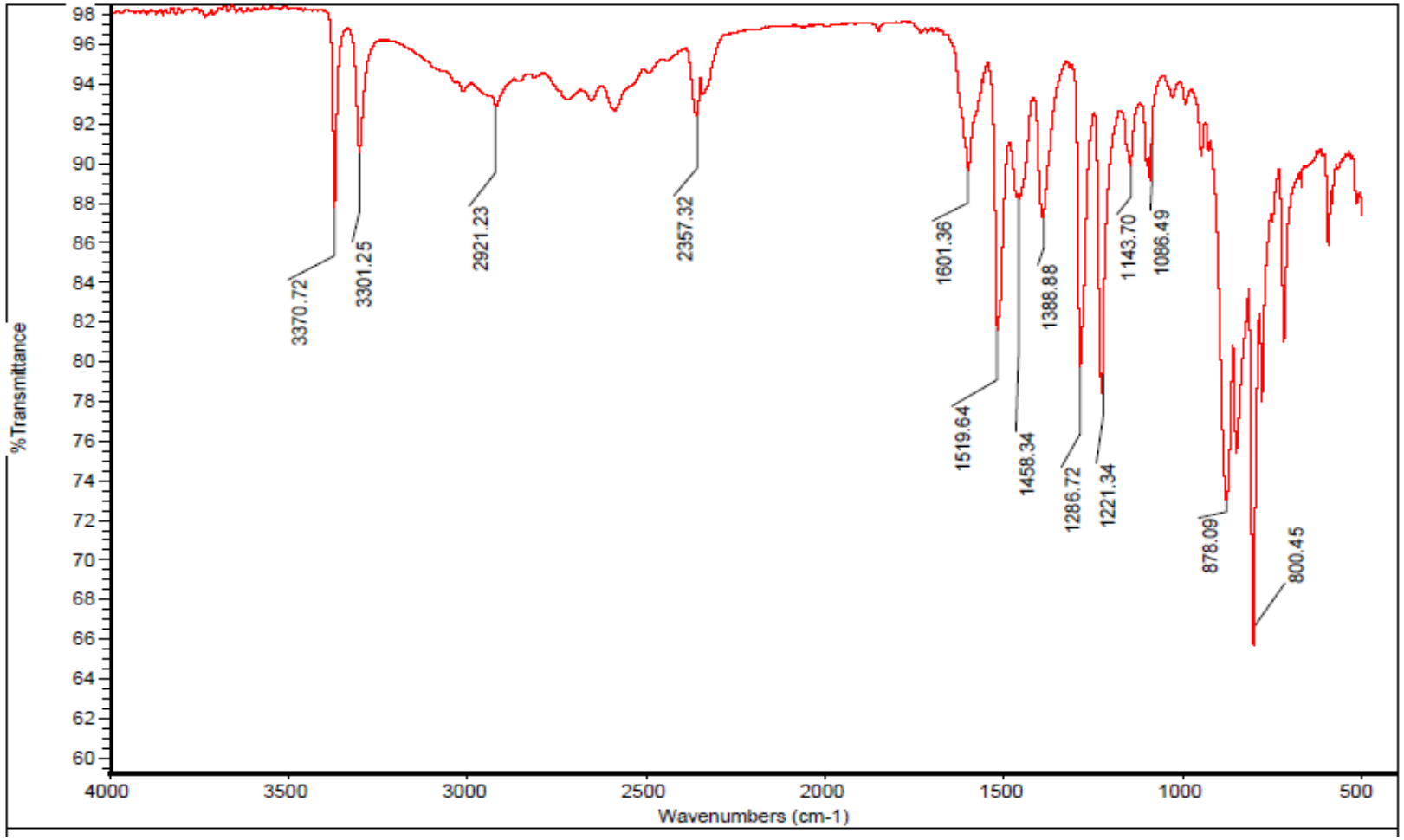

Compound 10 ^{1}H NMR

Acquisition Time (sec)	1.9945	***Comment***	STANDARD 1H OBSERVE			***Date***	Nov 16 2009
Date Stamp	Nov 16 2009	***File Name***	C:\USERS\KESHAR\DESKTOP\NMR\BOOK 5\KP-5-72-DP.FID\FID				
Frequency (MHz)	199.98	***Nucleus***	1H	***Number of Transients***	32	***Original Points Count***	5984
Points Count	8192	***Pulse Sequence***	s2pul	***Receiver Gain***	34.00	***Solvent***	CHLOROFORM-d
Spectrum Offset (Hz)	1002.0226	***Spectrum Type***	STANDARD	***Sweep Width (Hz)***	3000.30	***Temperature (degree C)***	AMBIENT TEMPERATURE

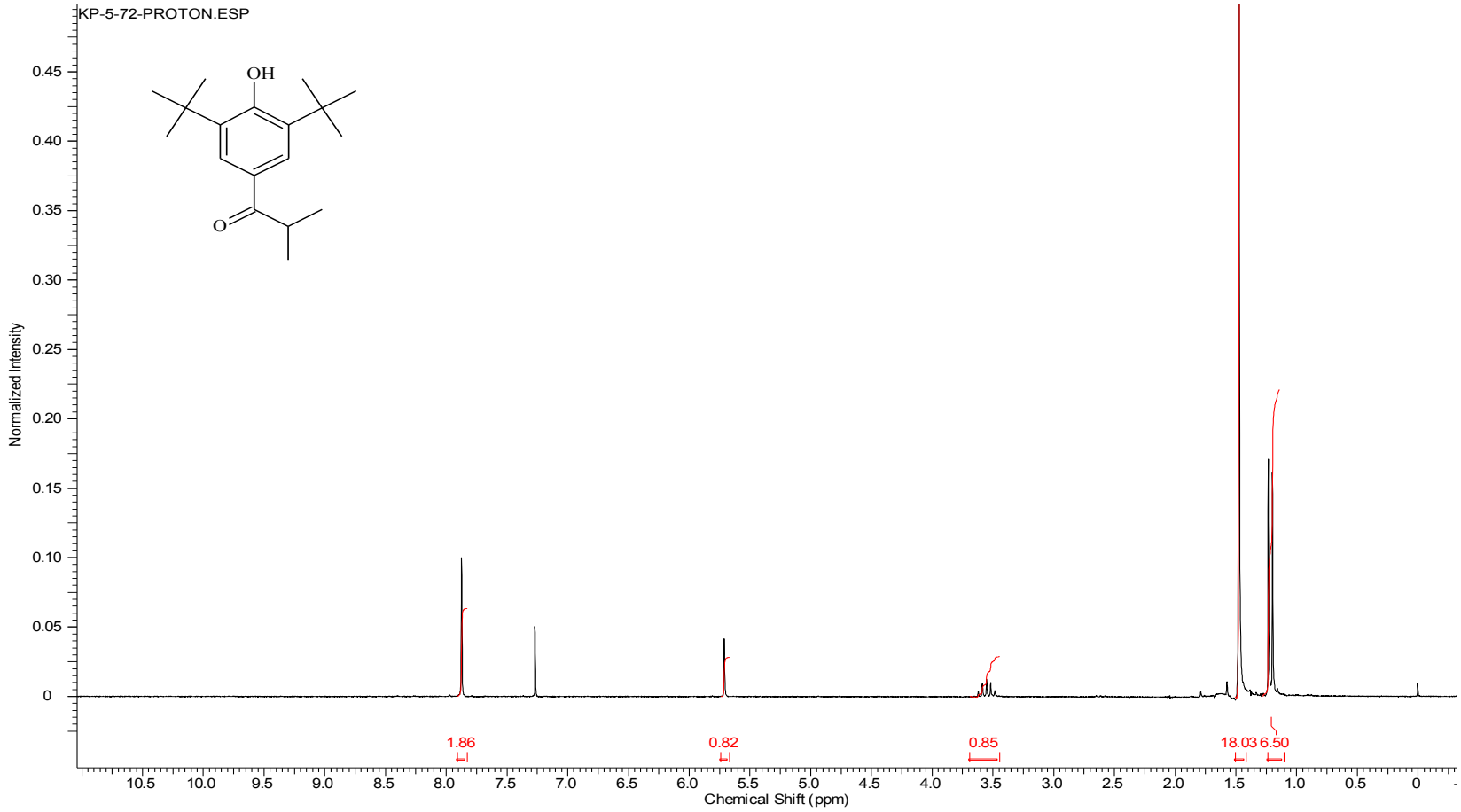

Compound 10 ^{13}C NMR

Acquisition Time (sec)	1.4976	***Comment***	13C OBSERVE□KP-5-72-Dp-C13			***Date***	Nov 18 2009
Date Stamp	Nov 18 2009	***File Name***	C:\USERS\KESHAR\KP-5-72-Carbon				
Frequency (MHz)	50.29	***Nucleus***	13C	***Number of Transients***	384	***Original Points Count***	18720
Points Count	32768	***Pulse Sequence***	s2pul	***Receiver Gain***	40.00	***Solvent***	CHLOROFORM-d
Spectrum Offset (Hz)	4878.5537	***Spectrum Type***	STANDARD	***Sweep Width (Hz)***	12500.00	***Temperature (degree C)***	AMBIENT TEMPERATURE

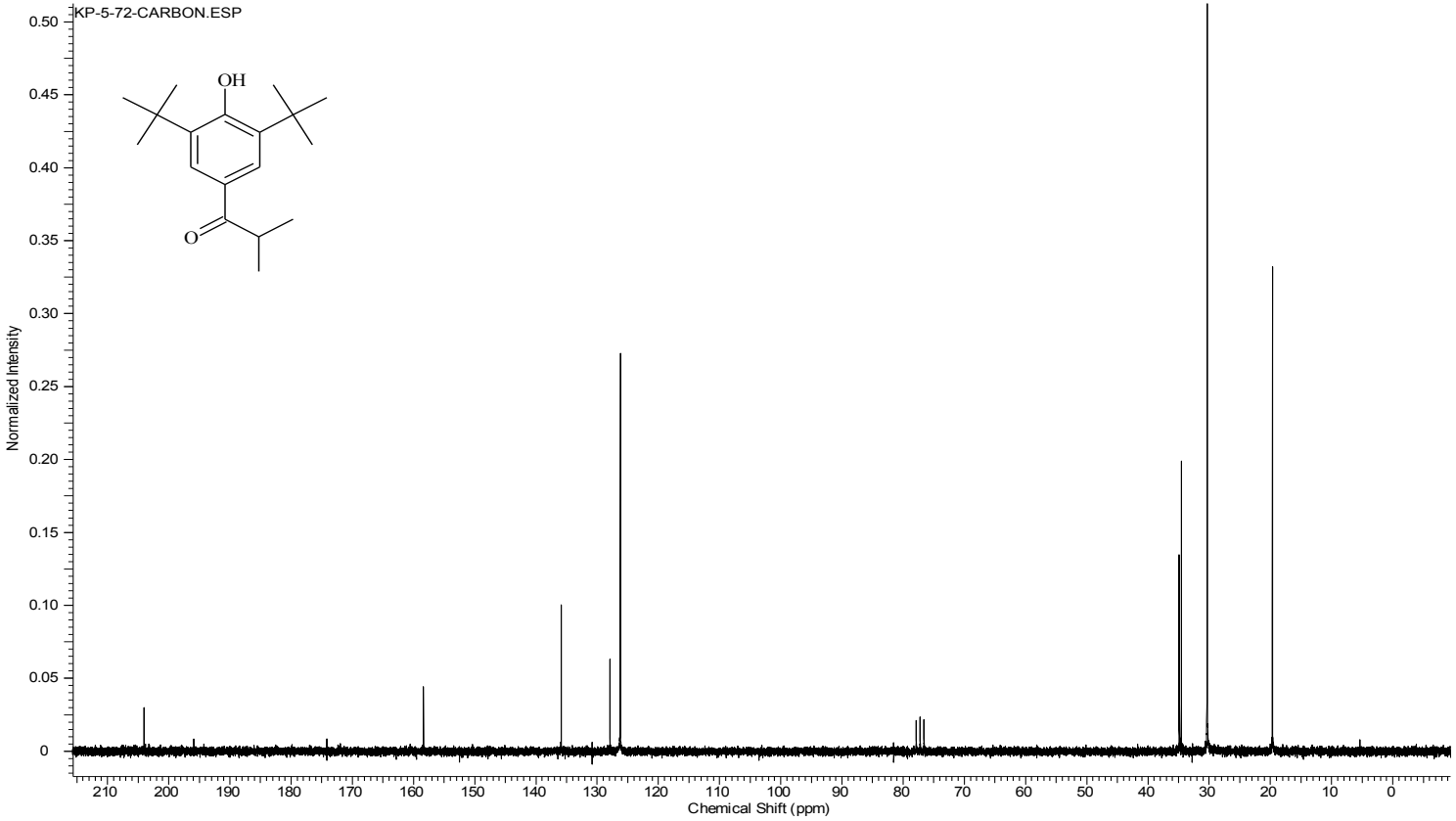

Compound 11 ^{1}H NMR

Acquisition Time (sec)	1.9945	***Comment***	STANDARD 1H OBSERVE			***Date***	Nov 17 2009
Date Stamp	Nov 17 2009	***File Name***	C:\USERS\KESHAR\DESKTOP\NMR\BOOK 5\KP-5-73-DP.FID\FID				
Frequency (MHz)	199.98	***Nucleus***	1H	***Number of Transients***	96	***Original Points Count***	5984
Points Count	8192	***Pulse Sequence***	s2pul	***Receiver Gain***	18.00	***Solvent***	CHLOROFORM-d
Spectrum Offset (Hz)	1002.7551	***Spectrum Type***	STANDARD	***Sweep Width (Hz)***	3000.30	***Temperature (degree C)***	AMBIENT TEMPERATURE

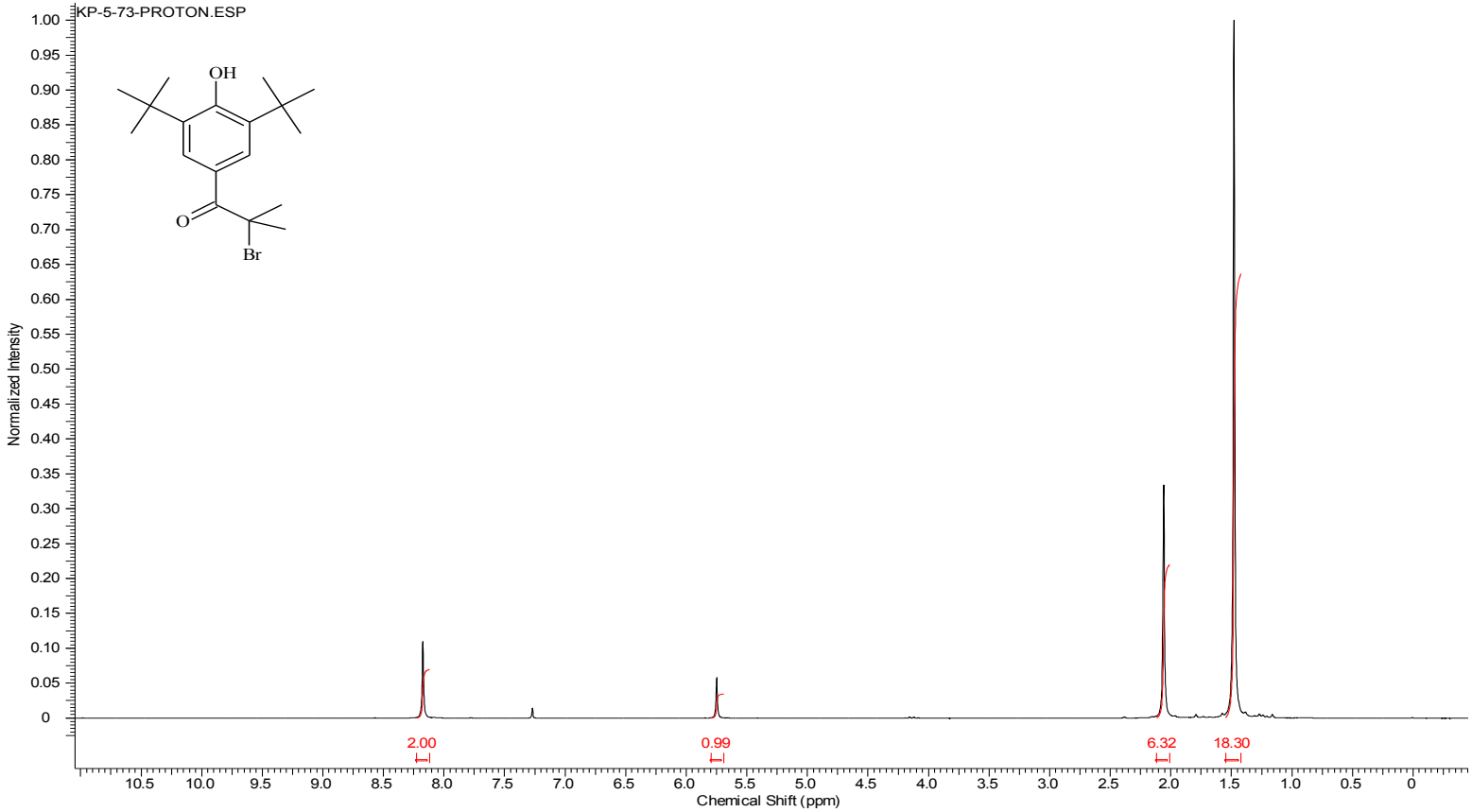

Compound 11 ^{13}C NMR

Acquisition Time (sec)	1.4976	***Comment***	13C OBSERVE	***Date***	Nov 18 2009	***Date Stamp***	Nov 18 2009
File Name	C:\USERS\KESHAR\DESKTOP\NMR\BOOK 5\KP-5-73-DP-C13.FID\FID					***Frequency (MHz)***	50.29
Nucleus	13C	***Number of Transients***	416	***Original Points Count***	18720	***Points Count***	32768
Pulse Sequence	s2pul	***Receiver Gain***	40.00	***Solvent***	CHLOROFORM-d		
Spectrum Offset (Hz)	4879.3164	***Spectrum Type***	STANDARD	***Sweep Width (Hz)***	12500.00	***Temperature (degree C)***	AMBIENT TEMPERATURE

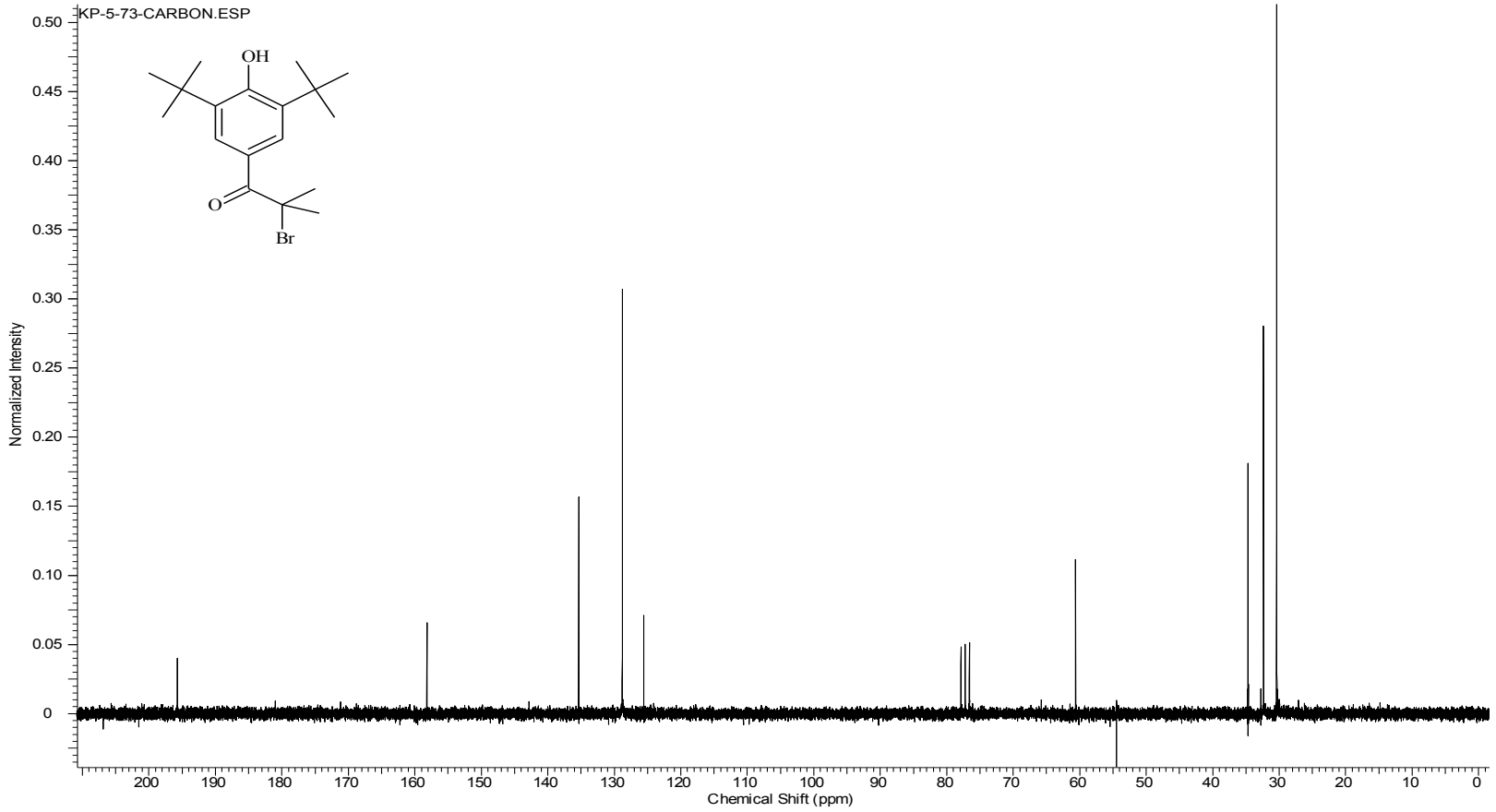

Compound 12 ^{1}H NMR

Acquisition Time (sec)	2.0487	***Comment***	Std proton	***Date***	Nov 23 2009	***Date Stamp***	Nov 23 2009
File Name	C:\USERS\KESHAR\DESKTOP\NMR\BOOK 5\KP-5-77-CRUDE.FID\FID					***Frequency (MHz)***	399.75
Nucleus	1H	***Number of Transients***	8	***Original Points Count***	13103	***Points Count***	16384
Pulse Sequence	s2pul	***Receiver Gain***	48.00	***Solvent***	CHLOROFORM-d		
Spectrum Offset (Hz)	2404.7087	***Spectrum Type***	STANDARD	***Sweep Width (Hz)***	6395.91	***Temperature (degree C)***	25.000

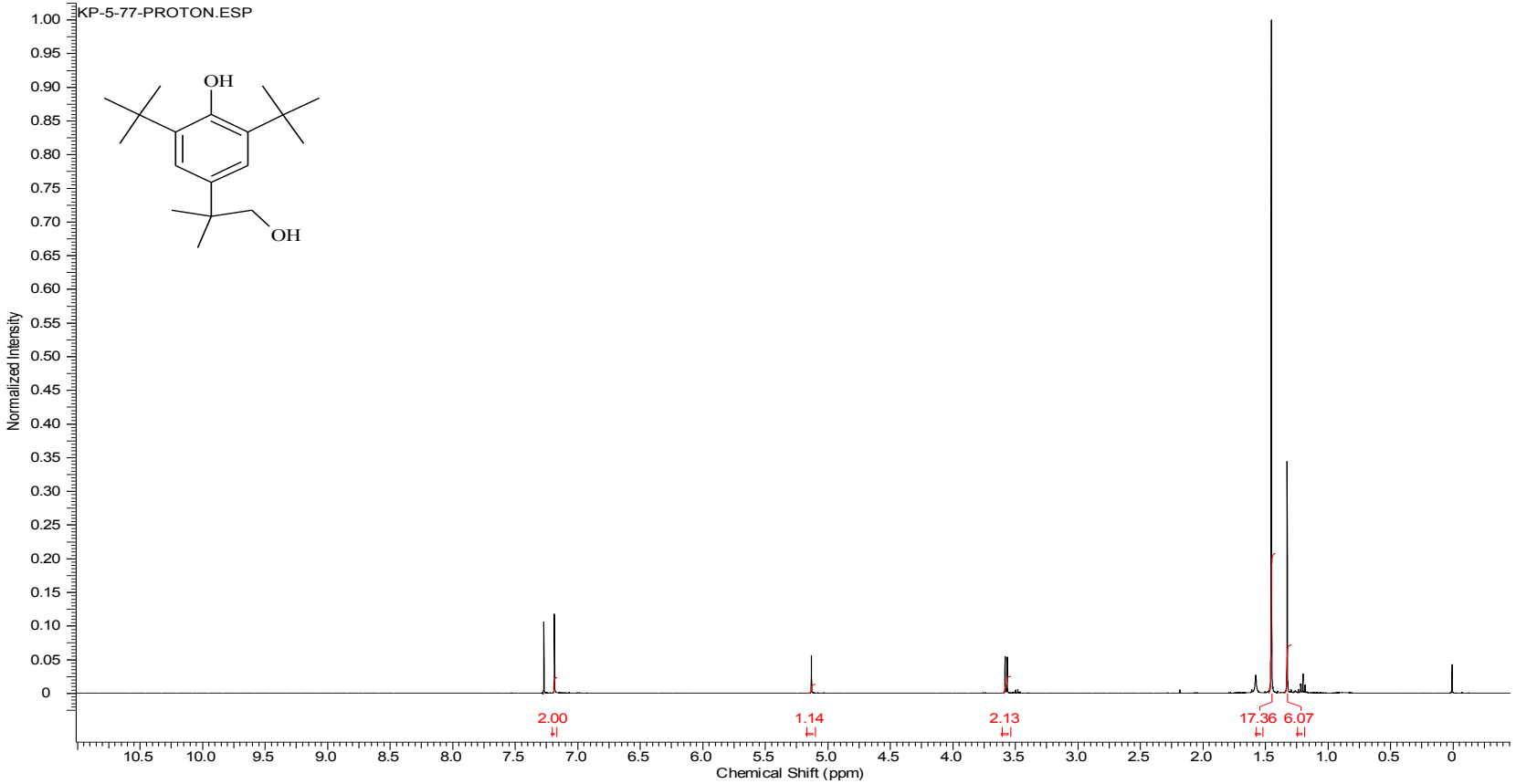

Compound 12 ^{13}C NMR

Acquisition Time (sec)	1.3005	***Comment***	Std proton	***Date***	Nov 23 2009	***Date Stamp***	Nov 23 2009
File Name	C:\USERS\KESHAR\DESKTOP\NMR\BOOK 5\KP-5-77-C13.FID\FID					***Frequency (MHz)***	100.53
Nucleus	13C	***Number of Transients***	512	***Original Points Count***	31375	***Points Count***	32768
Pulse Sequence	s2pul	***Receiver Gain***	30.00	***Solvent***	CHLOROFORM-d		
Spectrum Offset (Hz)	10550.8555	***Spectrum Type***	STANDARD	***Sweep Width (Hz)***	24125.45	***Temperature (degree C)***	25.000

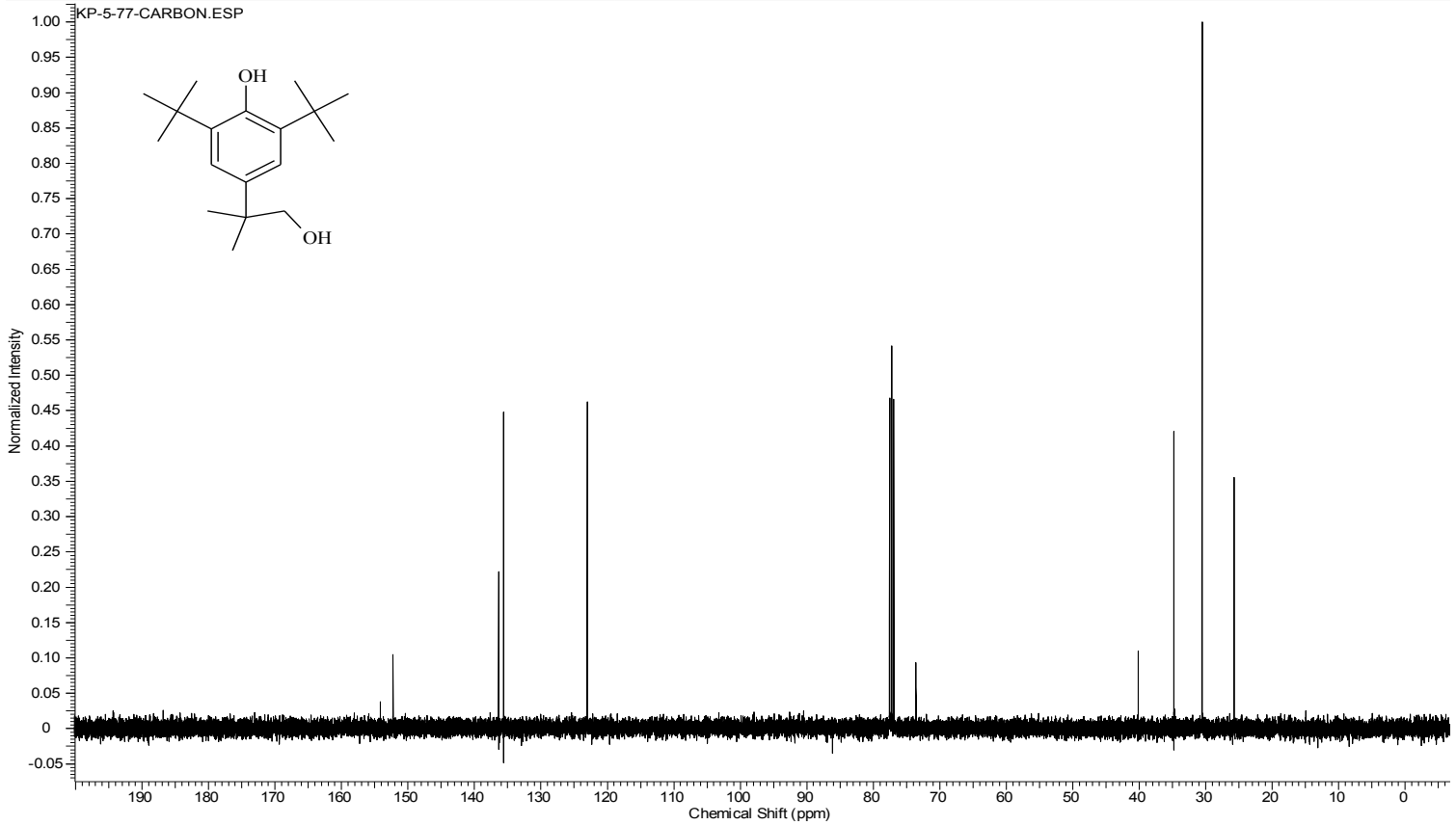

Compound 13 ^{1}H NMR

Acquisition Time (sec)	2.0487	***Comment***	Std proton	***Date***	Nov 24 2009	***Date Stamp***	Nov 24 2009
File Name	C:\USERS\KESHAR\DESKTOP\KESHAR NEW NMR BACKUP 2011\NMR BACK UP 4 AND 5\KP-5-78-DP.FID\FID						
Frequency (MHz)	399.75	***Nucleus***	1H	***Number of Transients***	4	***Original Points Count***	13103
Points Count	16384	***Pulse Sequence***	s2pul	***Receiver Gain***	36.00	***Solvent***	CHLOROFORM-d
Spectrum Offset (Hz)	2405.0991	***Spectrum Type***	STANDARD	***Sweep Width (Hz)***	6395.91	***Temperature (degree C)***	25.000

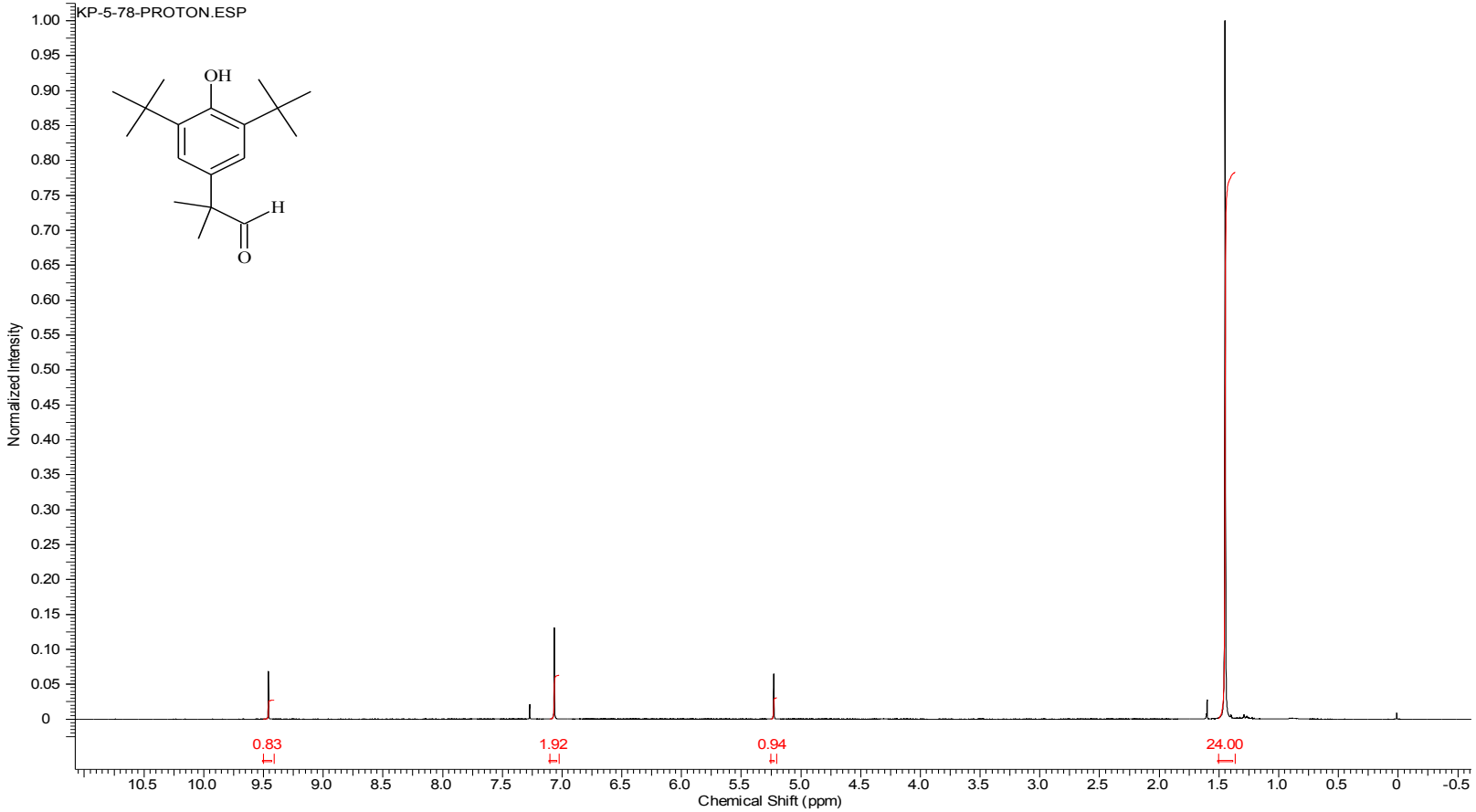

Compound 13 ^{13}C NMR

Acquisition Time (sec)	1.3005	***Comment***	Std proton	***Date***	Nov 24 2009	***Date Stamp***	Nov 24 2009
File Name	C:\USERS\KESHAR\DOCUMENTS\KESHAR NMR\KESHAR\COPY OF KESHAR NOVA 3-16-2011\KESHAR\KP-5-78-C13.FID\FID						
Frequency (MHz)	100.53	***Nucleus***	13C	***Number of Transients***	448	***Original Points Count***	31375
Points Count	32768	***Pulse Sequence***	s2pul	***Receiver Gain***	30.00	***Solvent***	CHLOROFORM-d
Spectrum Offset (Hz)	10551.5918	***Spectrum Type***	STANDARD	***Sweep Width (Hz)***	24125.45	***Temperature (degree C)***	25.000

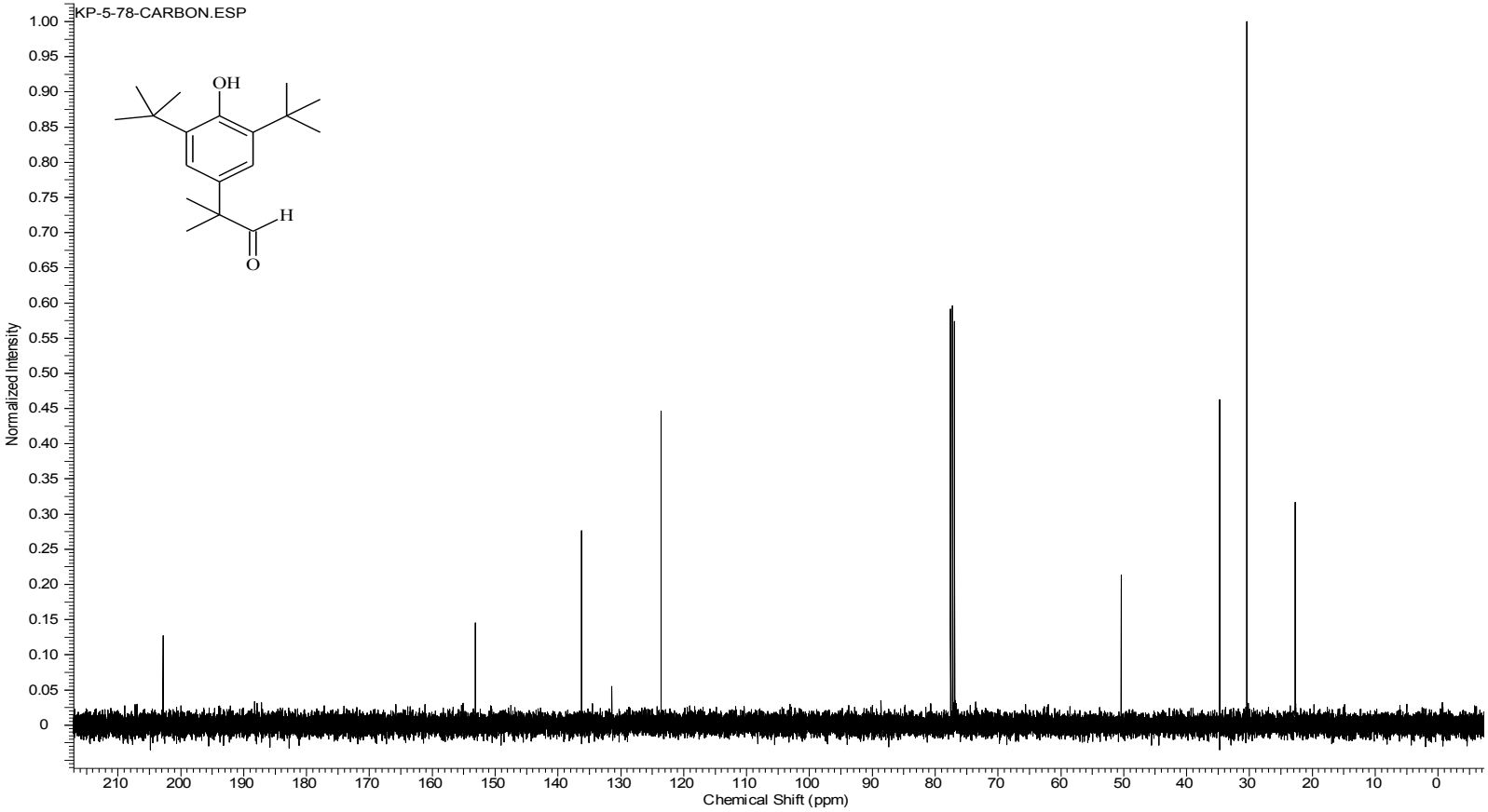

Compound 13 IR

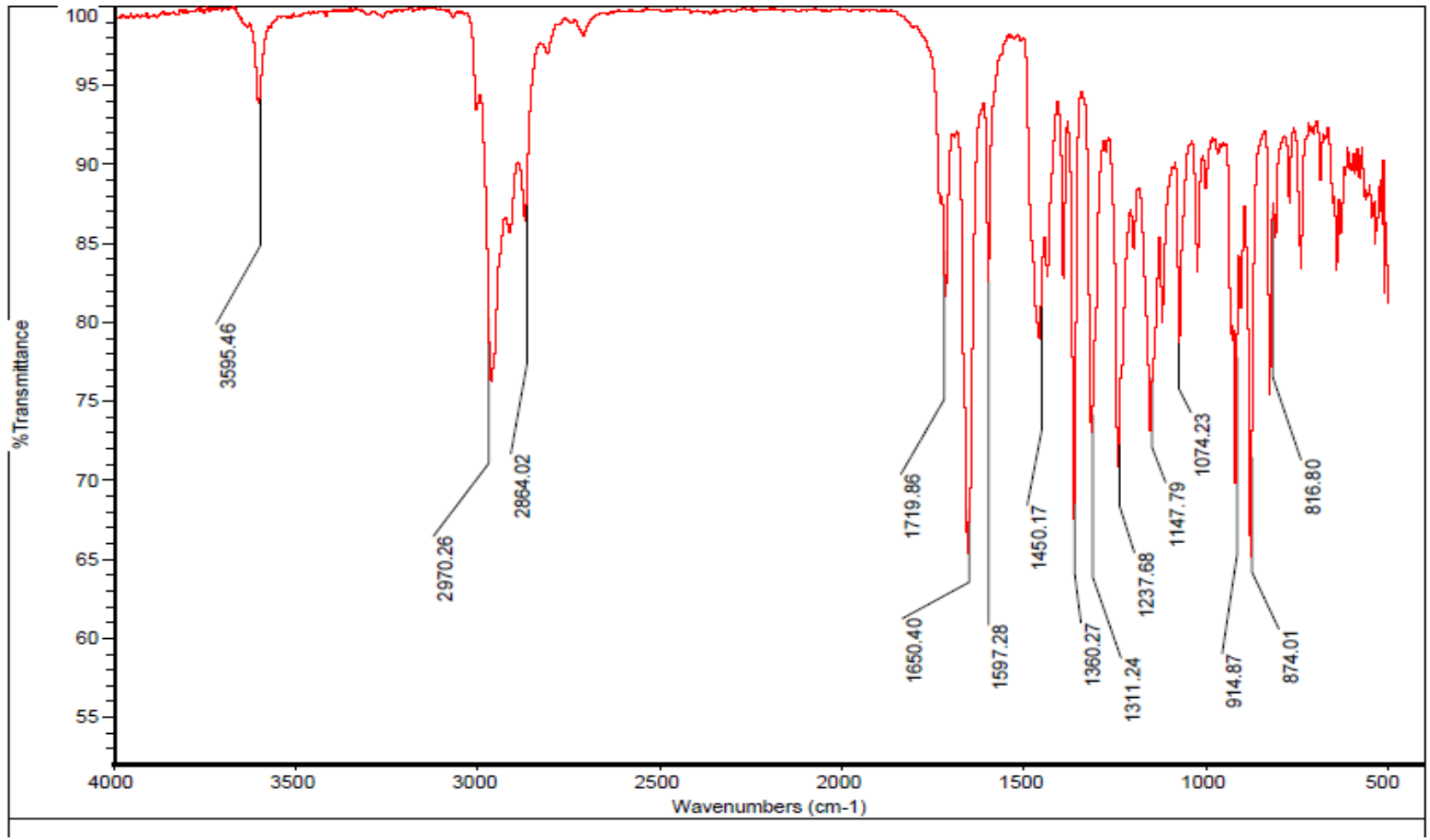

Compound 15 ^{1}H NMR

Acquisition Time (sec)	2.0487	***Comment***	Std proton	***Date***	Nov 25 2009	***Date Stamp***	Nov 25 2009
File Name	C:\USERS\KESHAR\KP-5-69-Proton						
Frequency (MHz)	399.75	***Nucleus***	1H	***Number of Transients***	16	***Original Points Count***	13103
Points Count	16384	***Pulse Sequence***	s2pul	***Receiver Gain***	32.00	***Solvent***	CHLOROFORM-d
Spectrum Offset (Hz)	2405.0991	***Spectrum Type***	STANDARD	***Sweep Width (Hz)***	6395.91	***Temperature (degree C)***	25.000

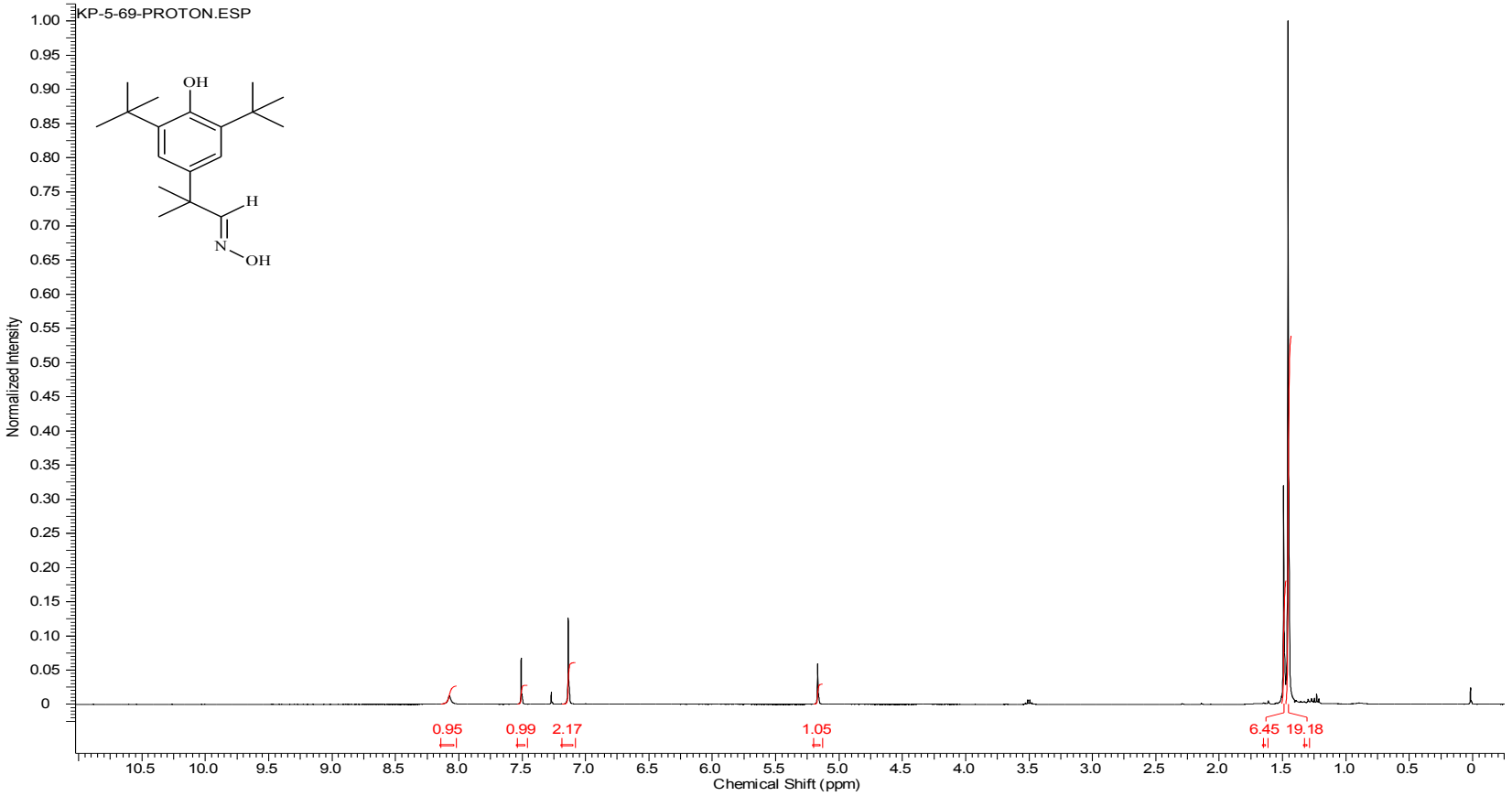

Compound 15 ^{13}C NMR

Acquisition Time (sec)	1.3005	***Comment***	Std proton	***Date***	Nov 25 2009	***Date Stamp***	Nov 25 2009
File Name	C:\USERS\KESHAR\KP-5-69-Carbon						
Frequency (MHz)	100.53	***Nucleus***	13C	***Number of Transients***	544	***Original Points Count***	31375
Points Count	32768	***Pulse Sequence***	s2pul	***Receiver Gain***	30.00	***Solvent***	CHLOROFORM-d
Spectrum Offset (Hz)	10551.5918	***Spectrum Type***	STANDARD	***Sweep Width (Hz)***	24125.45	***Temperature (degree C)***	25.000

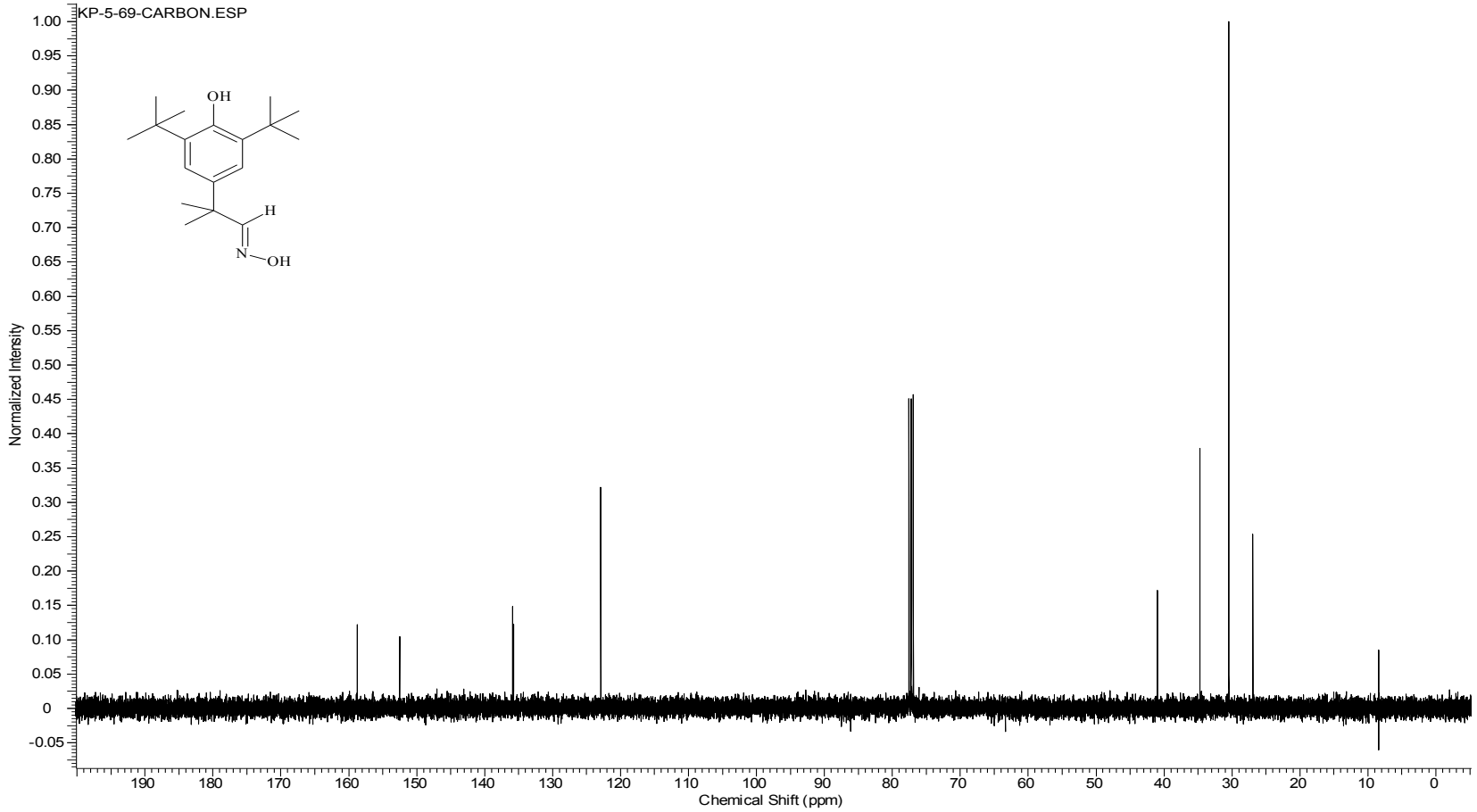

Compound 15 IR

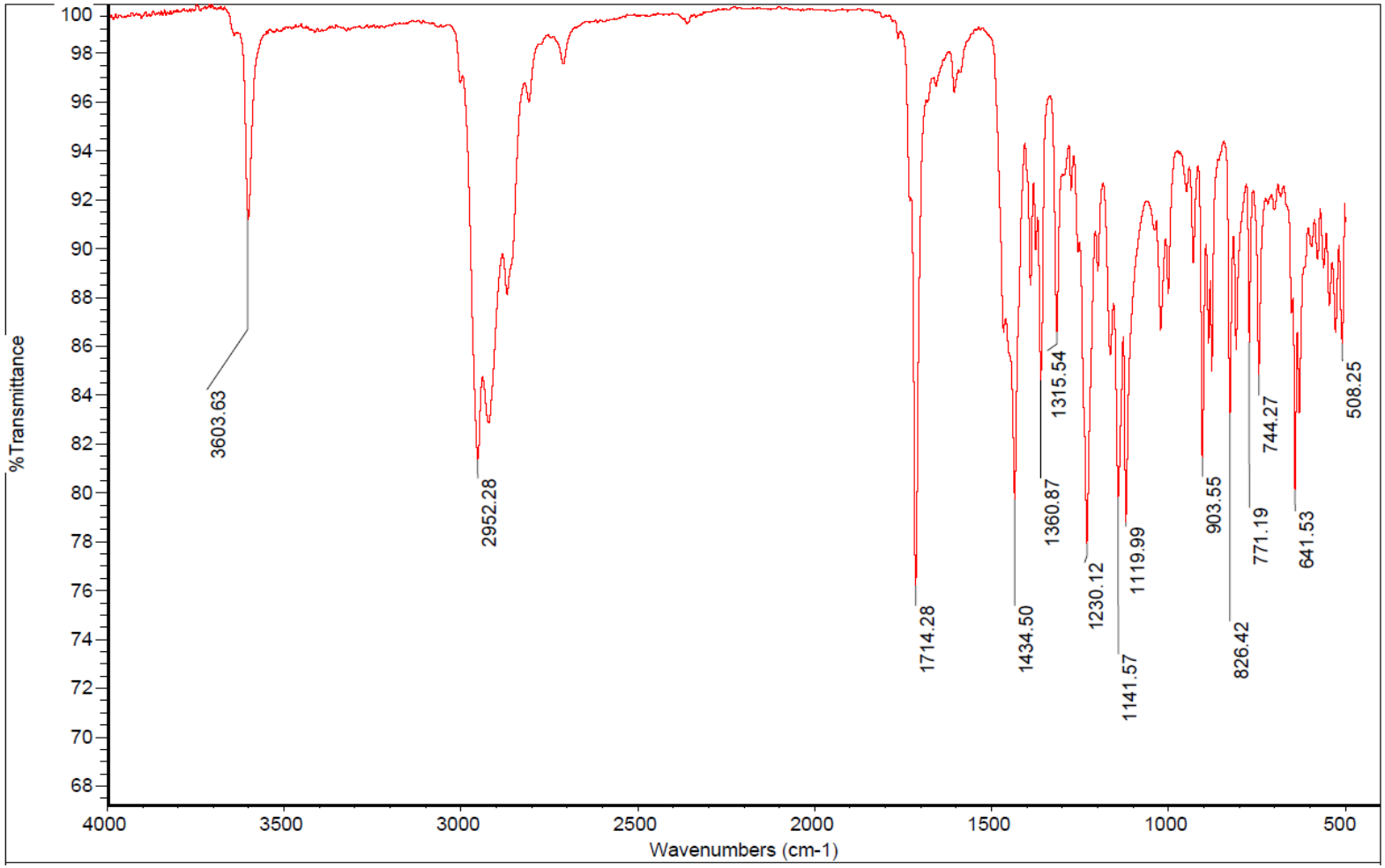

Compound 16 ^{1}H NMR

Acquisition Time (sec)	2.0487	***Comment***	Std proton	***Date***	Nov 29 2009	***Date Stamp***	Nov 29 2009
File Name	C:\USERS\KESHAR\DESKTOP\NMR\BOOK 5\KP-5-81-FRAC2.FID\FID					***Frequency (MHz)***	399.75
Nucleus	1H	***Number of Transients***	20	***Original Points Count***	13103	***Points Count***	16384
Pulse Sequence	s2pul	***Receiver Gain***	32.00	***Solvent***	CHLOROFORM-d		
Spectrum Offset (Hz)	2454.6799	***Spectrum Type***	STANDARD	***Sweep Width (Hz)***	6395.91	***Temperature (degree C)***	25.000

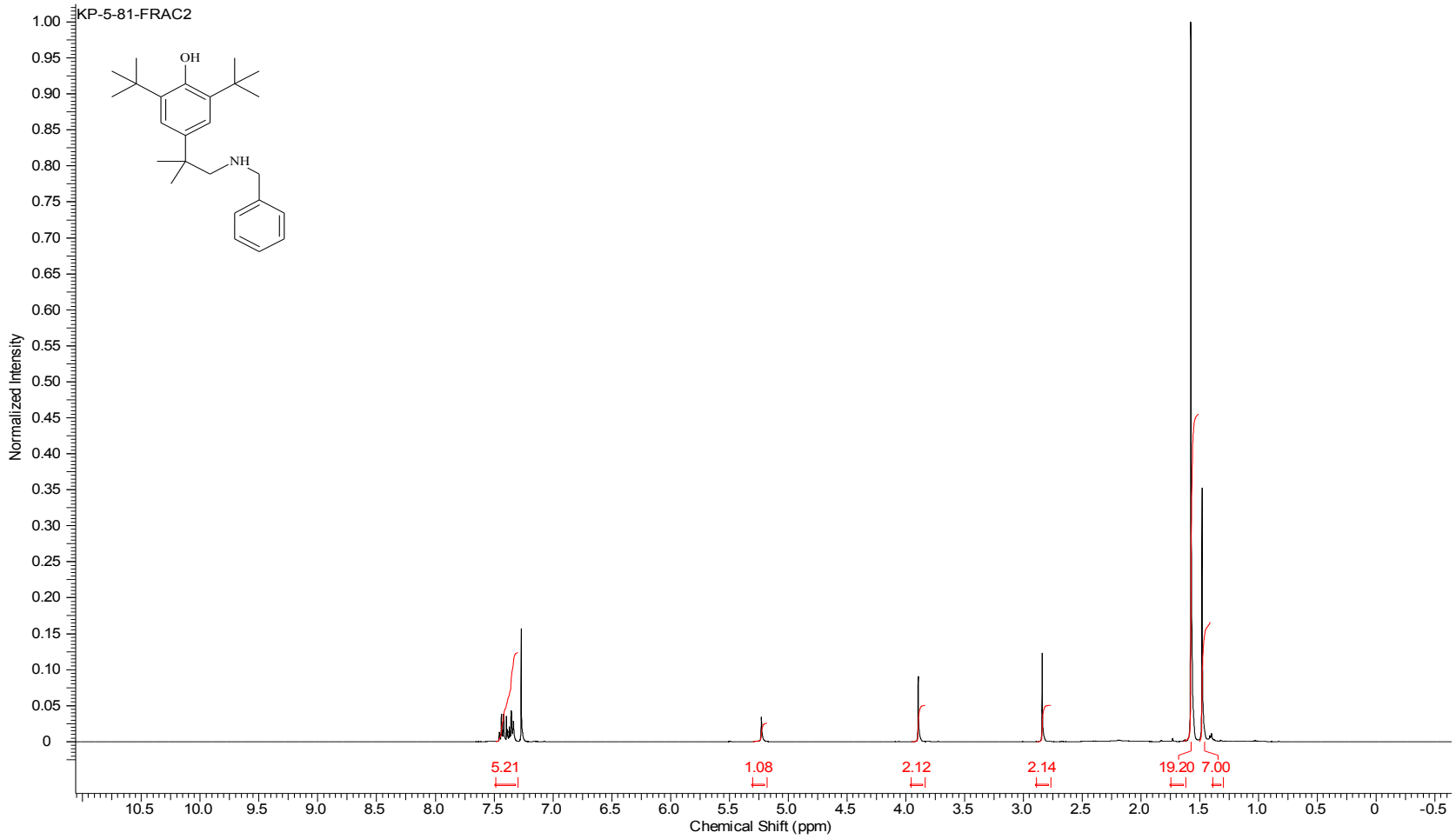

Compound 16 ^{13}C NMR

Acquisition Time (sec)	1.3005	***Comment***	Std proton	***Date***	Nov 29 2009	***Date Stamp***	Nov 29 2009
File Name	C:\USERS\KESHAR\DESKTOP\NMR\BOOK 5\KP-5-81-C13.FID\FID					***Frequency (MHz)***	100.53
Nucleus	13C	***Number of Transients***	1000	***Original Points Count***	31375	***Points Count***	32768
Pulse Sequence	s2pul	***Receiver Gain***	30.00	***Solvent***	CHLOROFORM-d		
Spectrum Offset (Hz)	10550.1191	***Spectrum Type***	STANDARD	***Sweep Width (Hz)***	24125.45	***Temperature (degree C)***	25.000

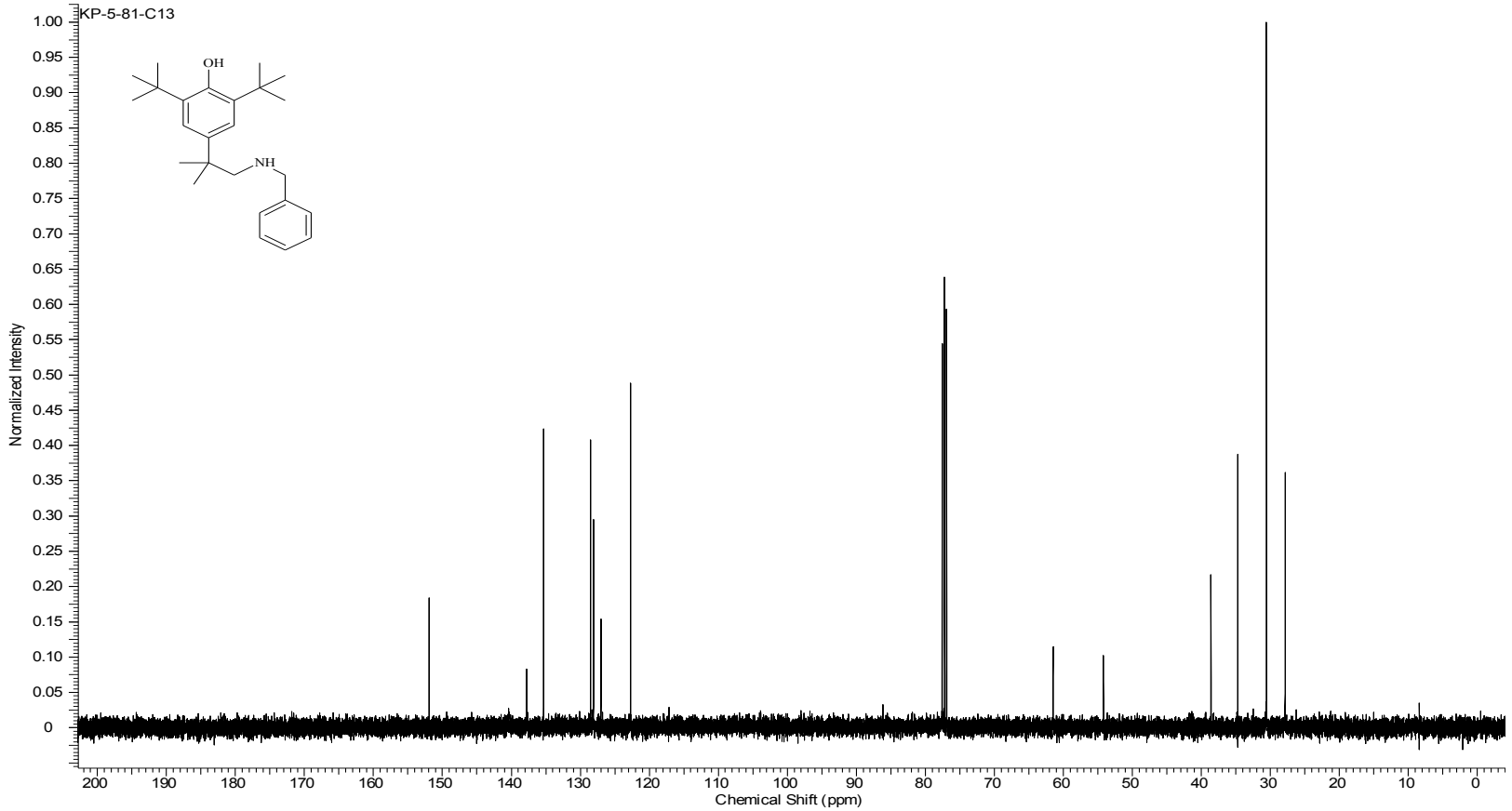

Compound 17 ^{1}H NMR

Acquisition Time (sec)	2.0487	***Comment***	Std proton	***Date***	Nov 23 2009	***Date Stamp***	Nov 23 2009
File Name	C:\USERS\KESHAR\DESKTOP\NMR\BOOK 5\KP-5-42-FRAC2-PURE.FID\FID					***Frequency (MHz)***	399.75
Nucleus	1H	***Number of Transients***	16	***Original Points Count***	13103	***Points Count***	16384
Pulse Sequence	s2pul	***Receiver Gain***	32.00	***Solvent***	CHLOROFORM-d		
Spectrum Offset (Hz)	2403.5376	***Spectrum Type***	STANDARD	***Sweep Width (Hz)***	6395.91	***Temperature (degree C)***	25.000

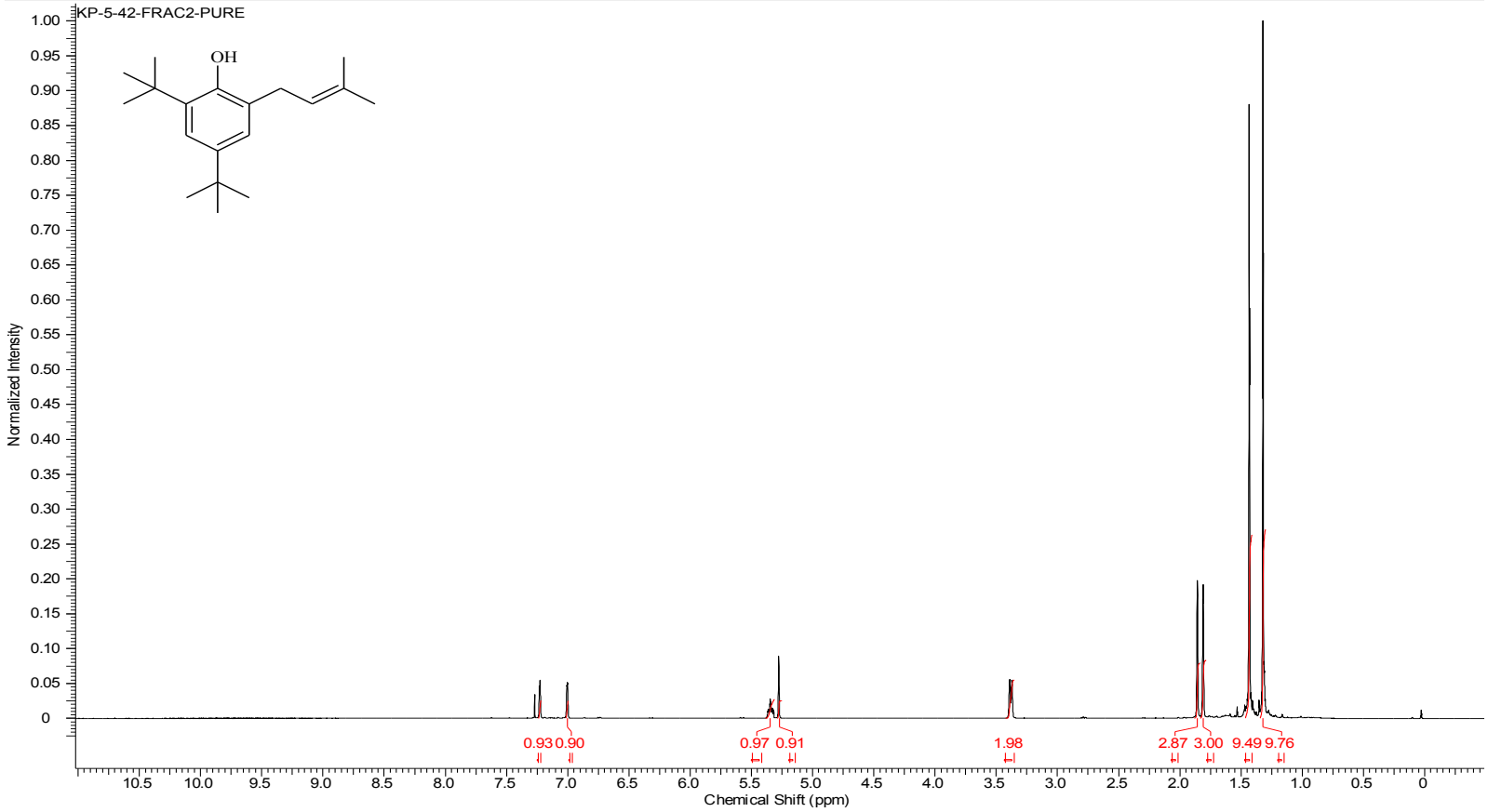

Compound 17 ^{13}C NMR

Acquisition Time (sec)	1.3005	***Comment***	Std proton	***Date***	Nov 23 2009	***Date Stamp***	Nov 23 2009
File Name	E:\KESHAR NMR REMAIN\KP-5-42-FRAC2.FID\FID			***Frequency (MHz)***	100.53	***Nucleus***	13C
Number of Transients	512	***Original Points Count***	31375	***Points Count***	32768	***Pulse Sequence***	s2pul
Receiver Gain	30.00	***Solvent***	CHLOROFORM-d			***Spectrum Offset (Hz)***	10550.8555
Spectrum Type	STANDARD	***Sweep Width (Hz)***	24125.45	***Temperature (degree C)***	25.000		

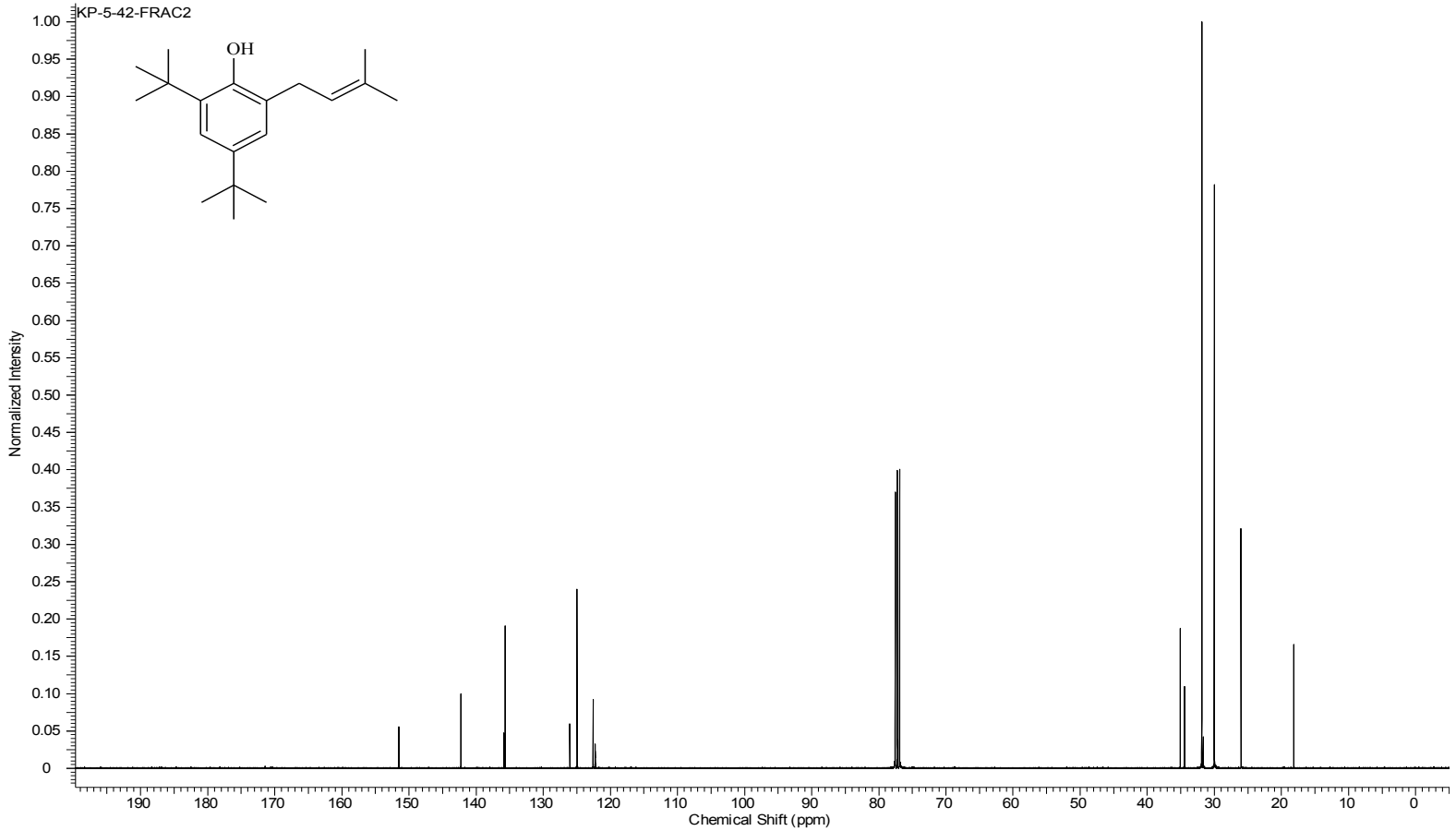

Compound 18 ^{1}H NMR

Acquisition Time (sec)	2.0487	***Comment***	KP-5-85-frac19			***Date***	Dec 3 2009
Date Stamp	Dec 3 2009	***File Name***	C:\USERS\KESHAR\DESKTOP\NMR\BOOK 5\KP-5-85-FRAC19.FID\FID				
Frequency (MHz)	399.75	***Nucleus***	1H	***Number of Transients***	28	***Original Points Count***	13103
Points Count	16384	***Pulse Sequence***	s2pul	***Receiver Gain***	42.00	***Solvent***	CHLOROFORM-d
Spectrum Offset (Hz)	2404.7219	***Spectrum Type***	STANDARD	***Sweep Width (Hz)***	6395.91	***Temperature (degree C)***	25.000

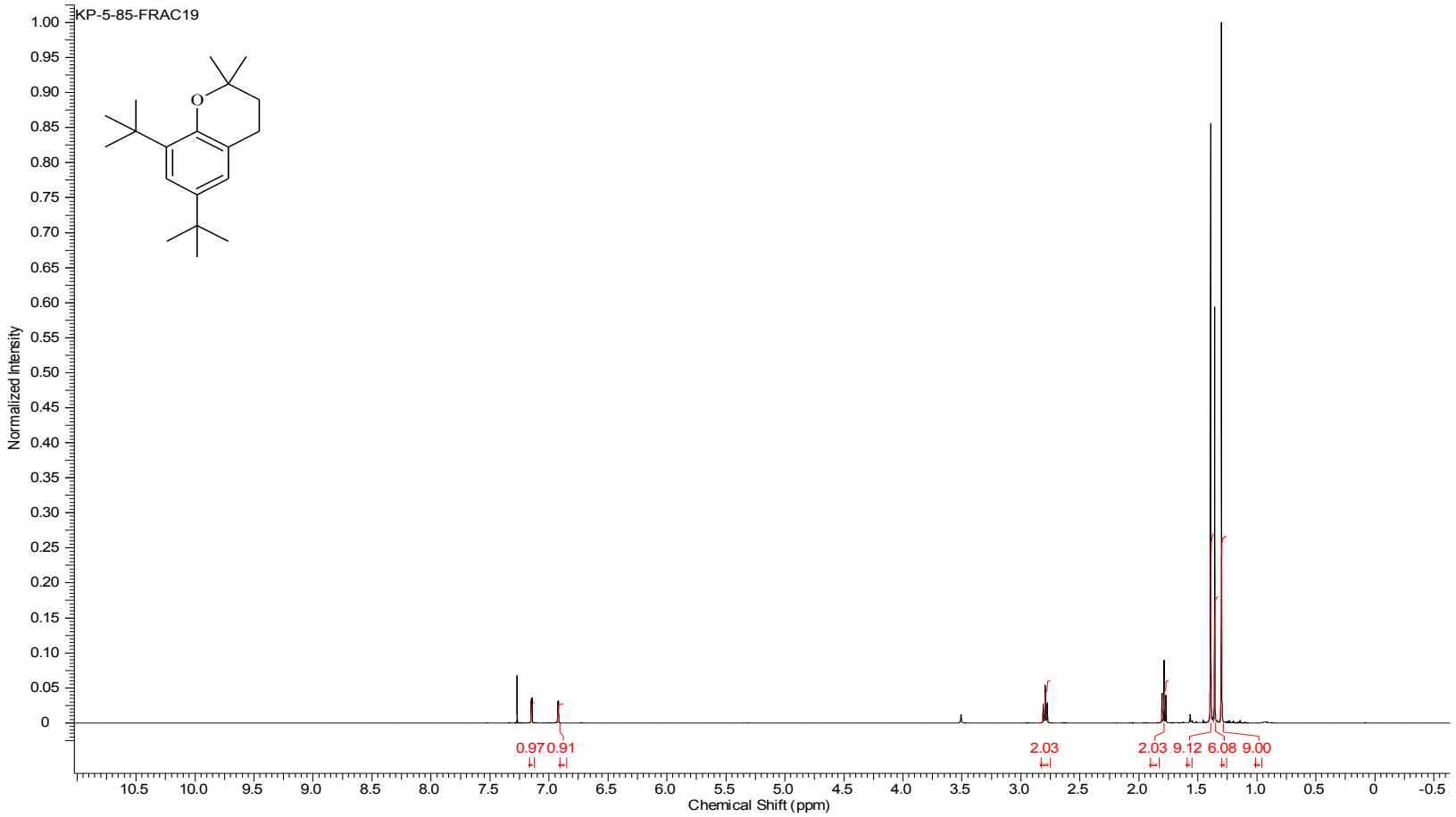

Compound 18 ^{13}C NMR

Acquisition Time (sec)	1.3005	***Comment***	Std proton	***Date***	Nov 25 2009	***Date Stamp***	Nov 25 2009
File Name	C:\USERS\KESHAR\DESKTOP\NMR\BOOK 5\KP-5-76-FRAC7-C13.FID\FID					***Frequency (MHz)***	100.53
Nucleus	13C	***Number of Transients***	512	***Original Points Count***	31375	***Points Count***	32768
Pulse Sequence	s2pul	***Receiver Gain***	30.00	***Solvent***	CHLOROFORM-d		
Spectrum Offset (Hz)	10551.5918	***Spectrum Type***	STANDARD	***Sweep Width (Hz)***	24125.45	***Temperature (degree C)***	25.000

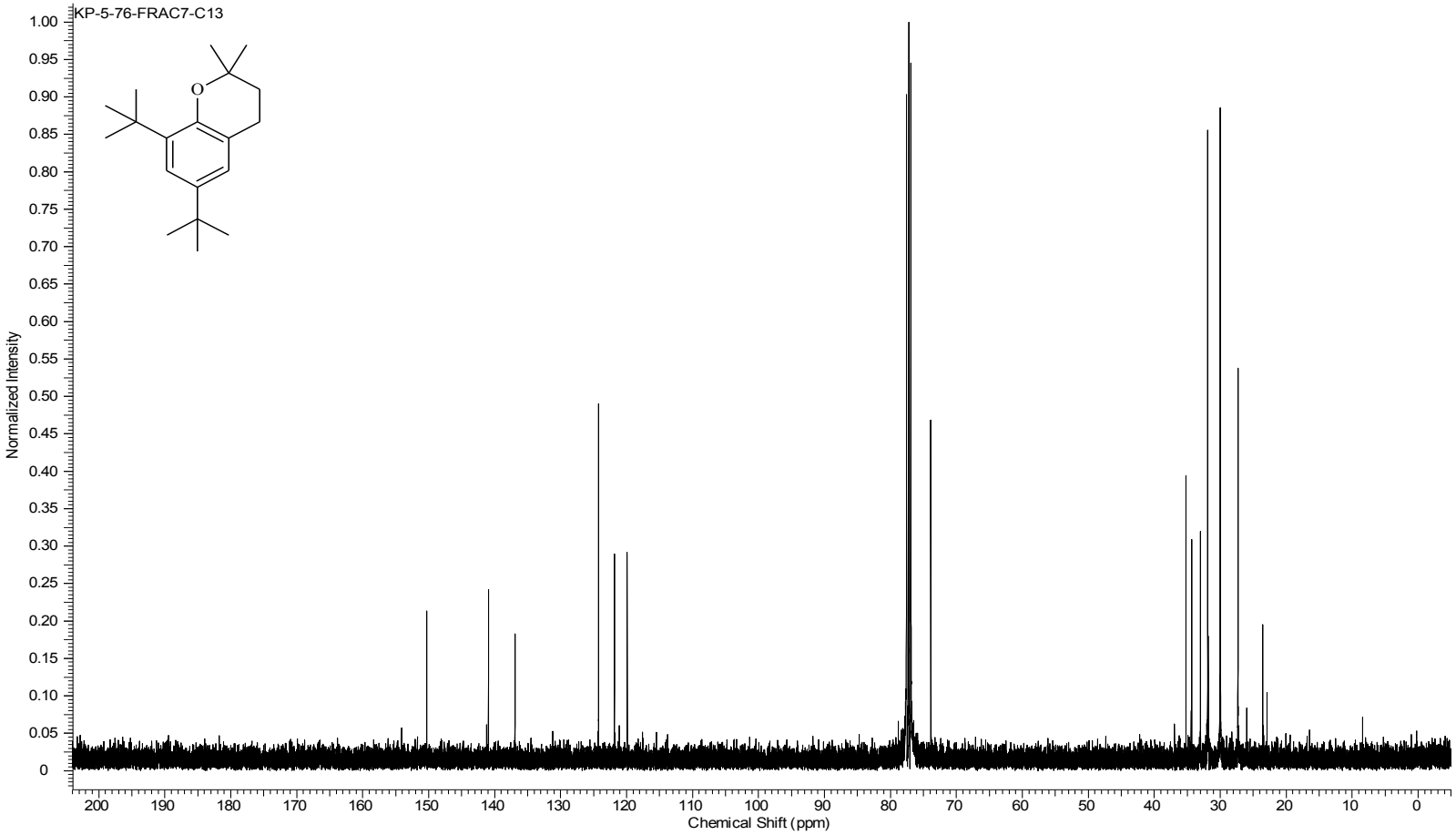

MON-0585 (compound 9) ^{1}H NMR

Acquisition Time (sec)	2.0487	***Comment***	Std proton	***Date***	Aug 24 2009	***Date Stamp***	Aug 24 2009
File Name	C:\USERS\KESHAR\KP-5-15-Proton						
Frequency (MHz)	399.75	***Nucleus***	1H	***Number of Transients***	40	***Original Points Count***	13103
Points Count	16384	***Pulse Sequence***	s2pul	***Receiver Gain***	36.00	***Solvent***	CHLOROFORM-d
Spectrum Offset (Hz)	2397.2451	***Spectrum Type***	STANDARD	***Sweep Width (Hz)***	6395.91	***Temperature (degree C)***	25.000

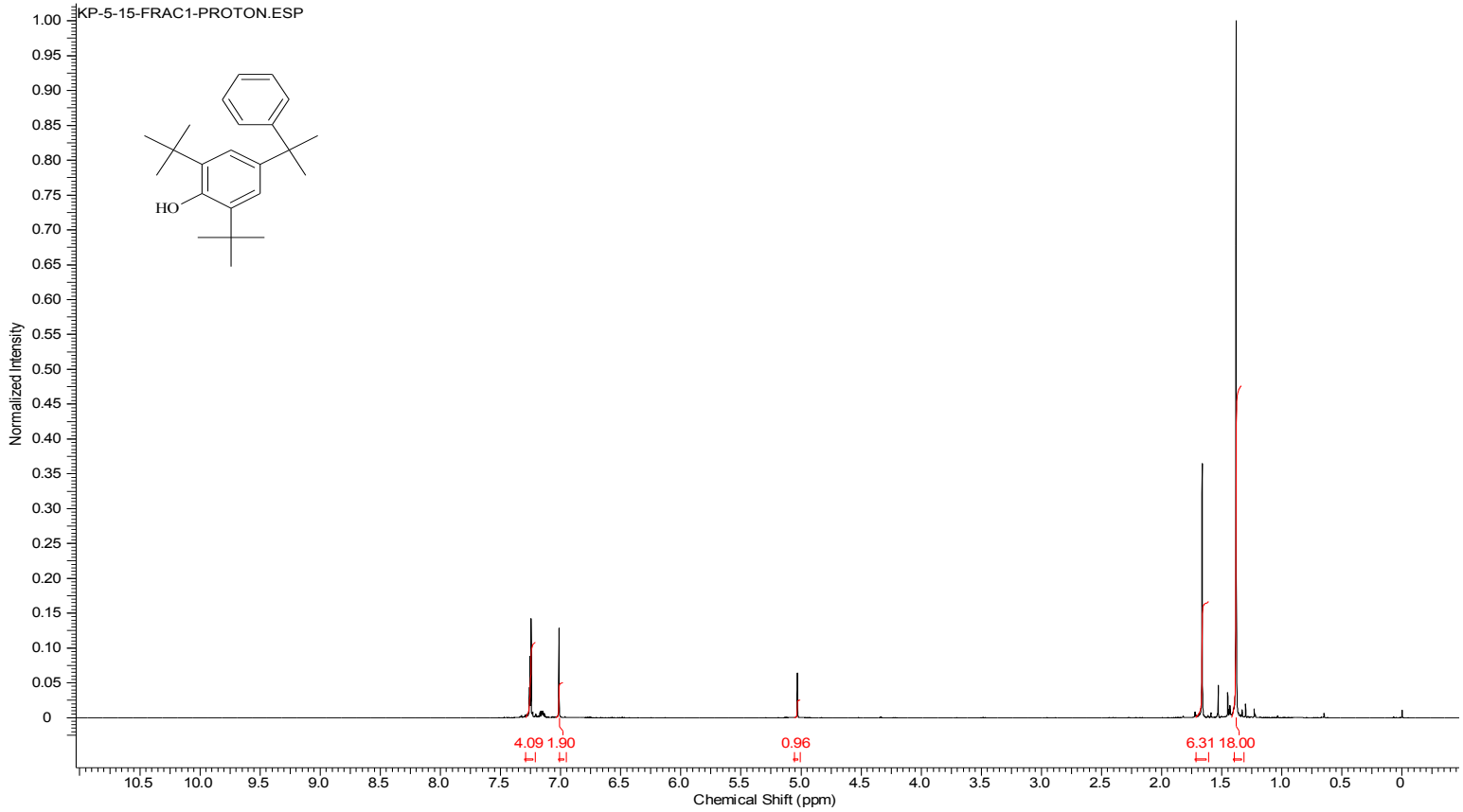

Compound 52 ^{1}H NMR

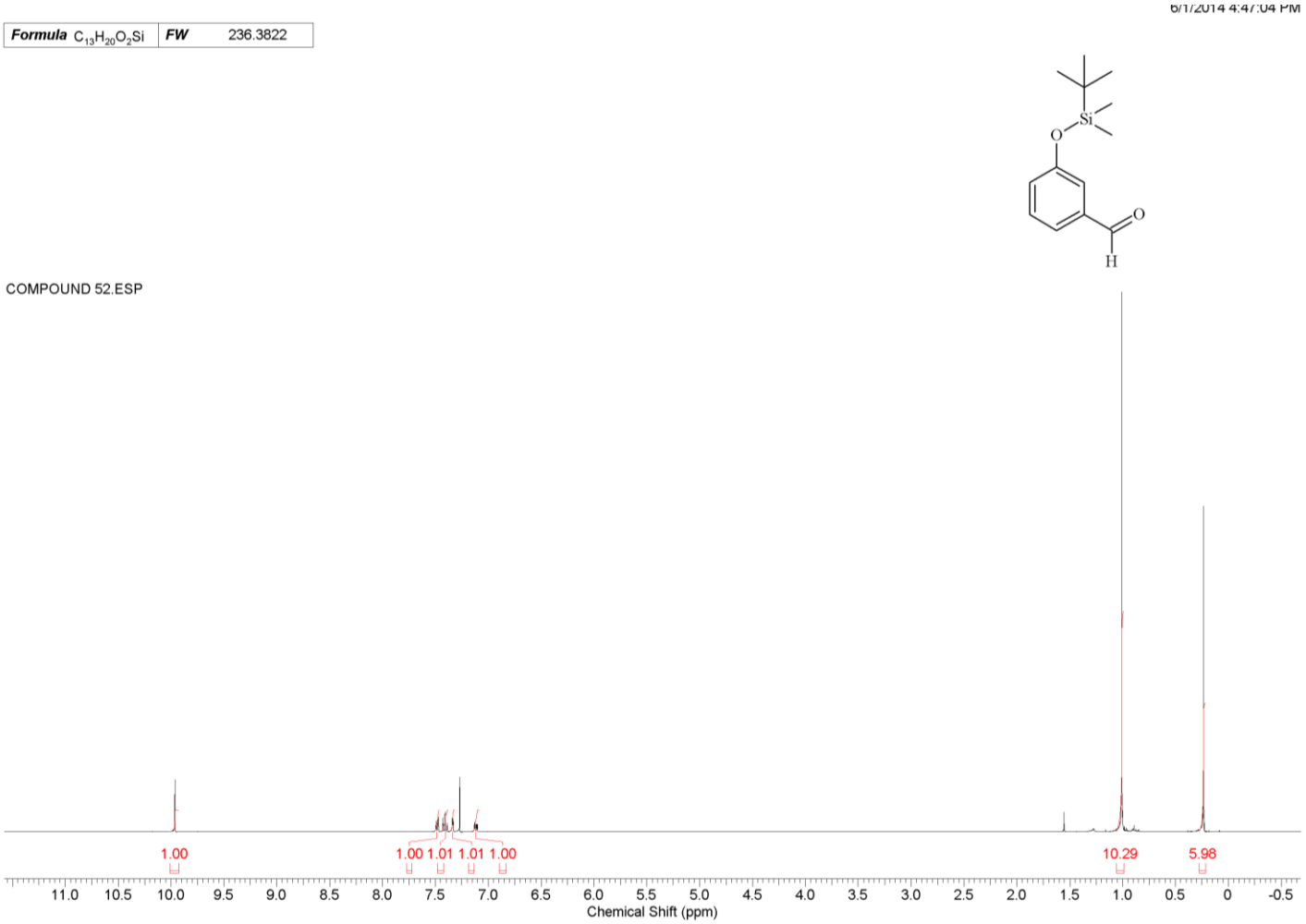

Compound 53 ^{1}H NMR

Formula	$C_{13}H_{22}O_2Si$	FW	238.3981

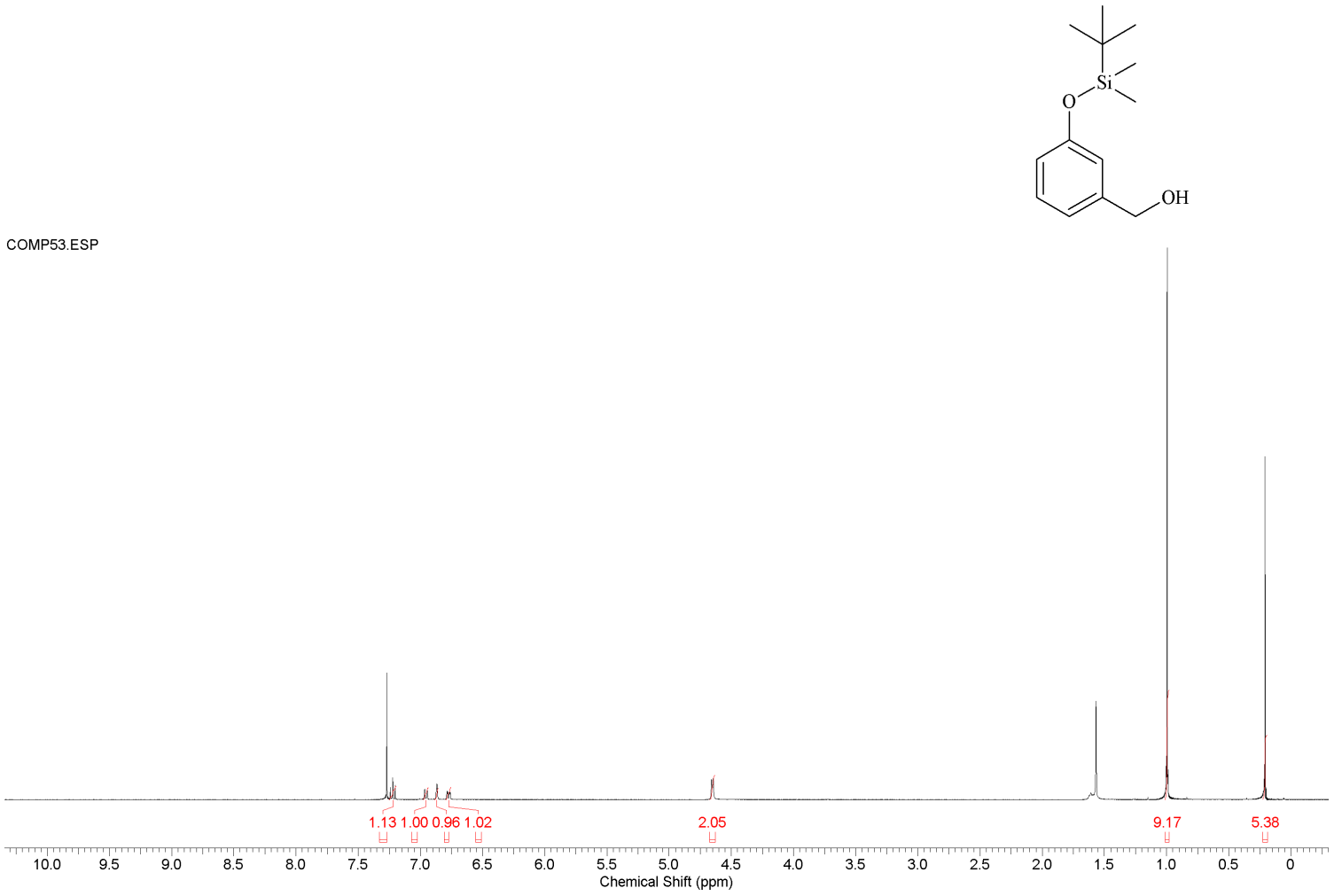

Compound 54 ^{1}H NMR

Formula $C_{13}H_{21}BrOSi$	FW 301.2947

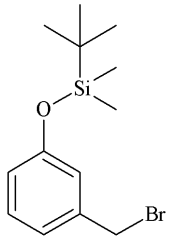

OMP54.ESP

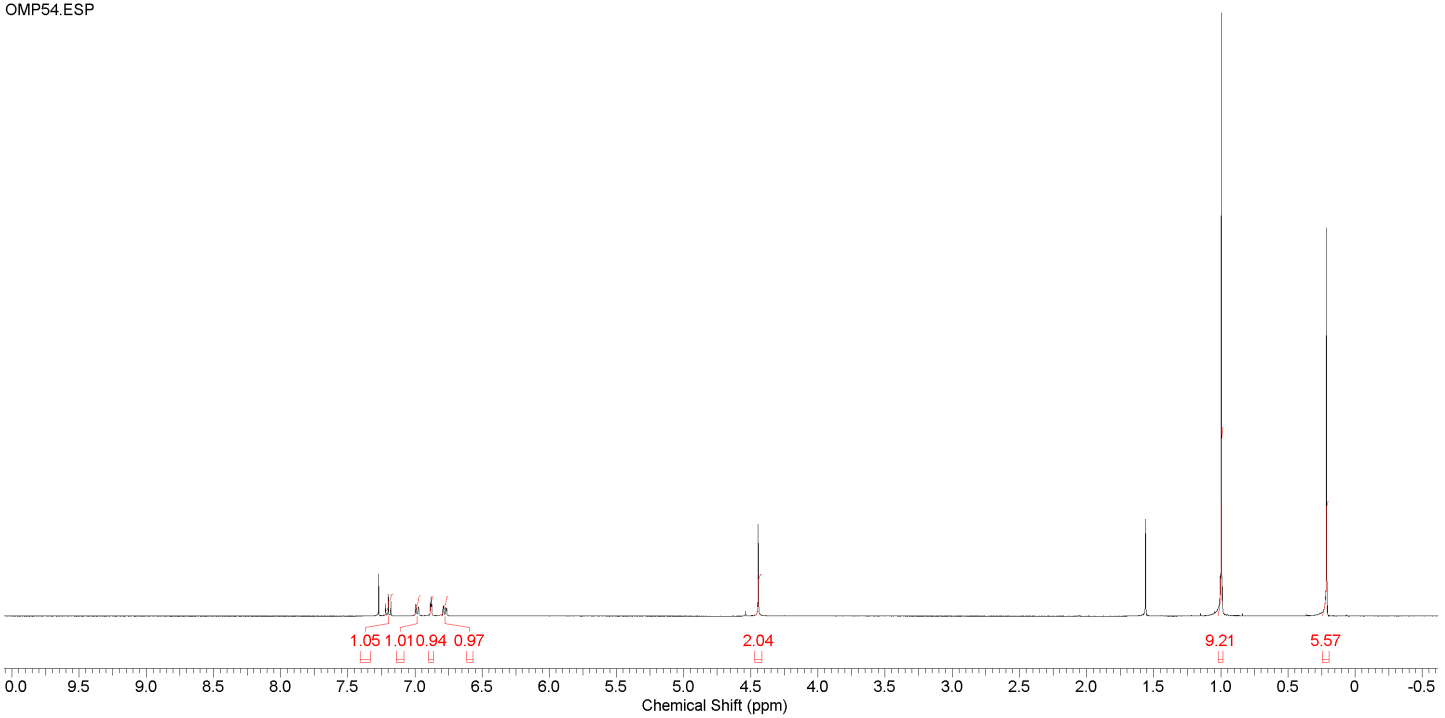

Compound 54 ^{13}C NMR

Formula	$C_{13}H_{21}BrOSi$	FW	301.2947

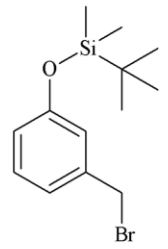

COMPD54-C13.ESP

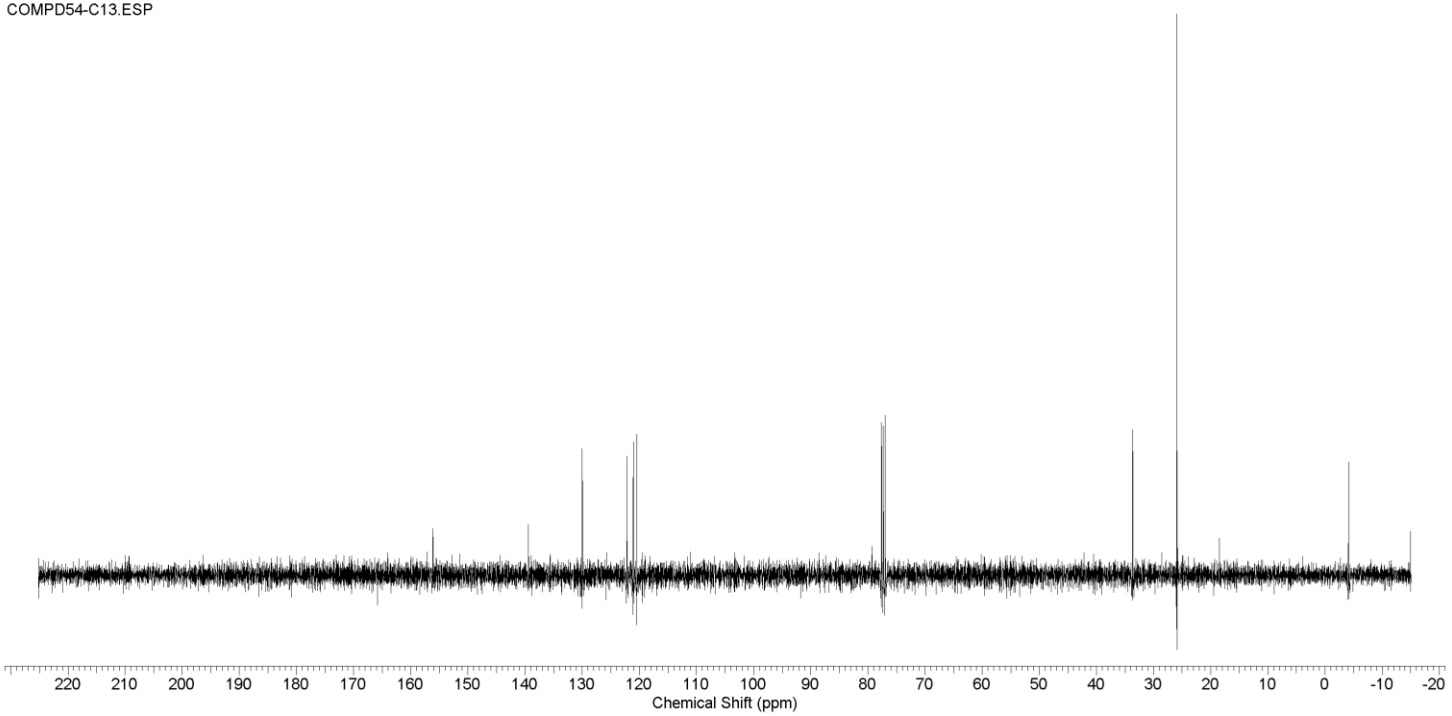

Compound 56 ^{1}H NMR

Formula $C_{24}H_{41}NO_6Si$	***FW*** 467.6709 (321.5297+73.0706+73.0706)

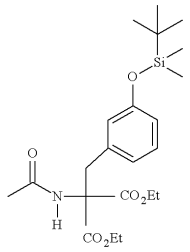

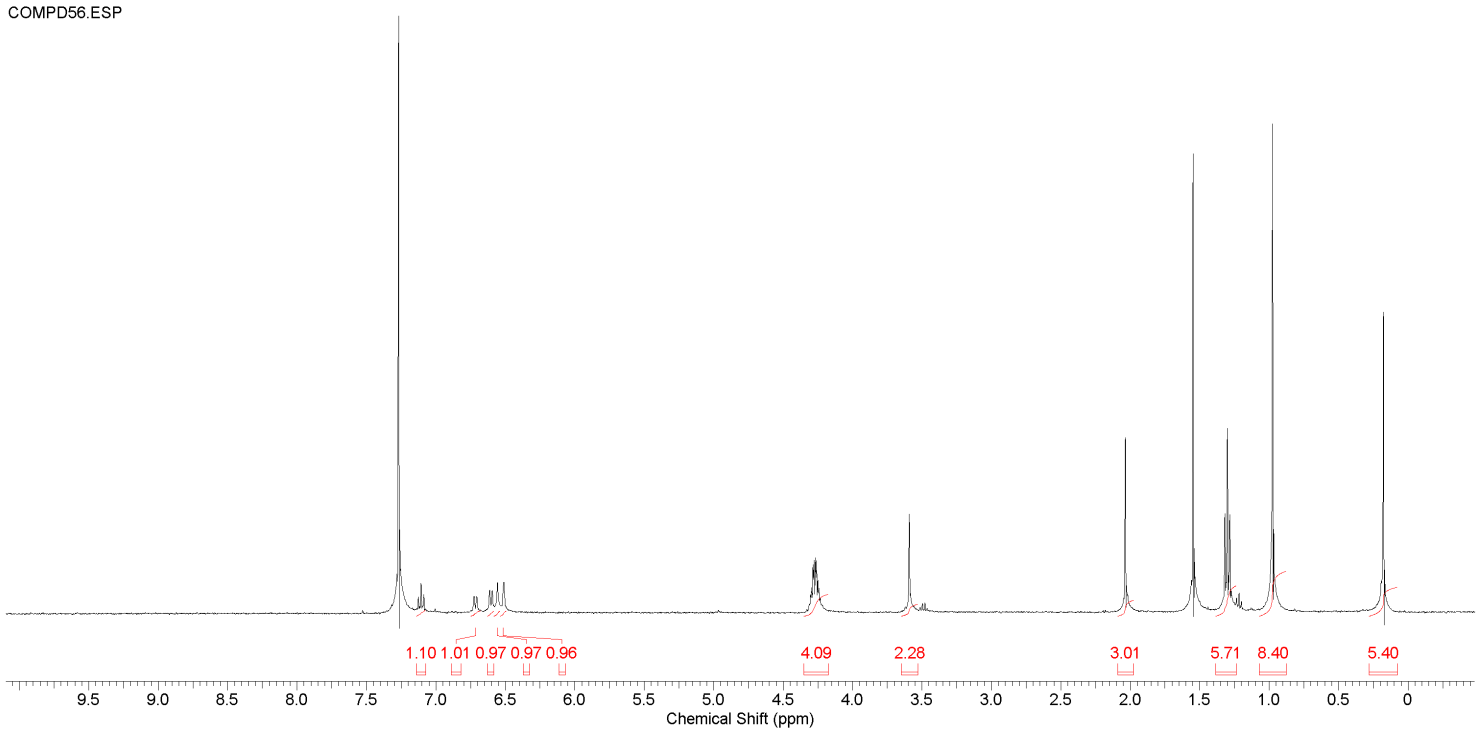

Compound 57 ^{1}H NMR

Formula $C_{16}H_{23}NO_6$	FW 325.3569 (45.0174+73.0706+207.2689)

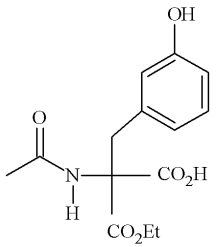

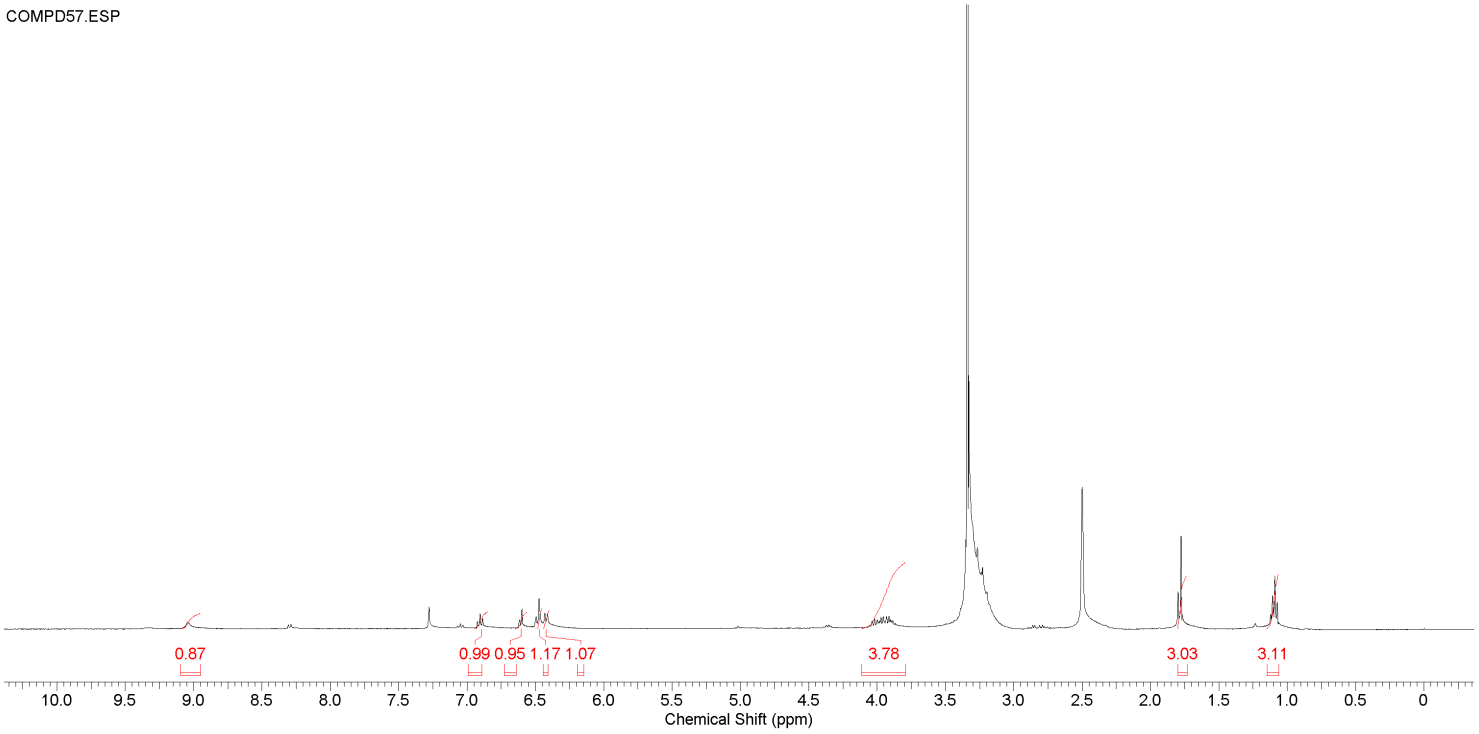

Compound 58 ^{1}H NMR

Formula $C_{13}H_{17}NO_4$	FW 251.2784

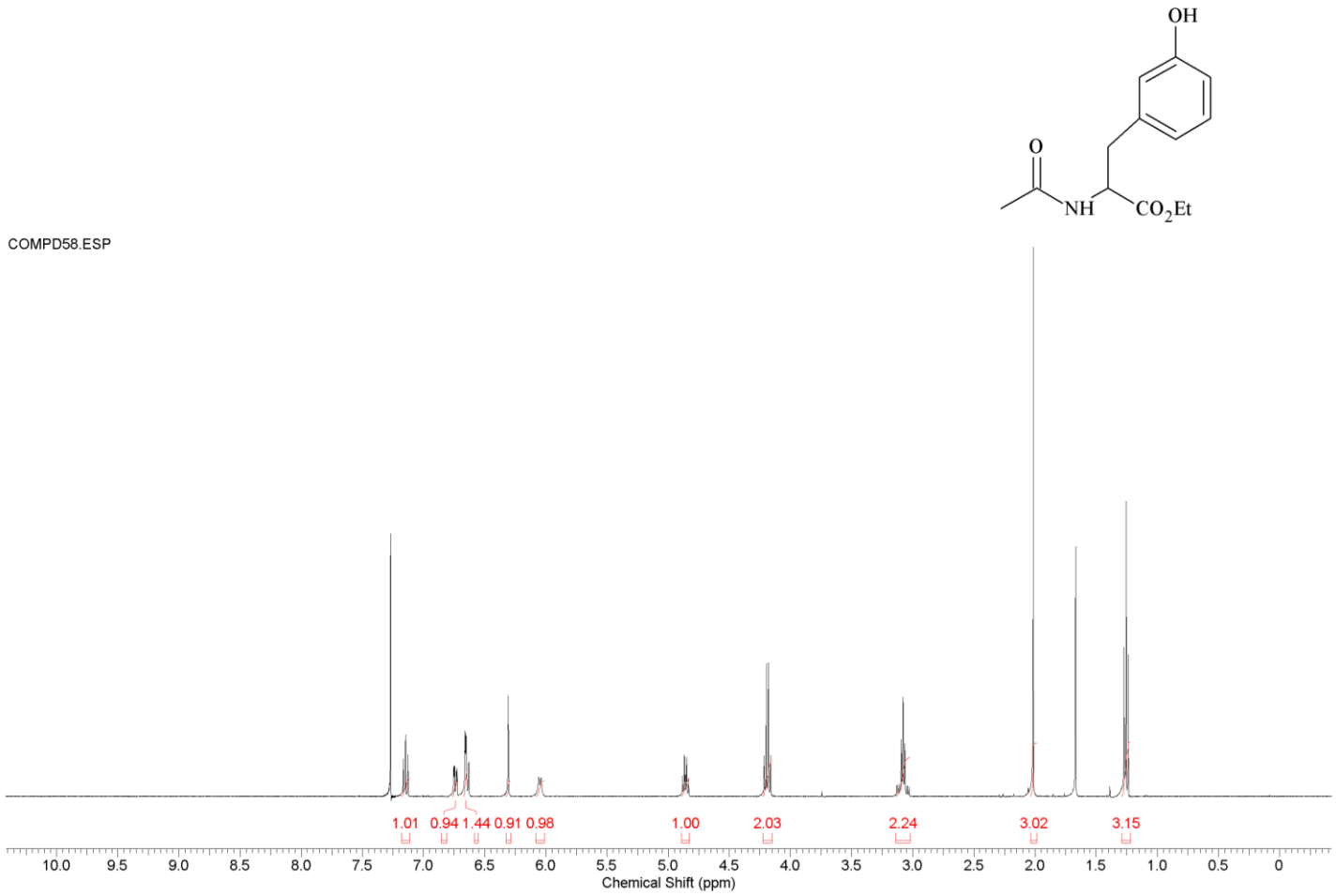

Compound 59 ^{1}H NMR

Formula	$C_{11}H_{13}NO_4$	FW	223.2252

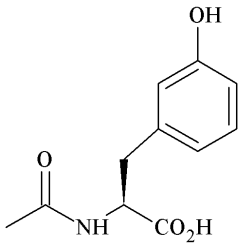

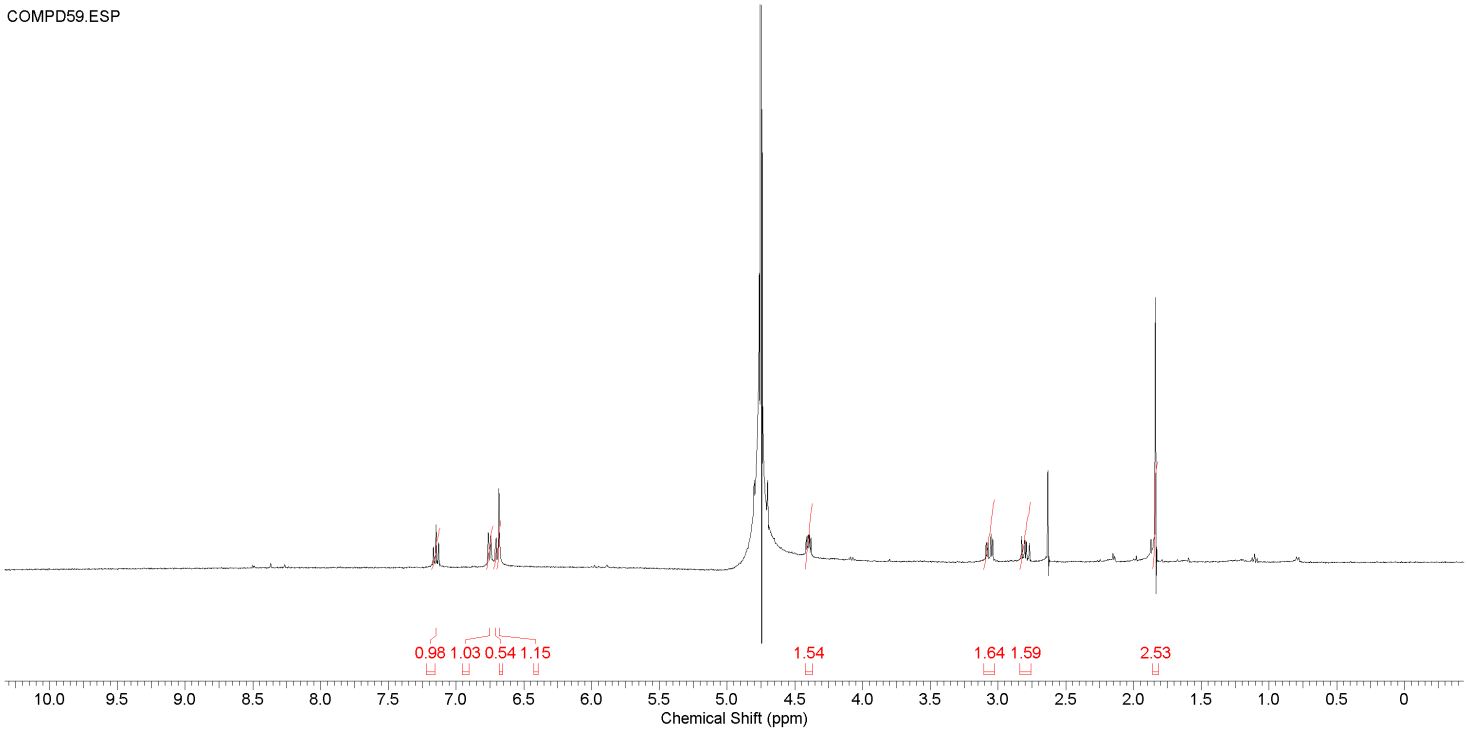

Compound 59 MS